AFML-TR-65-98
Volume I of III Volumes

June 1965

FINAL TECHNICAL ENGINEERING REPORT

CONTINUOUSLY CIRCULATING FISSIOCHEMICAL PROCESS DEVELOPMENT APPLICABLE TO HYDRAZINE SYNTHESIS

VOLUME I: PROGRAM SURVEY, PROCESSING, AND MATERIALS

TECHNICAL REPORT AFML-TR-65-98

JUNE 1965

Chemical Processing Branch
Manufacturing Technology Division
Air Force Materials Laboratory
Research and Technology Division
Air Force Systems Command
United States Air Force
Wright-Patterson Air Force Base, Ohio

MM Project No. 7-840a

Distribution Statement C:
Distribution authorized to U.S. Government agencies and their contractors.

DESTRUCTION NOTICE - For unclassified, limited documents, destroy by any method that will prevent disclosure of contents or reconstruction of the document."

Prepared under Contract AF 33(600)-42996 by
Aerojet-General Nucleonics, San Ramon, California;
J. H. Cusack, R. H. Black, R. L. Pearson, F. R. Standerfer, authors

NOTICES

DDC RELEASE TO OTS NOT AUTHORIZED. The distribution of this report is limited because the report contains technology identifiable with items on the strategic embargo.

Citation Format: Indexing

Accession Number:
AD0467239
Full Text (pdf) Availability:
View Full Text (pdf)
File: /UL/467239.pdf
Size: 9 MB
Citation Status:
Active
Report Classification:
Unclassified
Citation Classification:
Unclassified
Distribution Limitation(s):
02 - U.S. GOVT. AND THEIR CONTRACTORS
23 - AVAILABILITY: DOCUMENT PARTIALLY ILLEGIBLE
Abstract Classification:
Unclassified
Title Classification:
Unclassified
Identifier Classification:
Unclassified
Distribution Statement:
Distribution authorized to U.S. Gov't. agencies and their contractors; Administrative/Operational Use; Jun 1965. Other requests shall be referred to Air Force Materials Laboratory, attn: Research & Technology Div., Wright-Patterson AFB, OH 45433., Availability: Document partially illegible.
Date Citation Updated:
19 Jan 2005
Unclassified Title:
(U) CONTINUOUSLY CIRCULATING FISSIOCHEMICAL PROCESS DEVELOPMENT APPLICABLE TO HYDRAZINE SYNTHESIS. VOLUME 1: PROGRAM SURVEY, PROCESSING, AND MATERIALS
Report Date:
Jun 1965
Document Location:
DTIC
Media Count:
231 Page(s)
Pagination Code:
0
Corporate Author:
AEROJET-GENERAL NUCLEONICS SAN RAMON CA
Report Number(s):
AN-1425-VOL-1 *(AN1425VOL1)*
AFML-TR-65-98-VOL-1 *(AFMLTR6598VOL1)*
XC-TR-65-98-VOL-1 *(XCTR6598VOL1)*
Contract Number:
AF 33(600)-42996 *(AF3360042996)*
Project Number:
AF-7-840-A *(AF7840A)*
Monitor Acronym:
AFML
XC
Monitor Series:
TR-65-98-VOL-1 *(TR6598VOL1)*
AFML
Source Serial:
F
Descriptor Classification:
Unclassified
Geopolitical Code:
0614
Organization Type Code:
4
Organization Text:
INDUSTRIAL/COMMERCIAL
Annotation:
Continuously circulating fissiochemical process development applicable to hydrazine synthesis Vol. 1. Program survey, processing and materials. CONTINUOUSLY CIRCULATING FISSIOCHEMICAL PROCESS DEVELOPMENT APPLICABLE TO HYDRAZINE SYNTHESIS. VOLUME I: PROGRAM SURVEY, PROCESSING, AND MATERIALS -- Translation.
Fields and Groups:

070300 - Organic Chemistry

Personal Author(s):

Cusack, J H
Black, R H
Pearson, R L
Standerfer, F R

Descriptors:

(U) *HYDRAZINES, *HYDRAZINES, *NUCLEAR ENGINEERING, *NUCLEAR ENGINEERING, *CHEMICAL ENGINEERING, *CHEMICAL ENGINEERING, SYSTEMS ENGINEERING, SYSTEMS ENGINEERING, PRODUCTION, PRODUCTION, DECONTAMINATION, DECONTAMINATION, PROCESSING, PROCESSING, SYNTHESIS(CHEMISTRY), SYNTHESIS(CHEMISTRY), COMPATIBILITY, COMPATIBILITY, AMMONIA, AMMONIA, SLURRY FUELS, SLURRY FUELS, GAMMA RAYS, GAMMA RAYS, OXIDIZERS, OXIDIZERS, SEPARATION, SEPARATION, NUCLEAR ENERGY, NUCLEAR ENERGY, NUCLEAR REACTORS, NUCLEAR REACTORS, REACTOR FUELS, REACTOR FUELS, LIQUID ROCKET FUELS, LIQUID ROCKET FUELS, FLUORIDES, FLUORIDES, RADIOACTIVE ISOTOPES, RADIOACTIVE ISOTOPES, FISSION PRODUCTS, FISSION PRODUCTS, RADIOCHEMISTRY, RADIOCHEMISTRY, INDUSTRIAL EQUIPMENT, INDUSTRIAL EQUIPMENT, URANIUM COMPOUNDS, URANIUM COMPOUNDS, DIOXIDES, DIOXIDES, RADIATION CHEMISTRY, RADIATION CHEMISTRY

Identifiers:

(U) FISSIOCHEMISTRY

Abstract:

(U) The primary goal of this program was to design, construct, and operate a continuous in-reactor loop to further the development of the fissiochemical process; the conversion of NH3 to N2H4 was chosen as the demonstration synthesis, basic radiation chemistry, and new product development, and reactor physics. The AGN-6 loop experiment involved the circulation of a slurry of fully enriched particulate UO2 fuel in liquid NH3 through the high thermal neutron flux region of the Materials Testing Reactor, National Reactor Testing Station, Idaho; sampling and removal of the N2H4 product; separation and disposal of the radiolytic gases formed; and liquid NH3 feed makeup. The experiment was successfully operated in-reactor for 1440 hrs at nominal fission power levels of 0 to 9 kw. Initial fueled operations resulted in a hydrazine yield of 1.27 molecules per 100 ev of energy deposited, essentially confirming capsule-based predictions.

Descriptive Note:

Final technical engineering rept., Apr 1961-Jan 1965

Supplementary Note:

See also Volume 2, AD467256 and Volume 3, AD467257.

Source Code:

007250

Cost:

$14.60

FOREWORD

This Final Technical Engineering Report covers all work performed under Contract AF 33(600)-42996 from April 1961 through January 1964. On the basis of an agreement between the Air Force and the United States Atomic Energy Commission, follow-on work performed under AEC Contract AT (04-3)-368, Project Agreement No. 4, from February 1964 through January 1965, is also covered herein. The manuscript was released by the authors in May 1965 for publication as an AFML Technical Report. The Aerojet-General Nucleonics identification number for this report is AN-1425.

This Air Force contract with Aerojet-General Nucleonics, San Ramon, California, was initiated under ASD Project 7-840a, "Hydrazine Process Development Program." It was accomplished under the technical direction of Mr. Charles Tanis of the Chemical Processing Branch (MATC), Manufacturing Technology Division, AF Materials Laboratory, Wright-Patterson Air Force Base, Ohio.

Dr. J. H. Cusack was the Program Manager. Project Engineers on the program included Mr. F. R. Standerfer (Processing), Dr. R. L. Pearson (Materials), Mr. J. C. Whipple and Mr. H. T. Watanabe (In-Reactor Engineering), Mr. R. I. Miller (Support), Dr. L. G. Carpenter (Basic Studies), Mr. H. J. Snyder (Nuclear Engineering), and Mr. C. C. Groff and Mr. R. H. Black (Operations). Others assisting in the program included Mr. D. E. Bush, Contract Administration, Mr. H. E. Bohrer, Purchasing Administration and Mr. D. C. Camp, Technical Editor. Subcontract activities at the National Reactor Testing Station, Idaho were carried out under the direction of Mr. F. L. McMillan, Mr. L. L. Myers, Dr. R. L. Shank and Mr. J. H. Ronsich, of the Phillips Petroleum Co. Especially significant consultation was supplied by Dr. W. M. Garrison, UCRL Berkeley, and Mr. S. A. Reed, ORNL.

This project has been accomplished as a part of the Air Force Manufacturing Methods Program, the primary objective of which is to develop, on a timely basis, manufacturing processes, techniques and equipment for use in economical production of USAF materials and components. The program encompasses the following technical areas:

Metallurgy - Rolling, Forging, Extruding, Casting, Fiber, Powder
Chemical - Propellant, Coating, Ceramic, Graphite, Nonmetallics
Electronic - Solid State, Materials and Special Techniques, Thermionics
Fabrication - Forming, Material Removal, Joining, Components

Suggestions concerning additional Manufacturing Methods development required on this or other subjects will be appreciated.

ABSTRACT

CONTINUOUSLY CIRCULATING FISSIOCHEMICAL PROCESS DEVELOPMENT APPLICABLE TO HYDRAZINE SYNTHESIS

(VOLUME I: PROGRAM SURVEY, PROCESSING, AND MATERIALS)

J. H. Cusack
R. H. Black
R. L. Pearson
F. R. Standerfer

Aerojet-General Nucleonics
San Ramon, California

The primary goal of this program was to design, construct, and operate a continuous in-reactor loop to further the development of the fissiochemical process; the conversion of ammonia to hydrazine was chosen as the demonstration synthesis. Direct support included studies in decontamination, purification, fuel cycle, materials, chemical and energy deposition analysis, basic radiation chemistry, and new product development, and reactor physics. The ~~AGN-6~~ loop experiment involved the circulation of a slurry of fully enriched particulate UO_2 fuel in liquid ammonia through the high thermal neutron flux region of the Materials Testing Reactor, National Reactor Testing Station, Idaho; sampling/ and removal of the hydrazine product; separation and disposal of the radiolytic gases formed; and liquid ammonia feed makeup. The experiment was successfully operated in-reactor for 1440 hours at nominal fission power levels of 0 to 9 kw. Initial fueled operations resulted in a hydrazine yield of 1.27 molecules per 100 ev of energy deposited, essentially confirming capsule-based predictions. Product concentration rose, with time, to the 1 wt% equilibrium value expected at the existing power level; the ~~subsequent~~ product concentration decline was attributed to fuel plate-out. Hydrazine was successfully separated from loop filtrate and decontaminated by distillation and evaporation. Post-operational loop component inspection revealed no serious corrosion, erosion or wear problems. During the pre-operational developmental period, gas-liquid and solid-liquid separation techniques and appropriate equipment were developed; methods for improving the removal of radioactive contamination from the concentrated product were determined. The compatibility of materials of construction, particulate UO_2, and process chemicals was demonstrated.

****

PUBLICATION REVIEW

This volume has been reviewed and is approved.

FOR THE DIRECTOR:

(b)(6)

Chief, Manufacturing Technology Division
AF Materials Laboratory

MASTER TABLE OF CONTENTS

CONTINUOUSLY CIRCULATING FISSIOCHEMICAL PROCESS DEVELOPMENT APPLICABLE TO HYDRAZINE SYNTHESIS

Volume I: Program Survey, Processing, and Materials

MASTER TABLE OF CONTENTS (Continued)

Section Page

Volume II: In-Reactor Engineering, and Support

MASTER TABLE OF CONTENTS (Continued)

Volume III: Basic Studies, Nuclear Engineering, Plant Design, Loop Operations, and Appendices

MASTER TABLE OF CONTENTS (Continued)

TABLE OF CONTENTS

VOLUME I: PROGRAM SURVEY, PROCESSING, AND MATERIALS

TABLE OF CONTENTS (Continued)

TABLE OF CONTENTS (Continued)

TABLE OF CONTENTS (Continued)

LIST OF FIGURES

VOLUME I: PROGRAM SURVEY, PROCESSING, AND MATERIALS

LIST OF FIGURES (Continued)

LIST OF FIGURES (Continued)

LIST OF FIGURES (Continued)

LIST OF FIGURES (Continued)

LIST OF TABLES

VOLUME I: PROGRAM SURVEY, PROCESSING, AND MATERIALS

LIST OF TABLES (Continued)

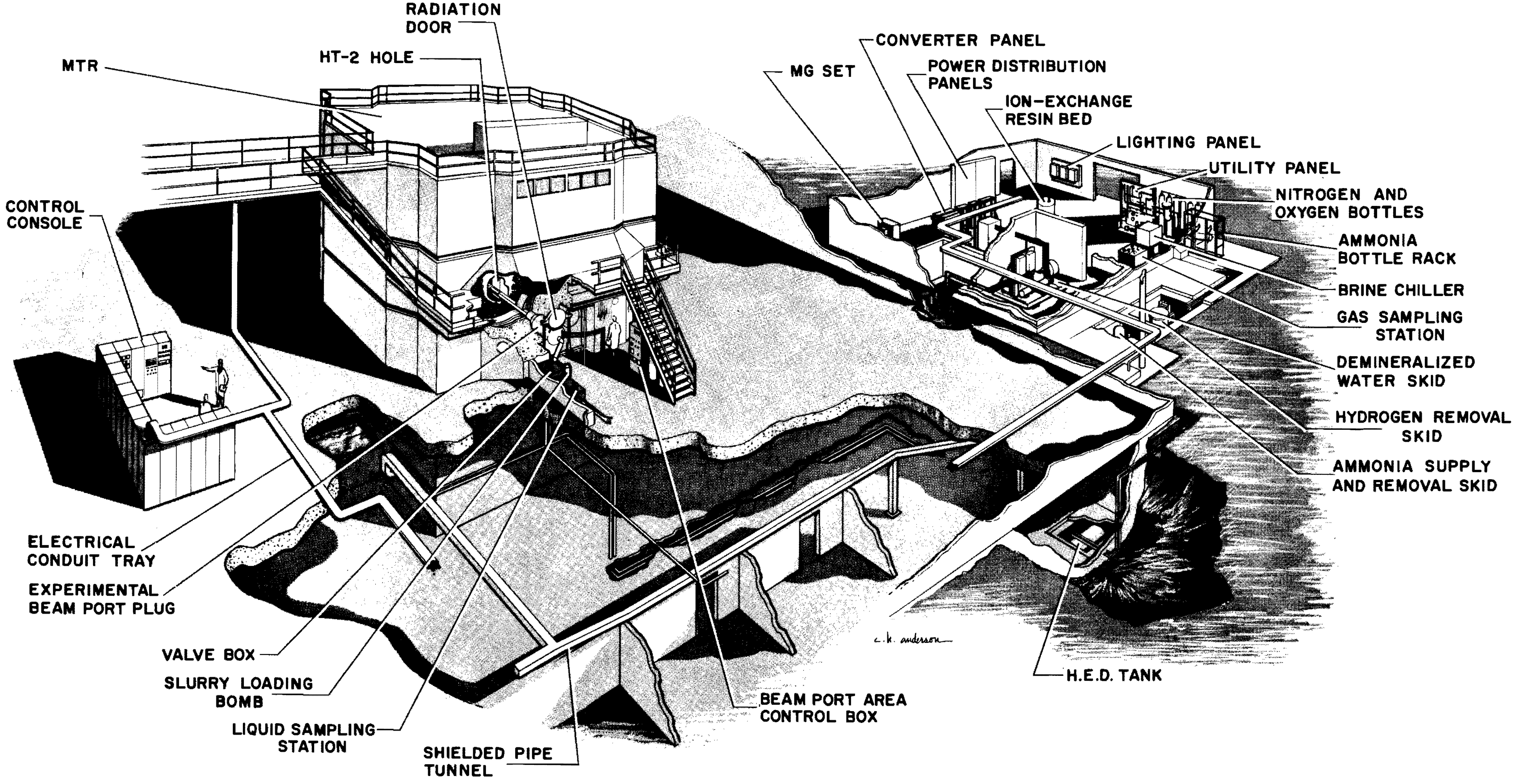

113-63-4044

AGN HYDRAZINE LOOP FACILITY

1.0 PROGRAM SURVEY

The primary goal of this program was to design, develop, construct and operate a continuous in-reactor hydrazine production loop using the fissiochemical process. Direct support for the development of the loop and its components included studies in decontamination, purification, fuel cycle, materials, chemical and energy deposition analysis, and reactor physics. Basic radiation and chemistry studies were undertaken to further elucidate reaction mechanisms and to extend the application of this process.

This final report fully describes the Hydrazine Process Development Program including the developmental phase from contract inception (April 1961) through the installation of the completely assembled experimental equipment into the reactor facility (November 1963), the operational phase (through April 1964), and the post-operational inspection and data reduction phase. Section 1 of the report summarizes all program activities, results, and conclusions; Sections 2 through 8 discuss developmental details in depth, including the design, construction and initial testing of all experimental equipment; Section 9 presents loop operation experimental data, product processing experience, and post-operational equipment inspection observations.

All Hydrazine Process Development Program efforts through January 1964, were funded by the U. S. Air Force under Contract AF 33(600)-42996, ASD Project 7-840a. At that time, on the basis of an agreement between the Air Force and the United States Atomic Energy Commission, the latter agency assumed cognizance and funding responsibility for the remainder of the program.

1.1 Background

1.1.1 Chemo-Nuclear Production Techniques

Since operation of the first nuclear reactor, the application to chemical production of the energy released has been a topic of general discussion. Most proposals have suggested using the energy evolved either as process heat or as ionizing radiation. In the process heat concept, nearly all of the liberated energy is available, but at temperatures limited by the properties of construction materials. Thus, the energy is degraded to relatively low temperatures before application to the chemical system.

The ionizing radiation concept utilizes reactor energy in the form of gamma photons. Energy is deposited along the photon path at densities equivalent to temperatures of 10,000^{o}K. Furthermore, the products formed under these conditions are subject to the fastest possible quench. Molecular collisions lower the ionization track temperature to the ambient level within less than a microsecond. However, this approach is severely limited in over-all efficiency by the fact that less than 7% of the fission energy is liberated as gamma photons.

The ideal system would be one which combined the advantages of these two systems without suffering from their disadvantages. Such a system was first experimentally demonstrated by Harteck and Dondes of Rensselaer Polytechnic Institute in 1956 when they utilized fission fragment recoil energy to bring about the combination of N_2 and O_2 to form nitrogen dioxide.

1.1.2 Fissiochemistry

This direct application of the kinetic energy of recoiling fission fragments to the production of chemicals has been termed fissiochemistry. Using this approach, up to 84% of the energy released by uranium fission may be applied to a chemical system at high energy densities, yet the products formed are quenched to ambient temperature in less than a microsecond. Thus, highly energetic compounds can be formed and preserved using this technique. Fissiochemistry was basically an undeveloped tool combining the experimental problems of a nuclear reactor with those of a chemical processing plant. Nevertheless, for particular systems or classes of compounds, the approach should prove to be economical.

The fission fragment approach shows at least two significant advantages over the use of gamma photons. Most obvious is the possibility that as much as 84% of the 200 Mev resulting from the fissioning of a uranium atom can be directly utilized, whereas gamma photons account for only 7% of the fission energy. A less obvious, but perhaps more important, advantage of fission fragments is concerned with linear energy transfer-- the rate of energy deposited per centimeter of track length. The average linear energy transfer of the fission fragment is about 4000 times higher than that of a gamma photon. If peak linear energy transfer rates are compared, this ratio increases by a further order of magnitude.

The gamma photon track might be considered as a string of disconnected expanding spurs, each containing relatively few active species, such as ions or free radicals. The very high linear energy transfer of a fission fragment results in a cylindrical expanding track wherein the active species are more highly concentrated and have greater opportunity for interaction. Multiple events within a single molecule may also become significant. The practical significance of this track difference is the resulting order-of-magnitude yield increase in certain chemical reactions. For example, fission fragment irradiation of ammonia results in a hydrazine G value (molecules of hydrazine produced per 100 ev of energy deposited) about tenfold greater than that obtained from the gamma-irradiation of ammonia.

Fission fragments consist of a wide variety of isotopes with an average weight of about 120 mass units, and an average charge of +20, at least during the early part of their recoil. These fragments have an extremely short range in fuel or fuel diluent; thus, fuel composition and geometry play a dominant role in over-all energy deposition efficiency. Care must be taken in the design of fuel elements so that the fission fragments can be efficiently introduced into a surrounding process stream without having to travel through significant thicknesses of fuel.

A solution of uranium in a reactant stream allows essentially complete utilization of the recoil energy; however, such an advantageous situation will usually be barred by process limitations. Small suspended particles, fibers, or thin slabs of fissile material have been suggested as promising alternatives. Incorporation of the uranium fuel in other materials such as metals, ceramics, or glasses may be necessary in the case of fibers and slabs in order to meet fuel element structural requirements. Harteck and Dondes have extensively studied fuel-loaded glass fibers for gaseous systems; Brookhaven National Laboratory is studying a wide variety of alloyed fuel plates of various designs. Aerojet-General Nucleonics has concentrated on micron-size suspended fuel particles, primarily because of their superior energy deposition efficiency, but also because of a variety of secondary considerations. A suspended particulate system will have an inherently safe negative temperature coefficient of reactivity; a fixed element design may, under certain circumstances, have a positive temperature coefficient of reactivity. Fuel inventory can be easily altered by the rapid addition or removal of easily fabricated fuel particles in a suspended system. Continuous slip stream fuel reprocessing may be considerably less expensive than the periodic refabrication of core made up of a large area of thinly plated elements.

1.1.3 Development History

AGN's initial interest in the fissiochemical field was concerned with the fixation of nitrogen. In this process, micron-size, fully-enriched UO_2 particles are suspended in high pressure air. Fission fragment irradiation results in the production of NO_2. Conventional processing steps are then used to produce nitric acid and fertilizer.

In 1957, following Harteck's initial experimental studies, AGN conducted a paper study of the nuclear nitrogen fixation approach. After making the necessary assumptions concerning yield and equipment development, it seemed reasonable to suggest a brief experimental program to determine possible yields from a suspended particle-type reactor.

An eight-month AGN experimental program aimed at the determination of fixed nitrogen yield was funded by the Atomic Energy Commission.* Results indicated that the process could, under certain circumstances, be of economic interest.** Fixed nitrogen is not, however, an expensive commodity in the United States, and there was no immediate interest in a reactor development program aimed at commercial nuclear nitrogen fixation. Continued research in the field is amply justified, however, and such work is continuing.

Since the fissiochemical approach appeared to offer no immediate advantage for the production of cheap industrial chemicals, AGN turned its interest to high-cost power and propellant materials, primarily of military and space interest. Such compounds are typified by hydrazine, a storable rocket fuel.

---

* USAEC Contract AT(04-3)-251, Project Agreement No. 2, February-October, 1959

** Final Report: TID-5693, November, 1959.

Work by other investigators in pyrolysis, glow discharge, and alpha and beta irradiation of liquid and gaseous ammonia indicated a wide variation in hydrazine yield. It was assumed that the following reactions would take place during the fission fragment irradiation of liquid ammonia:

$$2\ NH_3 \rightarrow N_2H_4 + H_2$$

$$2\ NH_3 \rightarrow N_2 + 3H_2$$

No accurate prediction of yield could be made, but preliminary economic calculations indicated that even a modest yield might result in a hydrazine production cost 1/4 to 1/10 of the production cost by conventional methods.

The Air Force initially funded a one-year experimental program* designed to determine hydrazine yield. Briefly, the plan was to irradiate about 200 milliliters of liquid ammonia containing 5 to 10 grams of suspended UO_2 in a stirred capsule. The assembly was placed in the base of a specially designed beamport in the 2 Mw Livermore Pool Type Reactor. In this position, incident neutrons from the reactor core brought about fissioning of the suspended fuel. The resultant fission fragments then passed through the liquid ammonia bringing about reaction.

The final result[1] of these capsule experiments can be summarized by an equation based on the ammonia decomposition and product yield experienced for each 100 electron volts of fission fragment energy deposited in the liquid ammonia:

$$6.8\ NH_3 \xrightarrow[100\ ev]{F.F.} 1.7\ N_2H_4 + 1.7\ N_2 + 6.8\ H_2.$$

---

*Contract AF 33(600)-40878; ASD Project No. 7-840; March 1960-March 1961.

By definition, the number of molecules of a product formed per 100 electron volts is termed the G-value. In this case, the maximum G-hydrazine was found to be 1.7. Each atom of uranium fissioned, then, produced about 2.7 million molecules of hydrazine. In somewhat more familiar terms, this yield is equivalent to 0.034 lb of hydrazine per kwh(th) or 813 lb of hydrazine per gram of U-235 burnup. About one-half of the ammonia reacted to form hydrazine, while one-half completely decomposed to nitrogen and hydrogen.

The resulting hydrazine yields were encouraging. A preliminary plant design, based on experimental yields,was undertaken. The plant was a large one, producing about 50 million pounds a year of hydrazine, a figure several times current consumption but consistent with possible future use. Based on reasonable engineering estimates, the 1960 capital cost for such a plant would be 50 million dollars; the production cost per pound of hydrazine, depending on the amortization method used, was estimated at 25-40 cents.

With encouraging first phase results at hand, the Air Force agreed that further studies were justified; the design, fabrication, and operation of a pumped, in-reactor loop was proposed as a second phase program. In April 1961, AGN was awarded a contract to carry out this program.

1.2 Goals and Organization

Some of the more important goals of the second phase program were as follows:

1) To define hydrazine yield as a function of the two most important operating parameters, hydrazine concentration and temperature;

2) To determine the combined mechanical and radiation effects on fuel size, form, composition and rheological properties;

3) To determine erosion and corrosion effects of a suspended fuel system under reactor conditions;

4) To provide heavily contaminated raw product for purification studies;

5) To provide general experience in operating pumped, suspended fuel loops having ex-reactor components;

6) To utilize all of these experimental determinations to increase confidence in plant design and production cost prediction; and

7) To investigate the fissiochemical formation of other products of interest.

For program control purposes, the work was divided into seven project areas, each of which was further subdivided into appropriate tasks.

A scheduling chart relating project milestones was prepared. An existing management approach known as the Program Evaluation Procedures (PEP) Network was utilized for this purpose. This approach allowed the computer programming of complex, inter-relating project tasks so that the effect of the early or delayed accomplishment of specific tasks on subsequent task scheduling could be determined rapidly and completely.

The seven major projects constituting the Hydrazine Process Development Program prior to in-reactor loop operation were defined as follows:

Processing: To determine the appropriate separation operations necessary to produce anhydrous hydrazine from the radioactively contaminated fuel-ammonia-hydrazine stream.

Materials: To determine the mutual suitability of materials of construction, fuel, process chemicals, and flow control components.

In-Reactor Engineering: To provide an in-reactor test program to determine G values under dynamic conditions of flow, pressure, and temperature, the stability of various chemical materials under irradiation, attack rate on components, and the characteristics and stability of slurry fuel.

Support: To develop appropriate sampling and analytical techniques and to continue the capsule yield studies initiated during the first phase program.

Basic Studies: To determine the basic mechanism by which fission fragments produce hydrazine from ammonia so that improvements in the process could be made from a theoretical understanding rather than by empirical variations in physical parameters, and to examine the possibility of making high energy fuel oxidizers such as nitrogen-fluorine compounds by fissiochemical means.

Nuclear Engineering: To determine appropriate fluid flow and heat transfer predictive techniques and to conduct reactor analyses to project future reactor development requirements.

Plant Design: Using information generated throughout the program, to update and improve plant design and economic analysis.

1.3 Pre-Operational Research and Development

During the period prior to in-reactor loop operation (April 1961 through November 1963), all supporting equipment and techniques were perfected; the in-reactor loop and all its ancillary apparatus were designed, fabricated, tested, and placed in an appropriate irradiation facility; a deeper understanding of fissiochemical mechanisms and applications to products other than hydrazine was gained; and the extent of future developmental requirements was more accurately outlined. Accomplishments in each of these seven major program areas are summarized below; a detailed report of the activities in each area is presented in later sections of the report (as indicated in the summary).

1.3.1 Processing (Section 2)

The primary goal of Processing Project activities was the development of equipment for the separation of pure decontaminated hydrazine from the dilute radioactive solution produced by fissiochemical irradiation. Concurrent long range studies aimed at building a technological foundation necessary for chemical processing in a self-critical pilot plant.

1.3.1.1 Processing Concepts

The original design concept for the in-reactor experiment envisioned a fully integrated apparatus including in-line separation and at least partial purification of product. This concept was altered after the selection of the MTR as the experimental site when space limitations and safety considerations required that the production and processing functions be separated. During this period the boundary conditions which established the design basis for the processing equipment were closely examined. These included the effect of various operating conditions upon gas production, ammonia use, fuel loss, and fission gas release rate. Gas production rate, in particular, set stringent equipment requirements; failure to disengage and remove gas promptly and efficiently from a circulating slurry could lead to a rapid and, perhaps, dangerous pressure rise or to pump failure.

1.3.1.2 Gas Separation

Gas separation developmental tests, as well as most other equipment testing and development activities described in this report, were conducted in a specially constructed 40 ft by 50 ft Butler building. The building was well equipped for safe and convenient testing and support of a variety of test systems. For example, each test system using ammonia was contained within a ventilated vapor cubicle which was kept under negative pressure and ventilated to an exhaust and scrubbing system.

The predicted radiolytic gas production rate at 15 kw loop fission power was 0.5 scfm. A literature and patent search revealed no information applicable to disengaging gas in this quantity from liquid in small equipment. The characteristics desired in the gas disengager included clean separation of gas and liquid, a minimum volume, a minimum slurry holdup or dropout, and a stable and measurable liquid level.

The earliest tests were performed with a water-air system and investigated two approaches: the formation of a thin liquid film from which bubbles would dissipate easily through a gas-liquid interface, and liquid centrifugation to force bubbles and liquid apart by density difference. Ultrasonic energy was tested as a means of coalescing bubbles to improve separation. While the first approach was successful in performing its prime function of gas disengagement, it was abandoned when no simple means could be devised to prevent fuel accumulation nor could the liquid-gas interface be detected instrumentally with sufficient accuracy to permit control of the operation. Subsequent effort was confined to the development of a cyclonic type gas disengager.

Numerous gas disengager models, varying in dimension and geometry, were tested, using ammonia, before an efficient device could be designed to fit within the restricted space available in the beamport plug. All models tested were basically similar in design: the feed containing the dispersed gas entered a vertical cylinder tangentially which gave a cyclonic effect thrusting the gas voids to the center and up out of the liquid. The down-flow rate in the unit was low enough so that the gas bubbles could rise and leave the liquid. The straightening vane was situated at the bottom of the unit to prevent the formation of a vortex which could carry gas voids into the exit stream. The bottom was conical to preclude fuel particle deposition in the base of the unit. The final recommended design called for a 4 - in. diameter cylindrical vessel providing a capability for at least a 2 -in. variation in liquid level and with liquid level instrumentation installed in a sidearm such that the cylindrical walls of the disengager above the vortex breaker would be smooth and uninterrupted.

1.3.1.3 Fuel Separation

Projected fissiochemical plant design as well as the original concept of the in-reactor loop envisioned in-line solids separation. Of the techniques considered, filtration, centrifugation, and evaporation all tend to compact the fuel into a cake; hydroclones ideally separate a slurry into an essentially solids-free supernate and a concentrated slurry stream which can be easily diluted with fresh feed and returned to the irradiation section.

Hydroclone tests began early in the program when ammonia handling facilities were not yet available; hence this early work was performed with aqueous slurries. A major effort was applied to reproducing some of the more pertinent tests performed by others and in developing techniques for sampling and analysis. By the time ammonia handling facilities were available, the hydroclone requirement had been eliminated from the in-reactor loop at the MTR and hydroclone tests were discontinued. It had become apparent by this time, however, that the development of an efficient solids separation system while feasible, would require more (and higher level) effort than could be expended appropriately at this time.

1.3.1.4 Separation of Hydrazine from Ammonia

While the reference method of separating hydrazine and ammonia was by evaporation, more economical methods might result if hydrazine could be removed from the crude product fluid without the necessity of vaporizing the bulk of the ammonia. Preliminary examination was made of four such methods: liquid-liquid extraction, hydrazination of an insoluble salt, hydrazination by replacement in an insoluble coordinated salt, and the molecular sieve retention of hydrazine. While each of these proposed methods suffers from its own deficiencies, none can be cursorily dismissed and all would be worthy of more detailed investigation in a future program.

The development of vapor-liquid equilibrium relationships from previously reported data served as a guide to the designs of an evaporator and a distillation column. The evaporator was an essentially simple device used primarily to develop instrument and control techniques. The packed column distillation apparatus was designed to separate 50 cc/min of a 2.7 mol% (5.0 wt%) hydrazine in ammonia mixture into a 99.9 mol% hydrazine overhead stream and a 7.8 mol% hydrazine bottoms stream. Only 1.5 theoretical plates are necessary for such a separation whereas the 18 inch height of Cannon protruded packing in the column was predicted to be equivalent to 4.4 plates. Extensive testing showed the distillation to operate smoothly on automatic control. The information and experience gained during this experimental work was to have formed the basis for continuous separation of hydrazine and ammonia as part of the in-reactor test apparatus.

While this requirement was later replaced by a batch separation requirement, the knowledge gained remained valid as a basis for design of the reference experimental apparatus.

1.3.1.5 Decontamination

A slurry reactor producing fissiochemical products will contain solid, liquid, and gaseous phases; the distribution of fission products among these three phases must be known in order to design effective product decontamination processes. The opportunity to study highly radioactive materials prior to the in-reactor loop test was presented when three slurry samples were irradiated at Battelle Memorial Institute reactor to fuel burnups as high as 0.03%. While the prime purpose of these irradiations was to determine fuel effects, they also served as a source of samples for fission fragment distribution studies. Careful analysis of the samples using both spectrometric and radiochemical techniques indicated a strongly preferential distribution; the liquid phase contained essentially all of the iodine-131 and approximately half of the ruthenium-103 in solution. All of the barium-lanthanum-140, zirconium-niobium-95, strontium-90, cerium-144, and cesium-137, and the remaining ruthenium-103 were with the UO_2 solids. Iodine and ruthenium together accounted for 20% of the total fission product activity after one day of decay (equivalent to 3% after one year). Xenon-131 and xenon-133 were the only radioisotopes found in the gas; no trace of iodine nor radioactive daughter products of rare gases were present in the gas phase.

Based on the above determinations it appeared likely that distillation alone could lead to almost complete product decontamination. An ammonia-hydrazine solution spiked with the radioactivity resulting from a capsule irradiation was separated in the distillation column described above. Resultant decontamination factors (based on the feed activity) were about 2000 for the ammonia distillate and about 200,000 for the hydrazine distillate. Less than 2% of the residual radioactivity was found in the distillation column packing, the remainder was in the still from which it could be rinsed with reasonable ease.

Several ion exchange resins and absorbers were selected as candidate materials to remove the relatively slight residual activity of the distilled hydrazine. One of these, Dowex AG 1X resin (Cl^-), showed significant promise when used as a packed bed column 5 cm long. Decontamination factors as high as 365 were observed.

1.3.1.6 Processing Test Apparatus for the In-Reactor Experiment

The experience gained in the separation and decontamination development studies described above led to the design and construction of a skid-mounted device for the processing of five-liter batches of loop product. The apparatus was designed to perform a 3-step processing sequence: the first step was a continuous distillation in which the ammonia and volatile fission products were vented while hydrazine plus nonvolatile fission products collected in the reboiler. During the second step, hydrazine was evaporated from the nonvolatile fission products into a product receiver; as a third step, the final clean-up of distilled hydrazine could be accomplished by passing it through experimental beds of absorbers and ion exchange materials. The apparatus was installed in the Idaho Chemical Processing Plant Hot Cell and thoroughly tested in preparation for use with radioactive loop product.

1.3.1.7 Chemical Changes in a Fissiochemical Hydrazine Production System

Two fissiochemical production systems models were briefly considered to outline some of the effects of long-term slurry reactor operation. Each model assumed an enclosed liquid ammonia - UO_2 slurry system from which hydrazine, radiolytic gases, and volatile fission products were withdrawn. Fuel and ammonia were added consistent with criticality and inventory requirements. The models differed in that no fuel reprocessing was assumed in the first model while a constant removal of non-volatile radioactive contaminants was assumed in the second. The changes in concentration of U-235, U-238, U-236, UO_2, total solids, fission products, and water were calculated as functions of operating time. Such information aids in establishing the controlling parameter for fuel processing. The controlling parameter might, for example, be an upper limit on fission product concentration. The consequences of such a choice may be far reaching and not obvious upon cursory inspection. For example, if a fission product concentration limit of 1.1 wt % is assumed, the consequence is that the entire fuel inventory must be reprocessed for fission product removal every 500 hours; if fuel loss during reprocessing is as much as 1%, hydrazine production costs would increase 2¢ per pound.

1.3.2 Materials (Section 3)

The initial experimental efforts of this group involved the determination of the mutual suitability of materials of construction, fuel, and process chemicals for use in the in-reactor loop. The culmination of this effort was the testing of all major loop components interconnected in their reference geometry.

1.3.2.1 Erosion

Specifications for the materials of construction for the hydrazine in-reactor test loop required that they be able to withstand the inter-related erosion/corrosion action of an ammonia-urania-hydrazine slurry. Dynamic tests were performed on candidate materials in a toroid rotator, a device successfully used in a similar test program at Oak Ridge National Laboratory. This convenient and economical device allows the exposure of test coupons to temperatures of up to 220°F, pressures up to 2000 psia, and slurry flow velocities up to 45 ft/sec yet does not require a pump and uses only a small amount (20-25 millileters) of test solution. Selected materials (e.g., stainless steels) when exposed to reference loop conditions showed erosion rates considerably less than 1 mil/yr. Direct experimental erosion rate comparisons with conditions previously tested at ORNL indicated that the hydrazine loop erosion should be at least an order of magnitude lower than that experienced in the Oak Ridge thoria-water slurry loop. This later loop had run successfully in-pile for over 3000 hours; thus it could be concluded that erosion rates in the hydrazine in-reactor slurry loop should not be a serious problem.

1.3.2.2 Hydrazine Decomposition

While it is known that hydrazine is easily decomposed by many materials (e.g., copper, molybdenum) at moderate temperatures, little was known about the decomposition of hydrazine in hydrazine-ammonia mixtures. The toroid assembly was adapted for use in determining such decomposition rates. None of the structural materials tested caused any appreciable decomposition of hydrazine; apparently the ammonia present inhibits reactions. Certain high surface powdered materials (e.g., UO_2, copper, Fe_2O_3), on the other hand, did initiate hydrazine decomposition. Since UO_2 was to be the reference fuel for the loop, it was of interest to determine the quantitative significance of the decomposition rate noted. Under the conditions assumed for a hydrazine production plant, the UO_2-induced decomposition would lead to a production loss of less than 1%.

1.3.2.3 Fuel Preparation

The stability of particulate UO_2 in both air and ammonia, its ready availability in a wide range of particle sizes, and its well developed technology led to its selection as the reference fuel for the loop experiment. Since the normally available low-fired uranium dioxide powder is relatively soft, high firing techniques were developed to reduce its resistance to degradation. The fuel pretreated for use in the loop was 93% enriched UO_2 particles ranging in diameter from 0.7 to 1.0 microns. The material was fired at 1300°C (just below its clinkering point) in dry hydrogen, cooled, crushed and screened.

Under subcontract to AGN, W. R. Grace & Co. conducted a preliminary investigation of another fuel form, a uranium dioxide sol. The availability of a stable sol might overcome some of the difficulties inherent in handling a slurry of UO_2 powder (particle settling, slurry caking, etc.) While Grace was not successful in preparing a truly stable urania-ammonia sol, their partial success indicates that the difficulties encountered could be overcome if the material is of sufficient interest. Since these efforts were less in direct support of the in-reactor experiment than in support of possible future phases of operation, the work was terminated.

1.3.2.4 Effect of Irradiation on Suspended Fuel

Previous investigations of the effect of irradiations upon water-urania suspensions (conducted by the Dutch and English) indicated the formation of significant quantities of colloidal material at relatively low fuel burnups. The unexpected appearance of such an effect during the hydrazine in-reactor loop experiment would lead to severe operational difficulty and perhaps the termination of the experiment. Since the results of the water slurry investigation could not be extrapolated to an ammonia slurry, it was deemed necessary to remove or at least reduce the uncertainties of fuel behavior by conducting capsule experiments prior to loop operations. Four capsules were prepared, each loaded with 1/2 gram of fully enriched UO_2 in 200 cc of liquid ammonia; suspension of the particulate fuel was maintained by ultrasonic vibrations. Three of the capsules were irradiated to 0.01, 0.022, and 0.056% fuel burnup in the Battelle Memorial Institute reactor; the fourth capsule was maintained as a control. Alteration of fuel properties with irradiation was surprisingly small; even after the highest burnup experienced, relatively few fines were present and no colloidal material was apparent. That some reduction in particle size did occur was indicated by the change in surface area from 0.6 meters^2/gram for the unirradiated material to 2.0 meters^2/gram for the highest burnup case. While irradiation did not significantly change the shape of most of the solids, a few of the particles showed definite crystal formation and several quite perfect single crystals were found. This crystal growth was somewhat unexpected but can be described as growth from a low supersaturation solution dependent upon a step defect in a low index face, a phenomenon which has been demonstrated for many types of crystals.

The results indicated no reason to doubt that particulate fuel would be a satisfactory fuel for the in-reactor loop test. The effect of crystal growth, if it should occur in a pumped loop, would be unpredictable however, and could conceivably result in fuel growth on the loop walls or the cementing of individual particles into large fuel agglomerates.

1.3.2.5 Component Testing Program

Because of the complexity of the in-reactor loop and the reliability assurance deemed necessary, a component test loop was constructed and operated. The test loop was arranged to closely resemble the geometry of the in-reactor loop so that the major components (main circulating pump, backflush filter, test section, gas disengager, and instrumentation) could be thoroughly tested under reference conditions. Temperature and fuel loading were varied throughout the test so that all anticipated slurry densities were included. The interdependency of pump power input, input power frequency, pressure head, and flow rate was determined for all conditions tested. Filter behavior, including pressure drop, was thoroughly investigated. The efficiency of the gas disengager at various disengager liquid levels was determined at gas injection rates considerably above those expected in an in-reactor loop.

At the conclusion of the test, a careful inventory was made of fuel so as to determine the extent of fuel laydown and trapping. No significant plateout of fuel was noted in the test section during the almost 600 hours of test loop operation. At times, loop flow was stopped, the fuel allowed to settle, and loop flow reinitiated; no difficulty was experienced in resuspending the fuel.

All in-reactor components operated throughout the testing program without malfunction. Post-operation inspection of the pump showed only minor changes in bearing and journal dimensions of the order expected during initial run-in periods.

1.3.3 In-Reactor Engineering (Section 4)

The major goal of the hydrazine process development program was the design, fabrication and operation of apparatus allowing the high flux neutron irradiation of a fissile-ammonia slurry to bring about the continuous fissiochemical production of hydrazine. While many ancillary activities were necessary, all were in direct or indirect support of this first engineering demonstration of a unique process. The insertion of the loop into the beamport of the Materials Testing Reactor in Idaho and the placement and testing of supporting equipment culminated a lengthy involved developmental effort and preceeded the relatively short but highly informative and significant in-reactor operational period.

1.3.3.1 Initial Design Concept

The development of initial loop design was influenced, to a large degree, by two earlier experimental programs. One of these, the fissiochemical capsule study at AGN demonstrated the technical possibility of producing hydrazine from liquid ammonia by utilizing the recoil energy of fission fragments under controlled conditions. The second was the Oak Ridge National Laboratory Homogeneous Reactor Program which involved design, construction and operation of an in-reactor slurry loop (in support of power reactor development) and provided significant practical experience in the techniques of handling slurries.

Three general loop concepts were considered: the large conventional loop, wherein the main components are located some distance from the reactor; the dynamic capsule concept, wherein all the loop components are contained in a small package close-coupled to the reactor core; and the beamport concept wherein the main components are housed inside or close to the biological shield of the reactor yet are reasonably accessible for purposes of control, sampling, etc. The last named concept was chosen partly because of the type of irradiation facilities available and partly because it allowed a significant engineering advance, at relatively moderate cost, over the work previously accomplished.

The initial loop concept was established prior to final irradiation facility selection and before any significant component development work had been accomplished. Thus, this concept was expected to guide facility selection and developmental planning, as well as to point out potential operational difficulties. Under this initial concept, a 5 gpm slurry flow would pass adjacent to a reactor core at controllable temperatures ranging from 125^{o}F to 220^{o}F and pressures from 500 to 1000 psia. Continuous separation of fuel-free liquid would take place in hydroclones, providing a feed stream for a processing section whose effluent would be partially decontaminated and concentrated hydrazine. The radiolytic gas produced would pass through charcoal absorbers for xenon and krypton removal prior to atmospheric discharge. Complex interlocking instrumentation circuitry was planned to allow close automatic control of all loop conditions and to allow rapid response to the onset of any potentially hazardous condition.

1.3.3.2 Selection of Irradiation Facility

It was originally proposed to the Air Force that the AGN-6 experiment be installed in the Georgia Nuclear Aircraft Laboratory Radiation Effects Reactor at Dawsonville, Georgia. Shortly after contact was established with the Lockheed operators, this facility was shut down and hence was unavailable. A lengthy and often frustrating series of contacts and negotiations with the operators of commercial and Government reactor facilities ensued. More than a year passed before final approval was received, allowing the use of the Materials Testing Reactor in Idaho, an AEC owned and Phillips Petroleum Co. operated facility. Highlights of this period included instances of large upward revisions of cost estimates between preliminary and final bids from potential facility operators and the decision by another reactor operator to shut down his facility just prior to negotiation of a final facility use contract.

1.3.3.3 Design Support Activities

During and subsequent to the period of initial design and facility selection, the gathering of support information necessary to the final design of experimental equipment continued.

In the early months of the program a series of meetings was held with personnel from the ORNL who had worked on the HRE Program to insure that the Hydrazine Program would have the full benefit of their experience gained in a similar slurry loop project. Extremely valuable general and specific recommendations resulted. Their extensive experience with slurry pump and bearing design was perhaps of most immediate value allowing the project to almost completely bypass pump development activities per se, and to procure essentially off-the-shelf equipment.

In view of the many unique features of this program, it was considered necessary to conduct a thorough component testing operation at AGN; complete testing programs were considered especially necessary for the main slurry circulator and the filter unit. The detailed requirements for such a test program were established and its conduct assigned to the Materials Project.

After the test facility had finally been established, an experiment was designed to determine the neutron flux profile in the assigned beamport. The flux measuring element was basically a mechanical and nuclear mockup of the anticipated test section. The ammonia-urania slurry was simulated with polyethylene pellets containing a dispersion of UO_2 particles. Cobalt wires and shielded and unshielded cobalt foils were appropriately placed to allow accurate determination of the total flux and the thermal neutron flux. The flux measuring experiment was inserted in the HT-2 beamport at the MTR on 1 November 1962 and was irradiated for 30 minutes at a low, known reactor power. The peak thermal flux was found to be 8.8×10^{13} n/cm^2-sec in the upper fuel tube and 8.3×10^{13} n/cm^2 sec in the lower tube extrapolated to full MTR power. The averaged flux over the fueled section was used to calculate the fuel loading necessary to obtain the desired fission power levels in the in-reactor loop.

1.3.3.4 Evolution of Final Design Concept

The initial design concept described above was based on prior experience, some general assumptions, and a desire for maximum operational flexibility. The final, firm design was dependent upon the results of initial out-of-reactor testing, the particular restrictions of the irradiation facilities selected, and information gained through other design support activities. From the beginning of the program until the final design was established, the over-all design concept was in a continuous state of revision as new information became available.

The first major change, required by space restrictions at the Westinghouse Test Reactor (the then current facility choice), separated the slurry system components into two physical units, the beamport plug and an outside equipment cubicle. Two main circulators were placed in parallel to allow backup in case of pump failure; the hydroclone fuel removal capability was replaced by a filter approach due to difficulties experienced in initial hydroclone testing; all support equipment was to be located in a shielded and an unshielded cubicle located immediately adjacent to the beamport. An in-line product processing capability was retained in this revised concept.

The next series of modifications took place after selection of the MTR facility. These involved, sequentially: adaptation of the system designed for the WTR to the MTR; the removal of various auxiliary equipment from the reactor floor to a position outside the main MTR building; the design of a separate demineralized water system; a completely revised design for in-reactor cooling; a totally revised concept of gas disposal whereby the off-gas stream was passed through a sophisticated catalytic system for hydrogen removal followed by long term underground storage to allow activity decay prior to atmospheric venting; and, finally, the elimination of the external shielded cubicle and the placement of all slurry handling components within the beamport plug. This last modification required the elimination of the standby circulator capability; however, sufficient spare parts were retained so that an entire replacement beamport plug could have been built if a major failure in the original beamport plug so required.

1.3.3.5 Final Design

The size, shape and location of the various pieces of hardware associated with the AGN-6 experiment were determined to a large extent by the facilities and equipment already existing at the test facility. The MTR is a thermal neutron reactor using enriched uranium as fuel, ordinary water as moderator-coolant, and beryllium as the primary reflector. One of the 17 large experiment holes leading from the reactor face to either the tank or active lattice is the "horizontal through-hole" facility which runs entirely through the reactor in a horizontal north-south direction. The south half of this facility, known as HT-2, is the location of the AGN-6 slurry loop. The hole is 4.75 in. square through most of its length but enlarges in several steps near its outer end to a horizontal cylinder about 2 ft in diameter and 4 ft long. This enlargement terminates in an equipment cubicle 6-1/2 ft square and recessed about 3 ft into the biological shield. The beamport plug containing the slurry handling components, together with necessary shielding, was designed to fit within this described space. A limited amount of equipment can be placed on the reactor floor adjacent to the beamport. Access to hot and cold drains, exhaust lines, and utilities is provided in the immediate area. Space for the control console was available on the reactor floor somewhat removed from the beamport location. An existing separate enclosure, Building 651, or the Annex Building outside the main reactor building was available to house supporting equipment. Two large unused underground tanks were available for temporary storage of fission gases prior to decay and atmospheric venting.

The four basic operational criteria of the in-reactor experimental system were as follows: pressure 1000 psia; temperature 125 to 220°F; flow rate 3 to 7 gpm; and fission power 0 to 15 kw. Safety criteria were set such that total fuel inventory could at no time be equal to a theoretical critical mass, all lines and equipment containing radioactive fluid would be doubly contained, and all contact dose rates and activity releases would be within facility allowances.

The over-all AGN-6 in-reactor loop experiment, as finally designed, was a highly complex system with many interconnected components located in four general areas at the MTR site. The Main Console

Area on the floor of the MTR building contained all major readout and control instrumentation. The Beamport Area in and near the HT-2 cubicle was the location for the experimental beamport plug proper and its associated components: the valve box, liquid sample station, product removal vessel, fuel induction apparatus, and associated shielding. The Annex Building, just east of the MTR building, housed the demineralized water system module, the gas sample station, and utility supply and control systems. The Equipment Pit Area, underground near the Annex Building, contained the ammonia supply and removal system module and the hydrogen removal system module.

The experimental beamport plug contained the entire slurry circulating system. The circulator pumped slurry through the in-line filter to the U-tube test section adjacent to the reactor core. Here, the fissiochemical reaction took place, producing hydrazine, hydrogen and nitrogen. From the test section the slurry flowed through the gas disengager and returned to the circulating pump.

The off-gases separated in the gas disengager were routed out of the beamport plug to the ammonia removal system where most of the contained ammonia vapor was condensed for return to the reaction system. The remaining gases passed through the gas sampling station to the hydrogen removal system where steam and oxygen were added prior to catalytic hydrogen combustion. After water condensation the residual gases (nitrogen and fission gases) were sent to underground holdup tanks for one month storage before exhaust to the atmosphere.

As the slurry flowed through the in-line filter in the beamport plug, a portion of the liquid was withdrawn as a clear stream through the porous filter element. About half of this fuel-free liquid was fed directly to the motor end of the slurry circulator to provide bearing back flush; the remainder was routed through a delay coil to the liquid sample station where large (5 liter) or small (1 milliliter) samples could be taken in shielded containers.

Each of the units, modules, and items of supporting equipment is a complex highly instrumented device carefully matched to the over-all system. The design, function, operation, and relationship to the over-all system of each is thoroughly discussed in the body of the report.

An over-all view of the system as installed is presented in the frontispiece of this report.

1.3.3.6 Hazards Evaluation

A detailed hazards report, discussing in depth those aspects of the experiment relating to safety and operation, was submitted to the MTR Safeguards Committee for review and approval. Committee approval, received 4 December 1963, was prerequisite to in-reactor experimental operation.

The system was designed such that automatic power reductions of the MTR were initiated by a loop alarm system if preset limits were exceeded in slurry tube temperature, slurry system gas pressure, cubicle radiation level, cooling water radiation level, or hydrogen concentration leaving the removal system. Depending upon the severity and potential danger of the signalled condition, the automatic reactor response could be a scram, junior scram, reverse, fast setback, or slow setback.

Maximum credible accident situations were examined to assure that none could lead to personnel injury, facility damage, or significant area contamination. The most severe such case would be the simultaneous failure of a slurry circulator and coolant water flow. Such a situation would result in the complete vaporization of the liquid ammonia in the test section and subsequent pressure rise within 2.2 sec after cessation of flow. The probability of a severe pressure transient was small; automatic pressure relief would prevent damage to the loop and facility.

Component testing had revealed no tendency for the UO_2 fuel particles to settle from the flowing slurry stream providing minimum transport velocity was exceeded. However, only limited confidence could be placed in these observations since the work of other investigators had indicated that the behavior of irradiated slurries is not totally predictable. Thus, as part of the Hazards Report, the consequences of slurry settling were investigated. It was found that, while such a condition would cause a sharp rise in slurry tube temperature, there was no possibility of burn-through and subsequent activity release.

1.3.3.7 Fabrication and Installation

All modules and subsystems were fabricated, assembled and inspected in the AGN shops. Pressure tests were conducted at 1.5 times design pressure and a functional checkout of individual subsystems was conducted covering as much as possible of the moving parts and instrumentation.

The installation of the experimental equipment within the MTR building proper was done by the reactor operator, Phillips Petroleum Co.; all external installation, including the equipment in the annex building and pits, was completed by an outside contractor, H. J. Ferguson Co.

The extensive pre-operational testing, operator training program, and the operational experience and results are discussed in Section 9.

1.3.4 Support (Section 5)

The prime purpose of the Support project was to provide ancillary information, data, and technology for the successful design and operation of an in-reactor loop. The various areas of effort included: 1) chemical analyses for N_2, H_2, N_2H_4, NH_3, corrosion products, and uranium; 2) fission product analyses for determination of total fissions, fission rate, or distribution of fission products; 3) theoretical evaluation of the efficiency of fission fragment emission by fuel bodies, including fission fragment ranges and energy dissipation rates; 4) measurement of the size distribution of powder fuels; 5) delineation of hydrazine G values and the effect of variables such as temperature, pressure, hydrazine concentration, and additives; and 6) the practical application of methods of chemical analysis, energy analysis, handling and operating requirements, etc., to the design and operation of the in-reactor loop.

1.3.4.1 Analysis

The chemical analysis of hydrazine was of fundamental importance throughout the program. A previously developed colorimetric method was modified many times and finally brought to the point of about 4% accuracy at low concentration ranges (approximately 0.1 to 1.0 ppm in aqueous solutions). The procedure was time consuming and inadequate for many samples which contained 1-5% hydrazine in ammonia.

A highly accurate coulometric titration method for hydrazine was developed for samples in the 0.01-1.0 milligram N_2H_4 range. This was later modified to extend to samples containing 0.5 μ g or more N_2H_4, so that this single rapid method was ultimately used for all cold samples.

Successive titrimetric analyses for N_2H_4 and NH_3 were developed by CPP Analytical Division for application to relatively large amounts of N_2H_4 found in highly radioactive loop samples; this method had a lower limit of about 0.5 mg N_2H_4 per sample.

Several other concepts for measurement of hydrazine concentration in ammonia were considered during the program, particularly from the standpoint of developing an in-line continuous analyzer. Gas chromatographic separation and measurement proved possible for samples containing 0.2% N_2H_4 or more in NH_3 but sample vaporization problems and leaks in high pressure sampling valves made the analysis inaccurate and unreliable. Ultraviolet absorption spectra were measured for liquid NH_3 and N_2H_4, showing no useful N_2H_4 absorption bands. A test to determine the effect of N_2H_4 on the dielectric constant of ammonia proved that ionic impurities normally present in both pure materials negate the usefulness of this measurement as a method of analysis. The related property of refractive index was not investigated due to the development effort required for a high pressure, corrosion-resistant refractometer. A method of determining very small amounts of hydrazine by reacting it with O_2 to form N_2 and H_2O, and analyzing N_2 by gas chromatography, had a detectable limit of about 0.05 μ g N_2H_4; unfortunately, contamination by air was so frequent that no confidence could be placed in the analysis.

Ammonia was analyzed customarily by acid-base titrimetry, usually after samples had been reacted with an excess of standard HCl or H_2SO_4. A second technique called for neutralization of the sample with acetic acid followed by oxidation with excess standard hypobromite. In each method, N_2H_4 reacted in a manner requiring correction for its presence.

Analysis of gases for H_2 and N_2 content was easily performed by gas chromatography, but column poisoning by NH_3 interfered with the direct application of this method in many situations. Attempts were made to set up a 2-column chromatograph with column position reversing for analysis of N_2, H_2 and NH_3 in single gas samples, but the system had many critical operating limits and had to be supplanted by mass spectrographic analysis. Krypton was analyzed after gas chromatographic separation; it was a tracer added to the gas phase of many capsule experiments.

Trace amounts of O_2 in the N_2 atmosphere of capsule containers were routinely analyzed by gas chromatography. A limit of 0.1% O_2 was placed on the capsule atmosphere; concentrations tenfold less were quickly and easily determined by gas chromatography.

Uranium analysis was performed by three methods: gross amounts of uranium in fuels, etc., were analyzed by a redox titration using Ce^{IV} oxidant, according to procedures well established by ORNL, CPP and other groups; a u.v. fluorescence technique, used in a non-conventional manner to obtain relative concentrations of UO_2 powders dispersed in H_2O, ultimately provided information on relative particle size distributions of UO_2 samples; polarographic measurement of the uranium present in filtered liquid NH_3 samples was made after reaction of the sample into aqueous acid. The last method was useful for samples containing greater than 10 μ g U; it proved valuable in determining leakage of UO_2 through mechanical filters and in determining the solubility of U compounds in liquid NH_3.

X-ray spectrochemical analysis was used to determine corrosion products from stainless steel; a solution technique was developed having good accuracy for Fe and Ni in concentrations above 10 μ g/cc, and Cr in concentrations above 50 μ g/cc.

1.3.4.2 Energy Deposition Analysis

A number of methods were developed for measuring the amount of energy deposited by fission fragments in all irradiation experiments. In the simplest technique, thermal neutron flux profiles were made by activation of gold foils or wires, and flux levels were assumed constant or were corrected using a monitor foil or wire in succeeding experiments. Knowledge of the thermal flux was used with U-235 weight and irradiation time to calculate the number of fission events occurring. Assumptions were then made in calculating factors for the efficiency of emission of fission fragments by the source, energy content after emission, and probability of expending energy in the desired chemicals. Errors in measuring absolute flux levels, changes in flux profiles, self shielding and chemical poisoning effects contributed to the lack of confidence in this technique.

Greater accuracy was obtained by running a calibration experiment in which a known amount of uranium in solution was successively irradiated in the same geometry and container. Fission product isotopes could be separated and analyzed to get several checks on the number of fissions in the run. This eliminated the requirement for absolute flux measurements, since only relative flux (by gold monitor foil, e.g.) is important in comparing experiments. Also, when two or more calibrations were performed using dissolved fuel and then dust or fiber type fuel, the efficiency of fragment emission and re-entry could be measured by comparing the amount of fission fragment isotopes in and out of the fuel. Only one assumption then remained in estimating the amount of energy deposited in a chemical system: the average energy per emitted fission fragment. The latter factor could be determined by irradiating a chemical system yielding a product of known G value. Such an irradiation made with water as the chemical medium yielding H_2 as the product, indicated that one type of powdered fuel was 76% efficient in depositing fission energy to the chemical medium; calculation of the efficiency from particle size distribution, fission fragment range-energy relations, and re-entry probability gave an efficiency of 79%.

Early in the program it was realized that halogen fission products, i.e., iodine and bromine isotopes, were soluble in the liquid ammonia system. Radio-chemical separation techniques were set up and, by using a sensitive beta flow proportional counter, the shielded Br^{82} isotope could be measured.

Gamma pulse height analysis of isotopes from the many irradiation experiments was a necessity throughout the program. For this work it was necessary to calibrate a pulse height analyzer system with several known isotope standards, and set up a method of stripping isotopes from composite curves. This in turn required calculation of buildup and decay data for all major fission product isotopes. These data compilations were all performed on an IBM-7090 computer with the data output in a form for easy interpolation.

Several fission fragment species were found partially soluble in liquid ammonia (e.g., Mo-Tc and Ru-Rh), while almost all the fission product inert gases appeared in the gas phase. Stable Kr was frequently added in capsule irradiations to help carry the Kr and Xe isotopes. (Krypton also acted as a tracer for calculating the size of gas samples removed from a capsule).

Radiochemical separation procedures were used for analyzing a number of fission products in calibration experiments. A radiochemical separation of iodine was performed routinely on liquid samples until it was determined that, after sufficient decay time, I^{131} could be analyzed accurately without separation.

During the first part of the program it became apparent that representative samples of hydrazine-ammonia liquid mixtures could not be obtained by merely attaching an evacuated bomb and opening the valve. A long study of sampling methods proved that there were ways of obtaining representative samples; these methods were ultimately applied to irradiated capsules and the in-reactor loop. One of the interesting observations made at this time was the fact that soluble fission products, namely I^{131}, behaved similarly to hydrazine; that is, any fractionation of sample resulted in equal enrichment or depletion of N_2H_4 and I^{131}. This fact permitted good measurements of G values from previously obtained poor (i.e., fractionated) samples, and allowed G value estimates even when it was impossible to set up a system for obtaining representative samples.

1.3.4.3 Fission Fragment Range-Energy Relationships

The support project initially undertook the consideration of fission fragment range-energy relations from both theoretical and experimental standpoints. The Bohr Equation was solved on Fortran and fragment ranges in UO_2 and NH_3 were calculated. Other formulations for stopping were analyzed in some detail, but were considered too complex for solution on a limited program. Experimental work quickly indicated that solid state detectors and fuel sources of known thickness could be used to obtain good data on range and energy; a significant enlargement of this program was instituted under the Basic Studies Task (Section 6.0).

1.3.4.4 Particle Size Distribution

The use of powdered fuels, such as UO_2 and U_3O_8 in particle sizes of 0.1 μ and larger, was both desirable and necessary in capsule work and loop work. Since no uranium compounds appeared soluble in liquid NH_3 to any significant degree, the use of solid fuel sources was required. The short range of fission fragments in uranium compounds (approximately 6 μ) made particles of less than 1 μ diameter desirable from the standpoint of efficiency. Handling problems and availability indicated that larger size particles were to be encountered. The necessity of a good technique for measuring the size distribution of powdered uranium compounds was apparent.

First attempts at sizing were performed with the view of applying the analysis directly to suspensions of fuel in liquid ammonia. The theory of sedimentometry was analyzed to show the requirements of x-ray or gamma-ray densitometry when used to analyze: 1) the build-up of a sedimenting layer and 2) the clearing of a homogeneous suspension.

A low energy gamma source for this work was delayed for six months because of vendors fabrication problems; because of this, an unfiltered 100 kvp x-ray beam was used as a source for the development of the sizing method. (X-ray densitometry did not provide the accuracy desired for a size analyzer, however).

Because of the need to analyze many samples of fuel early in the program, a Whitby Particle Size Analyzer system was used. A great deal of effort was required to find dispersing agents and mixing techniques suitable for analyzing UO_2 by this centrifuge-sedimentation method. In order to lower the fuel concentration and eliminate particulate streaming, a technique was developed for measuring the UO_2 with a u.v. fluorometer.

Checks on size analyses were performed by electron microscopy by an outside vendor. Significant difficulty was experienced in that work, again particularly in obtaining complete dispersion of the sample.

Although no clearly adequate method of particle size analysis was developed, sufficient information was obtained to permit estimation of the source efficiency of powder fuel used in irradiation experiments, to determine the sintering temperature of finely divided fuels, and to compare size distributions with vendor specifications.

1.3.4.5 Hydrazine Yield Structure

Capsule irradiation work at LPTR started in November 1961 and terminated in June 1963; about 40 irradiations were conducted. Capsules used in the previous Air Force program were redesigned to permit circulation of reactor pool water as a coolant. The primary pressure vessel was redesigned to use improved bearings and stirring devices; solenoid operated valves in the sampling lines were replaced by hand operated valves with extension rod drive. Irradiation procedures were changed so that a capsule could be removed from the beam tube without requiring reactor shutdown. No sampling was done at LPTR; instead, the capsules were irradiated for relatively long periods (6-24 hours), allowed to decay for 100 hours or longer, and removed to AGN for analysis. Increased size and weight of the capsules required installation of an electrically operated hoist and support assembly on top of the LPTR rod drive cab.

Previously, capsule orientation (rotational) in the beam tube had to be correct so that Au monitor foils would be in reproducible positions; the necessity for orientation was eliminated by the design of a ring around the outside of the capsule to which was attached a thin (1.5 mil) Au wire.

A transport box containing a 2-inch thick lead shield was used to carry an irradiated capsule from LPTR to AGN, where a lead brick storage facility was built to accommodate both capsules.

Three calibration irradiations were performed in the LPTR capsules to provide correlation of Au monitor wire activation with total fission rate. Fuel in solution (UO_2SO_4) was compared to UO_2 powder for H_2 formation, with the powder shown to be $\sim$ 76% efficient in energy deposition. Reasonable agreement was obtained in calculating the total fissions from 1) flux, fuel loading and time, 2) H_2 formation, and 3) fission product analysis.

Most of the capsule irradiation concerned N_2H_4 formation from NH_3 at temperatures of 110-125° F with a small pressure buildup (100-300 psia) in the gas phase during irradiation. Hydrazine concentration varied from 0 to 4.5% in capsule loadings and two attempts were made to build up the N_2H_4 concentration from zero to an equilibrium point by prolonged or consecutive irradiations of a single capsule loading. General conclusions from these tests were that: 1) $G_{N_2H_4}$ value at zero concentration was slightly more than unity, perhaps 1.2 to 1.4, although individual capsule runs gave values ranging from 0.5 to 2.2, 2) G_{N_2} and G_{H_2} were approximately 2 and 6, respectively, 3) hydrazine yield decreased nearly linearly with increasing concentration, and 4) the equilibrium N_2H_4 concentration was about 3 wt %.

Various individual runs were made which indicated: 1) increase in $N_2 + H_2$ overpressure (to ~ 600 psia) may provide a slight increase in hydrazine yield, 2) reduction of the gamma ray energy deposition (in relation to fission fragment energy deposition) results in a small increase in hydrazine yield, 3) radical scavenging and addition of a hydrazine complexing agent appear slightly beneficial in increasing yield, and 4) the only soluble fuel used (uranyl quinolate) appeared to precipitate under irradiation. The effect of temperature on yields was not determined in the capsule tests; a slight increase of temperature was possible by by-passing the coolant water flow, but the high vapor pressure of ammonia did not permit tests above ~ 160° F. No cooling system could be set up to provide temperatures lower than 100° F.

The LPTR capsule tests provided samples of fissiochemically produced hydrazine for decontamination studies, and gave significant impetus to the development of good sampling techniques, chemical and energy analysis techniques, and proper handling of radioactive gases, liquids, and fuels.

1.3.4.6 Loop Analytical Equipment

Chemical and energy analysis techniques for the in-reactor loop were initially intended to determine N_2H_4 concentration, N_2 and H_2 concentration, and fission rate on a continuous basis. Facilities for taking slurry samples, batch samples of liquid and gas, bleeding off liquid product and distilling liquid product were included as parts of the sampling station. A 2-column system was designed for gas analysis by gas chromatography. Batch liquid samples were to be reacted with metered quantities of standard acid, and aliquots of the aqueous-solution taken for analysis outside the reactor area. Fission rate was to be continuously monitored by a delayed neutron monitor on the liquid sample stream and a gamma pulse height analyzer system on the gas sample stream. Layout of the equipment and shielding required for this functional sample station indicated that the physical space required was many times the space available.

Experience with gas chromatograph sampling valves indicated that leakage could be expected and frequent maintenance would be required. Design and operational analysis of a delayed neutron monitor indicated that the flow rate of the filtered liquid stream must be measured and controlled with about 1% accuracy in the range of 10-50 cc/min; flowmeters and controllers for such low flow rates are not nearly this accurate. Also, the lack of a continuous monitor for hydrazine concentration made the continuous monitoring of fission rate less important. (The delayed neutron monitor system measured Br and I isotopes, and the delay time was chosen so that Br^{87} was the major neutron contributor. Other Br and I isotopes were known to be good soluble fission monitors that could be analyzed in batch liquid samples.)

Even elimination of continuous analyzing apparatus did not reduce the sample station size sufficiently to allow installation adjacent to the beam plug. Final decisions were made to: 1) locate the gas sampling equipment in the Annex Building to take advantage of a sample stream at low pressure in a place with adequate room for equipment, 2) place the gas stream pulse height analyzer on the sample stream in the Annex building, 3) eliminate reaction of liquid samples at MTR since only non-technical personnel would be available at that site, 4) eliminate concentration of product by distillation at the MTR site, and, 5) eliminate slurry sampling. The later two decisions were dictated by safety requirements as well as by space deficiency.

When the final sampling systems were built and operated, batch liquid samples of 1.4 cc volume and gas samples of 11.9 cc could be taken at a maximum frequency of one sample per hour and a normal frequency of one sample per shift. Samples could be analyzed at CPP for N_2H_4, NH_3, N_2, H_2 and fission products I^{131}, I^{133}, Xe^{133} and Xe^{133m} on a routine basis. Liquid product could be collected and stored in 5-liter vessels, transferred to CPP, and concentrated in a hot cell operation.

1.3.5 Basic Studies (Section 6.)

While the Hydrazine Process Development Program was primarily one of engineering development, the paucity of knowledge concerning fissiochemical theory indicated the need for modest efforts in such areas. Included within the scope of the program were investigations of 1) fission fragment energy loss prior to escape from fuel elements, 2) the detailed mechanism of ammonia radiolysis, 3) the solubility of uranium compounds in liquid ammonia, and 4) the possibility of the fissiochemical production of fluorine based high energy compounds.

1.3.5.1 Fission Fragment Range and Energy Deposition (FRED) Studies

While the theoretical analysis and prediction of fission fragment energy loss within solids had proved helpful (see Section 5), the indicated uncertainties suggested initiation of an experimental program designed to determine such losses directly. The recent refinements of solid state, gold plated, silicon surface barrier detectors suggested their use for this purpose. Experimental equipment was arranged to include a fuel source, solid state detector, the necessary amplification instrumentation, and a 128 channel pulse height analyzer. When the equipment was located so that a thermal neutron flux impinged on the fuel source, the resultant fission fragments penetrated the detector giving rise to energy pulses proportional in magnitude to the energy of the detected fragment. The pulse height analyzer automatically sorted these pulses by energy and summed the pulses in each energy interval. This observed spectral data was reduced by an IBM computer code to determine the fraction(S) of all fragments born within the source which were actually intercepted by the detector, the relative average escape energy (R) of the detected fragments; and the over-all energy deposition efficiency (E) for each source.

The sources analyzed by this technique included UO_2, uranium metal, and uranium aluminum alloy plates; U_3O_8 fibers; and UO_2 powders. The measured over-all efficiencies varied from 3.2% for a 28 micron thick uranium metal plate to 85% for an 0.31 micron thick UO_2 plate.

The techniques developed in this preliminary approach to a complex problem are being refined and expanded in applicability under Atomic Energy Commission funding.

1.3.5.2 Ammonia Radiolysis Studies

The purpose of these ammonia radiolysis studies was to measure the effects of temperature and additives on the fissiochemical G values for hydrazine, nitrogen, and hydrogen under the controlled conditions which would provide information on the radiolysis mechanism. This emphasis on mechanism thus differentiated this study from the more production-oriented stirred capsule runs discussed in Section 5.5. The radiolysis studies were conducted in small Pyrex glass ampules containing 3 to 5 grams of ammonia and about 0.15 grams of U-235 as uranium-loaded glass fibers. Studies of temperature dependence indicated a rather complex variation of hydrazine yield with temperature which suggests a variation in the relative importance of competing mechanisms as temperature increases. The effect of the addition of urea and other NH_2 radical source compounds upon hydrazine yield was determined. While the gamma radiolysis of ammonia has been investigated and discussed at lengths by others, certain apparent inconsistencies and contradictions among proposed mechanisms have heretofore remained unexplained. Consideration of the fissiochemical data from the present study in conjunction with the gamma work of other investigators allowed the development of an essentially complete mechanistic picture of ammonia radiolysis.

1.3.5.3 Soluble Fuel Studies

While it was known that no simple inorganic compounds of uranium were soluble in liquid ammonia, it appeared possible that certain complex organic compounds of uranium might show reasonable solubility. Of these, uranyl 8-hydroxyquinolate was selected for extensive testing. Initial indications of the solubility of this compound were qualified by the apparent dependence of solubility upon the total quantity of quinolate present. Subsequent investigations revealed that the initial rapid dissolution of the quinolate was followed by a slow ammonolysis forming an insoluble precipitate, apparently $UO_2 (NH_2)_2$. Radiation, too, appeared to induce precipitation of the soluble fuel. The value of continued investigation in this field appeared doubtful since no truly stable soluble compound had been found and, if one were found, its radiation stability was likely to be poor; the study was terminated.

1.3.5.4 High Energy Compounds

Energy-rich compounds, especially those containing fluorine, may be of significant value as future rocket fuel oxidizers. For this reason, a modest effort aimed at the fissiochemical production of such compounds was initiated. The highly reactive nature of the feed components and expected products required the development of unique radiation and analytical equipment and techniques. Assuming a reasonable yield of a postulated product, only a few micrograms would be available for detection from a single production run; thus very stringent requirements were imposed on analysis. Twelve production runs were performed utilizing various combinations of fluorine, nitrogen, NF_3, N_2F_4, and HF as feed materials. In only one run, involving a 65% fluorine 35% nitrogen mixture, was a fissiochemical product, NF_3, unequivocally produced. This was sufficiently interesting, however, to bring about the transfer of these synthesis efforts to a special classified program (AF 04(611)-9069) for the Air Force Rocket Propulsion Laboratory. Sufficient evidence of the formation of entirely new oxidizers has since been obtained to justify the extension of the program into its second year.

1.3.6 Nuclear Engineering (Section 7)

The efforts conducted under this general classification fell into two categories: experimental activities conducted to assure that conventional engineering approaches were appropriate to the prediction of loop fluid behavior, and theoretical studies of self critical reactor parameters preliminary to future pilot plant or production plant design.

1.3.6.1 Experimental Heat Transfer

Generalized forced convection heat transfer coefficients were experimentally determined for clear ammonia and for urania-ammonia slurries to assure the proper design and safe operation of loop heat removal equipment. A heat transfer test section was constructed as an adjunct to the component test loop thus avoiding the unnecessary duplication of equipment. The test section tubing was electrically heated to duplicate expected in-reactor conditions; the test section was extensively instrumented. The results of the tests indicated that the heat transfer characteristics of ammonia and ammonia-UO_2 slurries are best expressed by a form of the Seider-Tate Equation. A slight, and not practically significant, deviation from this relationship occurred at the high fuel loading of 190 grams/liter.

1.3.6.2 Experimental Fluid Flow

Early in the Hydrazine Process Development Program, the glass mockup of a curvilinear loop test section based on the preliminary loop concept was constructed. This apparatus allowed the early initiation of pump and filter tests and pressure drop investigation, using a non-reference water-uranium dioxide slurry. Its primary value was in allowing technical personnel to gain practical experience in the field of slurry handling and behavior. After this experience had been gained and after the loop design concepts had been considerably altered, water-UO_2 slurry investigations were terminated and supervision of component testing under reference condition was transferred to the Materials group.

Friction factor measurements were carried out simultaneously with the heat transfer investigations; no change in friction factor was found when heat was added to the test section. The minimum transport velocity, that velocity below which fuel particles begin to settle from the slurry, was measured for ammonia loaded with 160 grams/liter of uranium. The minimum transport velocity was found to vary from 5.2 ft/sec at a slurry temperature of 150°F to 8.0 ft/sec at 164°F.

Fluid flow and heat transfer correlations generally assume that the fluid under consideration is Newtonian in nature; i.e., a simple linear relationship exists between the internal sheer stress and the velocity gradient. Slurries, however, will form non-Newtonian fluids if the volume fraction of solids is large enough. Such non-Newtonian behavior, if not taken into account in the design of a loop, could cause severe operational problems. Since no rheological experiments had previously been made on a UO_2-ammonia slurry, a high temperature, high pressure viscometer was built so that the true slurry properties could be assessed. The equipment was initially tested with clear ammonia; the results agreed closely with literature values. Experiments with slurry showed the expected trend toward increasing viscosity with increasing solids loading but produced no evidence of non-Newtonian behavior.

1.3.6.3 Reactor Analysis

A parametric study was conducted to determine critical size, fuel loading, flux, power distributions, and reactor kinetics for a series of spherical self-critical ammonia-UO_2 reactors of production capacity. The study covered core diameters of 2-10 ft, mean temperatures of 60-200°F, void volumes of 0-10%, and hydrazine concentrations of 0-5%. The resultant core loadings which ranged from 100 to 500 kg of U-235 were only mildly dependent on core temperature and void concentration. Temperature and void coefficients of reactivity proved to be large and negative. Of interest also in terms of operating safety was the determination that fuel concentration surges of as much as 60% would not create a hazard.

Two potential hydrazine production reactor systems were analyzed to gain preliminary insight into their practicality. The first involved system heat removal by ex-reactor flash evaporation. The concentrated slurry resulting from the flashing operation was to be pumped back into the core; the flashed vapor was to be selectively condensed to remove hydrazine after which the remaining ammonia was to be recycled to the core. The second system envisioned a pump-assisted natural circulation reactor utilizing direct core boiling; hydrazine removal was to be by partial condensation as before.

Parametric relationships, power and equipment requirements, developmental requirements, and probable advantages and disadvantages of each system were determined in these preliminary analyses.

The flashing system offers a simpler approach to maintenance of core homogeneity, but this advantage may be offset by the high pumping power requirements, erosion problems in the flashing device, and fuel inventory control problems. The direct core boiling system avoids these problems but presents a much more difficult core design.

1.3.7 Plant Design (Section 8)

In order to maintain a reasonable economic perspective on fissiochemical hydrazine production potential, the preliminary plant design and cost estimation efforts initiated in the first phase of the hydrazine program have been continued. More generalized techniques have been developed allowing a rapid and approximate estimation of the fissiochemical production costs for any chemical. Alternate production and product separation techniques were also considered.

1.3.7.1 Plant Re-evaluation

Although the flashing and in-core boiling reactor concepts (discussed in Section 7.3) show promise, the more conventional fissiochemical plant design initially presented in the first phase program Final Report still appears to be the most practical approach to a self-critical production plant from the standpoint of developmental requirements. Even with this design, however, severe developmental problems remain to be solved. The maintenance of slurry suspension and homogeneity is less easily assured than had been originally anticipated; indeed no absolute assurance can be given that the problem is solvable. Unfortunately, the behavior of pumped, fissioning slurries has proved, both in this program and others, to be unpredictable from the results of simple relatively inexpensive experiments; hence investigation of this particular problem area would require further expensive and time-consuming in-reactor loop experiments. The magnitude of such an undertaking obviously requires considerable justification. Other developmental problems of varying severity (e.g., fuel separation from the product stream, yield optimization, hydrazine decontamination) have been investigated in sufficient depth to allow reasonable confidence that they could eventually be solved.

Capsule irradiation tests performed during this program indicate that the hydrazine G value and energy deposition efficiency originally assumed for plant design purposes may have been optimistic. Re-evaluation, based on the more conservative figures, would predict a 22.1 million lb/yr hydrazine production at an estimated FOB cost of 52¢/lb from a 175 Mw(t) plant. This compares with the earlier, more optimistic, estimates of 50 million lb/yr at 25¢/lb with the same power requirement.

1.3.7.2 General Cost Estimation Method

A reasonably simple equation was developed for the rapid estimation of approximate fissiochemical production costs. While the approach was developed specifically for the hydrazine production case, it can be converted to any other chemical system with minor adjustments for system peculiarities and molecular weights. The following five sources of expenditure were considered separately and then combined into an over-all expression: fuel inventory charge, fuel burnup cost, ammonia recombination and makeup cost, operations and maintenance cost, and capital charges. The final expression relates hydrazine production cost to the hydrazine net production G value, the ammonia destruction G value, the fission fragment energy deposition efficiency, and plant size in megawatts.

1.3.7.3 Alternate Production System Concepts

It is probable that development costs could be reduced substantially if a production loop rather than a self-critical reactor concept could be considered. Such a loop could be inserted into an existing large reactor such as a Hanford plutonium producer or one of the planned water desalination reactors. From the standpoint of chemical production costs, a loop type production system appears to show economic advantage over self-critical systems in plant sizes below about 100 Mw(t), and thus would be appropriate for chemicals having a low market volume (1-10 million lb/yr). Operational and control advantages are numerous.

The two reactor concepts discussed in Section 6.3 presume the vapor phase removal of hydrazine; the material and heat balance implications of such a product removal system were investigated. While this vapor phase removal approach bypasses the difficult and costly problem of fuel removal from a liquid stream, some of the potential savings will be offset by the requirement to operate the reactor at higher temperatures where hydrazine yield is not optimum.

1.4 Experimental Operation

In-reactor loop operational experience and results, processing data, and post-operational inspection observations are presented in detail in Section 9 and are summarized below.

The AGN-6 experiment was successfully operated in-pile for 1440 hr at nominal fission power levels of 0, 0.15, 2.5, and 8.0 kilowatts between December 1963 and April 1964. During this period, 48 liquid samples and 41 gas samples were taken to measure the various products of the fissiochemical reaction. In addition, several large (5 liter) samples were taken to investigate the problems of product separation and decontamination.

The slurry loop was removed from the HT-2 beamport at the end of April and transported to the Test Area North (TAN) facility at NRTS for post-irradiation disassembly and examination; this inspection took place during the period July through November, 1964.

1.4.1 Operations History

The installation of loop equipment at the MTR began in July and was completed on 6 September 1963. Equipment checkout and shakedown operation continued through mid-November; during this period all loop systems were operated intermittently out-of-reactor with the major effort directed toward optimizing the operation of the slurry system. An intensive operator training program was conducted for 36 consecutive shifts during the period 15-26 November 1963.

The first in-reactor operation took place during MTR Cycle 201[*] starting on 2 December 1963. No fuel was circulated during this period and hence no fissiochemical reactions took place. This non-fueled operation allowed the determination of gamma-induced hydrazine yield and equilibrium concentration. Additionally, it served as a thorough operational test of all equipment under reference conditions save for the presence of contaminating fission fragments.

Just after the conclusion of the unfueled Cycle 201 on 26 December, electrical indications of main circulator difficulties were noted; shortly thereafter this pump seized and could not be restarted. The beamport plug was withdrawn from the reactor and modifications were made to prevent recurrence of the problem during fueled operations. These modifications involved both operational and equipment changes, including improved venting and cooling, and resulted in the complete elimination of pump problems throughout the remainder of the experimental program.

---

[*] An MTR cycle is three weeks in duration. The reactor is down (not operating) during the first few days of each cycle for refueling and for insertion, removal or modification of experiments.

The first fueled operation took place during Cycle 205 starting on 25 February 1964. Sufficient fuel was circulated to generate a fission power of about 150 watts. During this cycle, 16 liquid samples and 14 gas samples were taken and no major problems were encountered. Procedural changes were made to prevent recurrence of minor activity releases which were noted during sampling.

The second fueled cycle (MTR Cycle 206) started on 16 March; sufficient fuel was added such that fission power varied from 2.2 to 4.4 kw during the ensuing operational period. During the third fueled cycle (MTR Cycle 207) starting April 9, fuel addition brought the loop to its maximum power, 9 kw. At final shutdown, the loop had been operated in-reactor for 1440 hours at fission powers ranging from 0 to 9 kw.

Failure of a valve bellows at the mid-point of MTR Cycle 206, which would have been a minor maintenance problem under most experimental situations, required a major, carefully planned, repair effort because of the high radiation levels normal in the loop equipment. The secondary containment provided by the valve box operated, as planned, to confine activity release to the immediate area. The slurry pump was shut off and ammonia removed from the system on 25 March; the reactor remained in operation, however, and a fission power of approximately 3.4 kw was produced within the U-tube by residual fuel which remained after the ammonia was removed. Preparations were made for the semi-remote repair to take place at the conclusion of the cycle. During the scheduled shutdown period at the beginning of Cycle 207, the faulty valve was replaced and several of the liquid sample station valves were reworked to preclude similar problems in the future. Ammonia was reintroduced into the system, and normal loop operation resumed on 9 April. Only minor operating difficulties were encountered until 22 April when a radioactivity release in the Annex Building, probably as the result of operator error, caused loop shutdown. The major objectives of the experiment had been achieved and, since the anticipated delays incident to resuming loop operation would have delayed another experiment scheduled by PPCo for the HT-2 test hole, the decision was made to terminate the experiment. At the conclusion of the cycle (27 April), the beamport plug was removed from the reactor into its storage coffin.

After transfer to the Test Area North (TAN) site, the beamport plug was dissassembled and its components examined in the RML cell. Evidence of corrosion, erosion, wear, and fuel plateout was sought in the U-tube, pump, gas disengager and filters. Selected sections of the U-tube and filters were examined metallographically to ascertain metal microstructure and filter pore-loading; uranium content was determined chemically.

A processing test apparatus was designed based on the results of preliminary tests using simulated loop product. The fabricated equipment was installed in the Multicurie Cell of the Idaho Chemical Processing Plant (ICPP). Two five-liter loop fluid samples were processed in a 3-step procedure: distillation to remove ammonia leaving contaminated hydrazine in the still, evaporation of relatively pure hydrazine from the non-volatile radioactive contaminants, and final product clean-up using a variety of ion-exchange materials. Analysis of the various fractions allowed determination of decontamination factors.

1.4.2 Experimental Results

The non-fueled operation of the loop during MTR Cycle 201 allowed the determination of gamma-induced nitrogen, hydrogen, and hydrazine yields, ammonia destruction, and hydrazine equilibrium concentration. Radiation-induced product yields are usually expressed as G values, the number of molecules of product formed per hundred electron volts of energy deposited. In this case, the measured yields were: $G_{N_2H_4}$, 0.05; G_{N_2}, 0.50; G_{H_2}, 1.50; and G_{NH_3}, - 1.0.

During initial gamma operations, the product concentration in the loop rose to 0.039 wt % hydrazine in ammonia. When a 5 liter sample was removed from the loop, the concentration fell to 0.026 wt% and rose again gradually to about 0.04 wt %.

These gamma-induced yields and product concentrations confirmed previous capsule results and indicated that, as expected, valid data could be obtained from loop operations.

The initial fission fragment-induced hydrazine yields also bore out capsule-based predictions generally. The G_0 value, the product yield at a concentration of zero wt % hydrazine, determined from data gathered during Cycle 205 was 1.27. Hydrogen and nitrogen yields were determined by several techniques; that considered most reliable indicated a G_{H_2} of 7.0 and a G_{N_2} of 2.33.

The hydrazine equilibrium concentration to be experienced during fueled operations was expected (on the basis of capsule results) to be a strong function of the ratio of deposited fission fragment kinetic energy to deposited gamma energy. Based on this relationship, a maximum hydrazine concentration of about 1.0 weight percent was expected during the first fueled operation where the fission fragment energy deposition (150 watts) was about equal to the gamma energy deposition. The concentration rose at the expected rate, reaching 0.97 wt % after nearly three days operation. At that point, however, and contrary to all expectations, the hydrazine concentration declined steadily from this high point to about 0.15 wt % near the end of the cycle. Because of operational and equipment difficulties, sampling was not sufficiently frequent during succeeding cycles to completely delineate concentration variation. However, it was possible to observe that hydrazine concentration increased sharply after each fuel addition and then went into an almost immediate decline. Each concentration maximum was lower than its predecessor even though it represented operation at a higher fission power.

The anomalous behavior of hydrazine concentration was the subject of intensive, inductive consideration. The slurry loop operated under conditions considerably different from the laboratory conditions employed for capsule experiments. Each capsule experiment is of short duration and starts with a clean system and pure feed components; the loop, on the other hand, is, by its nature, a concentrator of impurities. These impurities could include water, spent fission fragments, corrosion products, or trace hydrocarbons from the feed ammonia. Strongly adverse effects upon hydrazine concentration of these impurities, while unexpected, could occur.

A time-or dose-dependent change in fuel behavior could also, and perhaps more probably, be the cause of hydrazine concentration decline. Calculations showed that the concentration decline was remarkably consistent with a postulated fuel plateout on the internal surfaces of the slurry loop. Such fuel plateout, if uniform throughout the entire system, would not diminish total measured fission power but would drastically reduce fission fragment energy deposition within the circulating ammonia. As progressively larger amounts of fuel plated out, an increasing fraction of fission fragment energy would be deposited uselessly within the fuel cake. For this fuel behavior to be the true explanation for hydrazine concentration decline, a plateout would have had to occur at a rate sufficient to reduce fission fragment energy deposition efficiency from 75% at the beginning of fueled operations to 0.15% at the conclusion of the experiment. Such a decline in efficiency is not at all unreasonable and would result from fuel deposits about 0.01 in. thick.

Post-irradiation examination of the loop showed that a relatively uniform layer of fuel 0.002-0.003 in. thick coated all internal surfaces, that patches of fuel greater than 0.01 in. thick were scattered throughout the U-tube, and that insignificant quantities of suspended (and hence efficient) fuel had been circulating at loop shutdown. Although impurity effects upon hydrazine formation mechanisms cannot be ruled out, it is apparent that fuel plating alone is sufficient explanation of the low concentration attained. No definitive explanation of this observed fuel plateout can be given at this time. Capsule irradiations of UO_2-ammonia slurries to similar burnup showed no such effect although evidence of crystal growth was seen. Again, impurities may have played a part, perhaps by "cementing" the particles together and to the wall. Alternatively, the crystal growth phenomenon noted in the capsule studies may have been more pronounced in the loop, leading to interlocking or fusion of particles to each other and to the wall. Detailed electron-micrographic examination of fuel samples, underway at the Oak Ridge National Laboratory, may help clarify the causes.

Post-operational loop component examination indicated no serious corrosion, erosion or wear problems except for an anticipated erosion of the U-tube tip and scattered pitting. The latter may be associated with high temperatures experienced in the fuel layer when cooling was inadvertently reduced following loop shutdown. No significant wear was experienced in the slurry pump and the sintered metal filters suffered no appreciable plugging.

The low hydrazine concentration in the loop prevented the full product processing tests initially planned. The processing equipment had been designed to separate decontaminated hydrazine from 5 liter batches of crude product containing 5wt% hydrazine. Alteration of procedures, however, including the addition of hydrazine to the low concentration loop product, allowed the meaningful determination of decontamination factors. These ranged from 2000 to greater than 24,000 depending on the isotope studied. Extrapolation of the results indicate that ammonia removal by distillation followed by a simple hydrazine evaporation would yield a product sufficiently low in activity that final purification could take place in essentially unshielded conventional equipment.

1.5 Conclusions

The AGN-6 experiment fulfilled its primary objective of circulating a UO_2-liquid ammonia slurry in-pile to produce hydrazine by a fissiochemical process. None of the many equipment problems encountered were basically deterrent to the future of fissiochemistry; all such problems could easily be resolved in a second generation loop design.

Severe slurry fuel behavior problems remain to be solved. While initially determined product yields confirmed earlier capsule investigations, the decline in hydrazine concentration with time indicated that the behavior of pumped fissioning slurries is not totally predictable from the results of simple, relatively inexpensive, experiments, a fact noted in other similar studies. Post-irradiation inspection confirmed the suspicion that essentially all fuel had plated out on internal surfaces, leading to a severe reduction in fission fragment energy deposition efficiency. While the seriousness of this finding in terms of future practical slurry system utilization is undeniable, it should be noted that its cause is still under investigation. Practical means of maintaining slurry homogeniety might well be found should fissiochemical system requirements dictate. It is likely that such an investigation would require further expensive and time consuming in-reactor loop experiments; the magnitude of such an undertaking would obviously require considerable justification.

Simple, conventional techniques were shown to be adaptable to the concentration and decontamination of fissiochemically produced hydrazine.

While detailed refinement of an over-all processing scheme was not attempted in this program, sufficient development was accomplished to indicate that no major difficulty exists in this area.

It can be stated, finally, that the loop accomplished the job required of any first approach pilot plant, i.e., the determination on a small scale of those problems which must be solved prior to large scale development. As with any experiment of this sort, many more questions were asked than were answered. Those process areas easily amenable to scaleup have been pointed out and, more important, those areas wherein serious technical problems remain to be solved have been outlined. The over-all value of the experiment will become even more apparent as fissiochemical technology is broadened in the future through the efforts of the government laboratories, private industry, and foreign groups currently at work.

1.6 Future Work

Many of the activities initiated in this program are continuing under government and joint government-private funding. Examples are: the search for new rocket fuel oxidizers, the development of new fissiochemical fuel forms, the delineation of fissiochemical mechanisms, the quantification of fission fragment energy losses within various materials, a search for candidate products of commercial interest (e.g., fertilizers), preliminary plant design activities for a variety of products, and the determination of the economic implications of the entire process.

2.0 PROCESSING

2.1 Introduction

The processing project had the immediate task of developing equipment for the processing of crude slurry product from the in-reactor experiment; a concurrent, longer range task was the building of the technological foundation necessary for chemical processing in a self-critical pilot plant. The evolution of the concepts and facilities necessary to these tasks is discussed below. Later sections describe the detailed efforts in gas separation (2.2), fuel separation (2.3), hydrazine separation (2.4), decontamination (2.5), and long range chemical changes (2.6).

2.1.1 Processing Concept

The original design concept for the in-reactor experiment involved two major sections: a fission fragment irradiation section, and a chemical processing and decontamination section. The sections could be constructed to operate as a single, integrated apparatus or as two independent units. If the combined apparatus approach was chosen, the experiment would be conducted in one location with the possibility of continuous processing and would have centralized control. If the separated approach was chosen, the experiment would be more flexible but crude radioactive product would require transportation from one apparatus to the other and product processing would be performed in batches. The former approach would provide an example of a fully integrated pilot plant, and the latter approach would result in a simpler unit at the nuclear reactor face.

During the early stages of the program, processing emphasis was directed toward developing the necessary technology to build the combined apparatus. The program was reviewed and evaluated frequently from the standpoint of the combined vs the separated apparatus.

The apparatus design was reviewed again after the MTR was finally selected as the site for the experiment and after preliminary discussions with the PPCo technical and safety engineers. Several factors mitigated against the combined apparatus concept: Space close to the reactor face was severely limited; many of the apparatus instruments would be incorporated into the reactor power reduction controls(several of these instruments were at least moderately interacting which imposed restrictions on operation, particularly on the rate of corrective changes); concentrated hydrazine, especially when radioactive, was considered by the MTR safety engineer to be undesirable in the reactor building. These factors, plus the delays in obtaining a site, dictated that chemical processing of the product be performed at a location other than the MTR and the processing section be independent of the irradiation section.

Much of the emphasis in developing processing equipment for the in-reactor experiment was underway and required redirection after the decision to separate the units was made firm.

2.1.2 Parametric Study

The initial boundary conditions established for the in-reactor experimental apparatus were examined in conjunction with the best data on fissiochemical reaction efficiencies to gain a perspective on the chemical processing problem. Graphs were prepared, and are included in this section, showing gas production, ammonia use, fuel loss, and fission gas release rates all based on various operating conditions. These parametric studies helped to establish the design basis for the processing equipment.

The original design parameters, chosen prior to final test site selection and, hence, subject to reappraisal, were:

Fission power:	0 to 15 kw
Gamma power:	25 kw
Total pressure:	500 - 1000 psia
Temperature, hot leg:	220°F maximum 160°F normal
cold leg:	100°F
Liquid in high flux:	1000 cc
Fuel form:	high-fired UO_2, 1 to 3 micron dia
Slurry concentration:	200 g/l maximum
Raw feed material:	liquid ammonia
Circulation rate:	5 gpm maximum
Processing stream composition:	1% to 3% (weight) N_2H_4 in NH_3-UO_2 slurry
Hydrazine production rate:	10 to 320 gm/hr
Processing stream flow rate:	1 gpm

The net production efficiencies used in this study were based on earlier studies:[1]

Condition	Molecular Species	G Values (molecules/100 ev)
No hydrazine present	N_2H_4	2
	N_2	2
	H_2	8
At equilibrium hydrazine concentration	N_2H_4	0
	N_2	4
	H_2	12

Gas is produced as a side reaction in the fissiochemical production of hydrazine. Removal or disengagement of this gas from the process liquid must be accomplished at a rate equal to the gas production rate in order to maintain a constant system pressure. Figure 2.1 shows the required gas disengagement rate at start-up and at equilibrium hydrazine concentration as a function of fission power level. The temperature at the disengager was taken as 100°F and ammonia vapor in the disengaged gas was assumed to be in equilibrium with the liquid at this temperature. Operational failure of the gas disengager without corrective action would result in a rate of pressure increase proportional to fission power. Figure 2.2 shows the maximum rate of pressure rise in a loop thus confined. Available vapor space volume is shown as a parameter. The time required for the pressure in the system to double is also shown in Figure 2.2; only a few minutes would be available for stopping the experiment in the event of disengager failure.

The rate at which ammonia is lost from the system (and, therefore, the required makeup rate) is established by the rate at which ammonia is destroyed to produce gas, the temperature at which this gas is disengaged, and the removal rate through the product stream. Figure 2.3 shows the calculated ammonia use rate due to fissio-chemical destruction plus gas disengager loss as a function of the loop power level. When a product stream is removed from the loop system for hydrazine recovery, ammonia will be lost at a rate depending on the hydrazine concentration and flow rate of

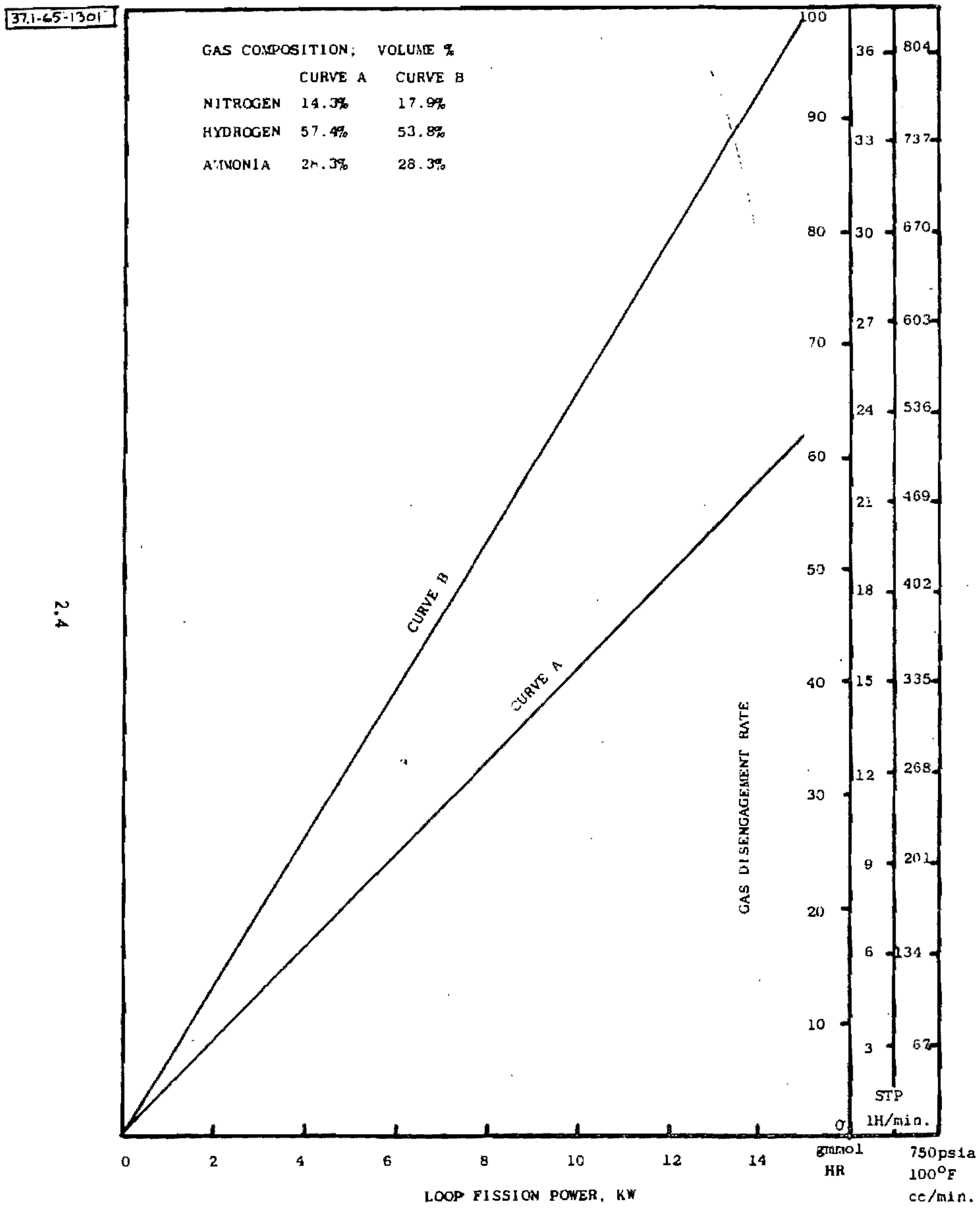

FIGURE 2.1 GAS DISENGAGEMENT RATE AT 100°F

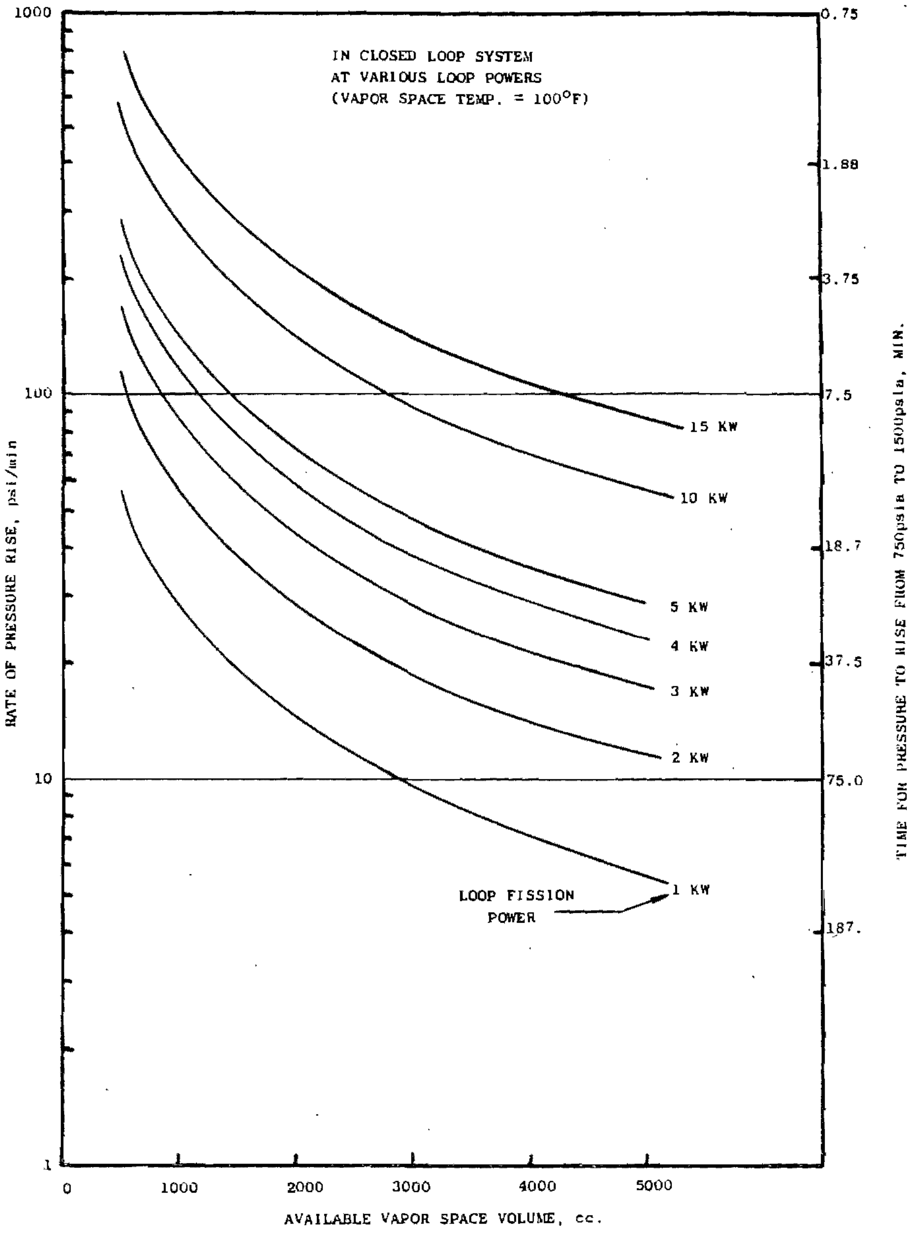

FIGURE 2.2 PRESSURE BUILD-UP RATE

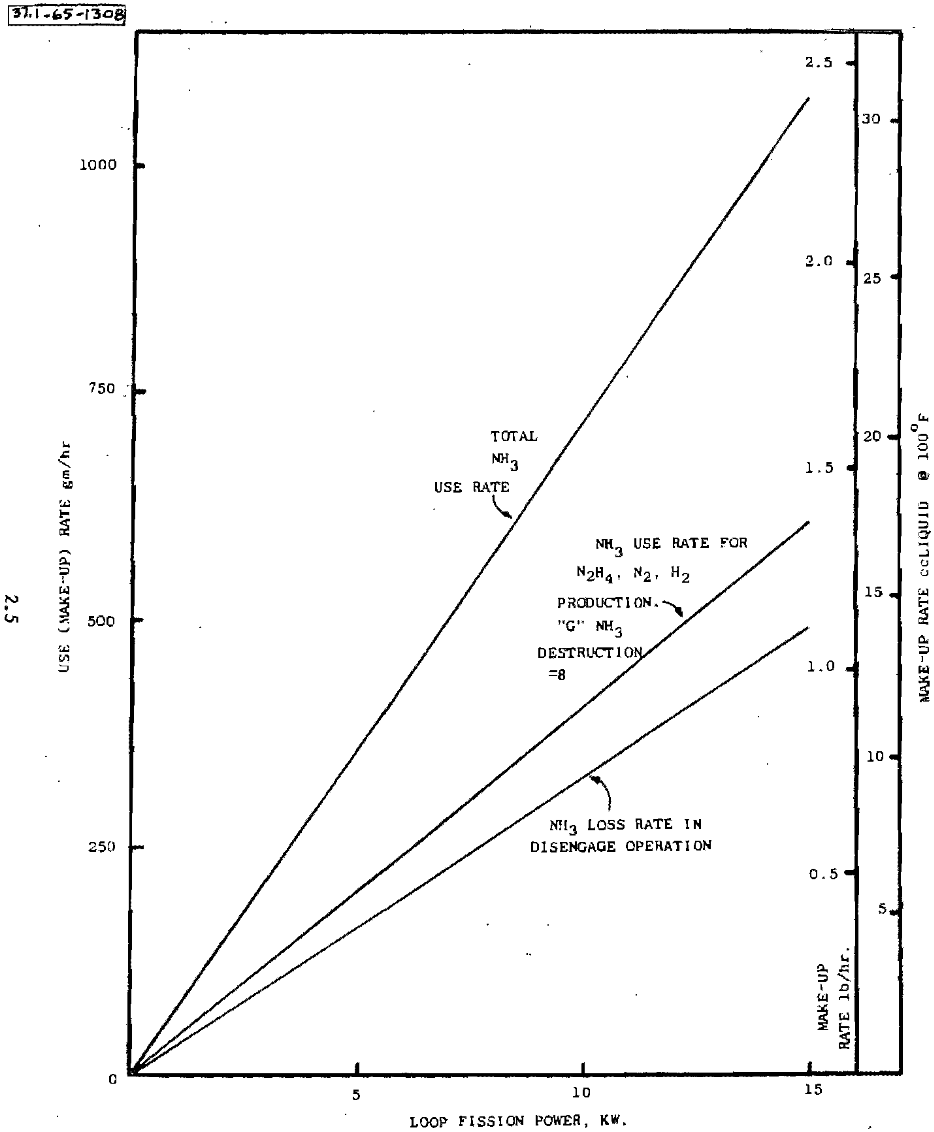

FIGURE 2.3 AMMONIA USE RATE VERSUS POWER, EQUILIBRIUM OPERATION

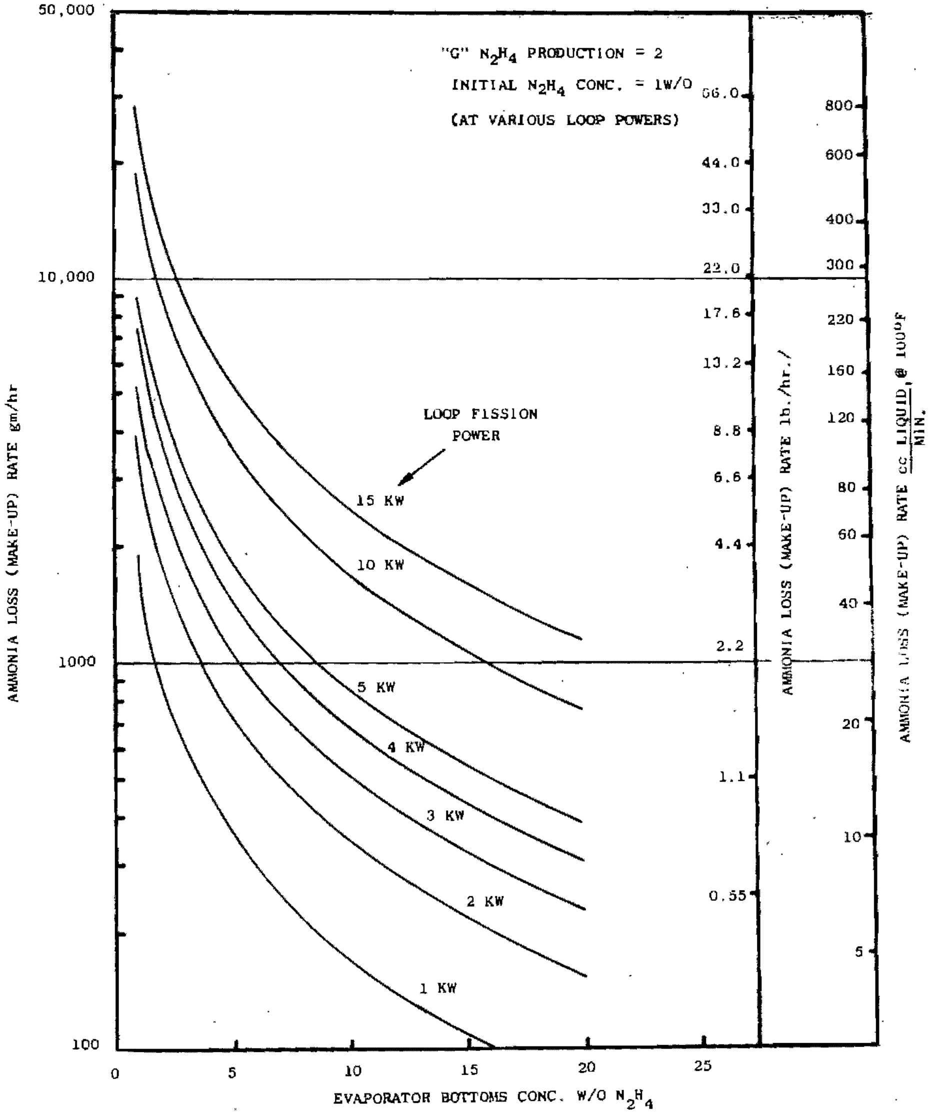

FIGURE 2.4 AMMONIA LOSS RATE FROM CONCENTRATED EVAPORATOR BOTTOMS

that product stream. Figure 2.4 shows the ammonia loss rate in the evaporator bottoms as a function of the bottoms concentration. In preparing Figure 2.4, it was assumed that (1) all evaporated ammonia was condensed and returned to the loop; (2) the base loop hydrazine concentration was 1% by weight, and (3) the net hydrazine production G-value was 2. The total ammonia use rate (ammonia destroyed, ammonia lost in gas disengagement, and ammonia in evaporator bottoms) is shown in Figure 2.5; it is significant that the bottoms loss rate has the greatest influence on the total loss rate, except at high bottoms hydrazine concentrations.

The UO_2 fuel will be lost from the reaction section through the one gallon per minute process stream at a rate dependent upon the efficiency of the fuel separator; in this case, the fuel separator is assumed to be a hydroclone. Figure 2.6 shows the UO_2 fuel loss rate during product removal as a function of the hydroclone over-all efficiencies, for various loop powers. In preparing this figure, it was assumed that all of the UO_2 passing through the hydroclones is lost from the system in the evaporator bottoms. The large fuel loss rates, even at high separation efficiencies, show clearly the need for a fuel makeup system to maintain reaction fission power and the need for an evaporator flushing system.

The vapors leaving the gas disengager will contain the fission product gases, krypton and xenon. Table 2.1 lists the gaseous mixed fission product activity release rate as a function of the hold-up time of these gases. In preparing this table, all twenty-one krypton and xenon isotopes having a half-life greater than one second were considered, the fission product families were assumed to have reached equilibrium, and standard decay and daughter growth equations were applied. Note that the decay of the predominant radioisotope Xe-135 (half life 9.2 hr) greatly reduces the total activity discharge rate between 10 and 100 hours; hold-up times longer than 100 hours do not appreciably lower the activity discharge rate.

These parametric studies helped to establish the design basis for the processing equipment.

37.1-65-1283

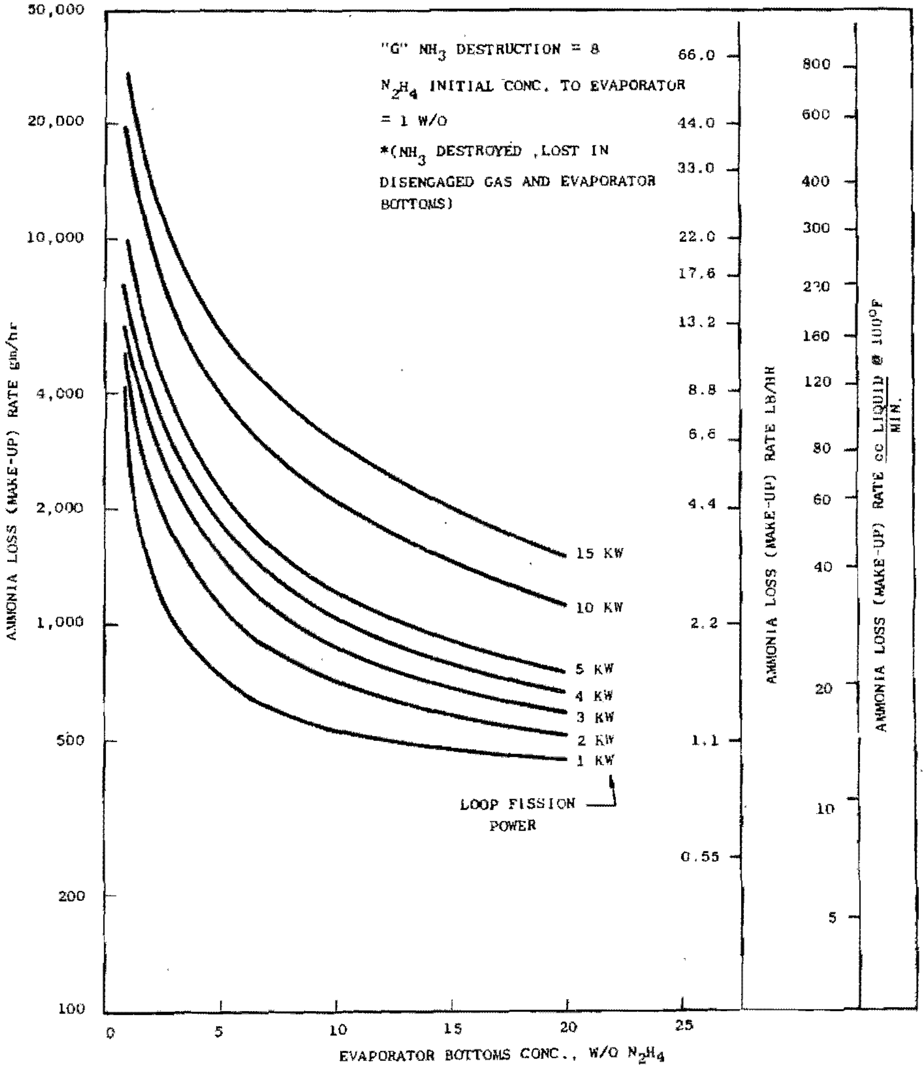

FIGURE 2.5 TOTAL AMMONIA USE (MAKE-UP) RATE AT VARIOUS LOOP POWERS

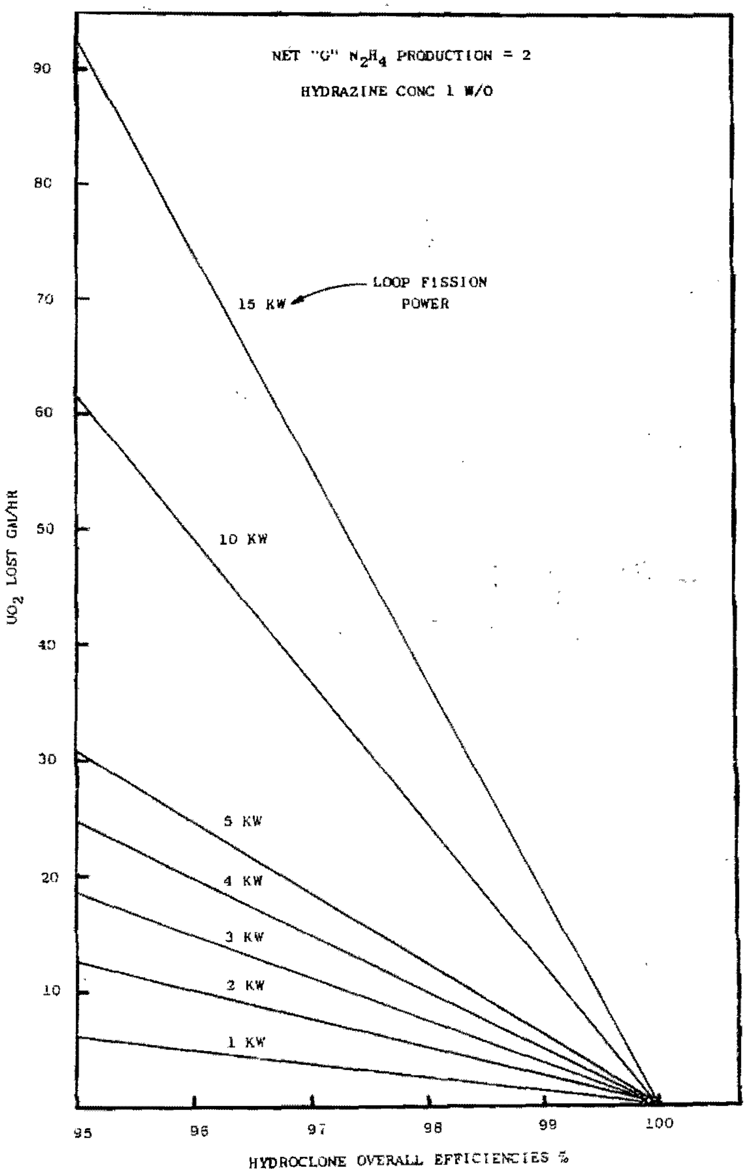

FIGURE 2.6 FUEL LOSS DUE TO HYDROCLONE EFFICIENCIES AT VARIOUS LOOP POWERS

TABLE 2.1

GASEOUS FISSION PRODUCT ACTIVITY RELEASE RATE FROM IN-REACTOR LOOP, CURIES/DAY

Loop Fission Power kw	Hold-Up Decay Time, (Hr)			
	1	10	100	1000
1	1550	552	12	7
2	3100	1104	25	14
3	4650	1656	37	22
4	6200	2208	50	29
5	7750	2760	62	36
10	15,500	5520	120	70
15	23,250	8280	186	108

2.1.3 Hydrazine Program Test Building

A 40 by 50 ft Butler building (Figure 2.7) was constructed (with company funds) for the Hydrazine Process Development Program. The floor area was divided approximately into thirds with the In-Reactor Engineering, Materials, and Processing Projects each assigned a test area.

The facilities in this building included: exhaust and scrubber system, ammonia dilution and discharge system, sprinkler system, building emergency blowers, a fire hose, chemical (wet and dry) fire extinguishers, and safety showers and eye washes.

Each test system using ammonia was contained within a ventilated vapor cubicle which was kept under negative pressure and ventilated by the exhaust and scrubbing system described below. These cubicles prevented small system leaks of ammonia vapor from entering the building, and minimized the amount of ammonia vapor escaping to the building in case of a large leak; they also confined any accidental spill of UO_2 to a local area.

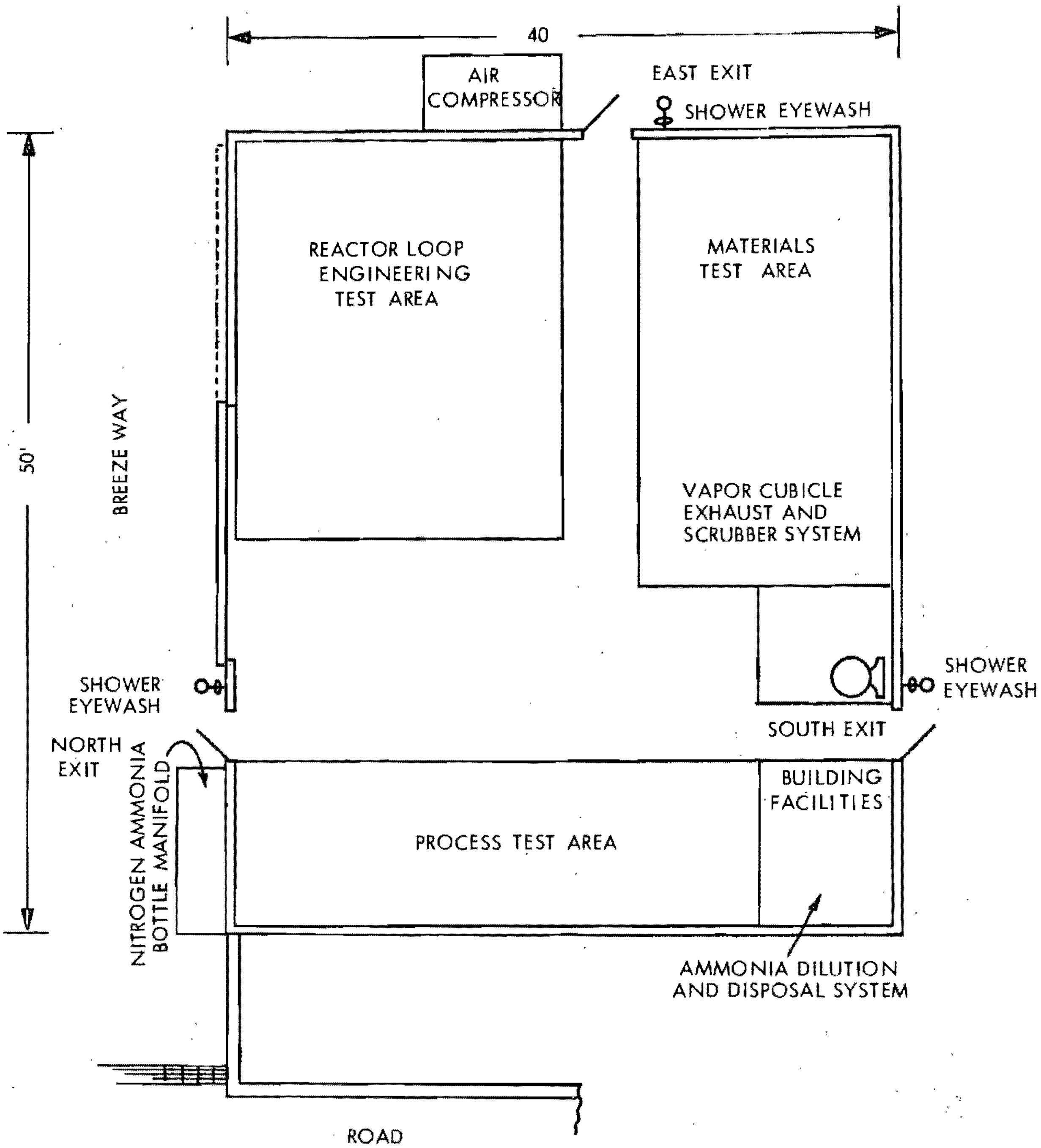

37.1-65-1302

FIGURE 2.7 NEW BUILDING LAYOUT FOR THE HPDP PROGRAM

An exhaust and scrubber system was installed in the building to apply negative pressure to the test system cubicles, each of which was separately ducted through an adjustable gate valve. The exhaust from the cubicles passed through a water scrubber to remove ammonia vapors before discharge to the atmosphere. The system was designed to allow a negative pressure of 5 to 10 in. of water at the cubicle if the cubicle were relatively air-tight and to maintain a 100 ft/min face velocity if 20 ft^2 face area were open. This was a corrective system; a separate ammonia-water reaction and sewer discharge system was installed to provide a safe method for the routine disposal of ammonia.

Two large blowers were installed in the roof of the building to quickly clear the air in the building. A safety shower and eye wash was installed outside the building at each of the three exit doors.

2.1.4 Processing Test Facility

Various process systems and equipment containing liquid ammonia, hydrazine, and UO_2 particles were tested at pressures up to 1000 psi. All of this test equipment was contained in an enclosure, consisting of an angle iron framework covered with sheet metal and partitioned into seven ventilated rectangular vapor cubicles connected to the building exhaust scrubber system. Figure 2.8 shows the process test area under construction.

A utility system, installed in the central three cubicles supplied gas, liquid ammonia, and slurry to the unit operations of the process system while they were under development. Two 150-pound ammonia cylinders in a storage rack were manifolded to supply liquid ammonia continuously through a diaphragm metering pump with a capacity of 0 to 3 gph at 1000 psi head. A four-cylinder manifold was provided for nitrogen gas service; individual valving permitted continuous supply. Vacuum to 10 microns was available from a portable vacuum pump.

Hydrazine was stored in 2-liter stainless steel vessels pressurized by purified, dry nitrogen at 5 psi. The hydrazine was discharged directly from the reservoir into other receptacles, or metered through a 25 ml or a 250 ml buret into the 1-liter stainless steel injector vessel.

37.1-65-722

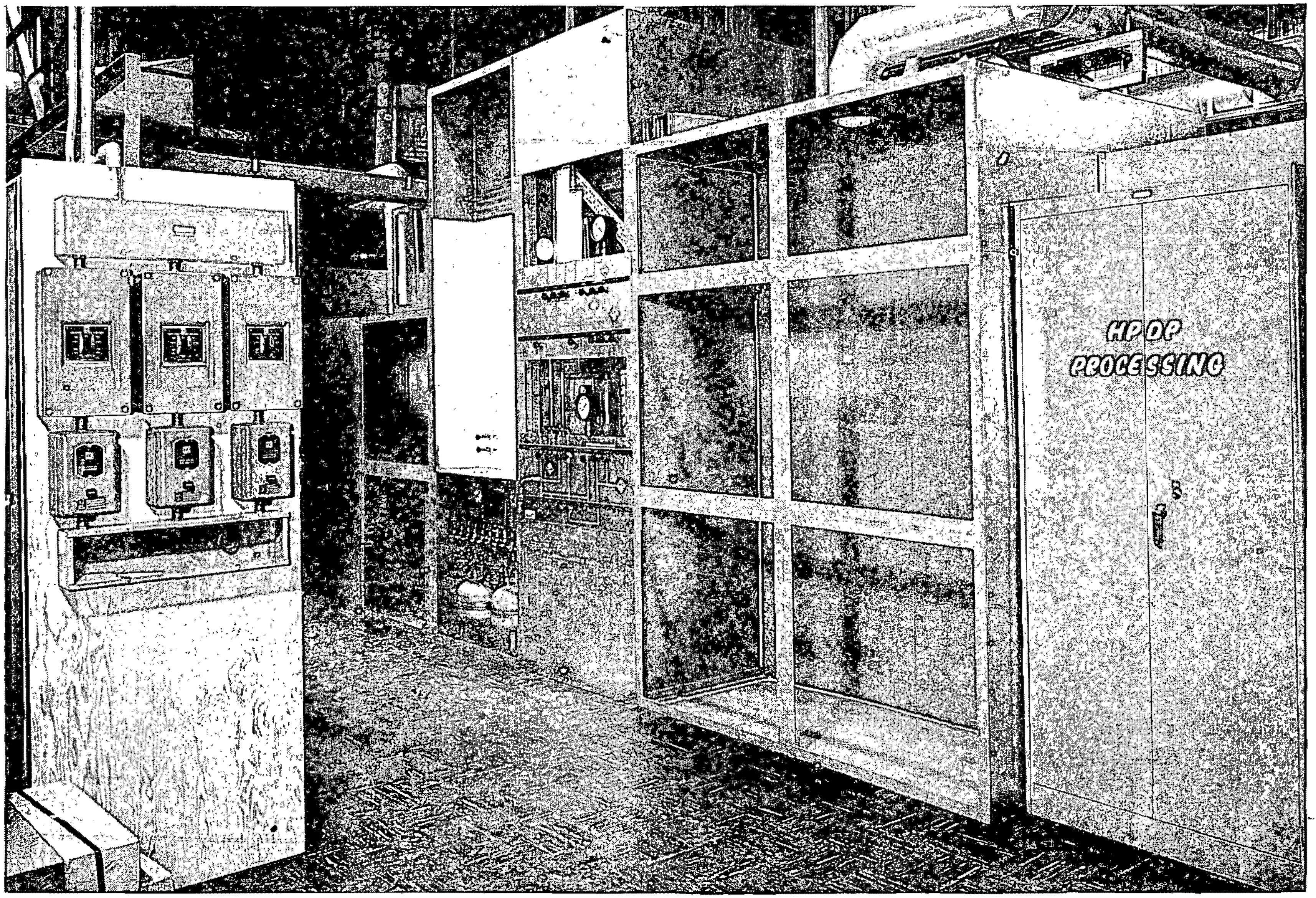

FIGURE 2.8. PROCESS CUBICLE AND TEST AREA

Ammonia could then be pumped into this vessel to give an ammonia-hydrazine solution. The injector vessel was supplied with high pressure nitrogen as required to force an ammonia-hydrazine solution through the delivery manifold to any of the process test systems. This delivery system (Figure 2.9) was located in the center cubicle of the process test section.

The working feed solutions for process test systems were prepared and stored in two 10-gallon, temperature controlled autoclaves (Figure 2.10). Autoclave #1, unstirred, was used for non-slurry solutions of liquid ammonia and hydrazine; autoclave #2, stirred, was used for slurries of liquid ammonia, hydrazine, and uranium dioxide powder.

Ammonia and slurry wastes were collected in a 2-gallon evaporator from which the liquid ammonia was allowed to vaporize leaving the UO_2 particles behind.

All major pressure vessels in the Process Test Area were protected with rupture disks or relief valves, or both. The lines from these safety devices terminated in a second waste evaporator reserved for relief discharges.

Samples were withdrawn from test assemblies and autoclaves through a central grab sampling system. During normal sampling operations, the sampler was evacuated, the line purged with a small amount of sample, and the final sample was then drawn; the sample line was then drained to the waste evaporator for disposal.

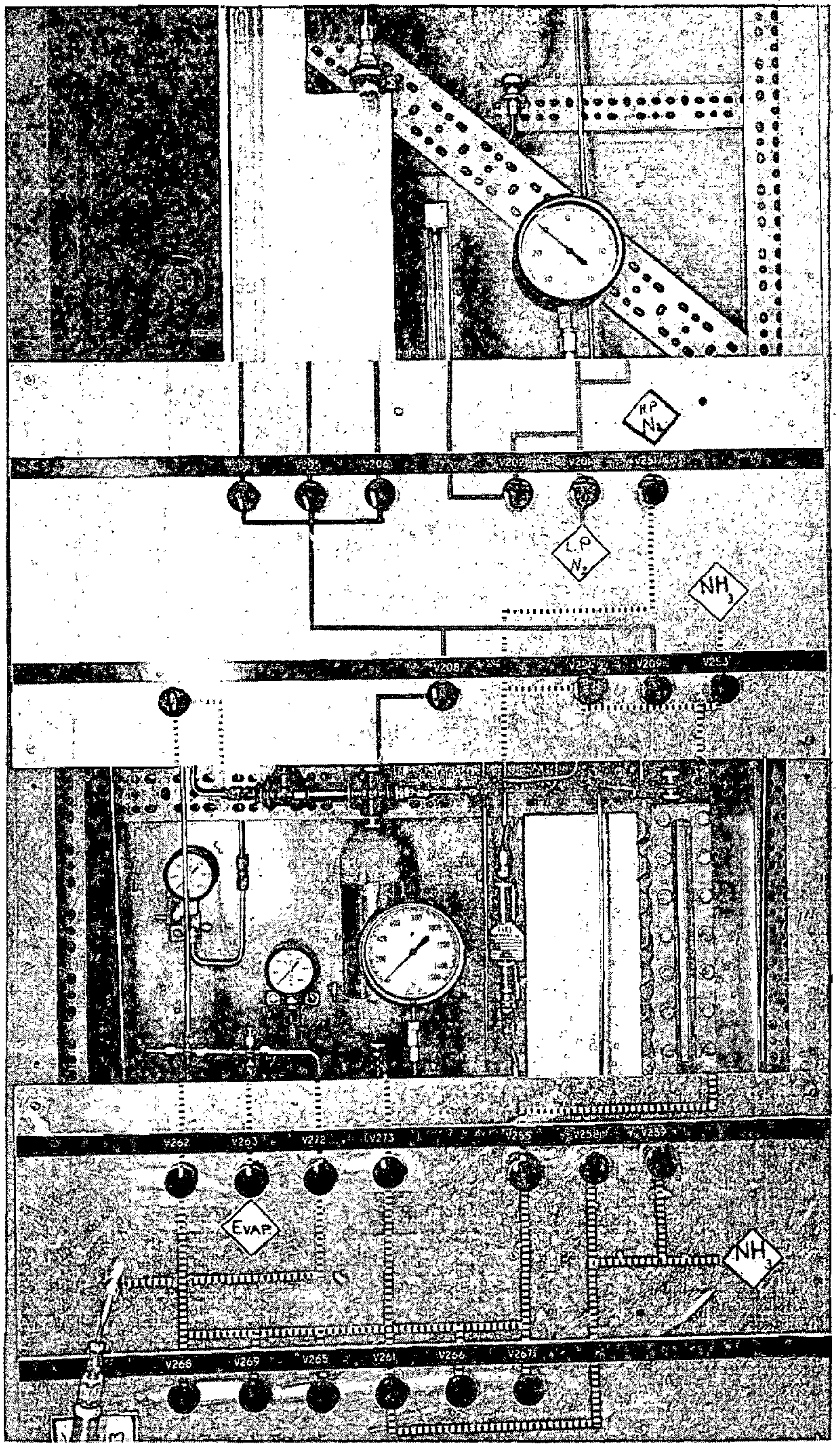

37.1-65-1287

FIGURE 2.9 HYDRAZINE-AMMONIA MIXING AND DELIVERY SYSTEM

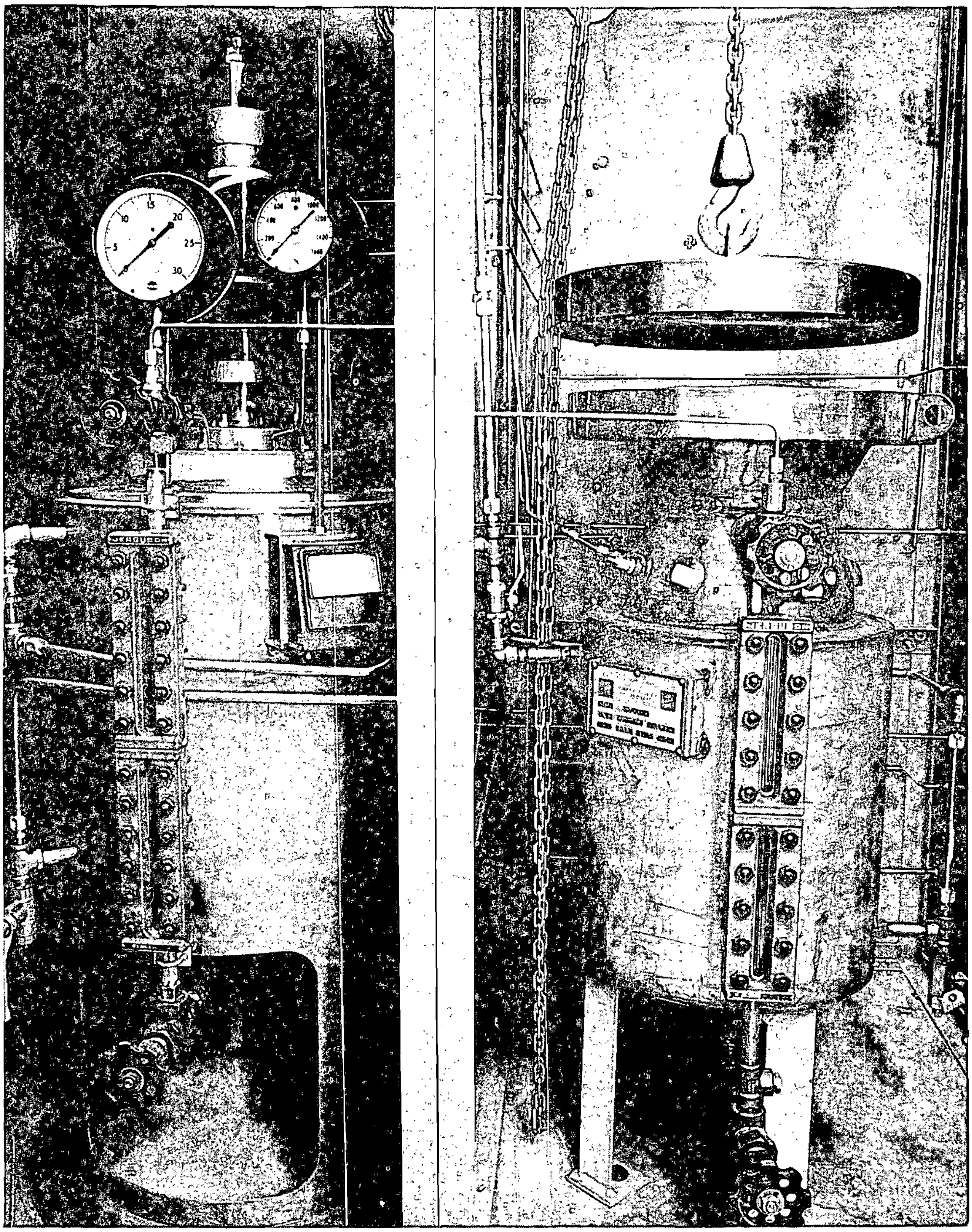

AUTOCLAVE #2 - STIRRED
FOR SLURRY APPLICATION

AUTOCLAVE #1 - FOR NON-SLURRY APPLICATION

FIGURE 2.10 PROCESS SYSTEMS FEED AUTOCLAVES
(FRONT CUBICLE PANELS REMOVED)

37.1-65-1291

2.2 Gas Separation

2.2.1 Introduction

The in-reactor loop produced radiolytic gas at a high rate directly proportional to fission power. The predicted radiolytic gas production rate at 15 kw fission power was 72 g-mol/hr or 0.5 scfm. Section 2.1.2 gives some of the relationships which illustrate the significance of successful gas-disengagement. Continuous and efficient gas removal at a rather steady rate was required to avoid loss of slurry into the gas exit line, pressure surges, and cavitation damage to the impeller of the main slurry pump.

A literature and patent search revealed no information applicable to disengaging gas from liquid in small equipment. Several references[2,3,4] described the application of ultrasonics to coalesce bubbles, thereby increasing their buoyancy.

Two gas-disengaging approaches were tested experimentally: 1) formation of a thin liquid film to expose bubbles to the liquid-gas interface where the bubbles would dissipate; and 2) centrifugation of the liquid to force bubbles and liquid apart by density difference. Ultrasonic energy was tested as a means of coalescing bubbles to improve separation.

The original operating parameters affecting the design of a gas disengager are listed below.

Slurry Composition		NH_3 Liquid Containing UO_2 Particles, 1 to 3 μ dia., at Concentrations up to 200 gm/liter
Maximum gas production rate		72 g moles/hr - 0.5 scfm
Operating pressure:	reference	750 psi
	maximum	1000 psi
	minimum	500 psi
Temperature:	reference	100° F
	maximum	150° F
Slurry flow rate:	reference	5 gpm

The size limitations originally imposed on the gas disengager resulted from the decision to place the unit inside the beamport to simplify slurry containment and shielding. At the time of this decision the prime candidate nuclear reactor for the in-reactor experiment was the Westinghouse Test Reactor (WTR). The maximum sized envelope for a disengager to fit the WTR beamport was a 6-in. diameter by 18-in. long horizontal cylinder.

The desirable characteristics of the gas disengager obviously included a gas-free exit-liquid stream and a liquid-free exit-gas stream, but the following were also important: 1) minimum liquid volume consistent with the pressurizer function, to reduce the required slurry inventory and thereby provide a higher average specific fission power, 2) minimum total volume, to reduce the amount of supplementary shielding which might be required by the gas disengager radioactivity levels, 3) absence of slurry holdup or dropout which would cause fission power to drop with time; and 4) pressurizer function, i.e., a liquid level which would be stable enough to instrument and which was sufficiently tolerant to level change to be used as a control point for ammonia addition.

2.2.2 Preliminary Testing

Early testing was performed with a water-air system at atmospheric pressure. Separation of gas from liquid by centrifugal action was attempted with spherical and pear-shaped cyclone vessels of up to 6-in. diameter. Entrance angle and height were varied; liquid exit position was varied; and shape was changed from spherical to conical. These designs did not disengage the small gas bubbles from the water, apparently because of insufficient liquid residence time or insufficient centrifugal action. However, the application of ultrasonic energy was helpful. Designs which emphasized centrifugal action created a vortex which sucked gas into the liquid outlet. It was found that an effective combination of forceful centrifugal action (with an effective vortex interruptor) and sufficient residence time was not possible within the six-inch height limit. The liquid film approach was tried with a horizontal cylinder 5-in. dia by 10-in. long fitted with an inlet to spread the water in a thin film over the cylindrical surface. A shallow reservoir was maintained at the bottom of the cylinder at a sufficient depth to prevent gas from entering the liquid outlet. Ultrasonic energy was applied to the cylindrical surface. This design was successful in disengaging gas from 5 gpm liquid; however, it was eventually abandoned, as no simple means could be devised to prevent a pile-up of fuel in the reservoir. In addition, no instrumentation was available for detecting the liquid-gas interface with sufficient accuracy to permit control of the operation.

When the MTR was selected as the irradiation facility, the size restrictions for the gas disengager were revised. The slurry processing equipment was required to fit within a 22-in. diameter horizontal beamport plug, therefore, a space of approximately 20-in. high by 6-in. diameter was allotted for the gas disengager. Subsequent effort was spent on developing a cyclonic type of gas disengager.

2.2.3 Liquid Ammonia Test Apparatus

An apparatus, shown schematically in Figure 2.11 was constructed for testing experimental gas disengager models. The apparatus, located inside a test cubicle, consisted of a canned motor pump, a bearing backwash filter, a heat exchanger, a gas introduction filter, a sight glass parallel to the test disengager, various control instruments, and a space for the experimental gas disengager.

The test apparatus was designed for liquid ammonia operation up to a temperature of 160°F and a pressure of 1000 psi. Tests used only slurry-free liquid ammonia to allow visual observation of the dispersed gas bubbles, and to allow rapid interchange of equipment without time-consuming decontamination.

During a typical run, (shown in Figure 2.12) gas was introduced into the fluid upstream of the disengager under test to simulate the radiolytic gases predicted for the actual in-reactor loop. This gas was dispersed into the flowing stream through a sintered metal filter. Gas disengagement efficiency could be determined by visual observation of the disengager feed and discharge streams through small sight glasses in the lines. The dispersed gas bubbles were clearly visible in the feed sight glass; when the disengager was removing all the inlet gas, the disengager outlet glass was clear.

For one test, instead of using the sintered filter to introduce gas, gas was introduced into the pump inlet so that the pump

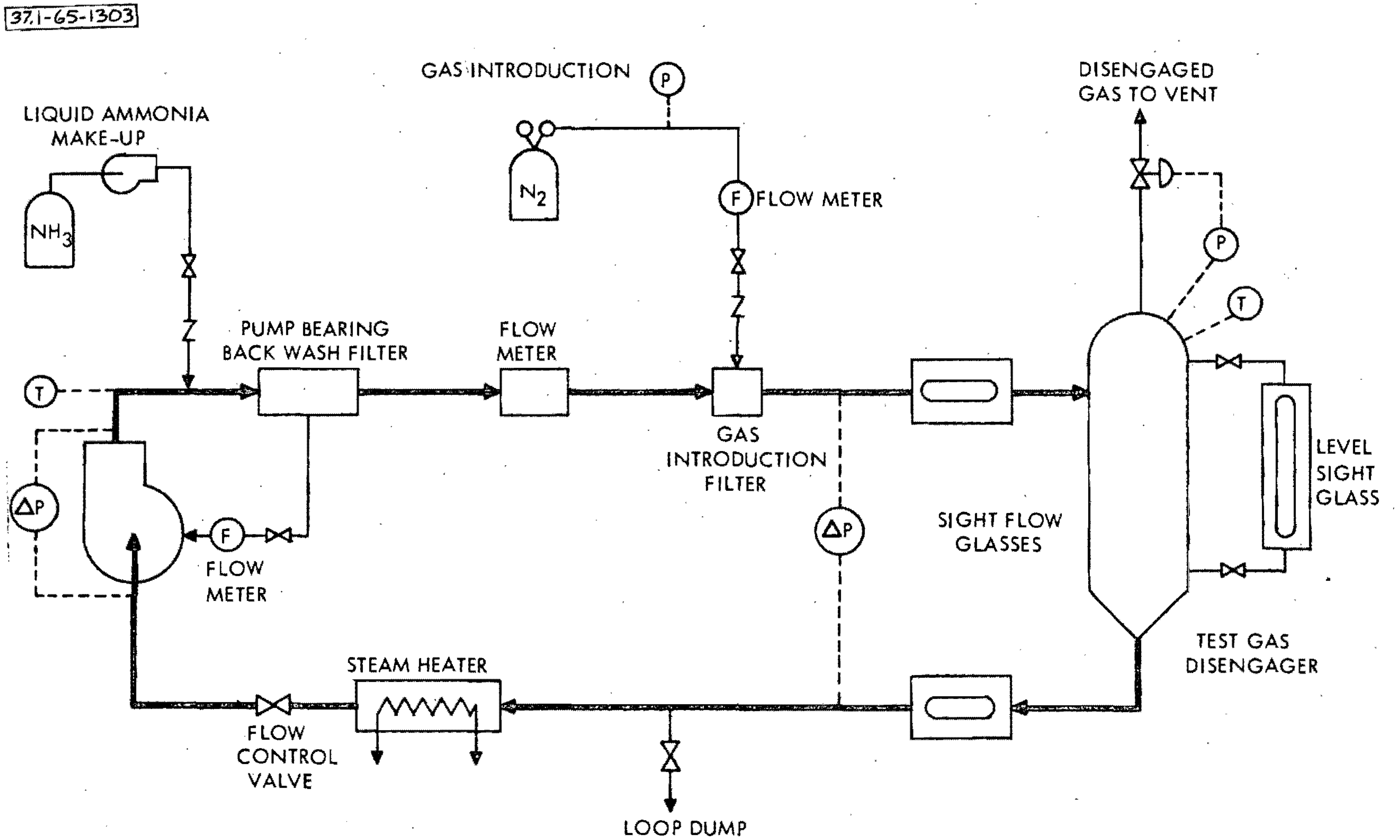

FIGURE 2.11 SCHEMATIC DIAGRAM OF GAS DISENGAGER TEST SYSTEM

37.1-65-1286

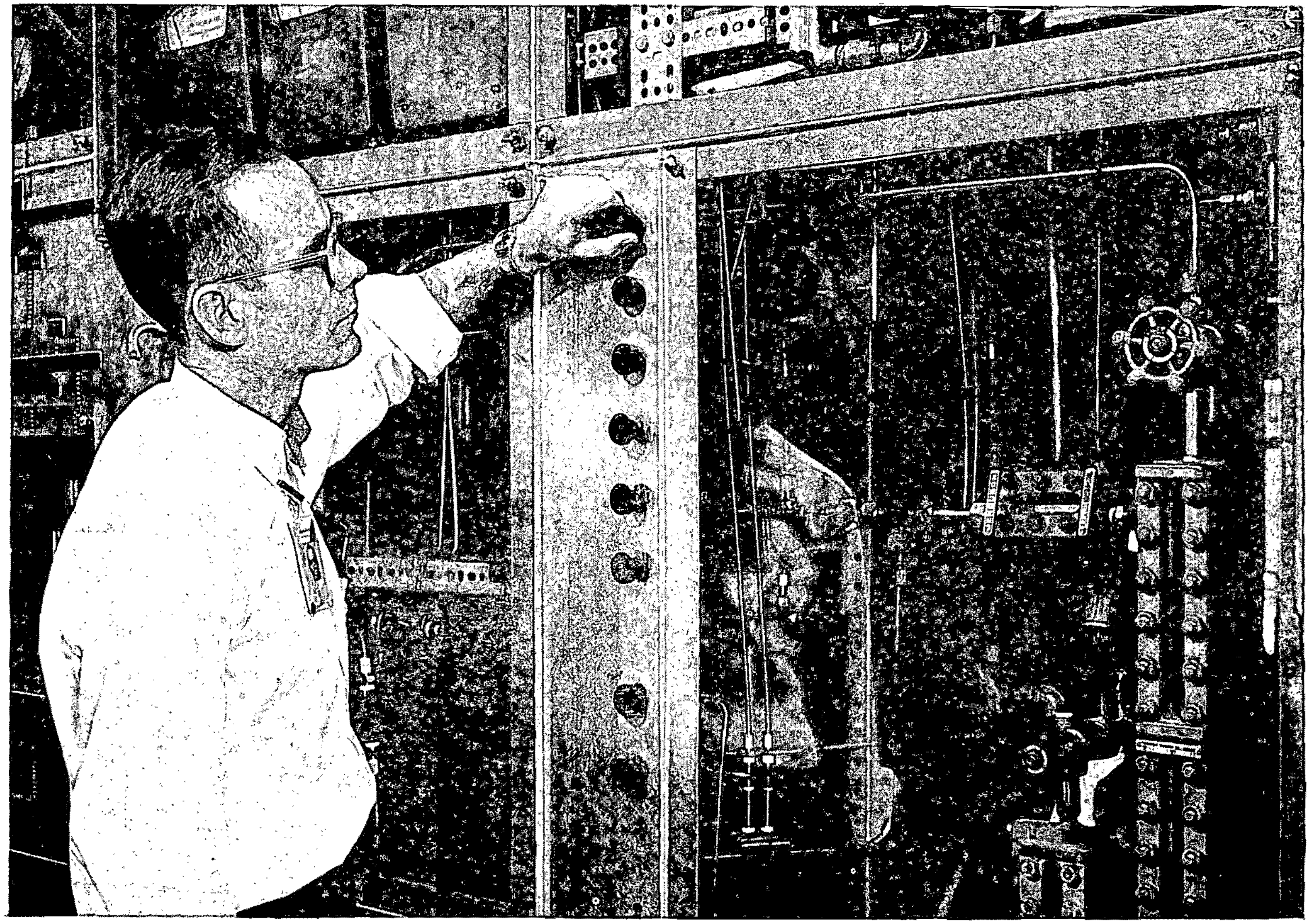

FIGURE 2.12 GAS DISENGAGER TEST APPARATUS

impeller could disperse the gas perhaps into tinier bubbles. This change did not affect the appearance of the inlet stream and it did not affect the disengagement efficiency, therefore, this gas introduction method was abandoned.

2.2.4 General Disengager Design

The general disengager design concept is shown in Figure 2.13. The feed, containing the dispersed gas, entered the vertical unit tangentially, which gave a cyclonic effect, thrusting the gas voids to the center and up out of the liquid. The downward flow rate in the unit was low enough that the gas bubbles could rise and leave the liquid. A straightening vane was situated at the bottom of the unit to prevent the formation of a vortex which could carry gas voids into the exit stream. The bottom was conical to preclude slurry particle deposition in the base of the unit.

Design variables which were tested included diameter, height (inlet-to-outlet), and vortex straightening vane position. Test conditions were:

○ Temperature	100 and 150° F
○ Pressure	750 to 1000 psia
○ Fluid flow	3 to 6 gpm
○ Dispersed Gas Introduction	0 to 1.50 scfm (N_2 gas)
○ Ultrasonics	on and off

2.2.5 Five-inch Model

Initial tests used a gas disengager with a 5-in. inside diameter. The disengager removed 100% of the dispersed gas down to a liquid height of about 12 in., the minimum level which could be observed for this model.

The maximum gas flow rate tested was 1.5 scfm, three times the maximum anticipated during the 15 kw in-reactor run. Since no visible effect on disengagement efficiency was noted, subsequent tests were run at 0.75 scfm, one and one-half times the maximum anticipated rate.

Ultrasonic energy was found to have no visible effect on gas disengager efficiency; its use was discontinued.

These encouraging results led to the construction of additional experimental disengager models to minimize the size and liquid volume of the final in-reactor model.

2.2.6 Four, Three, and Two and One-Half Inch Models

2.2.6.1 Tests

Three gas disengagers were fabricated from 4-, 3-, and 2-1/2-in. schedule 40 stainless steel pipe. In preliminary tests on each model, the distance between the entrance and exit was varied by inserting the outlet tube to various levels on the disengager axis. These tests indicated the approximate minimum liquid height required for disengagement; the models were then modified to reduce their over-all height. The models tested are listed in Table 2.2; those used for preliminary tests are identified as 4-1, 3-1, and 2.5-1.

The effects of temperature and gas composition were tested on the 4-inch models. The effect of inlet velocity was tested on models 4-3 and 4-3b. The effect of pressure was tested on the 3-inch models.

Gas introduction just above the vortex breaker was tested on model 4-3c, as this method was being considered for maintaining gas pressure of the in-reactor loop during shut-down and low power operation.

Pressure drop measurements were made on the 4-in. model across the liquid inlet and outlet and across the Purolator filter in the gas outlet.

2.2.6.2 Test Results and Discussion

The 4-inch unit required the least height of the three diameters tested. As flow rate was increased from 4 to 6 gpm, the liquid level height required for complete removal of gas bubbles from the exit liquid increased from 9 to 11.5 in. The variation among the models and test conditions gave a data spread of about ±1 in. The 3-in. models, 3.1 and 3.2, required a 14.5 in. liquid level height at 4.8 gpm, and 2 to 2.5 in. less at 3.5 and 6 gpm. At 4 gpm, a minimum in the efficiency of this diameter gas disengager appeared to exist which required about 2 in. additional liquid head to overcome.

TABLE 2.2

GAS DISENGAGER MODELS TESTED

Model No.	Inside Dia. (in.)	Bottom Shape	Distance		Notes
			Inlet-to-Vortex Breaker (in.)	Inlet-to-Outlet (in.)	
4-1	4.026	Hemispherical	5.5	26.0	
4-2		Conical	5.5	12.5	
4-3		Conical	7.0	12.5	0.635 in. ID entrance
4-3b		Conical	7.0	12.5	0.49 in. ID entrance
4-3c		Conical	7.0	12.5	Liquid inlet
			7.0	6.5	Inlet for 50% of gas
4-4		Conical	4.5	10.5	Special outlet
3-1	3.068	Hemispherical	8.0	26.0	
3-2		Conical	8.0	14.5	
2.5-1	2.469	Hemispherical	9.0	16.5	
2.5-2		Hemispherical	5.0	12.5	

The 2 in. models, 2.1 and 2.2, required even more liquid level height than the 3-in. models. Model 2.1 showed that the required liquid level decreased about one inch as flow rate was increased from 4 to 6 gpm; this suggested that perhaps a maximum required liquid level existed somewhere below 4 gpm.

The 3-in. and 2.5-in. models showed no performance improvement over the 4-in. models and required more height for efficient operation. Furthermore it was felt that these models were of such low volume that their use as pressurizers would be hampered. The 4-in. model, on the other hand, had sufficient volume to operate as a pressurizer and was low enough to fit easily into the allotted space.

Tests with the 4-in. models at 100°F and 150°F showed that temperature had only a minor influence on disengagement efficiency. The required depth of liquid was changed by an average of about one inch, but it was greater for model 4.2 and less for model 4.3 at 150°F.

The 3-in. models were operated at 750, 800 and 1000 psia. Pressure was found to have no detectable effect on efficiency.

The influence of inlet velocity, tested with models 4.3 and 4.3b, was found to be insignificant over a factor of 1.6.

The position of the vortex breaker, tested with models 4.2 and 4.3, had an average of 1 in. effect on the required liquid depth. Model 4.3 was less sensitive to changes in flow rate than model 4.2.

The results of the pressure drop tests are presented in Figure 2.14 over a flow rate of 3 to 6.5 gpm; pressure drop was approximately 0.3 psi at 4 gpm and rose linearly to 2 psi at 7 gpm. The gas pressure drop across the Purolator off-gas filter at 1.1 scfm was less than could be detected using a differential gauge of ± 0.3 psi sensitivity.

Model 4.3c, with 50% of the gas being added just above the vortex breaker, was found to be unsatisfactory for disengaging gas at liquid level heights lower than 12.5 in.

Nitrogen, which was the gas used for most tests, was replaced by helium for one test in order to bracket the density of the 3:1 hydrogen to nitrogen composition expected during the in-reactor experiment. No influence upon disengagement was observed.

2.2.7 Liquid Level Probe Tests

A set of test runs was performed after the liquid level instrumentation was selected. The sensing probes for this instrument were 6 3/4-in. OD cylinders arranged in a vertical line which penetrated the wall of the gas disengager 2-in. The purpose of the runs was to determine the influence of the probes on gas disengagement. This set of runs essentially covered the range of test conditions previously described. The 4-in. unit was modified using 3/4-in. steel stock as a mockup for the probes. These probes apparently disrupted the cyclonic action of the 4-in. unit and gas could not be disengaged. A 6-in. unit was similarly constructed and successfully disengaged gas. The mounting of the probes in the 4-in. unit was modified so that the probes entered essentially tangentially and parallel to the flow pattern; gas was disengaged almost as efficiently as in the 4-in. unit without probes.

37.1-65-1300

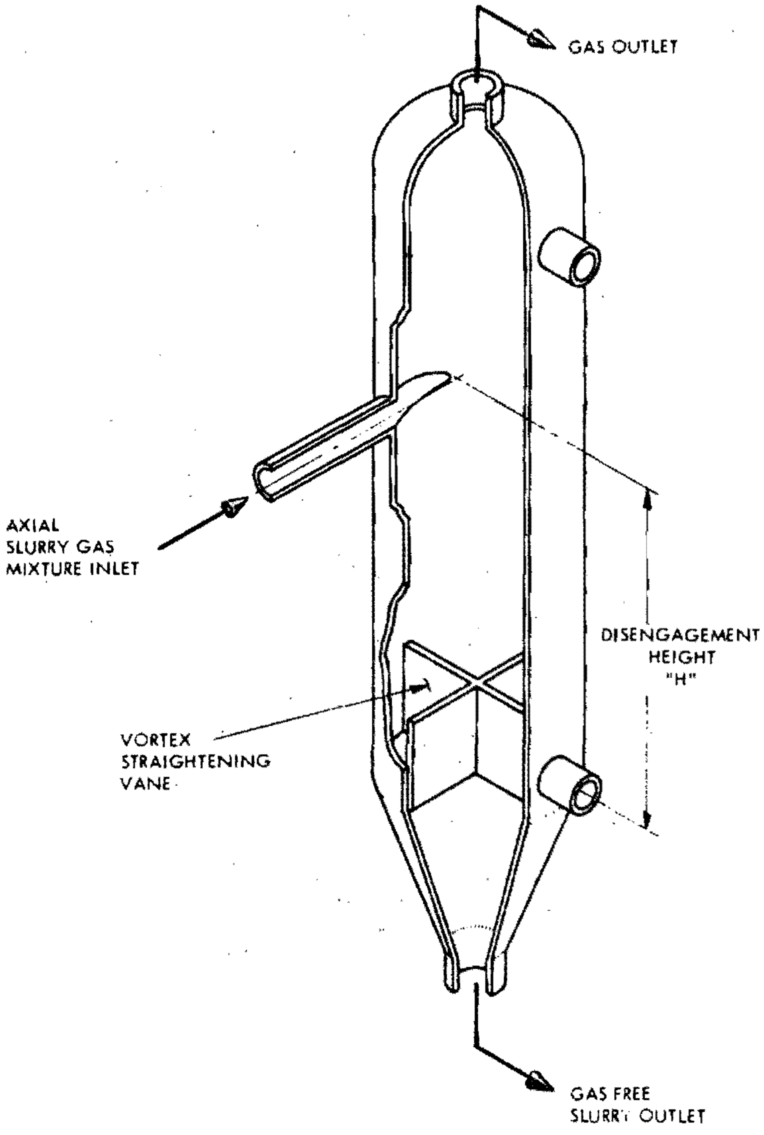

FIGURE 2.13 CUT-AWAY VIEW OF GAS DISENGAGER

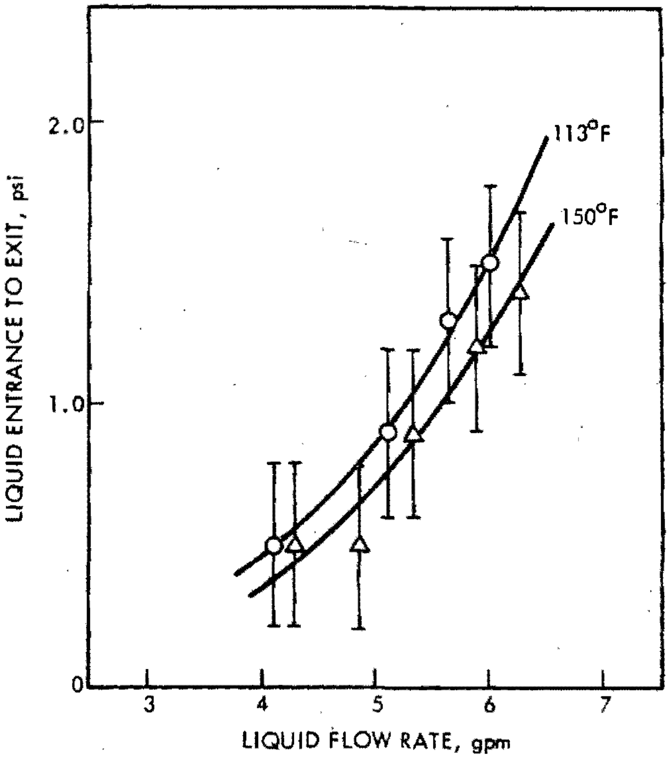

FIGURE 2.14 DISENGAGER PRESSURE DROP VERSUS LIQUID FLOW RATE

Up to this time, testing of the cyclonic type of disengager had been done using steel models and the cyclonic action could not be observed. A model of the 4-in. unit was constructed from transparent plastic in order to observe the vortex action. A transparent side arm, entering the unit below the vortex straightening vanes, was installed as a static level indicator. This unit was operated at one atmosphere using water at 5 gpm as a working fluid; no gas was injected. These tests showed that a "rooster tail" film approximately 1/8-in. thick was formed which climbed from the liquid inlet to about 3-in. above the inlet at 225° axially from the inlet position, (Figure 2.15). The effect was similar to that observed with flat-spray nozzles. Although this unit was not tested using level probes, it was evident that level probes inside the disengager would be unsatisfactory as they would cause considerable splashing which would deposit slurry over the inside of the in-reactor gas disengager and that, with such a vortex, there was little chance that liquid level probes would supply meaningful signals.

Liquid level measurements had been made by use of a sight glass in a side arm for all of the models tested. It was therefore assumed that a similar arrangement should be made for the liquid level probes. The sidearm was designed to minimize slurry holdup.

2.2.8 Conclusions

The following conclusions were drawn from the test program:

- Effective gas disengagement results from the proper combination of the buoyant rising of gas bubbles counter-current to liquid flow and the centrifugal thrust of liquid away from gas due to the cyclonic action. Buoyant rising is aided by low downward flow, i.e., large diameter, while centrifugal thrust is aided by rapid rotation, i.e., small diameter.
- Efficient cyclonic action requires a minimum liquid depth which is dependent upon disengager diameter and liquid flow rate. Liquid depth greater than this minimum does not affect disengagement efficiency.
- Temperature has a minor effect on gas disengagement efficiency.

37.1-65-1282

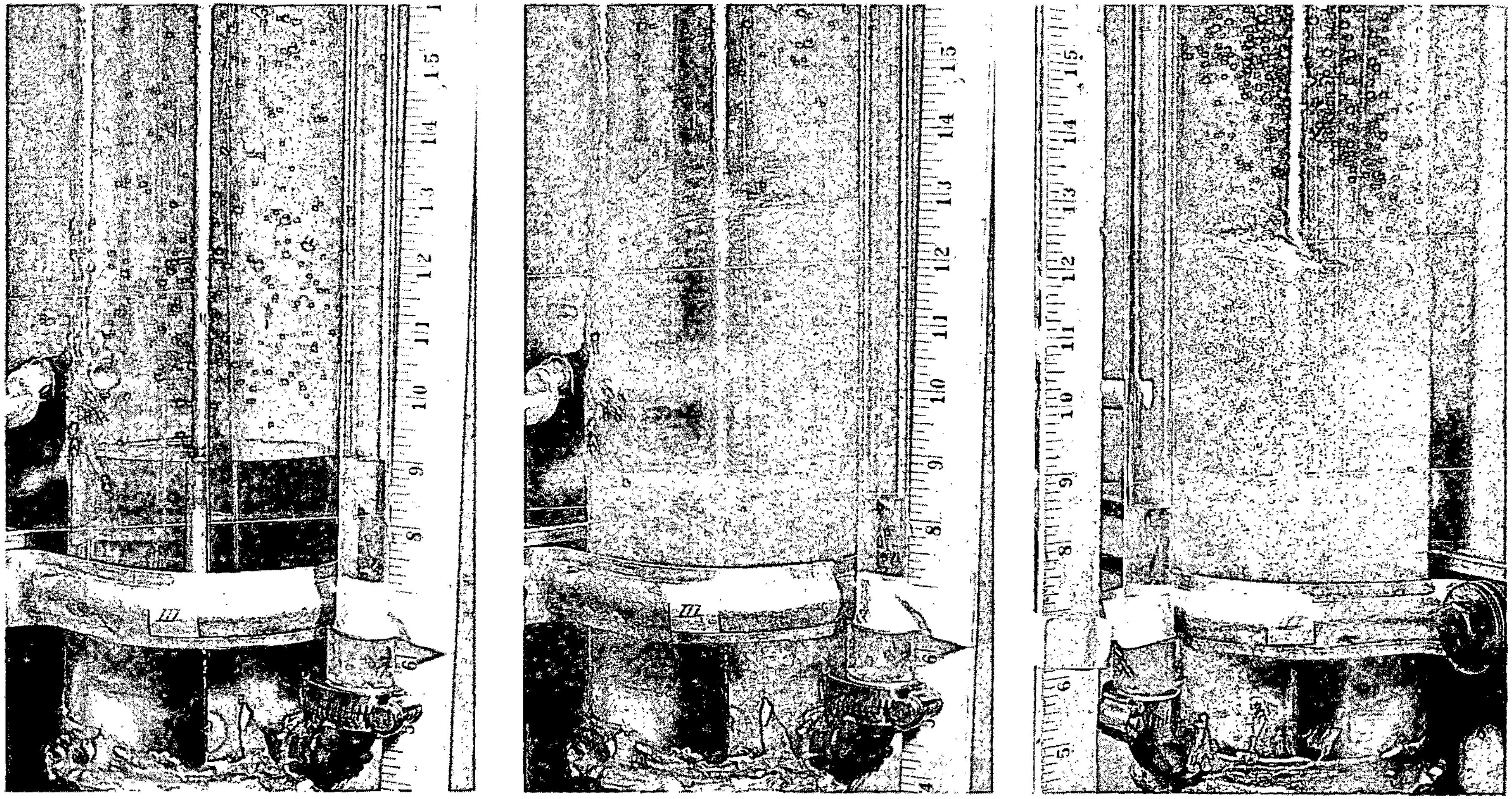

(A) STATIC (FROM RIGHT SIDE)

(B) OPERATING (FROM RIGHT SIDE)

(C) OPERATING (FROM LEFT SIDE)

FIGURE 2.15 GAS DISENGAGER FLOW MOCKUP RUN, LIQUID LEVEL 1 in. BELOW ENTRANCE

- Pressure has no effect on gas disengagement efficiency.
- Gas composition has no effect on gas disengagement efficiency.
- Make-up gas for the loop cannot be introduced below the liquid level without decreasing gas disengager efficiency.
- The entrance flow path must be smooth and free from obstructions such as level probes or thermocouples, otherwise the cyclonic action of the unit will be disrupted, severe splashing of slurry will occur, and the gas disengagement efficiency will be decreased.
- Level probes must be mounted in a side arm (similar to a sight glass installation) to supply a useful signal and to avoid undue splashing.
- Thermocouple heads, exit lines, etc., must be located high and, preferably, axially to reduce fuel buildup and eventual malfunctioning.

2.2.9 Recommended Design

The basic design recommended for the in-reactor gas disengager is shown in Figure 2.16. The 4-in. diameter represents the best combination of strong cyclonic action with a minimum height, which allows a reasonably low change in level per unit volume change for ease of liquid level control. The predicted performance is shown in Figure 2.17. This basic design provides a 2-in. variation in liquid level; additional working volume can be obtained if desired providing that the low level-to-vortex vane does not rise more than 0.5 in. above the liquid entrance. Exit option "A" requires a space of 1/8 in. between the bottom of the disengager and the exit tube to provide sufficient flow to keep slurry in suspension without unduly constricting the exit; it must leave the disengager below the top of the vortex vane to avoid disrupting the cyclonic action.

The liquid level probes should be installed in a side arm or "boot" similarly to the manner in which a sight glass would be installed, but taking precautions against solids pile-up. The cylindrical walls of the disengager above the vortex breaker must be smooth and uninterrupted.

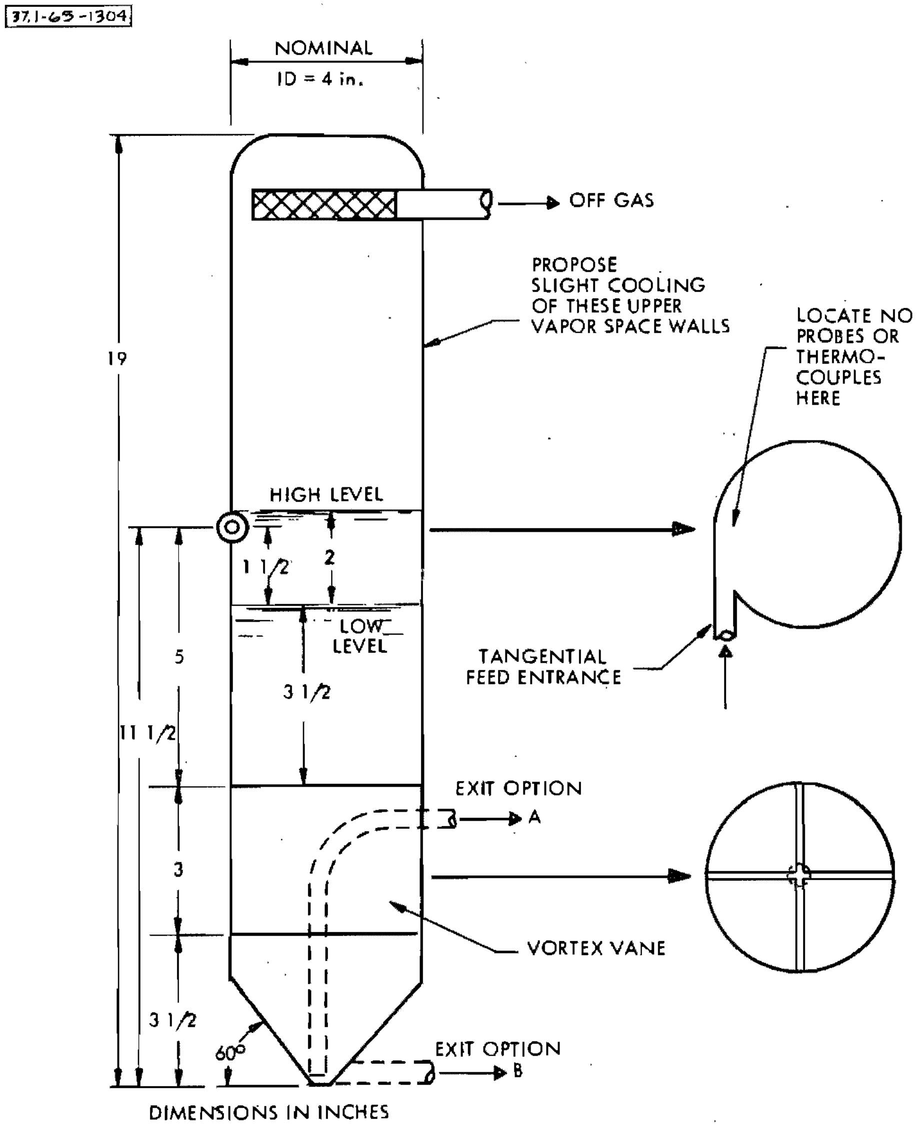

FIGURE 2.16 RECOMMENDED GAS DISENGAGER FOR THE IN-REACTOR LOOP

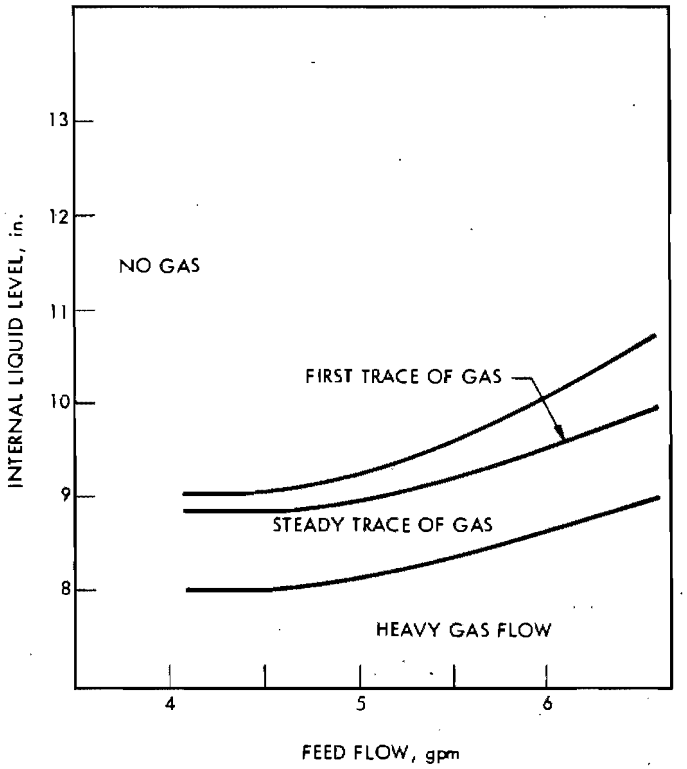

FIGURE 2.17 PREDICTED PERFORMANCE FOR RECOMMENDED GAS DISENGAGER DESIGN

2.3 Fuel Separation

2.3.1 Introduction

The projected fissiochemical production plant and the original concept of the MTR in-reactor loop included two major sections: the fission-fragment irradiation (or self-critical reactor section) and the chemical processing plant. Use of a circulating slurry in the irradiation section required that the slurry be confined to minimize fuel inventory and to isolate the slurry from the chemical processing plant. Several conventional solids concentration unit operations were available for consideration: filtration, centrifugation, hydroclone separation, and evaporation. Filtration, centrifugation, and evaporation all tend to compact the fuel into a cake. The resuspension of this cake, which would require some combination of mechanical and hydraulic action, would require considerable development in itself. Hydroclone separation of fuel from the product stream appeared to hold more promise and therefore was pursued in this study.

The hydroclones to be tested were designed for optimum performance with a given reference slurry feed. The slurry chosen was expected to represent, rather typically, one which would be most suitable for hydrazine production. The reference slurry contained UO_2 particles in the size range of 1 to 3 microns suspended in liquid ammonia at a slurry density of from 2 to 40 grams per liter.

The hydroclone tests began early in the hydrazine program. As ammonia handling facilities were not then available, the hydroclone work was performed with water or aqueous slurry. The major effort was applied to reproducing some of the more pertinent tests performed by others and in developing the techniques of sampling and analysis. By the time ammonia handling facilities were available, the hydroclone requirement had been eliminated from the in-reactor loop at MTR and the hydroclone tests were discontinued.

2.3.2 Theory

A hydroclone is a cyclonic separator in which a solid material of greater density than the suspending liquid is separated from the liquid by centrifugal action. The slurry enters the feed port tangentially to the cavity of the hydroclone (clone); a rotational motion is thus imparted to the body of fluid. (Figure 2.18). The resultant centrifugal action throws the solids toward the outside of the clone where they are carried out in the underflow. The liquid, partially depleted of solids, rises up the axis of the clone and is discharged into the overflow.

The size of particle which will be separated from the liquid is primarily dependent upon pressure drop and clone size for any given system, as these two parameters control the centrifugal force on the particles. The separation value of a given clone with a fixed pressure drop is described as the d_{50} value, that particle size at which 50% of the particles are centrifuged from the overflow stream. Essentially all particles with diameters twice d_{50} are removed. Equation 2.1, which describes d_{50}, was derived from Stokes law[5] and the constant was obtained experimentally.

$$d_{50} = \frac{5 \times 10^3 \mu^{0.5}}{(\rho_s - \rho_L)^{0.5}} \times \frac{D_c^{0.5}}{(\Delta P)^{0.25}} \qquad (2.1)$$

where:

d_{50} = the apparent Stokes diameter of the particle which the hydroclone will separate with 50% of the feed delivered to the underflow, (microns)

D_c = inside diameter of the hydroclone at the feed port (in.)

ΔP = pressure drop between the feed and the overflow ports (psi)

μ = viscosity of the liquid (lb/ft-sec)

$(\rho_s - \rho_L)$ = density difference between the solid and liquid (lb/ft^3)

Equation 2.1 which applies to clones with optimum dimensions and diameters less than one inch, shows that d_{50} is directly proportional to the square root of the clone diameter but that d_{50} decreases only by the 1/4 power of the pressure increase; i.e., separation is relatively insensitive to pressure change and cannot be improved to any appreciable degree by increasing the pressure drop.

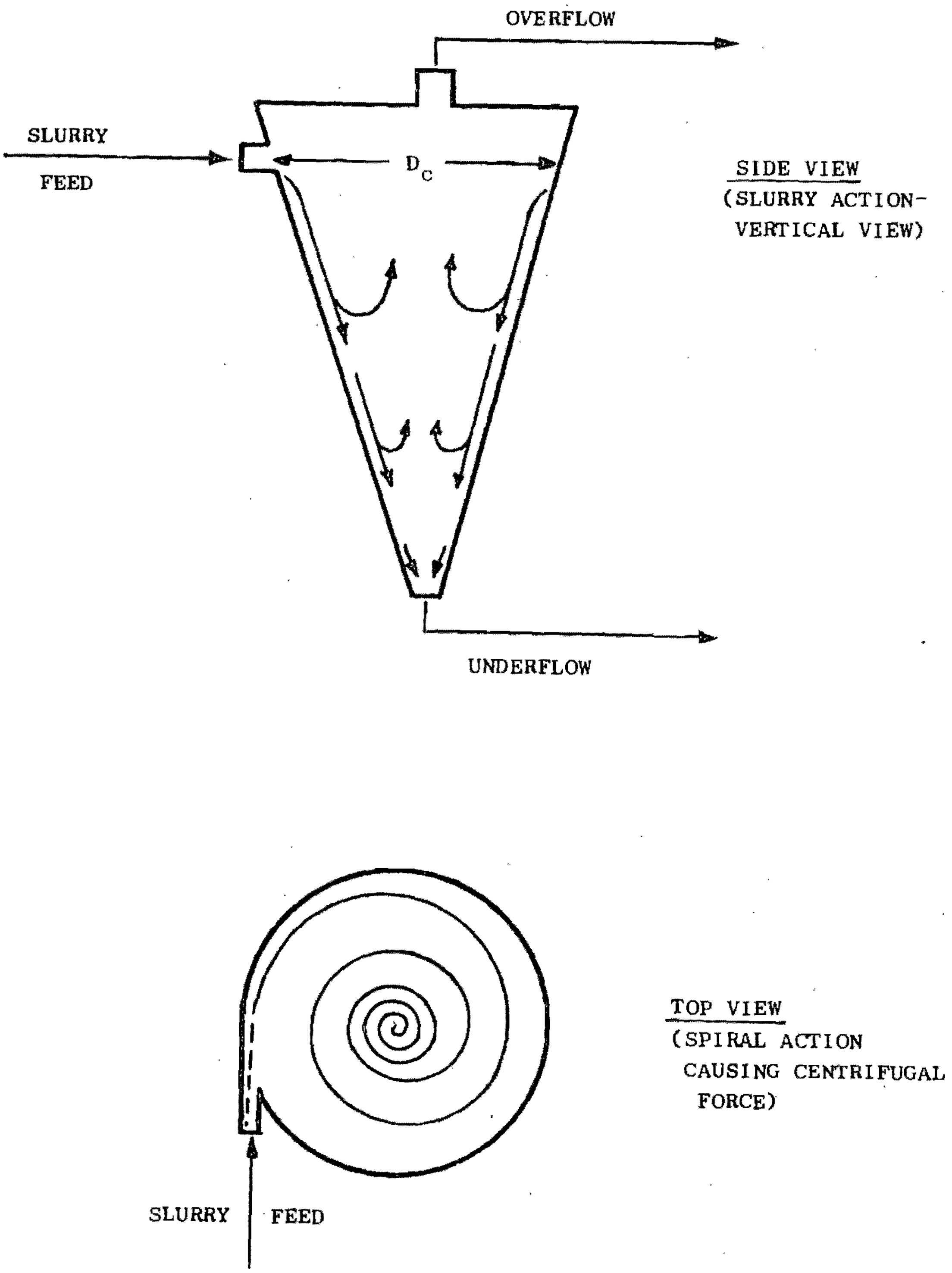

FIGURE 2.18 HYDROCLONE SCHEMATIC

37.1-65-1305

The efficiency of a hydroclone in separating particles of a given apparent Stokes diameter, d (which may differ from d_{50}) is called separation efficiency, E_o. Data relating E_o to the reduced diameter, d/d_{50}, has been compiled and developed by Haas[6] this is shown in Figure 2.19.

The underflow-to-feed ratio can be varied for a given clone to change its apparent efficiency for removing particles; this is due to the discharging of unseparated particles through the underflow stream. Equation 2.2[5] expresses the efficiency for removing a given particle size as a function of underflow rate.

$$E = E_o + (B/F)\ (1-E_o) \tag{2.2}$$

where

E = gross efficiency, or total fraction of feed solids, size d, discharged to hydroclone underflow

E_o = separation efficiency, fraction of feed solids, size d, discharged to underflow due to centrifugal separation, from Figure 2.19.

B = underflow liquid flow rate

F = feed liquid flow rate

As the B/F ratio approaches 1.00, the fraction of solids remaining in the overflow stream diminishes, but at the expense of the product stream flow rate.

A single hydroclone can be used to clean a recirculating slurry system by accumulating solids in an underflow receiver attached directly to the hydroclone underflow port; Figure 2.20 illustrates the principle. The underflow stream flows through the underflow port into the receiver and an equal volume of solution, with most of the solids settled out, returns axially through the underflow port. The underflow rate, B, is induced by the physical dimensions of the clone and by the pressure drop across it. Equation 2.3[6] expresses the B/F relationship in the range of 0.002 to 0.060:

$$\frac{B}{F} = \frac{2.3\ \Delta p^{0.25} Du^{1.8} Dc^{2}}{L^{3}} \tag{2.3}$$

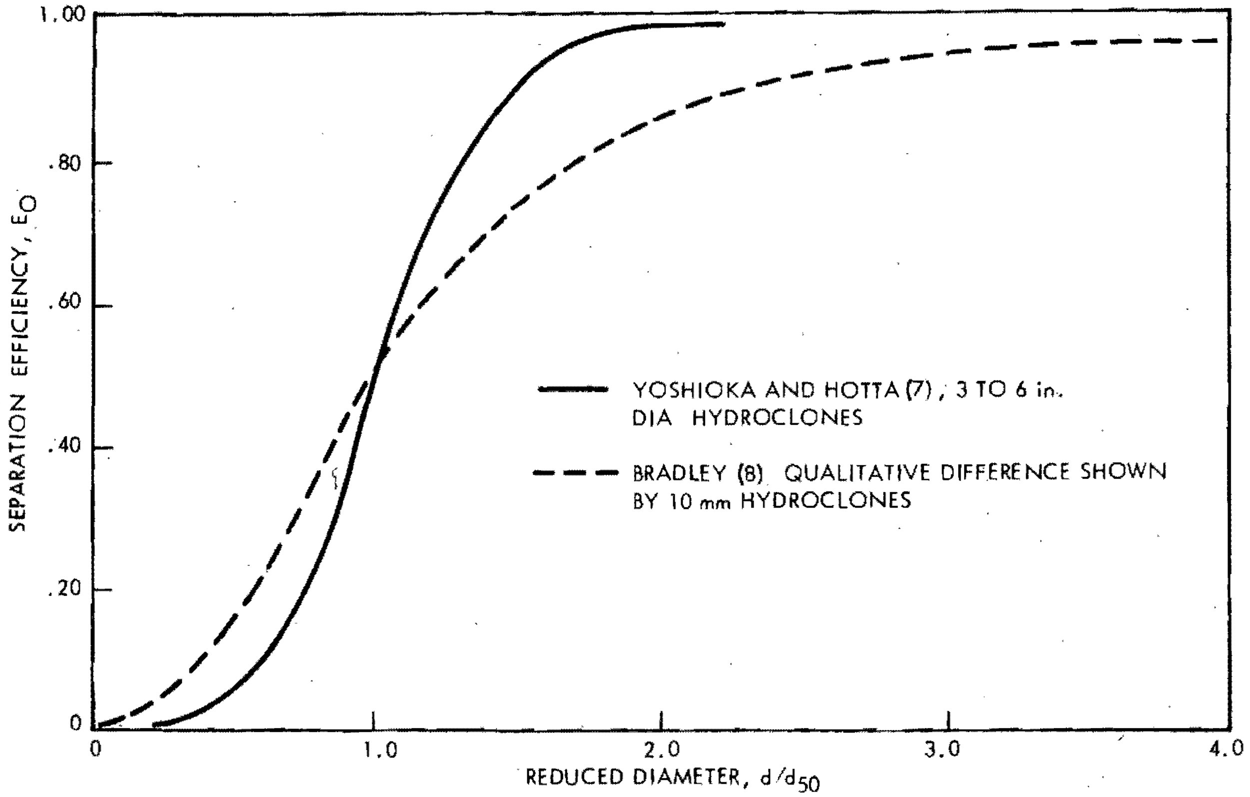

FIGURE 2.19 HYDROCLONE REDUCED EFFICIENCY CURVES

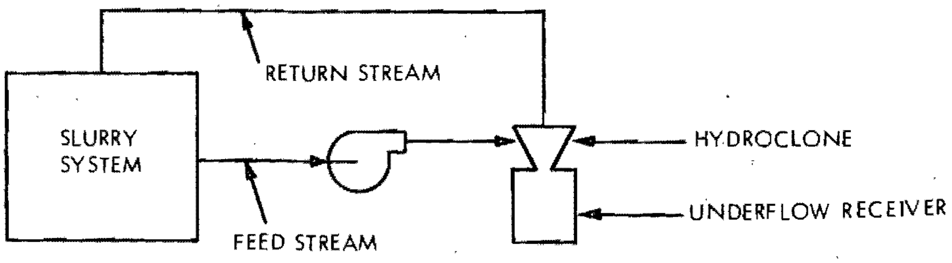

FIGURE 2.20 SCHEMATIC OF SLURRY REMOVAL SYSTEM

371-65-1285

where

Dc = inside diameter of the clone at the feed port (in.)

Du = underflow port diameter (in.)

L = inside length of clone from feed port to underflow port (in.)

The removal of solids from a slurry system by a hydroclone coupled to an underflow receiver can be expressed as a first-order relation;

$$\frac{C}{Co} = e^{-ES} \tag{2.4}$$

where

Co = initial concentration of a given particle size

C = final concentration of that particle size

S = (flow rate) (operating time)/system volume

E = efficiency (defined in Equation 2.2)

Solution of a problem using a real slurry containing a distribution of particle size requires a multigroup calculation.

2.3.3 Test Work

Three hydroclones were fabricated for test. A generalized cross-sectional view of the three clones, together with the individual interior dimensions[9] is given in Figure 2.21. These clone sizes were chosen because they could be operated to remove the particle sizes of interest. The hydroclones are shown in Figure 2.22. Three types of tests were run: a) aqueous flow rate as a function of drop, b) aqueous UO_2 slurry separation tests and c) aqueous UO_2 slurry with underflow receiver.

Flow rate as a function of pressure drop was measured for the three sizes of clones, using water. The apparatus constructed for this work is shown in Figures 2.23 and 2.24. Measurements were made at B/F ratios of 0 (all overflow) and 1.0 (all underflow). These results are presented in Figure 2.25.

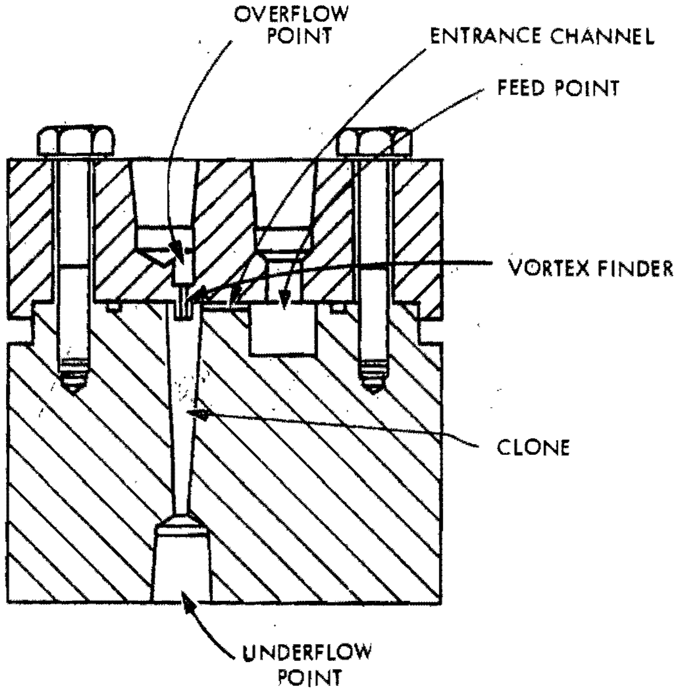

DIMENSIONS, INCHES				
NOMINAL SIZE		0.16	0.25	0.40
CLONE TOP ID		0.160	0.250	0.400
CLONE BOTTOM ID		0.050	0.070	0.100
VORTEX FINDER	ID	0.035	0.053	0.080
	OD	0.050	0.070	0.100
	LENGTH	0.125	0.125	0.1875
ENTRANCE CHANNEL	WIDTH	0.030	0.050	0.080
	HEIGHT	0.050	0.070	0.100
CLONE LENGTH		0.960	1.500	2.400

FIGURE 2.21 HYDROCLONE DIMENSIONS

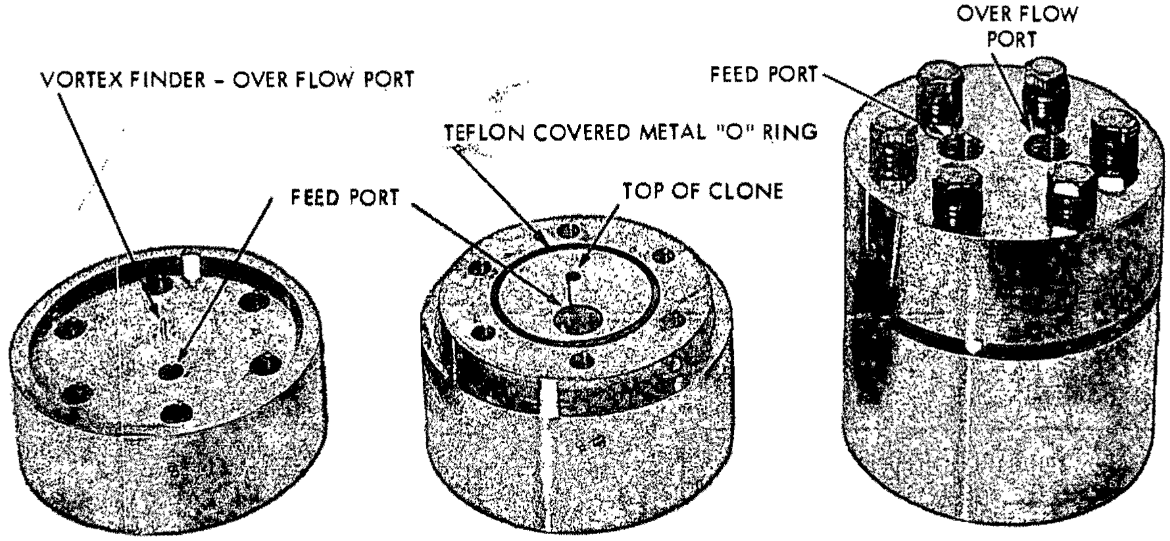

HEAD FROM 0.16 INCH HYDROCLONE

BODY FROM 0.25 INCH HYDROCLONE

ASSEMBLED 0.4 INCH HYDROCLONE

FIGURE 2.22 HYDROCLONES

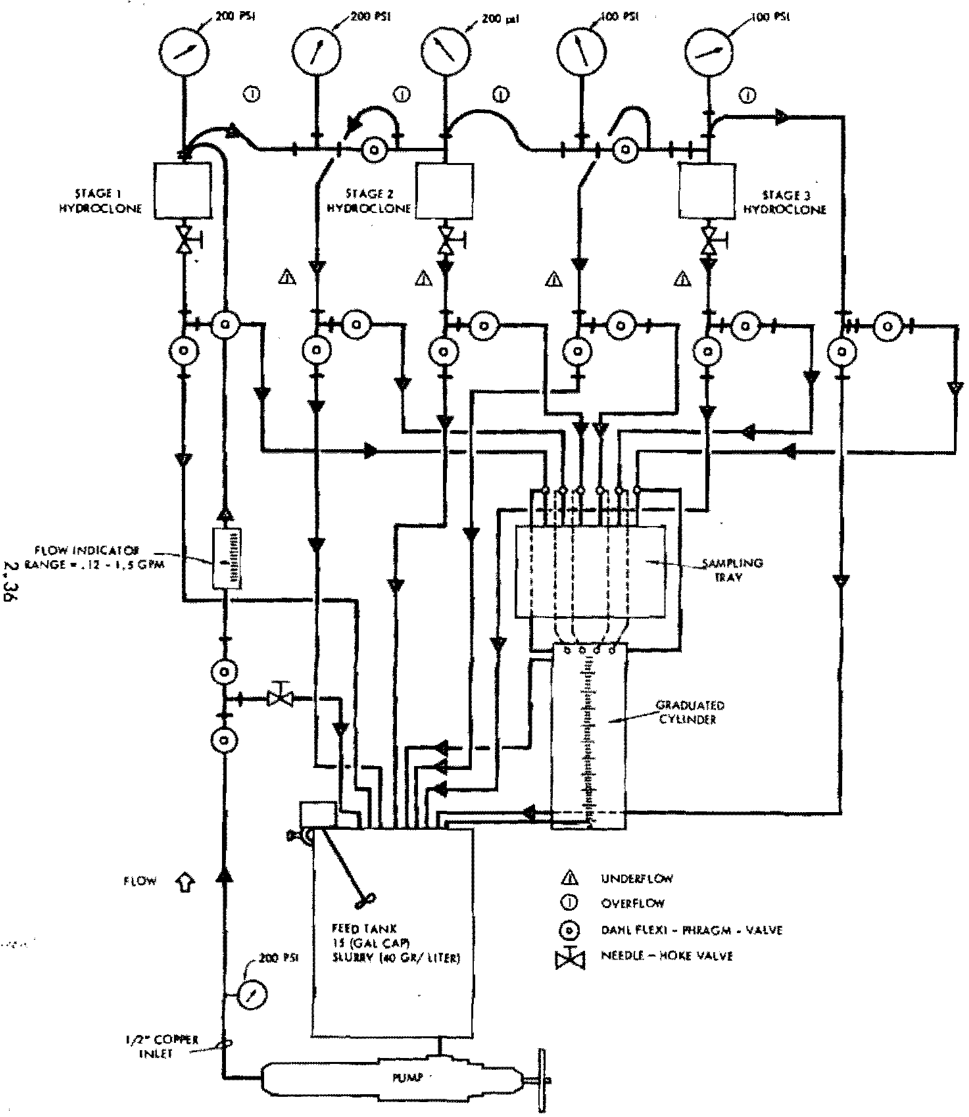

FIGURE 2.23 FLOW DIAGRAM OF HYDROCLONE WATER TEST SYSTEM

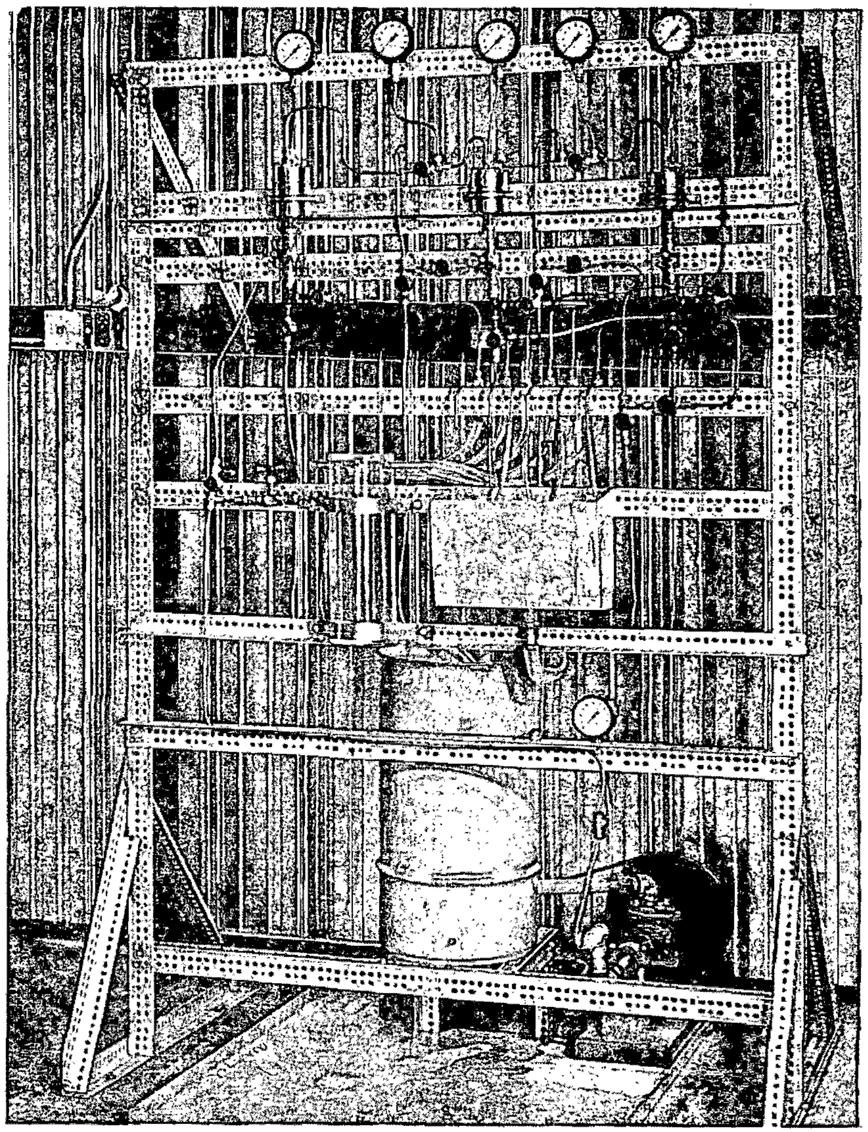

FIGURE 2.24 HYDROCLONE WATER TEST SYSTEM

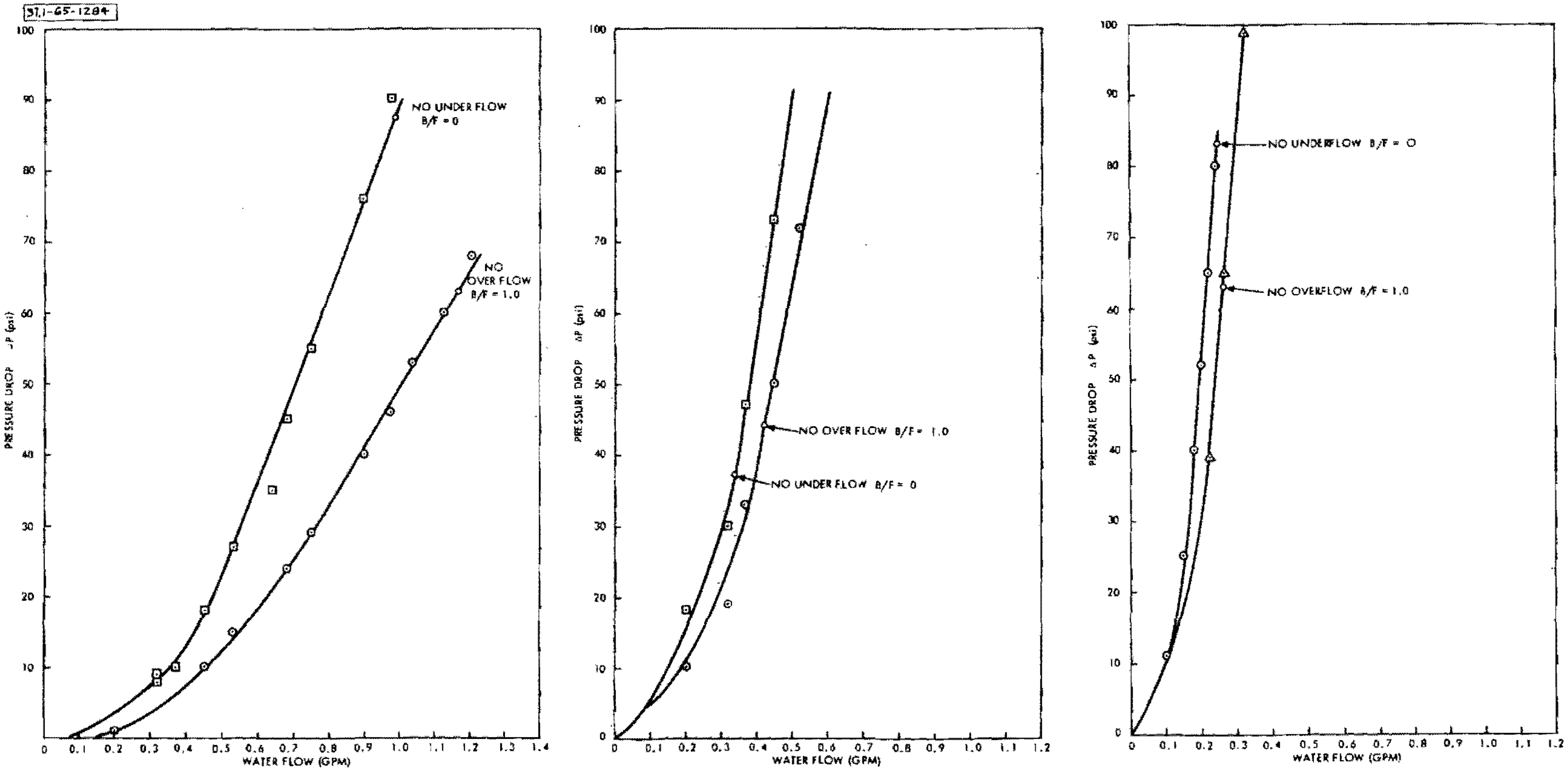

0.4 in. DIAMETER

0.25 in. DIAMETER

0.16 in. DIAMETER

FIGURE 2.25 FLOW VERSUS PRESSURE DROP FOR HYDROCLONES OF VARIOUS DIAMETERS

Separation tests using an aqueous UO_2 slurry were performed with the 0.40 in. and 0.25 in. hydroclones. The test system is shown schematically in Figure 2.26. The slurry was held in suspension in the 15-gal. slurry feed tank using a variable drive lightning mixer and pumped into the clone with a Moyno Model 3L2 screw pump. Test runs were made at set at pressure drops between 10 and 90 psi. Flow rate measurements and slurry samples of underflow and overflow were taken during each run. The hydroclones were operated at their natural B/F ratio for each ΔP.

Samples of the slurry feed were prepared and analyzed for particle size distribution. A typical photomicrograph showing the UO_2 is presented in Figure 2.27. Figure 2.28 gives the analysis of weight distribution; 50% of the fuel was less than 2.25 micron diameter and distributed normally on a logarithmic scale.

Table 2.3 gives the hydroclone test results. The removal efficiencies are plotted (and compared with predicted values taken from Figure 2.19) in Figure 2.29. The upper limit of the predicted efficiency was calculated from the Yoshioka and Hotta curve (3 to 6-in. clones) and the lower limit was calculated from the Bradley curve (0.39 in. clones). Both hydroclones performed best at low pressure drops; little was gained at pressure drops greater than 50 psi. The 0.4 in. hydroclone performed better than the 0.25 in. clone, and it also performed better than was predicted at pressure drops below 40 psi.

A single hydroclone fitted with an underflow receiver has been employed as a device for removing slurry from a circulating system[6]. This application was considered for final system cleanup during the early design phase of the in-reactor experiment. As can be seen from Equations 2.1, 2.3 and 2.4, a clone could be evaluated in such an apparatus by holding flow rates constant and sampling the slurry at intervals.

A system cleaning test was performed using the 0.40-in. hydroclone fitted with a 1.8 liter underflow receiver (Fig. 2.30). The hydroclone test system was modified as in the schematic of Figure 2.31. A slurry was prepared containing 1600 g of depleted, unfired UO_2 and 12.5 gal. of distilled water. The calculated slurry concentration was 33.8 g/l.

TABLE 2.3

HYDROCLONE TEST RESULTS

0.4-inch Hydroclone

		Flows (cc/sec)			Conc. g UO_2/1						
Run No.	P Psi	Feed	Under-Flow	Over-Flow	Feed	Under-Flow	Over-Flow	Clone d_{50}	$\frac{B}{F}$*	E** %	E_o*** %
1	10	24.0	19.0	5.0	25.6	31.4	3.6	1.66	0.793	97.0	85.6
2	20	33.6	29.6	4.0	29.2	32.6	2.3	1.38	0.880	98.6	92.9
3	30	38.3	31.2	7.1	26.4	35.4	3.8	1.25	0.815	98.2	90.4
4	60	57.6	46.7	10.9	28.9	34.8	3.7	1.05	0.810	97.6	87.4
5	90	67.2	58.3	8.9	36.8	32.6	2.3	0.760	0.860	99.1	93.3

0.25-inch Hydrocylone

1	20	14.4	9.3	5.1	19.6	28.8	3.0	1.02	0.645	94.6	84.9
2	30	17.9	11.4	6.5	24.2	28.4	3.7	0.937	0.635	93.4	82.6
3	40	19.4	12.4	7.0	21.5	32.1	2.7	0.876	0.640	95.4	87.4
4	60	22.6	15.4	7.2	21.6	30.0	3.7	0.787	0.682	94.6	80.8

* $\frac{B}{F}$ = underflow/feed flow

** $E = \frac{UO_2 \text{ leaving underflow}}{UO_2 \text{ entering feed}} (100)$

*** E_o = calculated from E using $E = E_o + \frac{B}{F}(1-E_o)$

371-65-1307

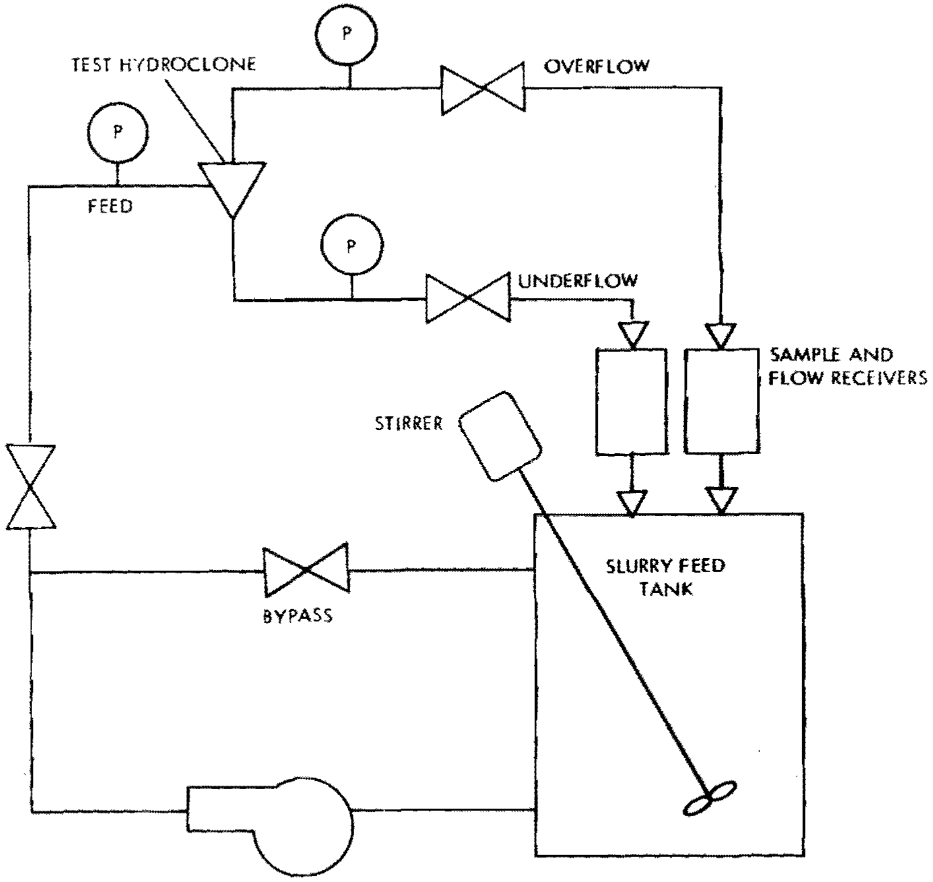

FIGURE 2.26 SCHEMATIC DIAGRAM OF SINGLE HYDROCLONE TEST SYSTEM

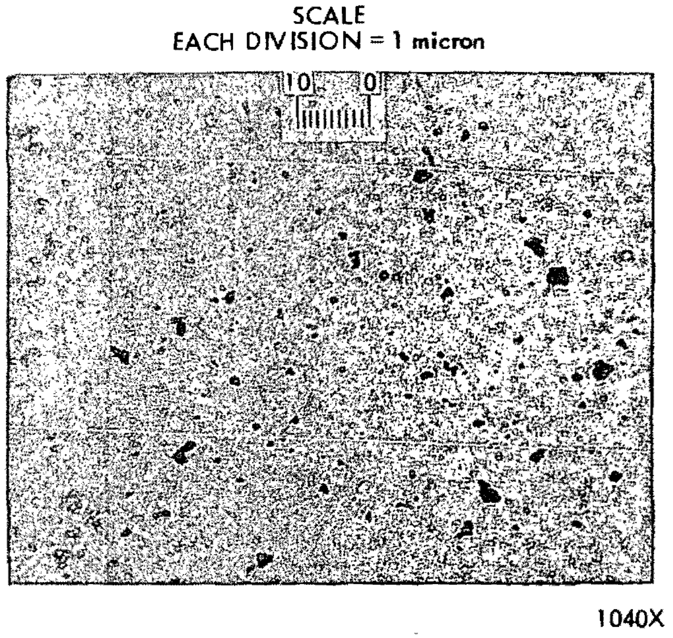

FIGURE 2.27 PHOTOMICROGRAPH OF SLURRY PARTICLES
PRIOR TO REMOVAL TEST

37.1-65-1294

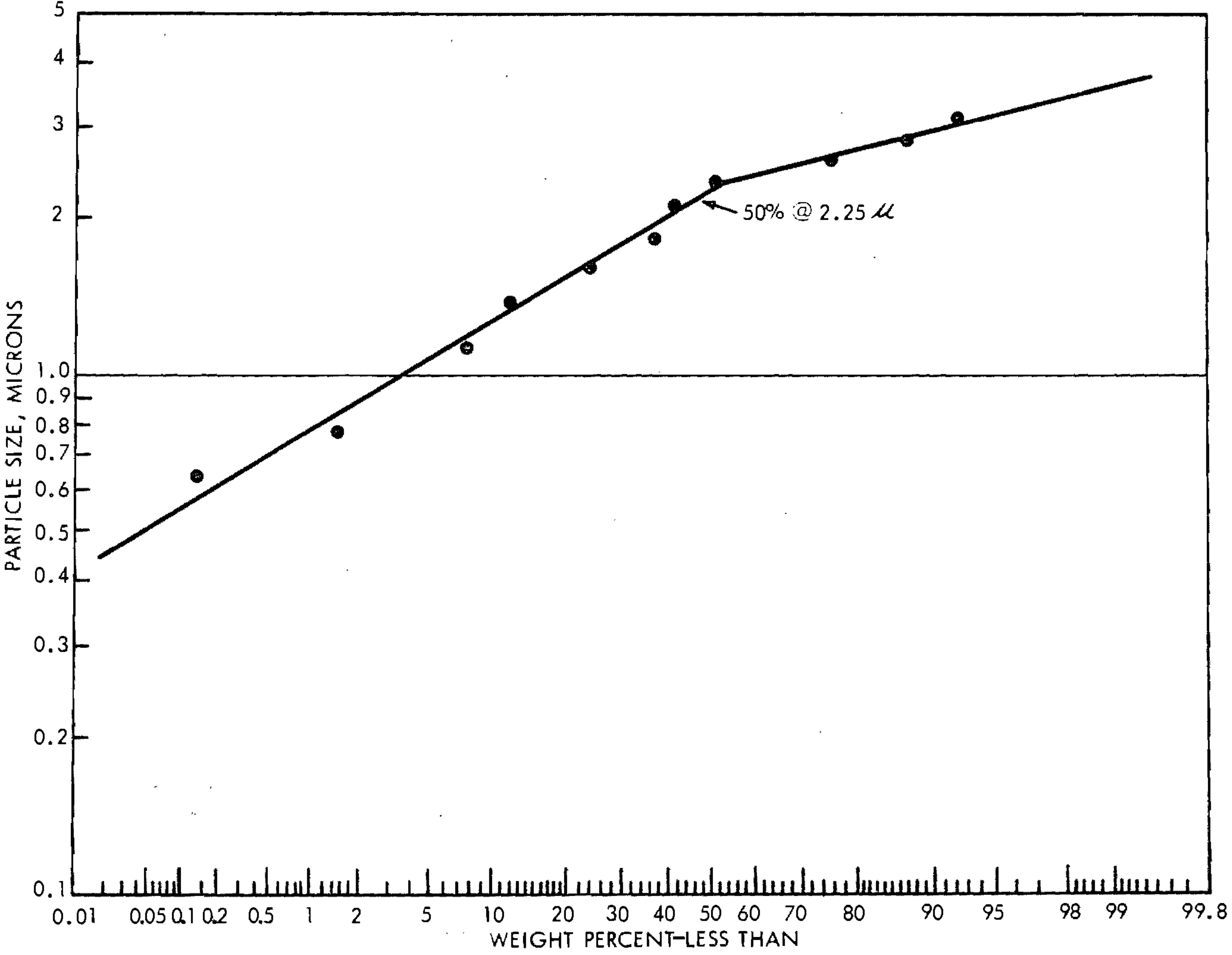

FIGURE 2.28 WEIGHT DISTRIBUTION OF FEED SLURRY

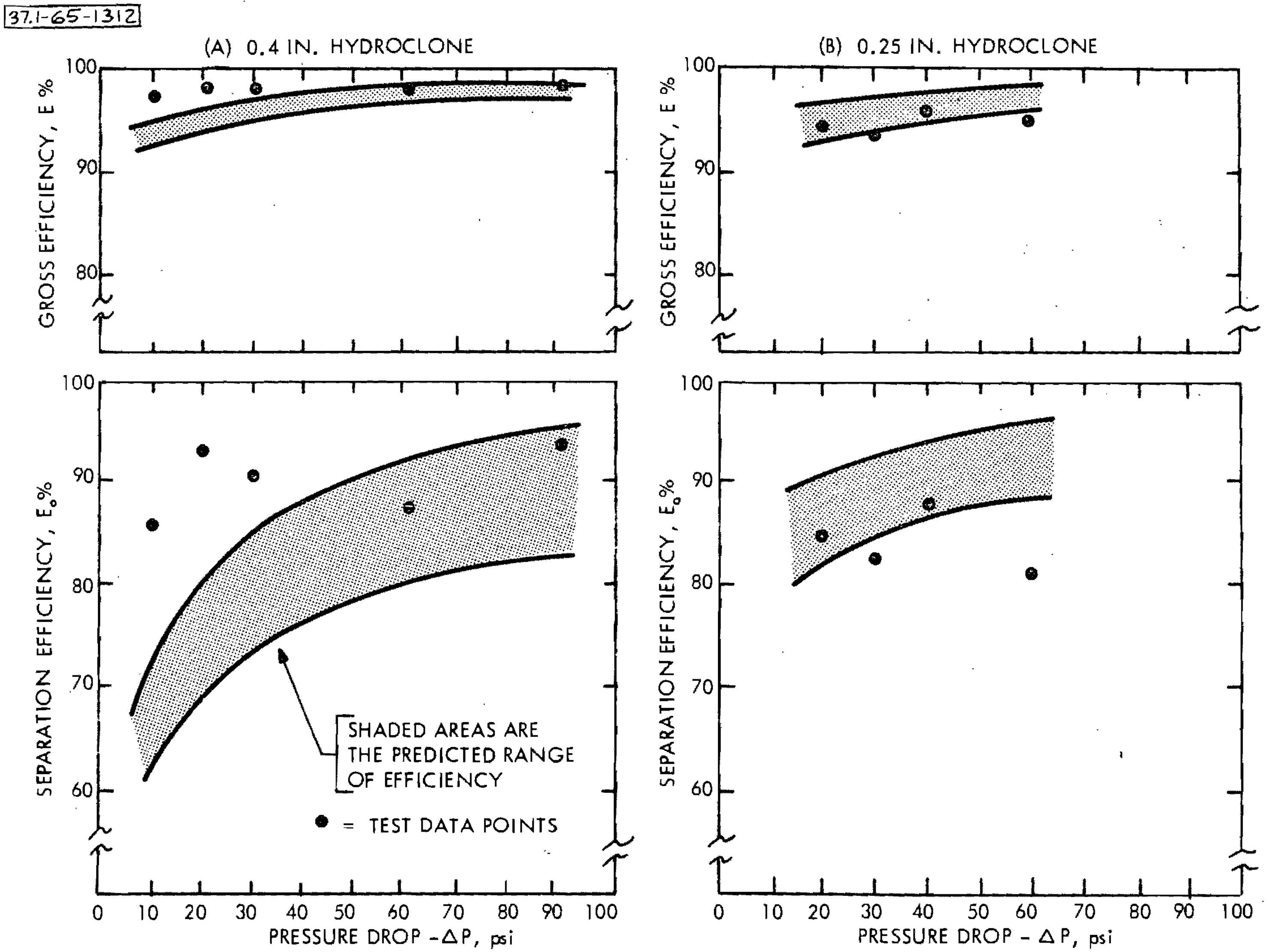

(A) 0.4 IN. HYDROCLONE

(B) 0.25 IN. HYDROCLONE

SHADED AREAS ARE THE PREDICTED RANGE OF EFFICIENCY

FIGURE 2.29 HYDROCLONE TEST AND PREDICTED EFFICIENCIES

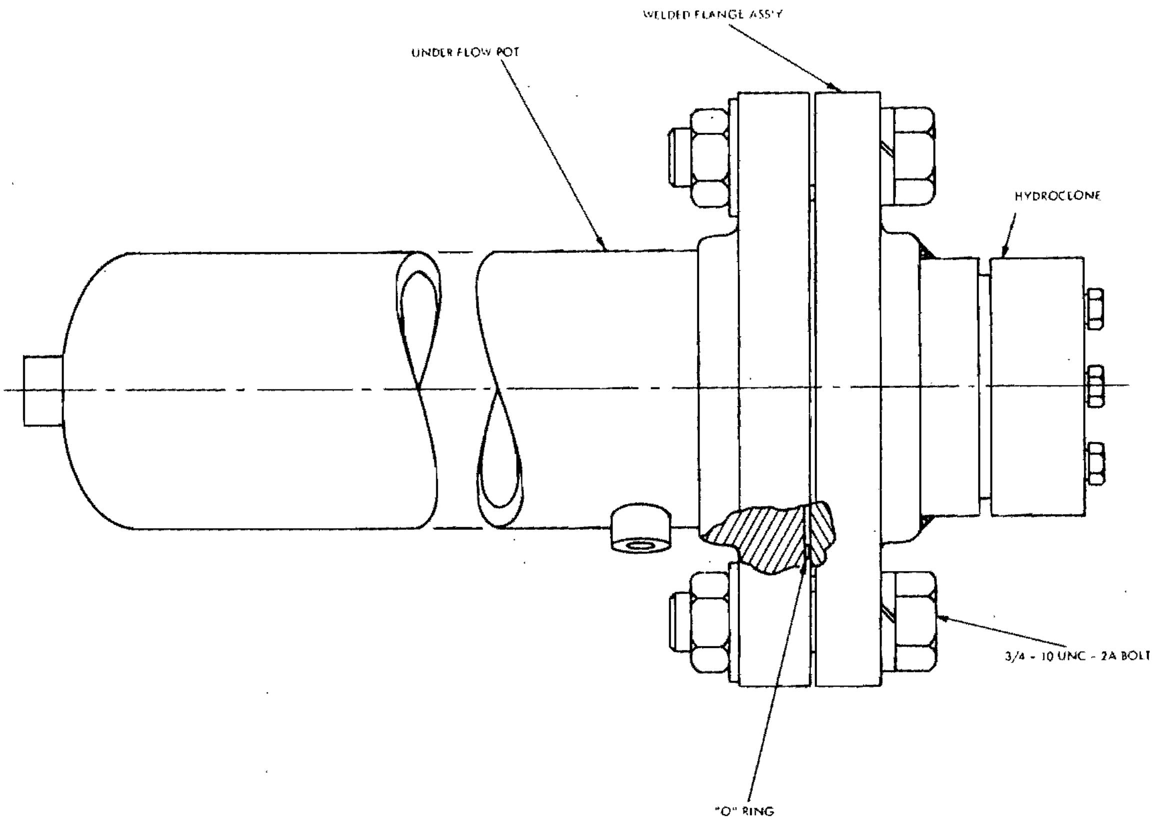

FIGURE 2.30 HYDROCLONE UNDERFLOW RECEIVER ASSEMBLY

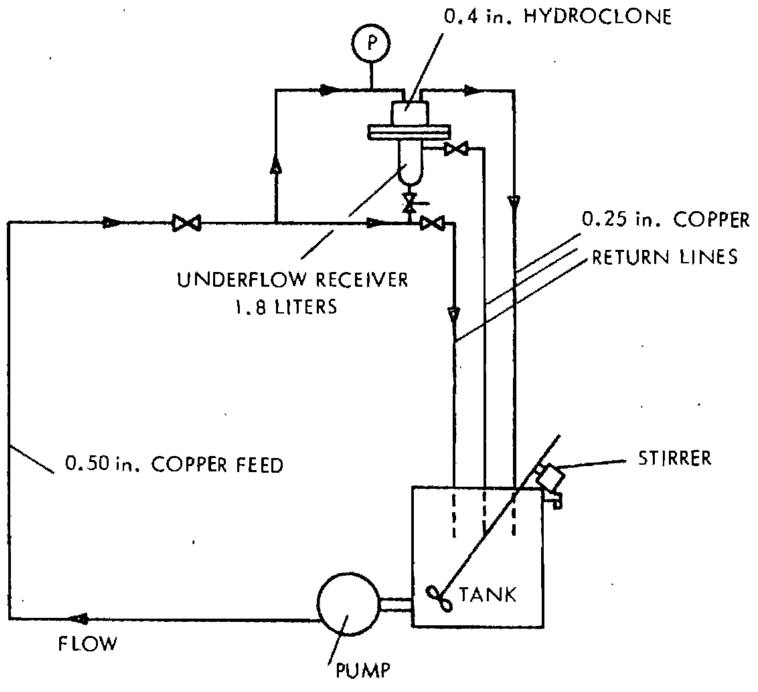

FIGURE 2.31 0.4 in. HYDROCLONE WITH 1.8 liter BATCH UNDERFLOW RECEIVER

Slurry samples were taken from several levels in the tank for particle size analysis and slurry concentration. The slurry was pumped through the hydroclone at 0.5 gpm giving a pressure drop of 90 psi across the clone. Slurry samples were taken from the tank periodically during the 15 hr run.

Figure 2.32 shows the particle size analysis. The results of the run are presented in Table 2.4 and Figure 2.33. The slurry concentration was found to be 24.6 g/l at all tank levels sampled; this indicated a loss of 9.2 g/l. When the test system was disassembled and cleaned, UO_2 was found in the pump suction, the rotameter, and valve bodies. These deposits qualitatively explained the discrepancy between calculated and observed slurry concentration. The substantial difference between the measured and predicted removal rates is believed due, in part, to the slow resuspension of slurry which had deposited. Other factors which may have contributed to the discrepancy are that equations 2.1 and 2.3 had been confirmed only for pressure drops up to 50 psi, rather than the 90 psi which was employed in this test, and the calculation of removal rate was based on the assumption of a single 1.65 micron diameter particle size rather than on a multigroup calculation. Both of these factors are considered to be of a much smaller magnitude in their effect than the slow resuspension of UO_2.

TABLE 2.4

RESULTS OF SLURRY REMOVAL RUN USING THE HYDROCLONE AND UNDERFLOW RECEIVER

Sample	Time of Sample, hr	Total Number of System Volumes Processed, Cycles	System Slurry Concentration, g/liter	Percent of Slurry Removed
1	0	0	24.6	0
2	4.8	11.5	5.0	79.6
3	10.0	24.2	1.7	90.0
4	14.3	35.4	1.3	94.7

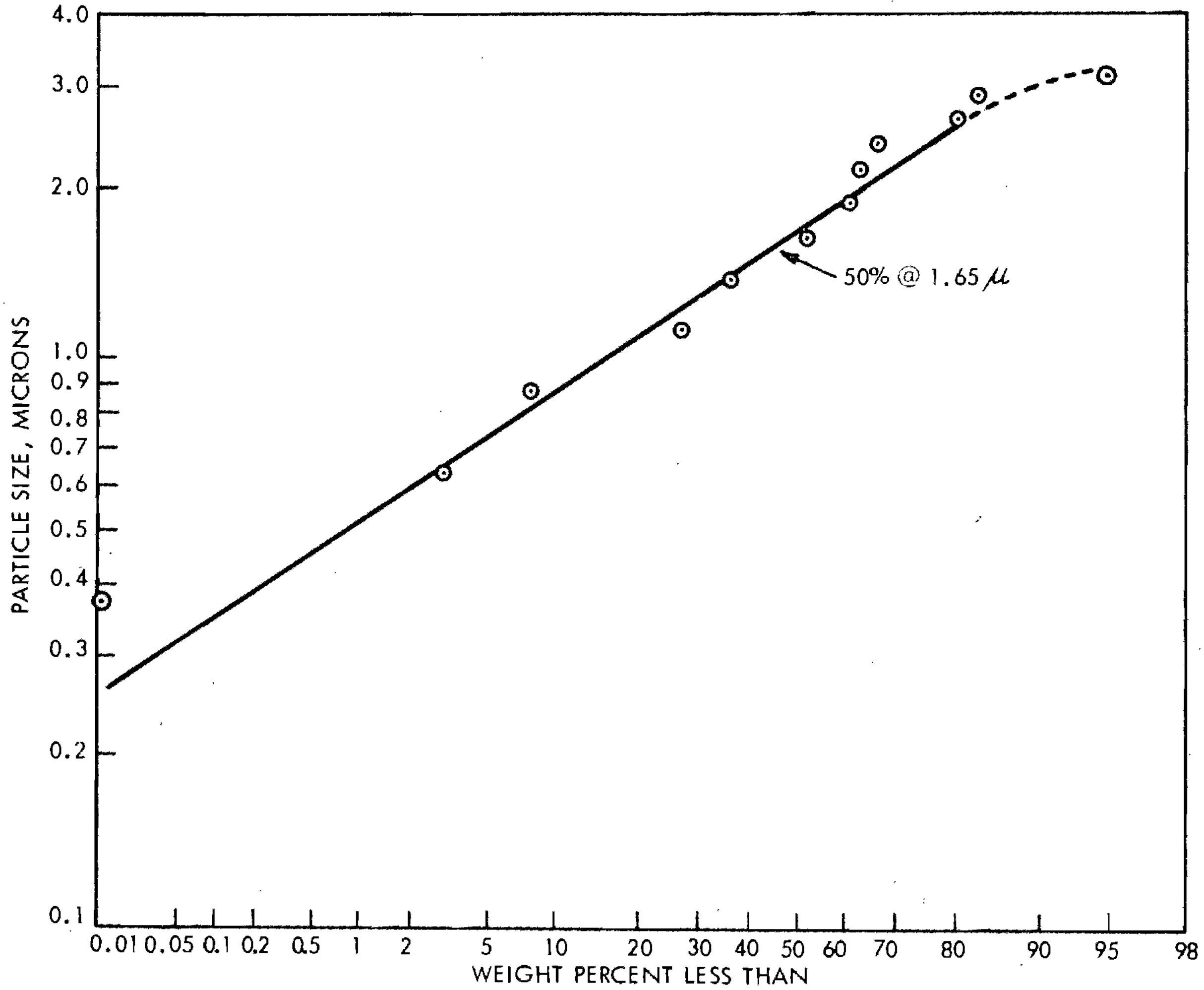

37.1-65-1293

FIGURE 2.32 WEIGHT DISTRIBUTION FOR INITIAL TEST SLURRY

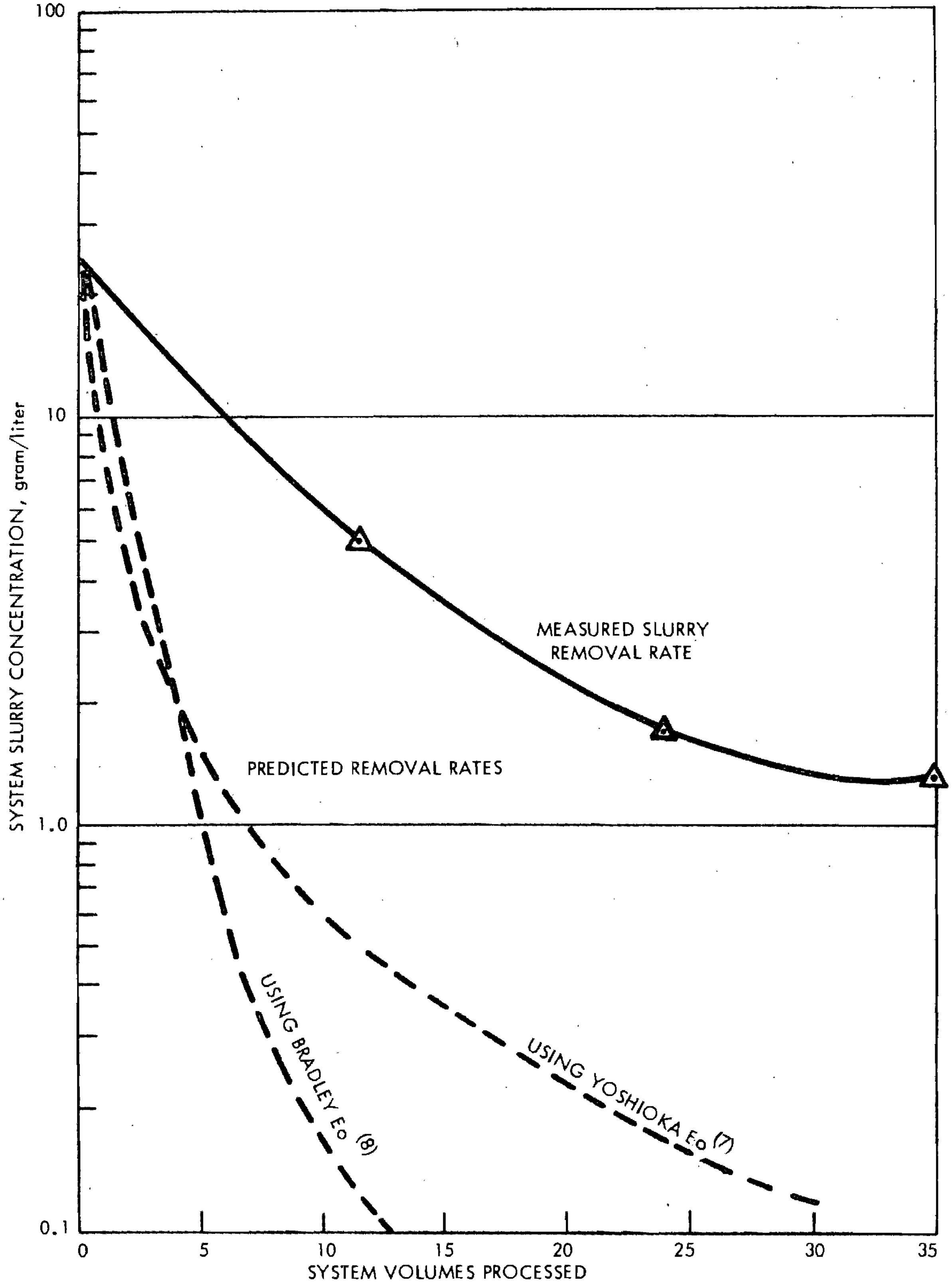

FIGURE 2.33 REMOVAL OF SLURRY PARTICLES USING A HYDROCLONE WITH UNDERFLOW RECEIVER

37.1-65-1309

2.3.4 General Remarks

This test series illustrated the magnitude of difficulty in the sampling and particle size analysis associated with performing slurry separation tests using hydroclones. The techniques involved in these aspects of the task were not fully mastered during this brief test. It was apparent that the development of a hydroclone for ammonia-UO_2 slurry would require more (and higher level) effort than could be expended appropriately on this portion of the program.

Hydroclones could be used in slurry systems to alter the particle size distribution or the slurry concentration. Potential application of this characteristic would be to optimize the performance of a filter; i.e., if fines tend to plug a filter, the filter could be placed downstream from the underflow of a hydroclone to minimize the problem. Another hypothetical application would be in the area of fuel processing; i.e., if fines are found to carry the preponderance of fission products, the fuel processing stream could be taken from the overflow of a hydroclone. Hydroclones (even in cascade) will not be sufficient to remove all the particles of any given size from a slurry stream.

2.4 Separation of Hydrazine from Ammonia

2.4.1 Introduction

The reference method of performing the separation of dilute hydrazine product from the ammonia feed was by evaporation. Hydrazine and ammonia are mutually soluble in any proportion, but the normal boiling point of hydrazine is 236° F while that of ammonia is -28°F which provides an easy separation by evaporation. The evaporator was to be designed to operate continuously from a clarified feed and to yield a bottoms product containing 10% by weight of hydrazine in ammonia. Further concentration and decontamination of the hydrazine was to be performed in the laboratory on a batch basis.

A competing separation method was by distillation using a packed column. The bottoms product from a distillation column would have a composition of approximately 95% by weight of hydrazine with only 5% ammonia. The distillation column was to be designed to operate continuously from a clarified feed.

Under the reference separation method, ammonia must be vaporized and recondensed prior to return to the reactor; a large heating and cooling load is required in the over-all process. Potentially superior separation methods might result from removal of hydrazine from the crude product fluid leaving behind liquid ammonia which could be directly recycled to the reactor.

The following four methods appear potentially feasible and are individually discussed in the following sections:

(1). Liquid-liquid extraction
(2) Hydrazination of an insoluble salt
(3) Hydrazination by replacement in an insoluble coordinated salt
(4) Molecular sieve retaining hydrazine but passing ammonia.

2.4.1.1 Liquid-Liquid Extraction

When a dilute stream of hydrazine in ammonia-water mixtures is acted upon by liquid benzaldehyde, the quantitative conversion of hydrazine into benzalzine occurs,[10,11]

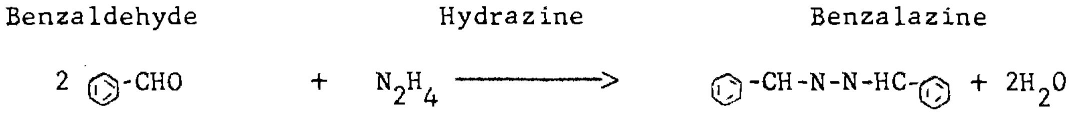

This product is insoluble in ammonia and dissolves in excess benzaldehyde.

Counter current liquid-liquid extraction equipment may be used to effect this reaction, with benzaldehyde flowing downward to hydrazine recovery and ammonia flowing upward to reactor recycle. The benzaldehyde bottoms would then be mixed with water and sulfuric acid in a still pot; reformed benzaldehyde and excess water would be distilled off. The benzaldehyde could be condensed and reused. Cooling the remaining pot liquid would precipitate hydrazine sulfate, which could be filtered and dried. The addition of anhydrous liquid ammonia to the hydrazine sulfate would free hydrazine and form insoluble ammonium sulfate. Any excess ammonia in solution with hydrazine could be distilled off, leaving hydrazine.

The water formed in the reaction will quickly react with ammonia to form ammonium hydroxide. Hence, recycling the ammonia-ammonium hydroxide stream will result in a steady increase in the water content of the stream. Furthermore, reaction between hydrazine and water may occur and retard the conversion of hydrazine to benzalazine. Hence, a means of removing the water must be found to make this method technically feasible. If successful dehydration methods must involve an energy expenditure not significantly lower than the evaporation-distillation reference method, then the use of extraction as a separation method may not be justified.

The solubility of benzaldehyde in ammonia is unknown, and would have to be determined. Means of removing this benzaldehyde from ammonia are also subject to investigation. In addition, other liquid extractants, notably organophosphoric compounds, should be examined for their ability to recover hydrazine from ammonia.

2.4.1.2 Hydrazination of Insoluble Salt

If hydrazine selectively forms a hydrazinate (rather than ammonia forming an ammoniate) with an insoluble, nonreactive salt, and if this salt complex is also insoluble in ammonia, then such a salt may be the basis of a feasible method of hydrazine separation. For example, anhydrous zinc sulfate forms an insoluble hydrazinate[12]. However, the solubility in ammonia, and the ammoniate-forming ability of zinc sulfate are currently unknown. Final separation of the complex to reclaim the purified hydrazine and dry salt might be accomplished by simple heating in vacuum.

2.4.1.3 Hydrazination by Replacement in an Insoluble Coordination Salt

Hydrazine might be recovered in a form that is insoluble in ammonia by using the ammonia-hydrazine liquid medium to effect a hydrazination by replacement in an insoluble coordinated salt.

It has been shown that while hydrazine sulfate reacts with anhydrous ammonia to give free hydrazine and the corresponding insoluble ammonium sulfate, hydrazine mono and diphosphate do not[13]. Hence a dilute solution of hydrazine in ammonia may react with insoluble ammonium phosphate in a replacement reaction which would liberate ammonia to the bulk stream and fix the hydrazine as insoluble hydrazine phosphate.

2.4.1.4 Molecular Sieves

The feasibility of using a molecular sieve material, Linde AW-500, was tested by determining if it would selectively adsorb hydrazine and if hydrazine could be recovered from it with little decomposition.

A schematic diagram of the apparatus used is shown in Figure 2.34. Two runs were performed. In each the apparatus was cleaned and evacuated, the test sampler was filled with sieve material, and the storage bomb was filled with a hydrazine-ammonia solution of about 6% by weight. Pressure within the apparatus was equalized by opening all internal valves except V5. At this point the test sampler became warm during each run, probably indicating that ammonia was adsorbing onto the sieve material. When the test sampler had cooled, V5 was opened to fill the test sampler with liquid test solution from the storage bomb. The test sampler was then isolated and allowed to equilibrate. During the three day equilibration period of the first run, the pressure rose from 135 to 195 psig indicating a calculated decomposition of less than 3% of the hydrazine in the test sampler (assuming that all the pressure increase is due to hydrazine decomposition). For the second run the test sampler was allowed to equilibrate only until the sampler cooled to room temperature again; no pressure rise was noted. The liquid was then drained from the test sampler and analyzed for both ammonia and hydrazine. The test sampler was heated to 120-150° F under vacuum for 20 min.; the vaporized contents were collected in a trap cooled by liquid nitrogen and analyzed for hydrazine. The sieve material was then washed with acid and the wash was analyzed for hydrazine. Table 2.5 gives the results of these runs.

The results show clearly that the hydrazine-ammonia solution exposed to the molecular sieve material became depleted in hydrazine, and that very little of this hydrazine was decomposed. The second run showed that the hydrazine was strongly associated with the sieve material and could not be removed effectively by heat and vacuum, but could be removed by acid wash.

These brief tests demonstrated that molecular sieves may have application in separating hydrazine from ammonia, but that difficulties in the non-destructive removal of hydrazine from the sieve material may limit this process.

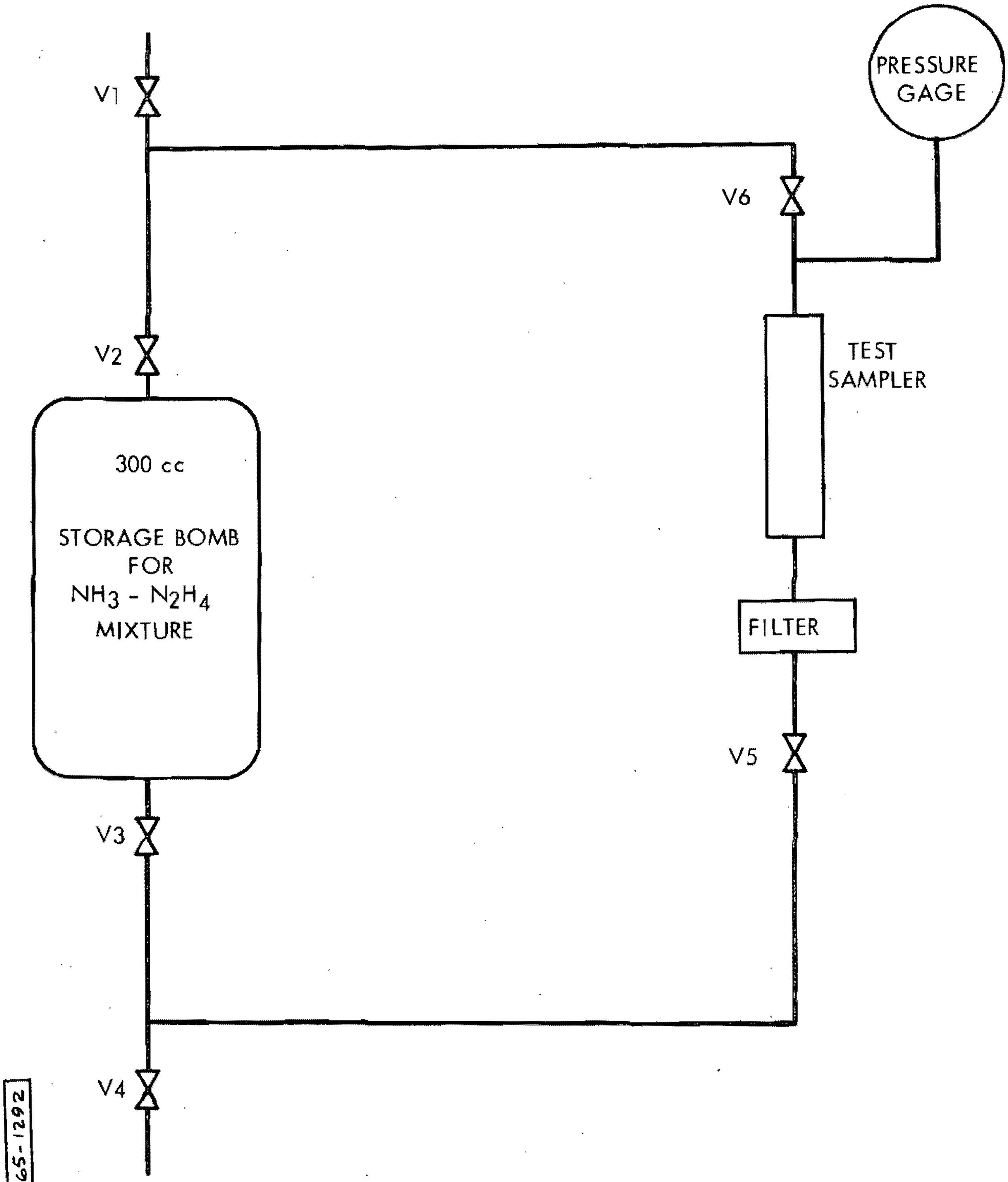

371-65-1292

FIGURE 2.34 SCHEMATIC DIAGRAM OF TEST ASSEMBLY USED IN HYDRAZINE-AMMONIA SEPARATION STUDIES

TABLE 2.5

MOLECULAR SIEVE TEST RUNS

	First Run	Second Run
Storage solution (wt % N_2H_4)	6.13	6.26
Solution drained from test sampler (wt % N_2H_4)	2.2	3.52
Total hydrazine adsorbed (calculated)(g)	-	0.18
Hydrazine recovered by heating (g)	-	0.007
Hydrazine recovered in acid wash (g)	0.005	0.15

2.4.2 Vapor-Liquid Equilibrium Data

In order to calculate any distillation, vaporization, or condensation problem, it is necessary to know the vapor-liquid equilibrium constant, K, over the temperature, pressure, and composition range of interest.

Preliminary vapor-liquid equipment data for the ammonia-hydrazine system was obtained from the literature. The data show that, in the ammonia-hydrazine system, the liquid phase activity coefficient for hydrazine varies considerably at low concentrations. The vapor phase activity coefficient varies widely for both hydrazine and ammonia. Because of the high pressure of the system, the fugacity of ammonia becomes an important consideration.

Previously reported data[14] were analyzed using the following relationships where:

Y = mol fraction of a component in the vapor phase

X = mol fraction of a component in the liquid phase

K = vapor-liquid equilibrium ratio

P = vapor pressure of the pure component, (psia)

π = total system pressure, (psia)

f_p = fugacity of a component as a pure saturated liquid (or vapor) of a vapor pressure corresponding to the system temperature, (psia)

f_π = fugacity of a component as a pure vapor at the equilibrium temperature and pressure of the system, (psia)

ϕ = fugacity coefficient obtained from generalized correlation using reduced pressure and reduced temperature. ϕ_L = the liquid phase, and ϕ_v = the vapor phase.[15,16,17]

f = fugacity function (psia)

γ = liquid phase activity coefficient

The conventional K value was derived from the equation:

$$K = \frac{Y}{X} \quad . \tag{2.5}$$

Ideally,

$$K = \frac{Y}{X} = \frac{P}{\pi} \quad . \tag{2.6}$$

However, since the system is not ideal, fugacity must replace vapor pressure:

$$\phi_L P = f_p \text{ (for the liquid)}, \tag{2.7}$$

and the system pressure must be replaced with fugacity (vapor phase activity coefficient):

$$\phi_v \pi = f_{\pi} \tag{2.8}$$

Thus:

$$K = \frac{Y}{X} = \frac{f_p}{f_{\pi}} \quad . \tag{2.9}$$

To simplify the graphs, ϕ_L and ϕ_v may be combined by defining the fugacity function as:

$$f = \frac{\phi_L P}{\phi_v} \quad . \tag{2.10}$$

Thus:

$$K = \frac{Y}{X} = \frac{f}{\pi} \quad . \tag{2.11}$$

Equation 2.11 takes into account compressibility and vapor activity, but not composition. The small error in fugacity may be absorbed into the liquid phase activity coefficient, γ .

$$\gamma = \frac{x\pi}{Xf} \quad . \tag{2.12}$$

Then γ can be calculated using Equation 2.12.

The X, Y, and π for this calculation were taken from Drago and Sisler[14] and f was calculated using Equation 2.10. The results of these calculations for ammonia and hydrazine are given in Tables 2.6, 2.7, 2.8, and 2.9 and in Figures 2.35 through 2.38.

Using these results, the value of K at various temperatures, pressures, and compositions can be calculated by the following equation:

$$K = \frac{Y}{X} = \frac{\gamma f}{\pi} . \qquad (2.13)$$

2.4.3 Evaporator

The evaporator was designed to process a 1% hydrazine-99% ammonia solution at a feed rate of 0.008 to 0.043 gpm. A schematic diagram of the apparatus is given in Figure 2.39. Instrument control governed the normal operation; test conditions were varied by changing the set points. Control was applied to feed flow rate by a flowmeter, to evaporator liquid temperature by a heater controller, and to evaporator pressure by a pressure regulated vent.

The evaporator was operated at 96° F to 100°F and at 185 psig. Heat was applied only while the heating coils were completely immersed. Product was withdrawn periodically during sustained operation to prevent overfilling the evaporator.

Six experimental runs were performed using this evaporator. Operation and control was uncomplicated and smooth. Sampling the bottoms gave no problem, but sampling the overhead vapors, while operationally successful, gave extremely erratic results. The problem was traced to unavoidable oxides in the metal samplers reacting with the low amount of hydrazine present in the vapor. Overhead sampling was somewhat more successful using specially cleaned samplers.

The experimental value measured for the activity coefficient of hydrazine was 2.70 compared with the theoretical value of 3.35. This discrepancy indicates a lower-than-theoretical amount of hydrazine and is attributed primarily to continuing sampling problems rather than inaccuracies in the theoretical value.

TABLE 2.6

LIQUID PHASE ACTIVITY COEFFICIENT FOR NH_3 (IN HYDRAZINE)

Temp. °F	π System Press. psia	Mol Fract. NH_3 in Liquid x	Mol Fract. NH_3 in Vapor y	NH_3 f psia	NH_3 Liquid Phase Act.Coef. γ
191.5	685	.9571	.99805	700	1.020
191.5	564	.8107	.99327	676	1.022
191.5	558	.8011	.99177	670	1.031
191.5	495	.7043	.99158	652	1.069
191.5	464	.6407	.99009	640	1.120
191.5	380	.5171	.9867	622	1.166
191.5	323	.4123	.9833	618	1.2464
191.5	273	.3435	.9799	602	1.2936
191.5	273	.3419	.9797	602	1.3172
191.5	214	.2470	.9764	595	1.4217
191.5	198	.2242	.9751	585	1.4720
212.5	853	.9514	.99685	900	.9930
212.5	793	.9031	.99499	872	.9510
212.5	790	.9000	.99462	872	.9977
212.5	787	.8946	.99463	872	1.0034
212.5	705	.8035	.99099	850	1.0229
212.5	564	.6321	.9858	805	1.0926
212.5	467	.5112	.9824	778	1.1535
212.5	389	.3979	.9780	755	1.2663
212.5	329	.3236	.9726	750	1.3184
212.5	326	.3180	.9723	750	1.3290
212.5	259	.2420	.9680	730	1.4191
212.5	223	.2049	.9634	725	1.4462

TABLE 2.7

LIQUID PHASE ACTIVITY COEFFICIENT FOR N_2H_4

Temp. °F	π System Press. psia	Mol Fract. N_2H_4 in Liquid x	Mol Fract. N_2H_4 in Vapor y	N_2H_4 f psia	N_2H_4 Liquid Phase Act.Coef. γ
191.5	685	.0429	.00195	9.50	3.278
191.5	564	.1893	.00673	8.60	2.332
191.5	558	.1989	.00823	8.55	2.700
191.5	495	.2957	.00842	8.30	1.698
191.5	464	.3593	.00991	8.10	1.580
191.5	380	.4829	.0133	7.65	1.368
191.5	323	.5877	.0167	7.5	1.224
191.5	273	.6565	.0201	7.2	1.1608
191.5	273	.6581	.0203	7.2	1.1695
191.5	272	.6640	.0203	7.2	1.1549
191.5	214	.7530	.0236	7.0	.9581
191.5	198	.7758	.0249	6.9	.9210
212.5	853	.0486	.00315	16.5	3.351
212.5	793	.0969	.00501	16.3	2.515
212.5	790	.1000	.00538	16.3	2.607
212.5	787	.1054	.00537	16.3	2.4599
212.5	705	.1965	.00901	16.0	2.0203
212.5	564	.3679	.0142	13.9	1.5661
212.5	467	.4888	.0176	13.0	1.293
212.5	389	.6021	.0220	12.2	1.1650
212.5	329	.6764	.0274	12.0	1.1105
212.5	326	.6820	.0277	12.0	1.1033
212.5	259	.7580	.0320	11.4	.9591
212.5	223	.7951	.0366	11.2	.9165

TABLE 2.8

FUGACITY FUNCTION OF AMMONIA

$$f = \frac{P\,(f_p/P)}{(f_\pi/\pi)}$$

System Press, π psia	System Temp. °F	Vapor Press, P psia	Critical Press, P_c psia	Reduced System Press. π/P_c	Reduced Vapor Press. P/P_c	System Temp. °R	Critical Temp, T_c °R	Reduced Temp. T_R	Vapor Press Fugacity Coef f_p/P	System Press. Fugacity Coef. f_π/π	Fugacity Function f
200	100	210	1657	.1207	.1267	560	731	.766	.895	.895	210
200	150	433		.1207	.2613	610		.834	.825	.915	390
200	200	795		.1207	.4798	660		.903	.755	.938	640
300	100	210		.1810	.1267	560		.766	.895	.850	221
300	150	433		.1810	.2613	610		.834	.825	.875	408
300	200	795		.1810	.4798	660		.903	.755	.908	661
400	100	210		.2414	.1267	560		.766	.895	.800	235
400	150	433		.2414	.2613	610		.834	.825	.836	427
400	200	795		.2414	.4798	660		.903	.755	.877	684
500	100	210		.3017	.1267	560		.766	.895	.755	249
500	150	433		.3017	.2613	610		.834	.825	.793	450
500	200	795		.3017	.4798	660		.903	.755	.848	708
750	100	210		.4526	.1267	560		.766	.895	.655	287
750	150	433		.4526	.2613	610		.834	.825	.705	507
750	200	795		.4526	.4798	660		.903	.755	.770	780
1000	100	210		.6035	.1267	560		.766	.895	.570	330
1000	150	433		.6035	.2613	610		.834	.825	.625	572
1000	200	795	↓	.6035	.4798	660	↓	.903	.755	.695	864

TABLE 2.9

FUGACITY FUNCTION OF HYDRAZINE

$$f = \frac{P\ (f_p/P)}{(f_\pi/\pi)}$$

System Press, π psia	System Temp. °F	Vapor Press, P psia	Critical Press, P_c psia	Reduced System Press. π/P_c	Reduced Vapor Press. P/P_c	System Temp. °R	Critical Temp, T_c °R	Reduced Temp. T_R	Vapor Press Fugacity Coef. f_P/P	System Press. Fugacity Coef f_π/π	Fugacity Function f
200	100	0.60	2130	.0938	0	560	1140	.491	1.0	.86	.698
200	150	2.25		.0938	0	610		.535	1.0	.865	2.601
200	200	7.30		.0938	0	660		.579	1.0	.873	8.38
300	100	0.60		.1408	0	560		.491	1.0	.795	0.755
300	150	2.25		.1408	0	610		.535		.805	2.795
300	200	7.30		.1408	0	660		.579		.820	8.902
400	100	0.60		.1877	0	560		.491		.740	0.811
400	150	2.25		.1877	0	610		.535		.755	2.980
400	200	7.30		.1877	0	660		.579		.773	9.444
500	100	0.60	2130	.2347	0	560	1140	.491	1.0	.687	.873
500	150	2.25	2130	.2347	0	610	1140	.535	1.0	.700	3.214
500	200	7.30	2130	.2347	0	660	1140	.579	1.0	.718	10.167
750	100	0.60	2130	.352	0	560	1140	.491	1.0	.580	1.035
750	150	2.25	2130	.352	0	610	1140	.535	1.0	.595	3.780
750	200	7.30	2130	.352	0	660	1140	.579	1.0	.615	11.850
1000	100	0.60	2130	.470	9	560	1140	.491	1.0	.495	1.213
1000	150	2.25	2130	.470	0	610	1140	.535	1.0	.510	4.420
1000	200	7.30	2130	.470	0	660	1140	.579	1.0	.532	13.700

37.1-65-1295

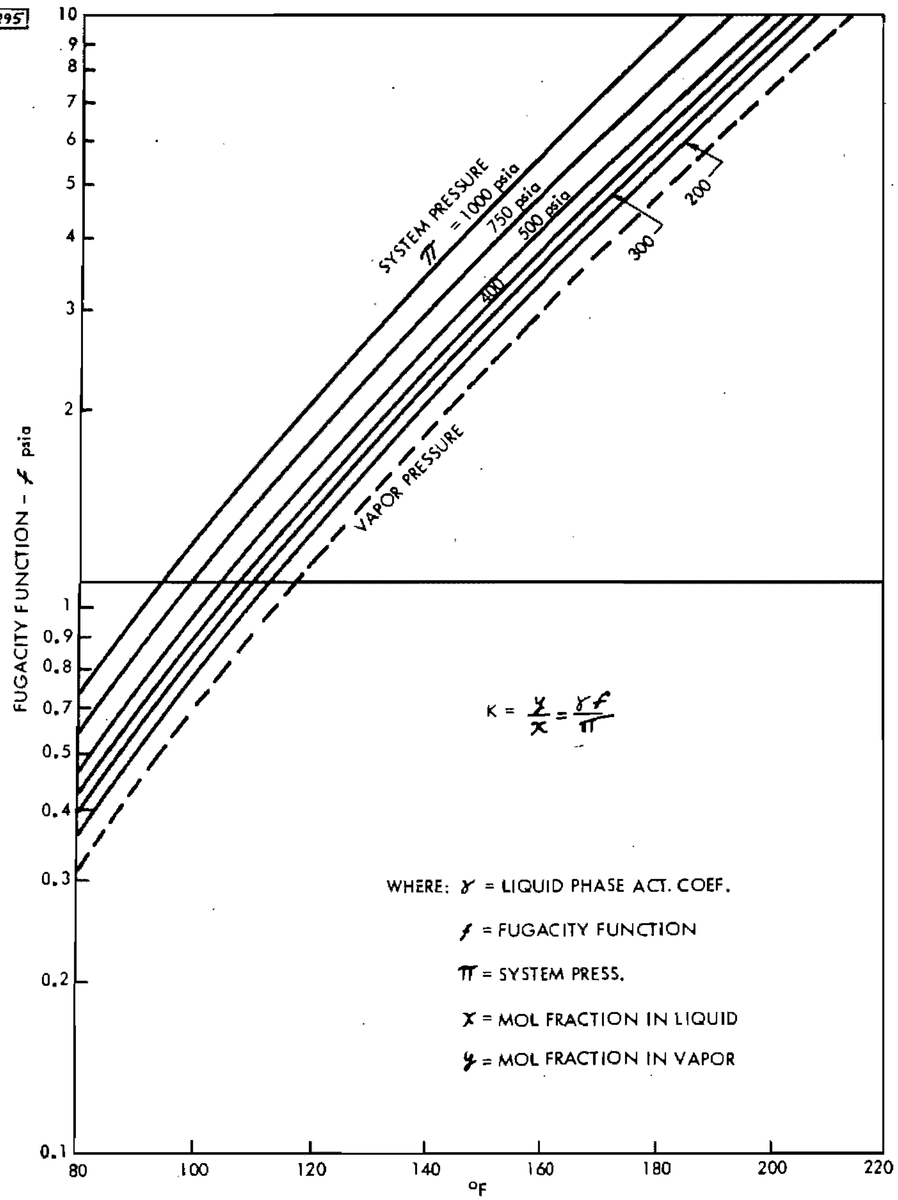

FIGURE 2.35 VAPOR PRESSURE AND FUGACITY OF HYDRAZINE

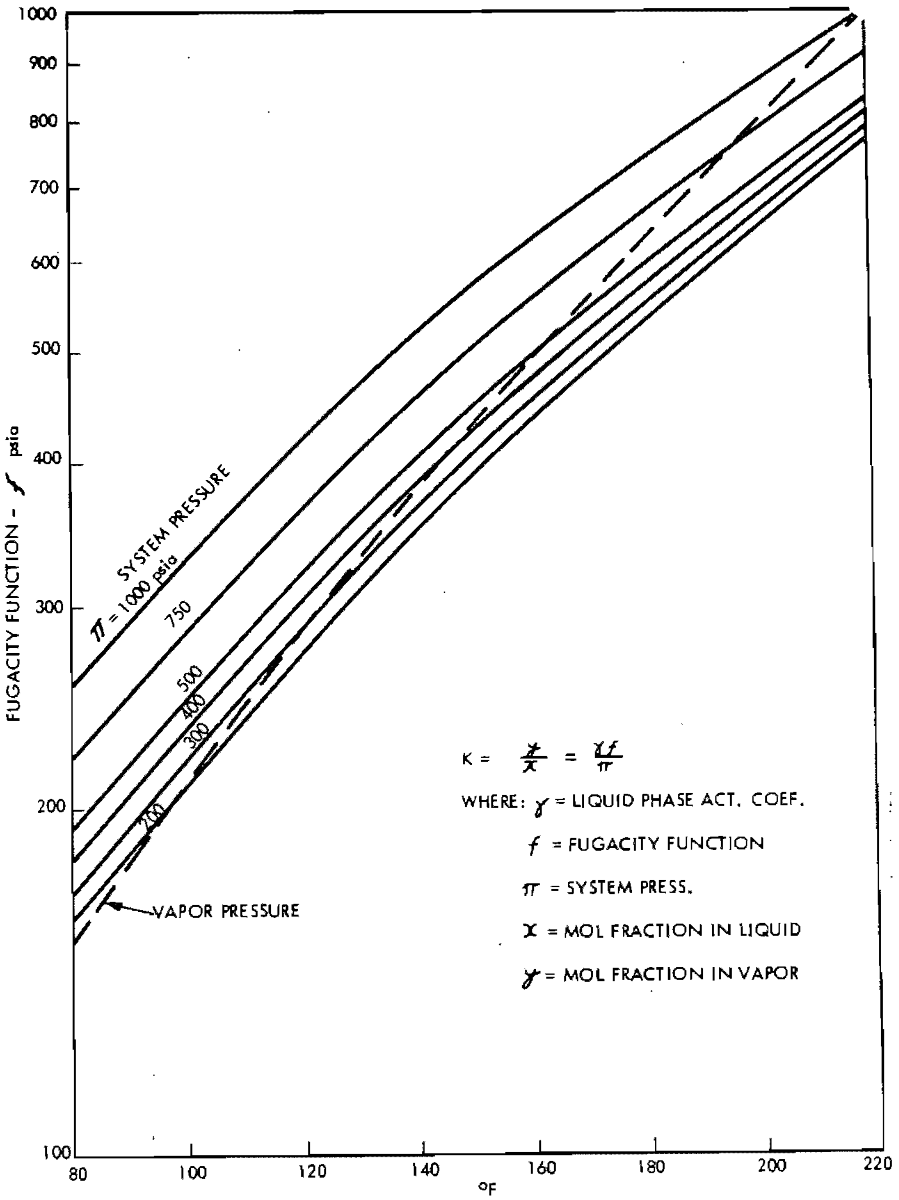

FIGURE 2.36 VAPOR PRESSURE AND FUGACITY OF AMMONIA

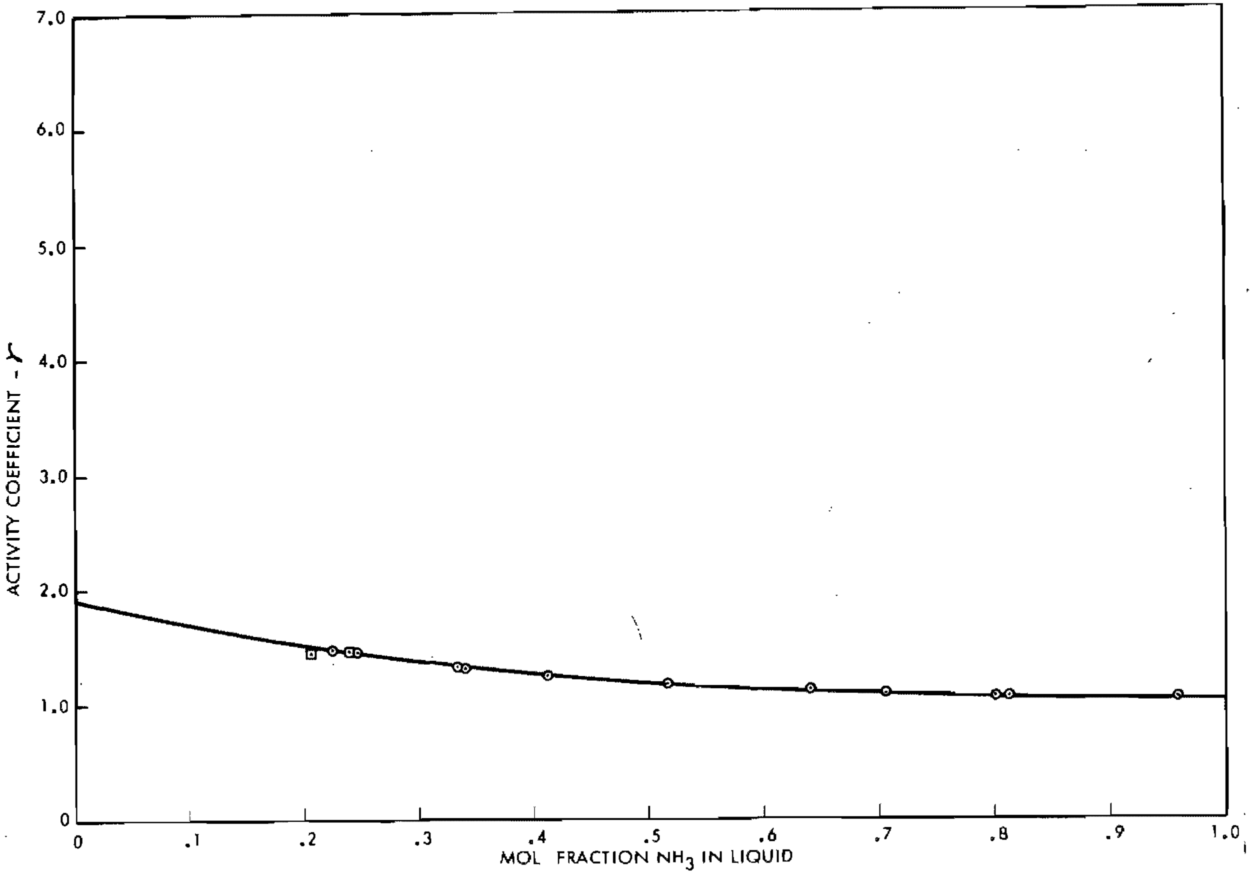

FIGURE 2.37 LIQUID PHASE ACTIVITY COEFFICIENT FOR AMMONIA

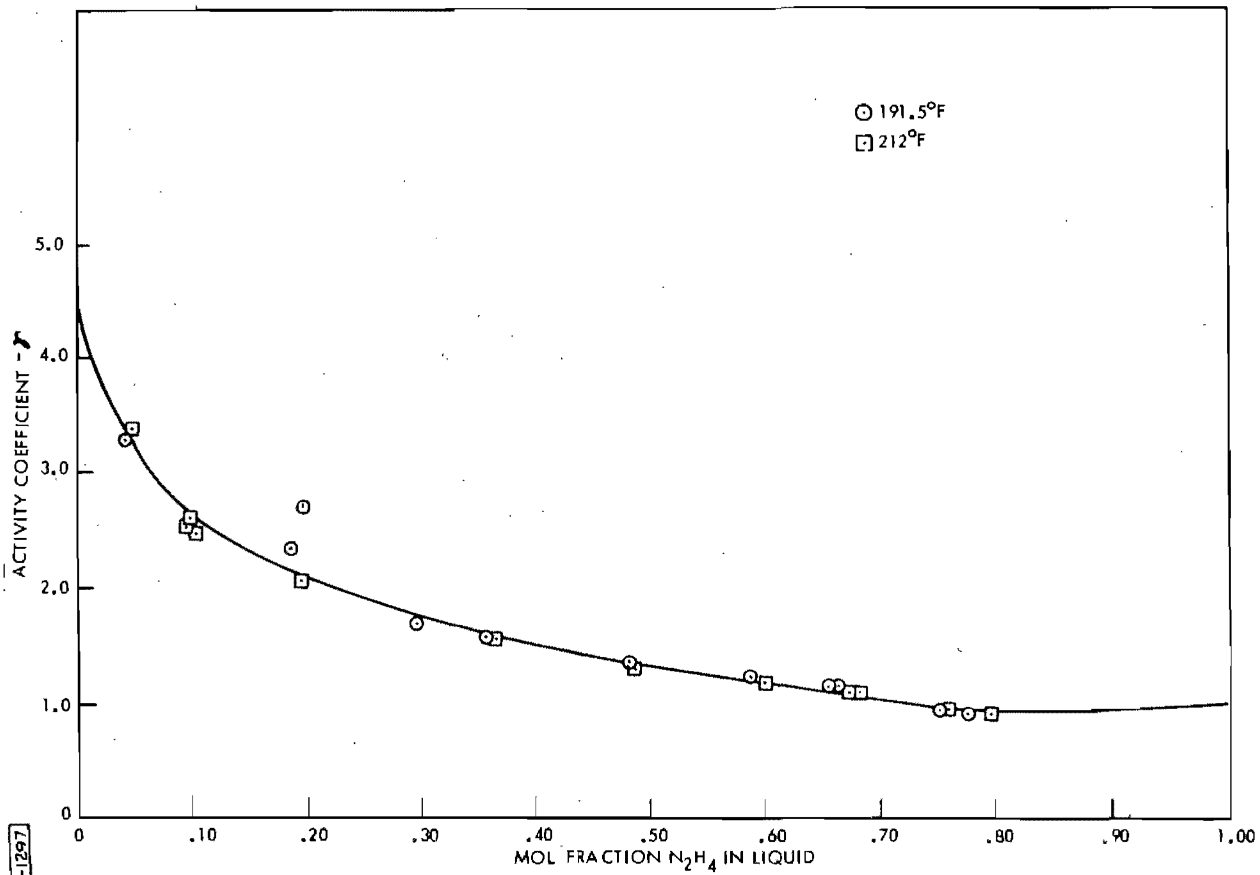

FIGURE 2.38 LIQUID PHASE ACTIVITY COEFFICIENT FOR HYDRAZINE

37J-65-1297

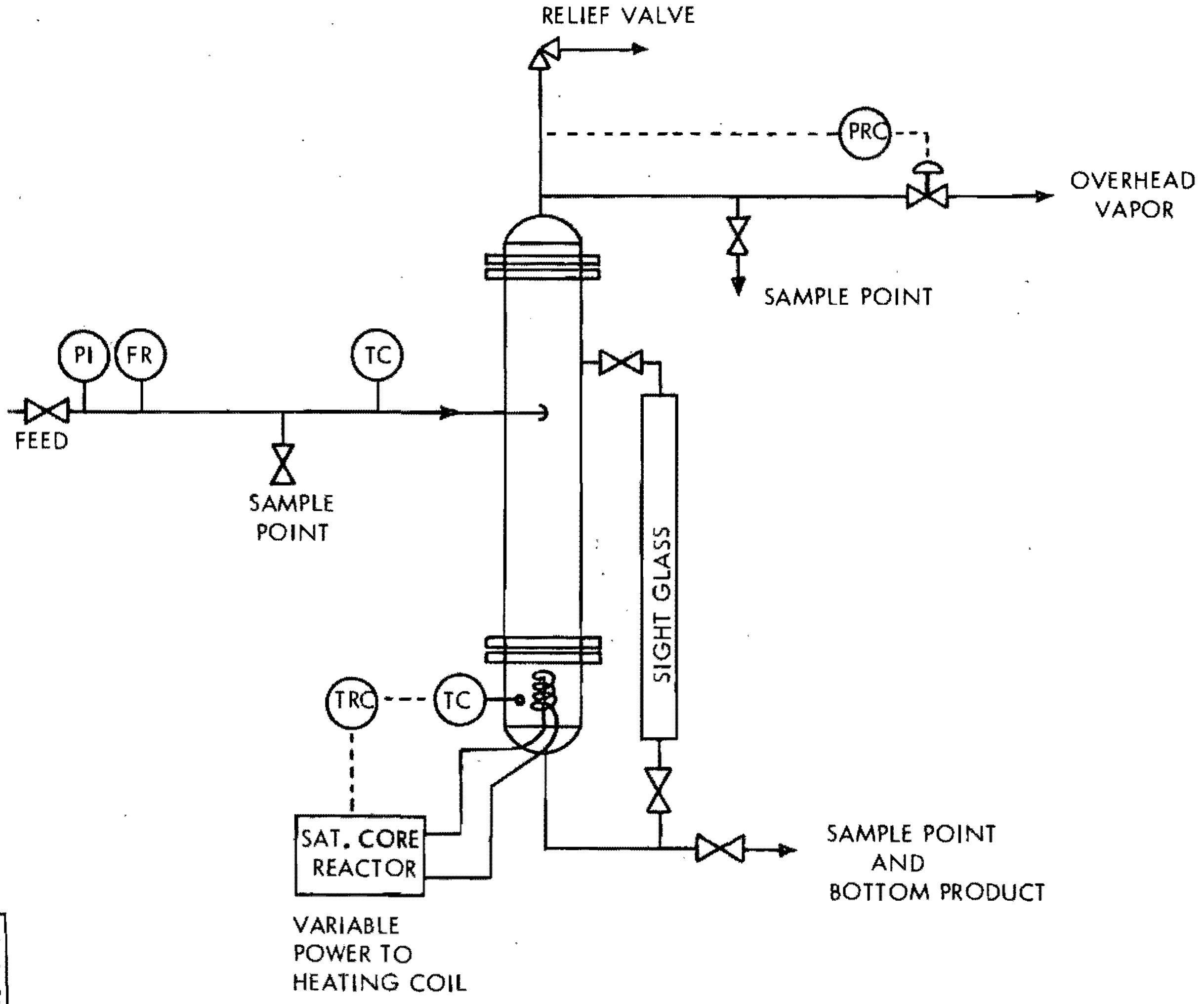

37.1-65-1296

FIGURE 2.39 SCHEMATIC DIAGRAM OF THE EVAPORATOR TEST SYSTEM

2.4.4 Distillation Column

A distillation column presents the opportunity to gain greater product concentration than is possible with an evaporator. The volume reduction thus realized would reduce the mass of radioactive shielding required for the hydrazine separation unit and subsequent units. A distillation column was therefore designed, constructed, and tested. Figure 2.40 shows the test apparatus. The distillation column was 24 in. high and 1.5 in. diameter; the column was packed with 0.16 x 0.16 in. Cannon protruded packing (Figure 2.41). The reboiler was heated by a Calrod heater brazed to the lower half of the reboiler exterior. Instrumental control governed normal operations; test conditions were varied by changing the set points.

Primary control was obtained by varying feed flow rate between 0 and 100 cc/min.; the feed entered the top of the column and was utilized as reflux. The reboiler temperature was maintained by varying heater power at a set point of up to 100°F. The pressure at the top of the column was regulated at approximately 10 psig by varying venting rate. Figure 2.42 is a schematic diagram of the distillation column test apparatus which shows the instrumentation and controls.

The column was designed to operate under the listed test conditions:

Feed Temperature	100° F
Feed Flow	50 cc/min
Feed Composition	5.0 wt % N_2H_4 (i.e., 2.71 mol%)
Reboiler Temperature	100° F
Column Pressure	10 psig

A bubble point calculation gave a predicted bottom liquid composition of 92.18 mole % N_2H_4. The hydrazine concentration was predicted to be sensitive to pressure and would lower as the pressure rose. Since there was no condenser on this column, the feed liquid would be the reflux. The overhead vapors leaving the column would be in equilibrium with the reflux. A heat balance and a flash calculation were made to determine the overhead vapor composition. The feed was flashed to the column pressure yielding a feed temperature of -6.5° F. The remaining feed liquid was

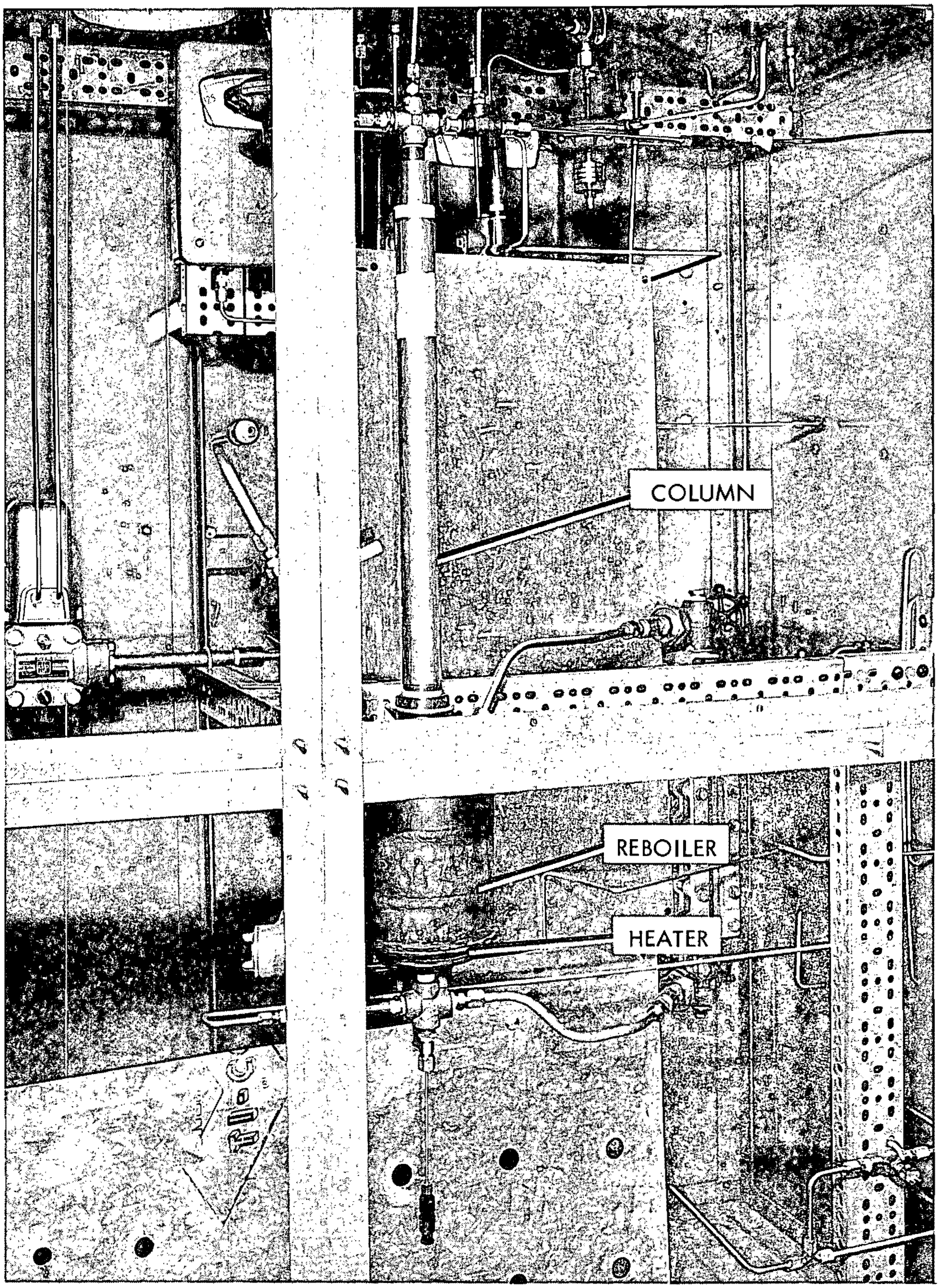

37.1-65-1298

FIGURE 2.40 TEST MODEL OF DISTILLATION COLUMN

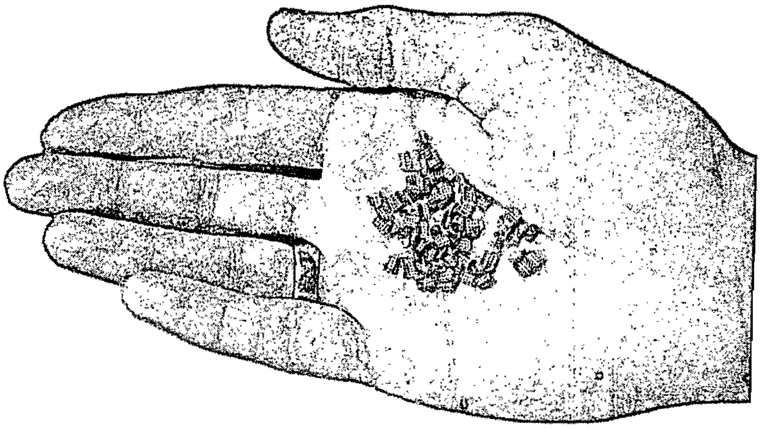

FIGURE 2.41
CANNON PROTRUDED
COLUMN PACKING

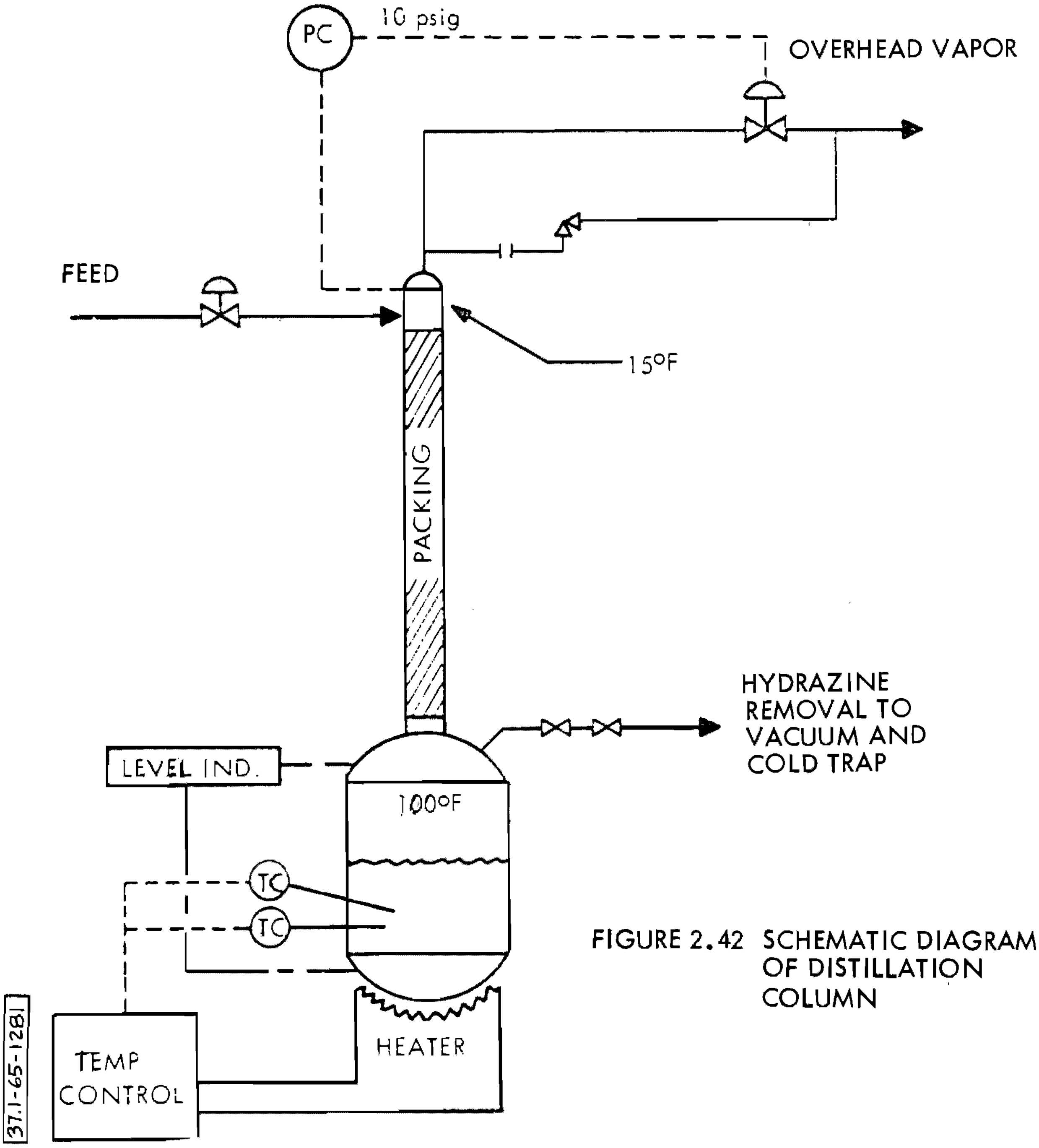

FIGURE 2.42 SCHEMATIC DIAGRAM OF DISTILLATION COLUMN

3.38 mol % N_2H_4. The composition of the vapor was predicted to be 0.00599 mol % N_2H_4 by a bubble point calculation on this flashed fluid. The quantity of material in the overhead (determined by an over-all material balance), multiplied by the mol % N_2H_4, gave 5.2×10^{-5} mol/min of N_2H_4 in the vapor. The complete material balance is given in Table 2.10.

TABLE 2.10

DESIGN MATERIAL BALANCE FOR THE DISTILLATION COLUMN

	Feed		Overhead		Bottoms	
Comp	mol/min	mol %	mol/min	mol %	mol/min	mol %
NH_3	0.88406	97.29	0.88011	99.9940	0.00395	7.82
N_2H_4	0.04655	2.71	0.000052	0.00599	0.04650	92.18

The minimum number of theoretical trays required to obtain the separation shown in Table 2.10 was derived using the Fenske equation[18]. This was calculated to be 1.535. The 18 in. packed bed was calculated to have 4.4 trays when operating just below the flooding point. The distillation column would therefore be able to operate at as low as 35% of flooding yet achieve the design separation. It should be noted that, with even lower flow rates, hydrazine loss rates would not be serious.

A series of tests was initiated to evaluate the distillation column. The first tests were instrument, control, and function checks. The distillation column was found to operate smoothly on automatic control. Overhead sample results using metal samplers were erratic; the scatter in sample results decreased considerably when glass samplers were used. The flooding point was to be determined during the second series of tests; however, the packing was of such high performance that the column would not flood even at 78 cc/min, the maximum rate which was obtainable with the heater. Area and void-fraction measurements were made to obtain a value for the packing factor; it was calculated to be ~520. A new column 0.75 in. in diameter was designed and constructed using this new value. The 0.75 in. column was designed to flood at 50 cc/min; the observed flooding point was 53 cc/min, an excellent check.

One test series was run to measure the composition of overhead vapors and reboiler liquid. This series was principally of academic interest as the hydrazine-ammonia separation by distillation is very easy, requiring only the assurance of reflux; as a result hydrazine losses through the overhead vapors were expected to be insignificant. The test series confirmed that the composition of the overhead vapors was determined by vapors in equilibrium with the feed. If for some reason hydrazine losses had to be further reduced, the column could be redesigned to introduce the feed at the appropriate intermediate point along the height of the column and supply reflux rather than introduce the feed above the packing as was done in this apparatus.

The information and experience gained during this development work was to have formed the basis for a continuous separation of hydrazine and ammonia as part of the in-reactor test apparatus. While the test series was being performed, the requirement for such a separation was eliminated and the requirement for the separation of a 5 liter batch of filtered ammonia-hydrazine product was substituted. The 5-liter batch was large enough for a continuous distillation of several hours, and so the distillation apparatus was used in tests to separate and decontaminate a radiotraced-fluid representing product from the in-reactor tests. This work is reported in the next section.

2.5 Decontamination

2.5.1 Introduction

The feed stream to the decontamination test apparatus was to be filtered liquid ammonia containing approximately 3% hydrazine. The types and amounts of fission products were unknown; therefore, experiments were devised to determine which radionuclides would be in this filtrate and what decontamination methods were most promising. The problem was studied in three sequential steps: 1) determination of the distribution of fission fragments in a liquid ammonia-UO_2 slurry; 2) testing of candidate decontamination methods and selection of a method for the decontamination test apparatus, 3) performance of decontamination tests on the filtrate from the in-reactor experiment.

The general problem of decontaminating an anhydrous hydrazine product is considerably aggravated by the lack of chemical knowledge and technology concerning anhydrous hydrazine. The candidate decontamination operations were adsorption, ion exchange, distillation or evaporation, electrodialysis, foam separation, precipitation followed by filtration, and solvent extraction. Foam separation appeared to show promise for a limited number of isotopes[19] but would require development of a controllable foam which was clearly beyond the scope of this study. Precipitation of slightly soluble isotopes through the use of carriers appeared attractive, as many of the fission products are barely soluble in hydrazine. Tests were performed which showed that isotopic exchange and co-precipitation of the radioisotopes with the carrier did not occur predictably and that very careful control would be required to maximize the effectiveness of this approach. Although ruled out for the specific purposes of this program, precipitation should not be discarded as a potentially useful hydrazine decontamination tool. Electrodyalysis and solvent extraction were considered to require entirely too much development before they could be considered for hydrazine decontamination studies. Distillation and evaporation were selected because these would not require advanced techniques. Adsorption and ion-exchange could be attempted using small vials or packed beds of materials without the necessity of developing new techniques; both of these methods were tested to a limited degree.

2.5.2 Distribution of Fission Fragments

2.5.2.1 Objective

A slurry reactor producing fissiochemical products will contain solid, liquid, and gaseous phases: fuel, in the form of a finely divided solid, will be distributed throughout the liquid feed; over this slurry will be pressurized cover gas. The distribution of fission products among these three phases must be known in order to design effective decontamination processes for product recovery. The objective of this study was to determine the distribution.

2.5.2.2 Description of Test

Three capsules were irradiated at the Battelle Memorial Institute (BMI) reactor to nominal fuel burnups of 0.005, 0.01, and 0.03% to study the radiation effects on slurry. Samples were taken from all the principal phases and analyzed by gamma spectrometry for specific radioactive fission products. The data from these analyses were used to calculate the distribution and to estimate a material balance of fission products.

The capsules are described in detail and illustrated in Section 3.4. The capsules were designed to irradiate 0.5 g of UO_2 powder suspended (by ultrasonic vibration) in about 50 ml of liquid ammonia. The design included space for decomposed ammonia (gas), provisions for removing the capsule liquid and solids, and appropriate instrumentation. Irradiation was performed at BMI in a thermal flux of approximately 4×10^{12} neutrons/sec-cm^2.

Samples were withdrawn from each of the slurry irradiation capsules as soon as practicable, and their quantities and times recorded. Seven types of samples were taken from each capsule after its irradiation; these seven types from one capsule comprised a sample set as described below. Care was exercised in all steps to avoid sample loss and segregation of fission products.

Sample Type A: Supernate from Settling Test

These liquid ammonia samples were decanted from the fuel after conclusion of slurry settling experiments. All parts of the apparatus containing liquid ammonia were cooled with dry ice to minimize ammonia loss. Volumes were measured by observing the liquid meniscus in calibrated polypropylene centrifuge cores. After the liquid ammonia was decanted, it was reacted with water, brought to a known volume, and aliquots were taken for gamma spectrometry.

Sample Type B: Solids from Settling Test

These solid samples were taken after Type A supernate samples had been withdrawn. They were weighed, dissolved, brought to a known volume, and aliquots reserved for gamma spectrometry.

Sample Type C: Supernate from Centrifuge Test

These samples were withdrawn, by a method similar to that used for withdrawing Type A samples, after a portion of the supernate from the settling tests had been centrifuged in a Servall SS-1 centrifuge at 10,000 rpm for 5 min; the centrifuge was cooled by dry ice.

Sample Type D: Solids from Centrifuge Tests

These samples were taken by the method used for Type B samples; their masses were obtained by fluorimetric analyses on aliquots.

Sample Type E: Gas

Samples of gaseous products from the slurry irradiation capsule were collected in 10 milliliter samplers.

Sample Type F: Container

The can from the slurry irradiation capsule was rinsed with two portions of distilled water to remove the UO_2 solids; then the can was washed with three portions of 3 M HNO_3. These acid washings were combined to form Sample Type F. Aliquots were prepared for gamma spectrometry.

Sample Type G: Slurry Collection Bomb

These liquid samples were taken from the slurry collection bombs after the slurry had been allowed to settle for a long period; few solids were present. The weight of the sample was determined by titrating aliquots for ammonia.

Samples were analyzed by gamma spectrometry of unseparated sample aliquots and by radiochemical separation.

Multiple channel pulse height analyzers (RCL 128) were used to record the signals from a photomultiplier coupled to a thallium-activated, sodium iodide crystal. The crystal used at BMI was a cylinder 1-1/2 in. high, 2 in. in diameter, and having a 5/8 in. diameter well; the AGN crystal was a 3 by 3 in. cylinder. The spectrometers were calibrated for gamma energy versus channel number and efficiency. All samples were counted under identical conditions of geometry, calibration, and background at BMI, and under a separate set of known conditions at AGN. Samples were recounted after appropriate intervals to obtain decay data.

The net count rates of known peaks were calculated for all samples. These count rates were converted to disintegration rates using sodium iodide crystal efficiencies of Heath[20] and gamma abundance data from National Research Council Nuclear Data Sheets[21]. The fission yield data were obtained from Bolles and Ballou[22].

A few samples were selected for radiochemical separation and analysis. The isotopes were chosen for study on the basis of their importance as contaminants or because of unsatisfactory resolution by spectrometry alone.

2.5.2.3 Results and Discussion

The gamma spectrometer data from all samples were compared in an effort to locate major differences attributable to solid, liquid, and gaseous phases, and to irradiation time. After this comparison, two sample types were selected for radiochemical analysis: Type B samples from the settling tests, typical of the fuel solids, and Type G samples filtered from the slurry bombs and containing the fewest solids.

The radioisotopes which were studied, and the analytical method employed, are shown in Table 2.11. The energy of the gamma peak chosen for spectrometry is also shown.

TABLE 2.11

RADIOISOTOPES STUDIES

Radioisotope	Half-Life	Chemical Group	Gamma Peak (Mev)	Analysis Method Gamma	Analysis Method Chem	Notes
Ce-141	33 d	Rare Earth	0.145	X		
Ce-144	285 d	Rare Earth			X	
I-131	8 d	Halogen	0.365			
Ru-103	40 d	Noble Metal	0.498	X	X	
Zr-95	65 d	Zr-Nb	0.76	X	X	
Nb-95	35 d	Zr-Nb	0.76	X<	X	Daughter of Zr-95
La-140	40 h	Rare Earth	1.6	X		Daughter of Ba-140
Sr-90	28 y	Alkaline Earth			X	
Ba-140	12.8 d	Alkaline Earth	-	X		By observing La-140
Cs-137	29 y	Alkali Metal			X	

The gamma spectra of the UO_2 solids which settled out during the settling test are compared in Figure 2.43. No qualitative difference is observed from lowest to highest fuel burnup. Quantitative comparisons confirm that the proportion of each radioisotope in this sample type remained the same within the accuracy (± 10%) of the comparative analysis.

The spectra of the solids thrust down during the centrifuge test were compared with each other and with the spectra of solids from the settling test. Again, the proportion of each radioisotope remained the same within ± 10%, with one exception: the sample of low burnup centrifuged solids clearly showed twice the concentration of ruthenium in proportion to the other solid samples. Cerium-141, zirconium-niobium-95, lanthanum-140 (tracing the parent barium-140) and ruthenium 103 were the prominent radioisotopes. The presence of cerium-141 and ruthenium-103 were confirmed through decay studies. Iodine-131 was notably absent from all the solids samples. The broad peak at 0.3 Mev may contain some iodine, but certainly less than 15% of the iodine present in the liquid.

Radiochemical analysis confirmed the presence of ruthenium-103 and zirconium-niobium-95 in the solids; cerium was again shown by the isotope 144. Elements of interest which could not be seen by gamma spectrometry because of interference were strontium-90 and cesium-137; both of these radioisotopes were found radiochemically in the solids in substantial concentration.

Gamma spectrometry of liquid samples did not show such a clear proportional relationship of radioisotopes as did those of the solids. Figure 2.44 illustrates the difference between liquid decanted after the centrifuge test and liquid decanted after the settling test. Other liquid samples showed comparable variations. The differences among the spectra of liquid samples were similar to the spectra of solids, as indicated by comparison of Figures 2.43 and 2.44. Zirconium-95 was found in the smallest proportion in liquid samples and was considered to be a tracer of solids.

The net spectrum of the liquid samples indicated I-131 and Ru-103 as primary constituents with only very small amounts of the other radioisotopes.

37.1-65-1279

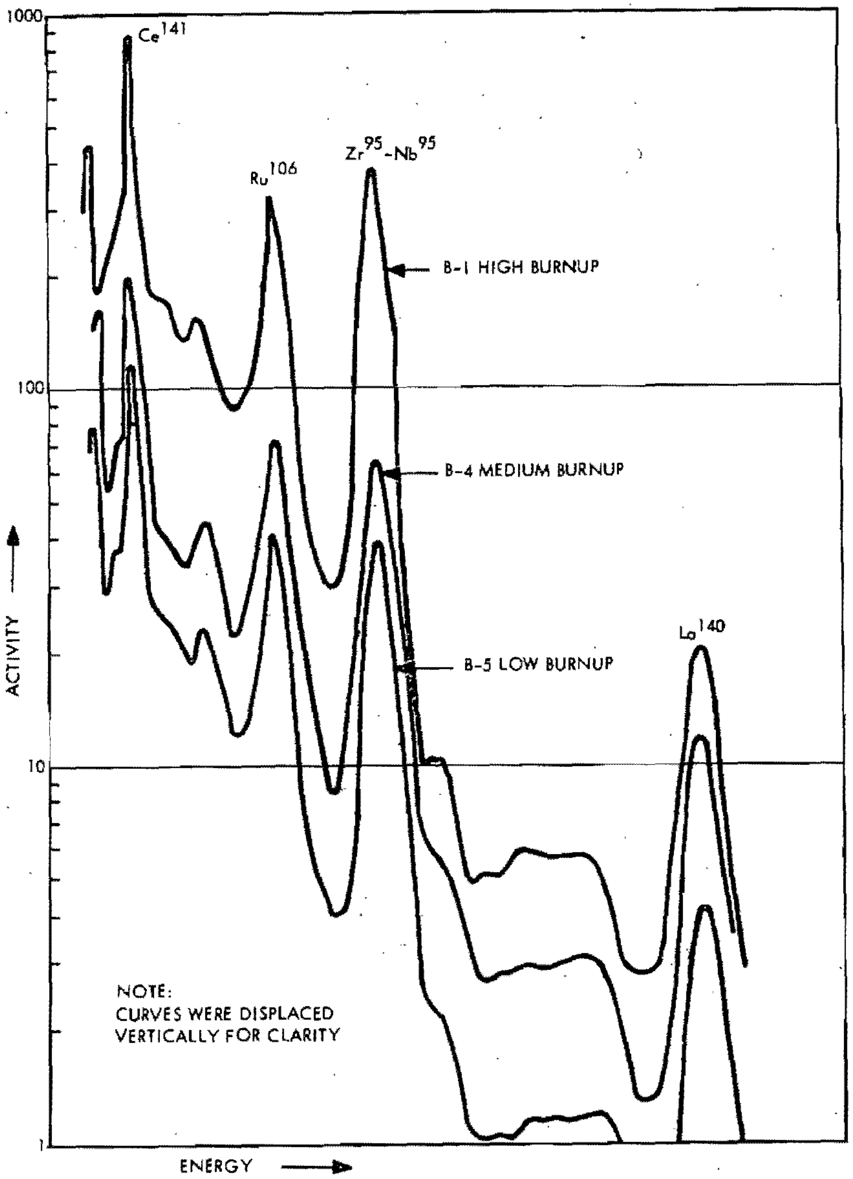

NOTE:
CURVES WERE DISPLACED VERTICALLY FOR CLARITY

FIGURE 2.43 GAMMA SPECTRA OF SOLIDS FROM SETTLING TESTS

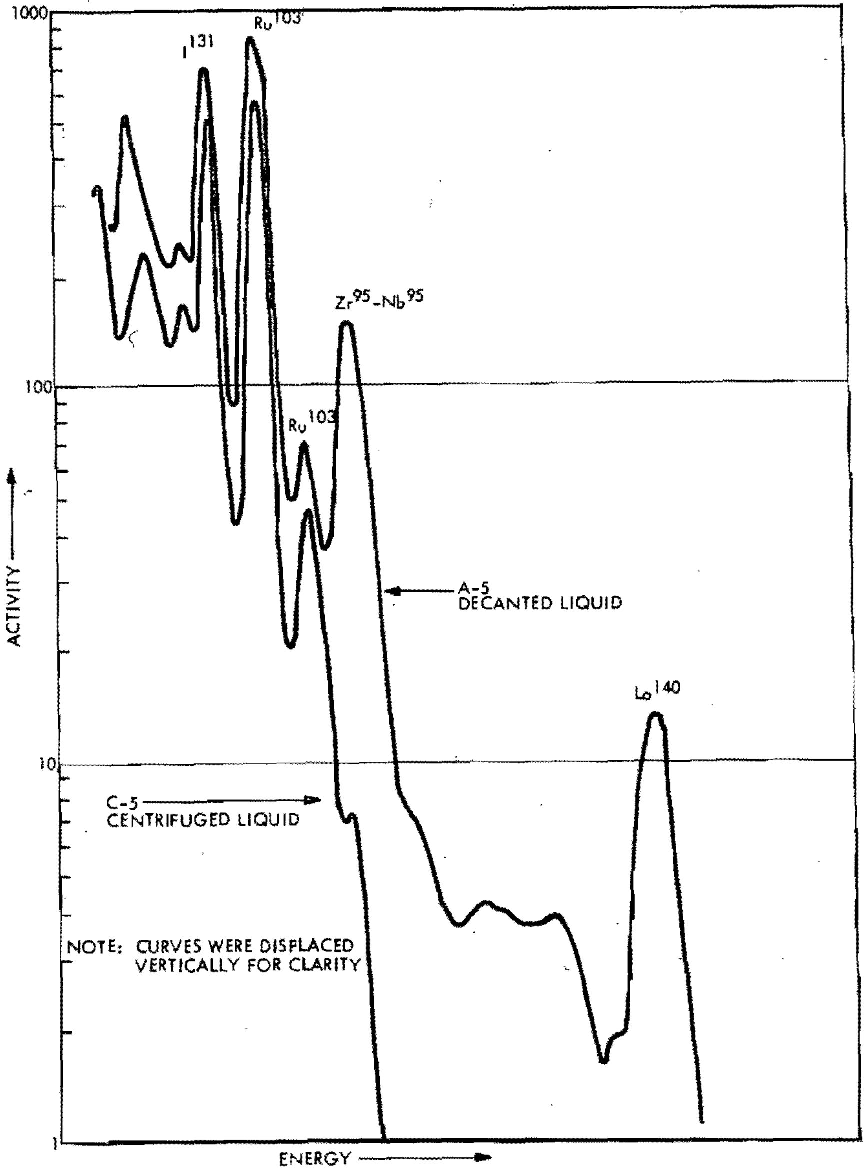

NOTE: CURVES WERE DISPLACED VERTICALLY FOR CLARITY

FIGURE 2.44 GAMMA SPECTRA OF LIQUIDS DECANTED FROM SETTLING AND CENTRIFUGE TESTS

Two filtered liquid ammonia samples were withdrawn from the slurry bomb approximately one month after irradiation. The spectra of both of these samples showed no La-140 and no Zr-95. I-131 and Ru-103 were prominent.

The three types of liquid samples (settled, centrifuged, and filtered), separated after various contact times with the solids (one week to one month), showed the presence of I-131 and Ru-103; however, there was little agreement in the proportions of these isotopes when samples were compared either within one type or among several types. Evidently, some important factor in determining the relative distribution of these isotopes was not closely controlled.

The radiochemical analysis results of the liquid samples showed ruthenium-103 only (iodine-131 was not sought). Zirconium-niobium-95 and cerium-144 were below detection limits; these results agree with the gamma spectrometry results. Strontium-90, which is a particularly undesirable radioisotope because it is a bone-seeker of long half-life and short-range ionization, was undetected in the liquid samples. Cesium-137 was also below the detection limit in these samples although, as an alkali metal, its presence was anticipated.

Xenon-131 and Xe-133 were the only radioisotopes found in the gas. Iodine was not found in the gas phase, nor were the radioactive daughter products from radioactive rare gases.

The distribution of fission products among the phases provides a basis for hypothesizing which chemical forms are present. The development of a sound hypothesis for explaining these findings would be a complex undertaking in itself, as the ammonia chemistry of much of the fission product spectrum is unavailable. Still, the environment can be generally described as considerably less ionizing than water, but more strongly reducing.

Even in neutral aqueous systems, the rare earths, alkaline earths, and zirconium-niobium tend to precipitate or plate onto surfaces; this tendency would appear to be even stronger in an ammonia system with its lesser solvent properties. The great surface area of the UO_2 particles would enhance the precipitation; a 0.01% burnup produces enough fission products to coat the UO_2 particles with only a 2.5×10^{-3} monatomic layer. According to Belloni, et al[23] coverage of 5×10^{-3} monatomic layer is observed as the maximum for the rare earths in aqueous systems.

The presence of cesium in the liquid ammonia phase was anticipated, as alkali metals of low atomic weight are very soluble. However, cesium could not be detected in the liquid; this fact is interesting with regard to the chemistry of alkali metals in liquid ammonia, but due to the qualitative nature of the analysis it cannot be considered conclusive.

The halogens, with iodine as the model, are soluble in liquid ammonia. In aqueous systems, iodine is usually rather volatile, however, iodine was not found in the gas phase. Iodine is presumed to be reduced to the non-volatile iodide (I^-) state in the liquid ammonia environment.

Ruthenium was found in both the liquid and solid phases. Noble metals have been observed to form complexes in aqueous ammonia systems; this reaction plays an important role in many electrodeless plating processes. Perhaps, to a limited degree, ruthenium forms complexes with liquid ammonia. Ruthenium was found in over twice the concentration in one sample of the centrifuged solids as in the others. Possibly contact with moist air, and consequent alteration of the pH of the solution resulted in a slight equilibrium shift toward the solids. As the solids comprised an extremely small fraction of the total liquid-plus-solid mass, the liquid was not noticeably depleted in ruthenium. Ruthenium was the only element observed to "wander" between liquid and solid phases. In a decontamination process involving filtration, this could create a significant problem.

The radioisotopes studied here are considered to be representative of their chemical groups. If this is true, about 90% of the fission product radioactivity can be accounted for. Figure 2.45 gives the hypothetical distribution of fission product activity, resulting from instantaneous fissioning, for increasing decay. The decay data for this figure were obtained from Bolles and Ballou[22]. Admittedly, calculations based upon instantaneous fissioning provide an oversimplified model for long irradiation times, especially if gases and products are withdrawn and liquid is added; nevertheless, the results of this study are indicative.

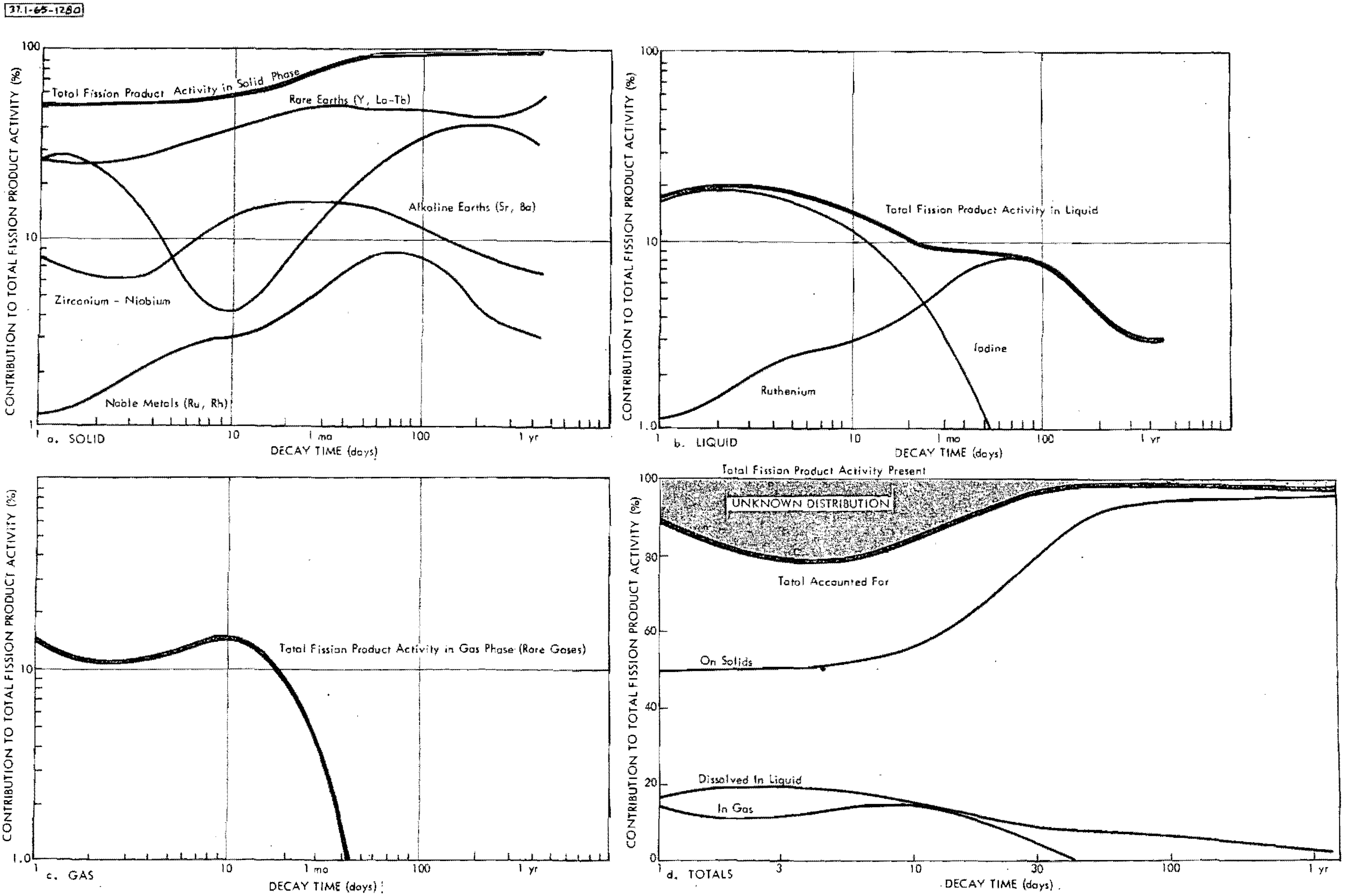

FIGURE 2.45 HYPOTHETICAL DISTRIBUTION OF FISSION PRODUCT ACTIVITY AMONG THE PHASES PRESENT IN A CAPSULE

2.5.2.4 Conclusions

The fission products resulting from the neutron irradiation of U-235 O_2-$NH_{3(1)}$ slurry were distributed preferentially among the phases present. The liquid phase contained essentially all of the iodine-131 and approximately half of the ruthenium-103 in solution. All of the barium-lanthanum-140, zirconium-niobium-95, strontium-90, cerium-144, and cesium-137, and the remaining ruthenium-103 were with the UO_2 solids. Iodine and ruthenium together accounted for 20% of the total fission product activity after 1 day of decay, but this slowly dropped to about 9% after 1 month, and to 3% after 1 year.

2.5.3 Distillation of Spiked Ammonia-Hydrazine Solution

2.5.3.1 Objectives

As mentioned previously, when the MTR was selected as the reactor for the in-reactor experiment, an apparatus consisting of two units (a slurry loop to produce hydrazine and a processing unit for concentrating and decontaminating hydrazine) was selected in preference to the fully integrated apparatus. Arrangements were then made to locate the processing unit at the Idaho Chemical Processing Plant (ICPP) in the multicurie cell. The experiment related below was devised to provide the information for the design of the apparatus to process and decontaminate the dilute crude hydrazine which would be delivered to the multicurie cell in 5-liter batches. The experiment had the following objectives:

- to obtain information which would be useful in calculating the radioactivity levels in the AGN-6 product decontamination experiments;
- to determine the radioactive distribution throughout the decontamination equipment; and
- to obtain data on hydrazine recovery.

2.5.3.2 Description of the Test

The distillation apparatus (Figure 2.46) consisted of a column having a 3/4-in. pipe filled with 0.16 by 0.16-in. protruded packing 16 in. deep, and equipped with automatic feed controls and instrumentation. The basic design was adapted from the distillation experiments reported in

371-66-835

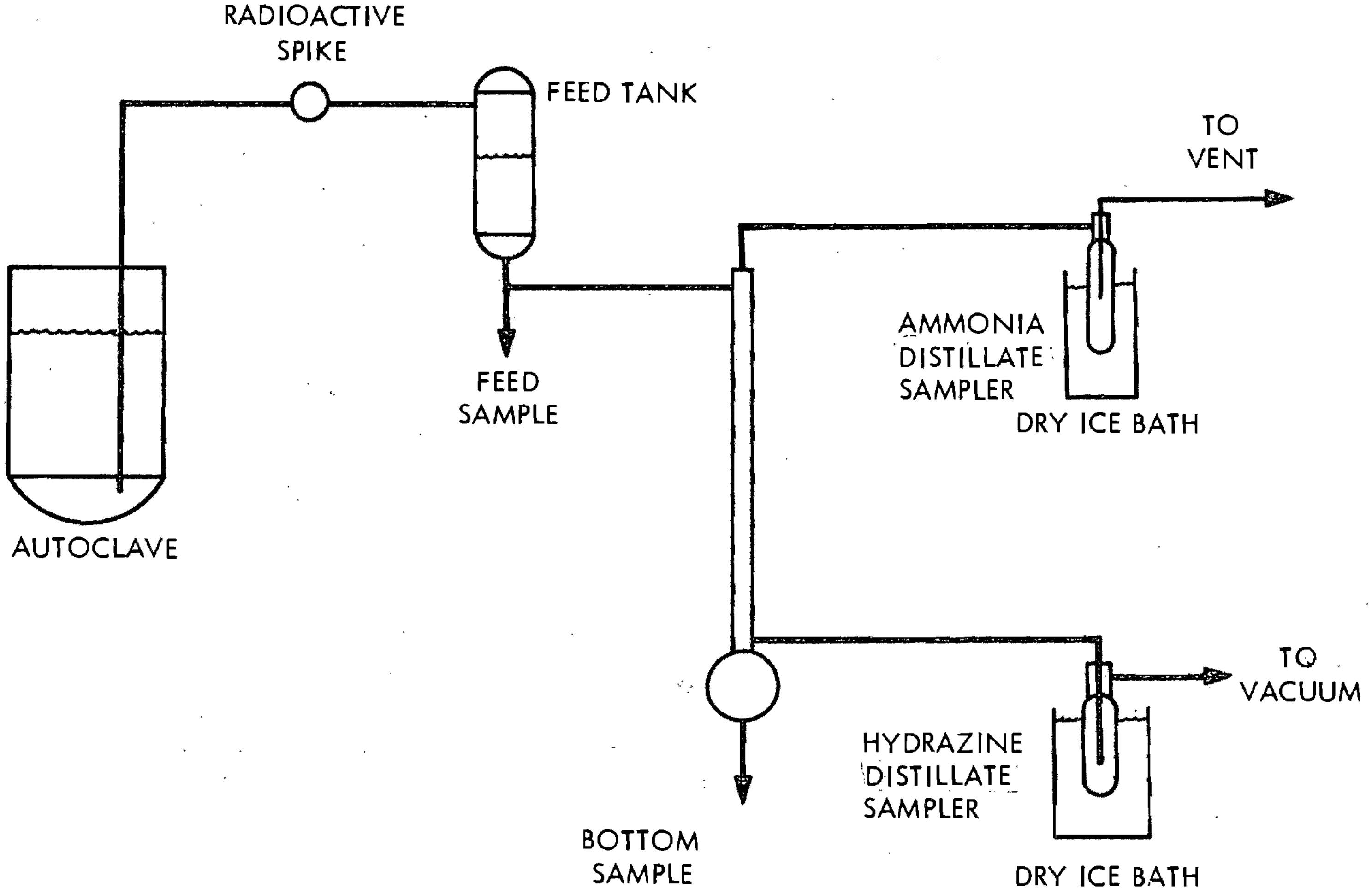

FIGURE 2.46 SCHEMATIC DIAGRAM OF DISTILLATION DECONTAMINATION APPARATUS

Section 2.4.4. A 10-gal autoclave was used to prepare the ammonia-hydrazine mixture. The spiked feed was stored and delivered from a 5-liter tank.

The first run contained 0.5 mc of activity and the second, 2 mc. Feed, ammonia distillate, bottoms, hydrazine distillate, and packing samples were taken. The first run was spiked with 10 ml of settled, unfiltered liquid from an LPTR capsule run reported in Section 5.7. The principal radioisotopes were iodine and ruthenium. On the second run, 300 cc of ammonia were added to the LPTR capsule and then decanted back to the 300 cc sample bomb after settling overnight. Approximately 2 mc of soluble fission products were obtained. The fission products used to spike the ammonia-hydrazine were produced during a fissiochemical experimental run using UO_2 slurried in liquid NH_3, and in that respect are "prototype" rather than "synthesized".

Feed samples, 12 ml in volume, were withdrawn near the beginning and end of each run. Ammonia distillate samples, 100 to 260 ml of liquid in volume, were taken near the beginning, middle, and end of each run. These samples were used to measure droplet entrainment from the feed into the vapor stream. Ten milliliter volume bottom samples were taken at the beginning and end. Hydrazine distillate samples, approximately 20 ml in volume, were taken at the start, middle, and end of each run.

The column packing was removed at the end of Run 2 and sampled from the top of the column and at 4-in. increments down the column to determine the plate-out of fission products.

The 5 wt% hydrazine in ammonia mixture, was prepared in an autoclave. Prior to each run, a sampler containing the spike was set in-line between the autoclave and the 5 liter tank, then flushed into the tank with ammonia-hydrazine solution. The distillation proceeded in two steps: Ammonia was continuously distilled until the 5 liters were discharged from the tank; the ammonia distillation was stopped and hydrazine was flashed and condensed as a product. All samples were chemically analyzed for ammonia and hydrazine. Gross gamma-counting, using a well counter of approximately 50% efficiency for I-131 and Ru-103, was performed on all samples. Selected samples were submitted to gamma spectrometry, using an RCL-128 analyzer with a 3 by 3 in. cylindrical crystal.

2.5.3.3 Results

Ammonia distillate samples accounted for approximately 10% of the total ammonia distillate stream, while the hydrazine distillate samples represent all of the hydrazine distillate streams. These results are presented in Tables 2.12 and 2.13.

TABLE 2.12

CHEMICAL MATERIAL BALANCE - RUN 1

Stream	Ammonia (grams)	Hydrazine (grams)	Hydrazine (%)	Total (grams)
Ammonia Distillate	2818.(a)	0.58	0.3	2819.
Hydrazine Distillate	0.64	120.8	76.5	121.4
Bottoms Sample	0	12.9	8.2	12.9
Unaccounted for	-	23.7(a)	15.0	23.7
Feed	2819.	158.	100.0	2977.

(a) By difference

TABLE 2.13

CHEMICAL MATERIAL BALANCE - RUN 2

Stream	Ammonia (grams)	Hydrazine (grams)	Hydrazine (%)	Total (grams)
Ammonia Distillate	2458.(a)	0.5	0.4	2458.
Hydrazine Distillate	2.47	97.9	80.2	100.4
Bottoms Sample	0.	12.8	10.5	12.8
Unaccounted for	-	10.8(a)	8.9	10.8
Feed	2460	122.0	100.0	2582.

(a) By difference

Aliquots of the samples were counted in a well counter, with the discriminator set to accept only those gamma counts above 0.26 Mev. Samples counted throughout a week were corrected for decay to the time of completion of the experimental run. The predominant radioactive isotopes were I-131 and Ru-103, in a radioactivity ratio 7 to 1 at the end of Run 2. A small amount of Zr-Nb^{95} was also present.

Decontamination factors (DF) were calculated for the distillations. The decontamination factor for the ammonia distillate was obtained by dividing the feed specific activity by the specific activity of the ammonia distillate. The decontamination factor for the hydrazine distillate was obtained by dividing the initial reboiler specific activity by the hydrazine distillate specific activity. The ammonia distillate DF for Run 1 was greater than 10^3. The results of Run 2 are given in Table 2.14 and the results of the individual hydrazine distillate samples are given in Table 2.15.

2.5.3.4 Discussion

Although Run 1 was performed primarily to satisfy radiological safety requirements, it was useful for checking out the operating procedure and sampling techniques. The ammonia distillate samples were too small and dilute to supply data for calculating a DF.

Considerable quantities of hydrazine remained unaccounted for in both runs. Some hydrazine was obviously lost during transfer of the distillate samples, and vapors were observed to emanate from the hydrazine distillate cold trap. A modified procedure was adopted in which the hydrazine vapor flow rate was reduced and the vapors cooled to reduce hydrazine loss.

The very small amount of radioactivity unexplained in Run 2 was within the margin of experimental error. The fact that 97% of the radioactivity was found in the reboiler was encouraging, as it meant that only the reboiler posed an equipment decontamination problem. A single ammonia flush reduced the contact radiation level in the reboiler from 5 mr/hr to 1.8 mr/hr. The large (1 gal.) volume of the reboiler increased the difficulty of cleaning it with small amounts of solution. The decontamination apparatus to be built for the AGN-6 work was designed with a 300-ml reboiler, requiring less ammonia to flush it out.

TABLE 2.14

RADIOACTIVE MATERIAL BALANCE - RUN 2

Sample	Specific Activity (cpm/gram)	Total Activity of the Stream (cpm)	Total Activity of the Stream (%)	Decontamination Factor
Feed	6.4×10^5	1.66×10^9	100	
Ammonia Distillate	3.2×10^2	7.90×10^5	0.048	2.0×10^3
Bottoms	1.4×10^7	1.61×10^9	97.0	
Hydrazine Distillate 1	2.1×10^4	2.70×10^5	0.016	680
Hydrazine Distillate 2 to 4	54	4680	0.0002	2.7×10^5
Packing		3.1×10^7	1.87	
Unaccounted for			1.1	

TABLE 2.15

HYDRAZINE DISTILLATE SAMPLES

Sample	Hydrazine (grams)	Ammonia (grams)	Specific Activity (cpm/gram)
N_2H_4 Distillate 1	10.52	2.47	2.08×10^4
N_2H_4 Distillate 2	54.25	0	40.6
N_2H_4 Distillate 3	29.81	0	75
N_2H_4 Distillate 4	3.30	0	45.2

Hydrazine evaporation began when the feed was exhausted. At this time, the column pressure was 10 psig and the reboiler temperature 100°F, with the reboiler containing 133.7 g of hydrazine and 2.47 g of ammonia. The hydrazine vapors were vented directly from the reboiler to a dry-ice cold trap whose discharge was connected to a vacuum pump. The vacuum pump was throttled to bring the cold trap to 740 mm Hg absolute when the first vapors, containing most of the 2.47 g of ammonia, left the column, after which the pressure in the cold trap was gradually reduced to 10 mm Hg absolute.

Rapid boiling, assumed to have occurred as pressure was reduced, apparently carried relatively large amounts of radioactivity. The first hydrazine distillate sample showed an unusual amount of activity (Table 2.16). On samples 2, 3, and 4, the pressure was at 10 mm Hg throughout the distillation. The activity in these samples was very low and fairly constant, even though, as the hydrazine flashing progressed, the radioactivity in the liquid remaining in the reboiler became more and more concentrated. It had been anticipated that each progressive hydrazine distillation sample would contain more activity. The activity in the distillate sample seems to be related to boiling rate as well as to reboiler concentration.

The distillation column packing presented a very large surface area in comparison with the rest of the apparatus and, therefore, warrants close scrutiny. The low observed radioactivity (Figure 2.47) was encouraging from an operational standpoint as it indicated that hydrazine could be distilled up through the packing, rather than being flashed through a vent at the top of the reboiler. The slightly higher concentration of radioactivity at the top of the packing probably resulted from the lack of self-washing at the end of the run; the procedure was therefore changed, by terminating a run with a 5- to 15-min. pure ammonia wash. The slight increase in the Ru-103/I-131 ratio at the top and bottom of the column probably resulted from the lower solubility of ruthenium. The comparatively great $Zr\text{-}Nb^{95}/I^{131}$ ratio at the top of the packing suggested that fuel or insoluble fission products plate out very quickly on the packing, which could pose a serious problem if large amounts of fuel were present in the feed, and if the hydrazine were distilled through the packing.

2.5.3.5 Conclusions

These two runs were designed to simulate the conditions under which the loop filtrate would be handled, and to provide information for the design of the decontamination apparatus for the AGN-6 experiment.

The ammonia distillate was found to have a DF of 2×10^3 with respect to the feed without the aid of vapor detrainment. Less than 2% of the radioactivity of the total feed remained in the distillation column packing. Permitting hydrazine to be distilled through the packing should improve the hydrazine DF.

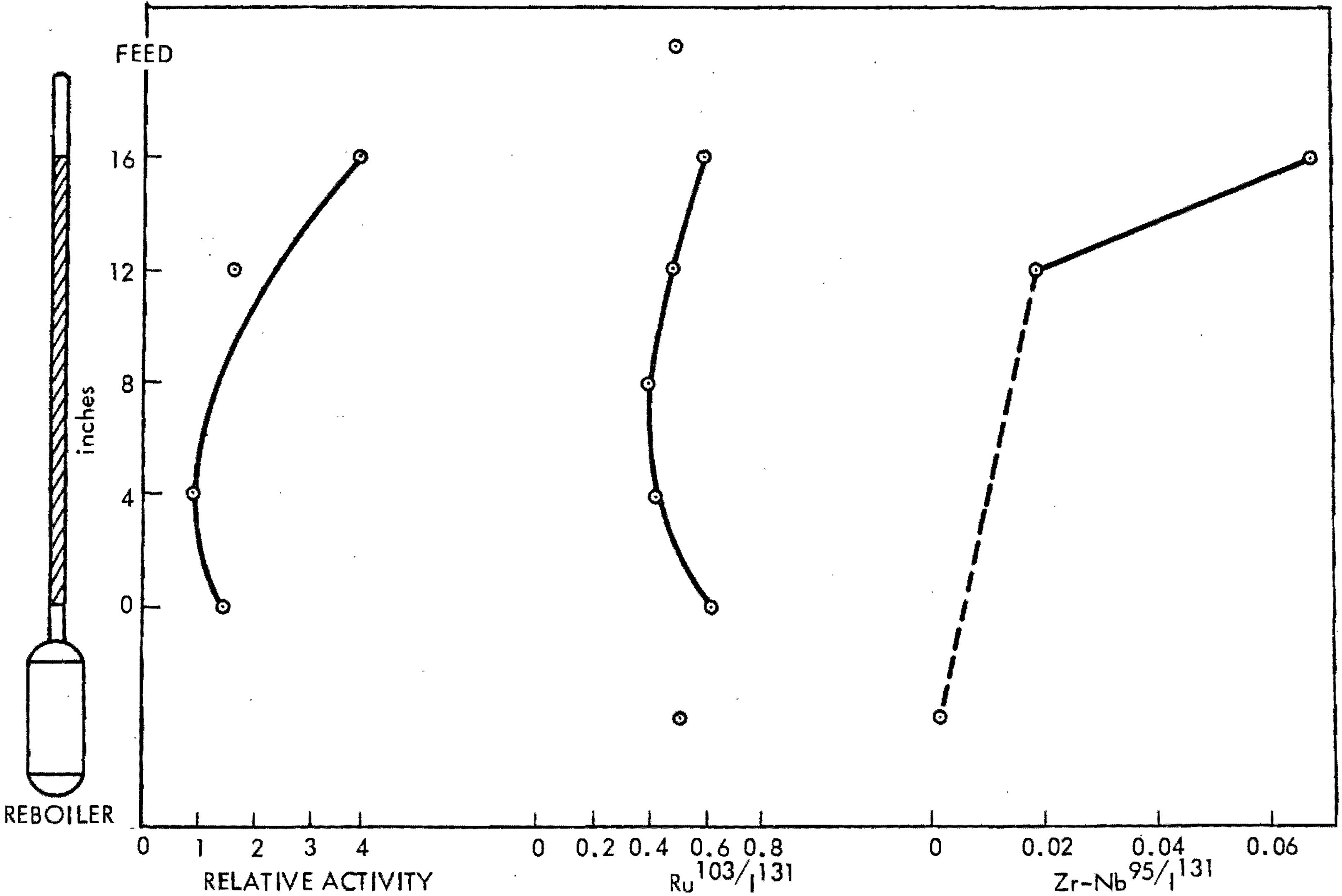

FIGURE 2.47 RADIOACTIVITY OF DISTILLATION COLUMN PACKING 13 DAYS AFTER RUN 2

At the end of the second run, 97% of the radioacticity was found in the reboiler bottoms; a single ammonia rinse reduced the radioactivity to approximately one-third its initial value. The first hydrazine distillate sample yielded the rather poor DF of 680, with subsequent samples averaging 2.7×10^5; modifications in operating technique were expected to improve the DF of the first sample. If the hydrazine from the AGN-6 filtrate could be distilled with a DF of 10^5, the remaining decontamination could be performed outside the multicurie cell.

2.5.4 Experiments with Decontamination Test Materials

2.5.4.1 Compatibility Tests with Hydrazine

Several ion exchange resins and adsorbers were selected as candidate materials to further decontaminate the distilled hydrazine withdrawn from the decontamination test apparatus. Samples of these materials were tested for compatibility with hydrazine by soaking them in hydrazine for 3 days (with periodic visual inspection), drying them to remove the hydrazine, and then recording their weights.

Activated charcoal was rejected as a decontamination test material because of its vigorous reaction with hydrazine, even though this reaction may have been caused by oxygen adsorbed onto the charcoal. No other samples reacted significantly. Two samples evolved noticeable heat when hydrazine was first added; the preparation procedure was modified so that materials to be used in a decontamination test would be pre-wetted with hydrazine to avoid any heat of adsorption during test.

2.5.4.2 Batch Decontamination Tests Using Iodine-131

Two sets of batch tests were performed, using 1-g samples pre-wetted with hydrazine (as described above). Excess hydrazine was decanted from the samples and 4 ml of hydrazine containing approximately 1.5×10^7 dpm/ml carrier-free I-131 (as I^-) were added to the first set of samples; the same solution, containing approximately 7μ gm/ml I^- carrier, was added to the second set of samples. Samples were agitated, allowed to settle, and a 200λ aliquot of hydrazine was withdrawn for counting. Decontamination factors (DF) were calculated by dividing the mean of the control count rate by the count rate of the settled liquid from the test samples. Results are presented in Table 2.16.

TABLE 2.16

REMOVAL OF IODINE-131 FROM HYDRAZINE BY VARIOUS TEST MATERIALS

Test Material	Adjusted Decontamination Factor Carrier-Free	Adjusted Decontamination Factor 7 μgm/ml Carrier
3 Controls (average)	1.0	1.0
Ion Exchange Resins:		
Amberlyst XN-1001	7.4	13.0
Amberlyst XN-1006	18.0	17.0
Dowex AG-1X10 (OH^-)	5.7	11.0
Dowex AG-1X10 (Cl^-)	10.0	20.0
Dowex AG-50W-X12(H^+)	0.9	0.9
Miscellaneous:		
Activated Alumina	1.0	1.1
Precipitated Silver	1.0	1.0
Granulated Lead	0.7	1.0
Silica Gel	0.9	0.9
Benzene	1.0	1.0

The two sets of tests bracket the iodide concentration expected from the in-reactor experiment loop filtrate. It is evident that the carrier-added set gave higher DF than the carrier-free set, and that ion exchange resins were the only materials which performed substantial decontamination. The fact that ion exchange resins work well in a hydrazine medium may be extremely important for the final decontamination step in a hydrazine plant.

2.5.4.3 Column Decontamination Tests Using Iodine-131

An experiment was conducted to separate I-131 from hydrazine by ion exchange. The ion exchange column, having a theoretical capacity of 10 milequivalents or 1.3 gm I^-, was filled with 6 ml N_2H_4 and 3.5 g Dowex AG 1 x 10 resin (Cl^- form) and dried at 110°C. The dried column was prepared for runs by loading it with 6 ml N_2H_4, letting it stand for 10 minutes, and flushing it with 10 ml N_2H_4. The finished bed was 5 cm long.

Three 6-ml portions of N_2H_4 containing I-131 and I^- carrier were passed through the column at 1.5 ml/min, followed by two 6-ml portions of N_2H_4 wash, each of which was collected separately. The I-131 concentration was 0.4 μc/ml; the I^- carrier concentration was 7 μg/ml. The total iodide ion added represented 0.01% of the column capacity. Two hundred lambda aliquots were withdrawn from each portion collected, pipetted onto KI crystals, dried, and counted.

The results of this experiment, summarized in Table 2.17, show that each addition of N_2H_4 to the column pushed through the preceding addition with no detectable mixing. Since the iodide ion remained bound to the resin, it could not contaminate the wash.

TABLE 2.17

DECONTAMINATION OF HYDRAZINE BY ION EXCHANGE

Addition No.	Content	Effluent Decontamination Factor
CV-1	$N_2H_4 + I^-$	No detectable count
CV-2	$N_2H_4 + I^-$	215
CV-3	$N_2H_4 + I^-$	325
CV-4	N_2H_4 wash	365
CV-5	N_2H_4 wash	No detectable count

This experiment was conducted in air with a short column, and the hydrogen ion concentration was not controlled; while these conditions may affect the operation of the ion exchange column, the results showed the decontamination factors to be 10 to 20 times higher than those observed in the batch test.

2.6 Chemical Changes in a Fissiochemical Hydrazine Production System

Two fissiochemical production system models (Figure 2.48) were briefly considered to outline some of the effects of long term slurry reactor operation. Each model assumed an enclosed liquid ammonia-UO_2 slurry system from which hydrazine, radiolytic gases, and volatile fission products were withdrawn and to which fuel and ammonia were added consistent with criticality and inventory requirements. The models differed in that no fuel reprocessing was assumed in the first model while a constant removal of non-volatile radioactive contaminants was assumed in the second.

2.6.1 System Without Slurry Processing

UO_2 and ammonia are the principal raw materials added to the operating system. A number of chemical and physical changes occur in a system when not all of the materials which are added or produced are removed. Where slurry is not processed, only the volatile waste products leave the system, producing the following obvious system changes:

- Buildup of non-volatile fission products
- Buildup of U-236 and U-237 from non-fission neutron capture of U-235
- (b)(3) [redacted]
- (b)(3)
- Buildup of total solids in the system
- Buildup of O_2 (probably as H_2O) from the fissioned U-235 O_2
- Buildup of C^{14} from the (n-p) reaction of N^{14}
- Possible change of part of the U into the UN_x form
- Possible changes in the average UO_2 particle size or integrity
- Possible changes in the flocculation of the solids

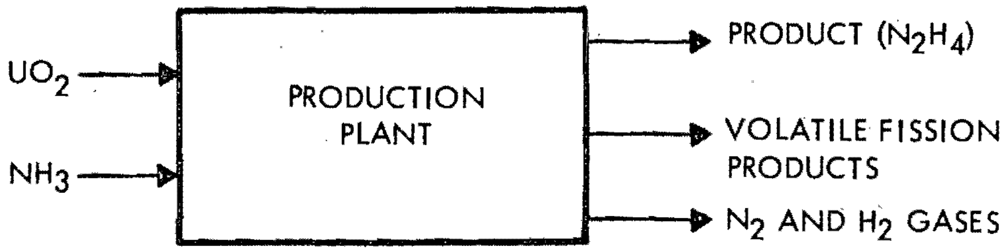

(A) NO SLURRY REPROCESSING

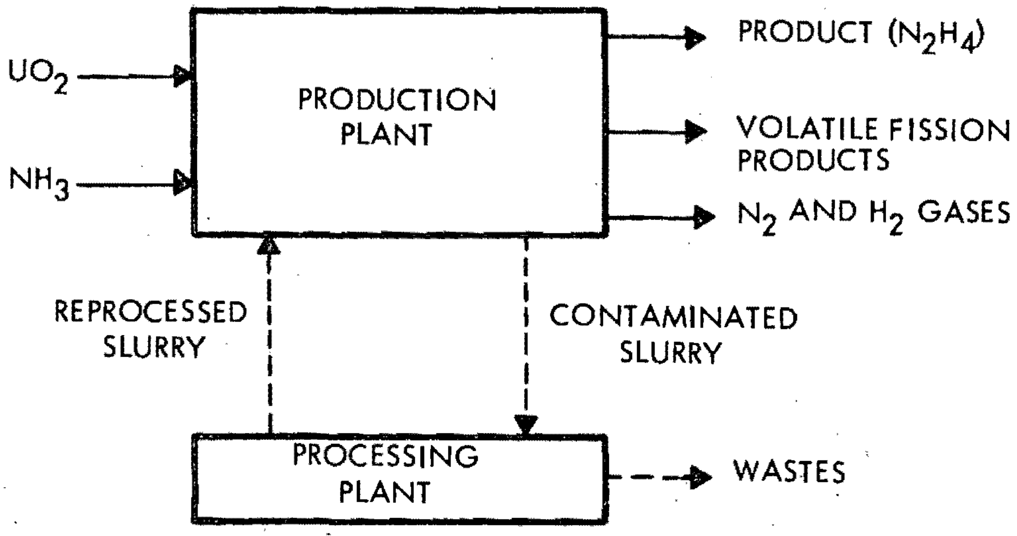

(B) WITH SLURRY REPROCESSING

FIGURE 2.48 FISSIOCHEMICAL PRODUCTION SYSTEM MODELS

37.1-65-1289

- Possible changes in the system surface chemistry
- Increase in the total system neutron absorption cross section (poisons)
- Buildup of impurities present in makeup UO_2
- Buildup of impurities present in makeup ammonia

The calculated rate at which these changes occur depends on the over-all average power density for the slurry system and the efficiency of the main- and side-reactions. The calculations are based on the following assumptions:

- (b)(3) [redacted]
- (b)(3) [redacted]
- Power Density. An over-all average power density of 25 kw/l was used, assuming a core power density of 50 kw/l and a total system volume equal to twice the core volume.
- Fission Products. It is assumed that 20% of the fission products will leave the system in the gas phase and the remaining 80% concentrate in the slurry. Since this calculation is concerned with system chemical changes, the changing of fission products due to radioactive decay and neutron capture is immaterial.
- Load Factor. 100% load factor is used.

The calculated changes in concentration of U-235, U-238, U-236, UO_2, total solids, fission products, and H_2O are shown as functions of operating time in Figure 2.49. In this calculation, the capture and decay products of U-238 and U-236 have not been separated from their parent nuclides. Note from Figure 2.49 that the fission products reach a concentration of 0.1 wt % after about 600 hr of operation (less than 1 month), after which they could affect some of the system chemistry. Also, the total solids in one year increase from 50 to about 66 g/l. The water will probably not build up as shown, since most of it will vaporize off at some point (probably as hydrazine hydrate).

(b)(3)

(b)(3)

2.6.2 System with Slurry Processing

It is difficult to establish at this point the controlling parameter for slurry processing. It could be a physical parameter such as particle size, or some nuclear parameter such as poison buildup. However, a chemical parameter such as the accumulation of impurities or fission products may well set the first requirement for slurry processing.

One processing scheme might be based on a simple wash of the UO_2 particles contained in a small fraction of the slurry bled from the plant through a filter. The UO_2 collected could be washed with water, acids, or other solvents, to dissolve the undesirable chemical components and remove them from the system. The UO_2 could then be dried and returned to the reactor by backwashing the filter with liquid ammonia.

Consider, for example, a requirement that the fission product concentration be limited to 1.1 wt %, and assume that the over-all power density is 25 kw/liter. Using this power density to calculate the fission product introduction rate, and further assuming that the wash removes

100% of the fission products, the required slurry processing rate would be about 2×10^{-3} l/hr per liter of total reactor slurry. This rate represents 0.2% of the total system volume per hour and the total system volume is changed every 500 hr. These rates seem small until fuel loss is considered. Assuming a fuel loss rate of only 1% and a base fuel concentration of 50 g/l, the fuel loss rate equals 55% of the fuel use rate resulting from burnup in the reactor. If 55% of the fuel is really lost, fuel burnup charges for hydrazine production will increase by 55%, and the hydrazine produced will cost 2¢ more per pound.

3.0 MATERIALS

A major materials effort was necessary to determine the compatibility of materials of construction, fuel, process chemicals and flow control components. This effort was initially important in terms of insuring the successful operation of an in-reactor loop; of almost equal importance was the determination of which materials problems would be most severe in terms of possible future reactor development.

Toroid experiments (Section 3.1) were conducted to determine the rate of erosion of typical materials of construction by reference ammonia-urania slurries. This same equipment allowed the determination of hydrazine decomposition rates induced by the materials environment anticipated in the in-reactor loop (3.2). Techniques were developed (3.3) for the treatment of uranium dioxide particulate fuel to assure its high strength and uniformity; preliminary experiments conducted by W. R. Grace and Company (3.3.2) suggested the possibility of the eventual development of a stable urania salt. In an attempt to obtain an early indication of the effects of irradiation upon a circulating fuel,a series of high flux, moderate burnup capsule experiments was conducted in the BMI reactor (3.4); it was expected that such predictive approaches would yield qualitative results at best. Type 304 stainless steel, the major loop material of construction, is especially prone to sensitivation; special tests were conducted (3.5) to assure that the necessary welding of this material would not induce significant intergranular corrosion problems upon exposure to ammonia. The culmination of the materials project effort involved thorough proof testing of all loop components under their inter-related reference conditions (3.6); a separate experiment (3.7) assured the operability of the selected fuel induction technique.

3.1 Erosion

When a particle-laden fluid, such as a slurry, encounters the surface of a solid in its flow path, the fluid will be deflected away from the solid; most of the particles, having greater inertia, will collide with the solid. This action will ultimately result in detectable erosion of the containing or obstructing solids and/or of the particles in the slurry. This effect was a significant consideration in selecting construction materials for the hydrazine in-pile test loop, and specifications for those materials required that they be able to withstand the eroding action of an ammonia-uranium slurry. Therefore, dynamic tests were performed on candidate materials, duplicating the flow conditions of the in-pile loop. The tests were performed with a toroid rotator since it was known that this device had been successfully used in the dynamic test program at Oak Ridge National Laboratory (ORNL).

3.1.1 Toroid Description*

The toroid rotator is an economical laboratory-scale device that provides a method of circulating fluids at known velocities up to approximately 45 fps without the use of a pump. The toroid itself is compact and requires only a small amount (20 to 25 ml) of test solution and materials. A heating system is provided for operation at temperatures up to 220°F, and pressures up to 2000 psia can be contained. The system pressure can be continuously measured and recorded.

The toroid rotator consists of rings of containment tubing (toroids) and a rotating device. The toroids contain the test liquid and the solid material to be tested. The rotating device moves the toroid through an ellipitical path. When this motion is imparted to a toroid half full of liquid, the liquid will circulate as an unbroken mass without gross voids; it is not uniformly distributed throughout the tubing as it would be if the toroid revolved about its own axis, but flows as a "slug" concentrated in about half the space in the tubing. It is apparent, therefore, that a toroid can be filled only about half full to function effectively.

The rotating device consists of a horizontal mounting plate attached at its center (by means of a bearing) to the shaft of a vertical

---

* Adapted from Oak Ridge National Laboratory Report ORNL-2870.

rotator arm (see Figure 3.1). The rotator arm is connected to the shaft of a variable-speed motor mounted vertically. The vertical center line of the shaft of the rotator arm, which is connected to the mounting plate, is offset from the center line of the motor shaft, thus creating a crank throw in the rotator arm. The horizontal plate, with attached toroid, is prevented from rotating about its own axis by a connecting rod installed between the plate and a rigid frame. The velocity of the rotating fluid is controlled by varying the speed of the motor.

Four 1/4-inch tubing caps are welded around the circumference of the toroid 90 degrees apart. A 3/16-inch diameter hole drilled through the bottom of the caps and the toroid wall permits the insertion of a corrosion pin specimen. The pin specimen is held firmly in a standard 1/4-inch tubing plug by a Teflon bushing slipped on the end of the pin, insulating it electrically from the rest of the apparatus. The pin specimen is 0.125 in. in diameter and 0.950 in. long; the portion exposed to the fluid in the toroid is 0.450 in. long and is not covered by the Teflon sleeve.

3.1.2 Calculated Erosion Rates

The basic principles of impingement on a body by solids in a fluid can be presented in terms of so-called "target" efficiencies. Target efficiency represents the fraction of particles in a flowing slurry contacting a solid surface which will impinge on that surface. Thus, for flow around a cylinder, as shown in Figure 3.2, all particles initially carried in the fluid between streamlines A and B will impinge on the body, and the target efficiency will be (X/D_b). It has been shown[24] that the target efficiency is equivalent to

$$\frac{X}{D_b} = V_o D_p^2 (\rho_s - \rho)/18\mu D_b \qquad (3.1)$$

where:

V_o = average velocity of the particle-laden fluid

D_b = representative dimension or diameter of the body impinged upon

D_p = diameter of the particle

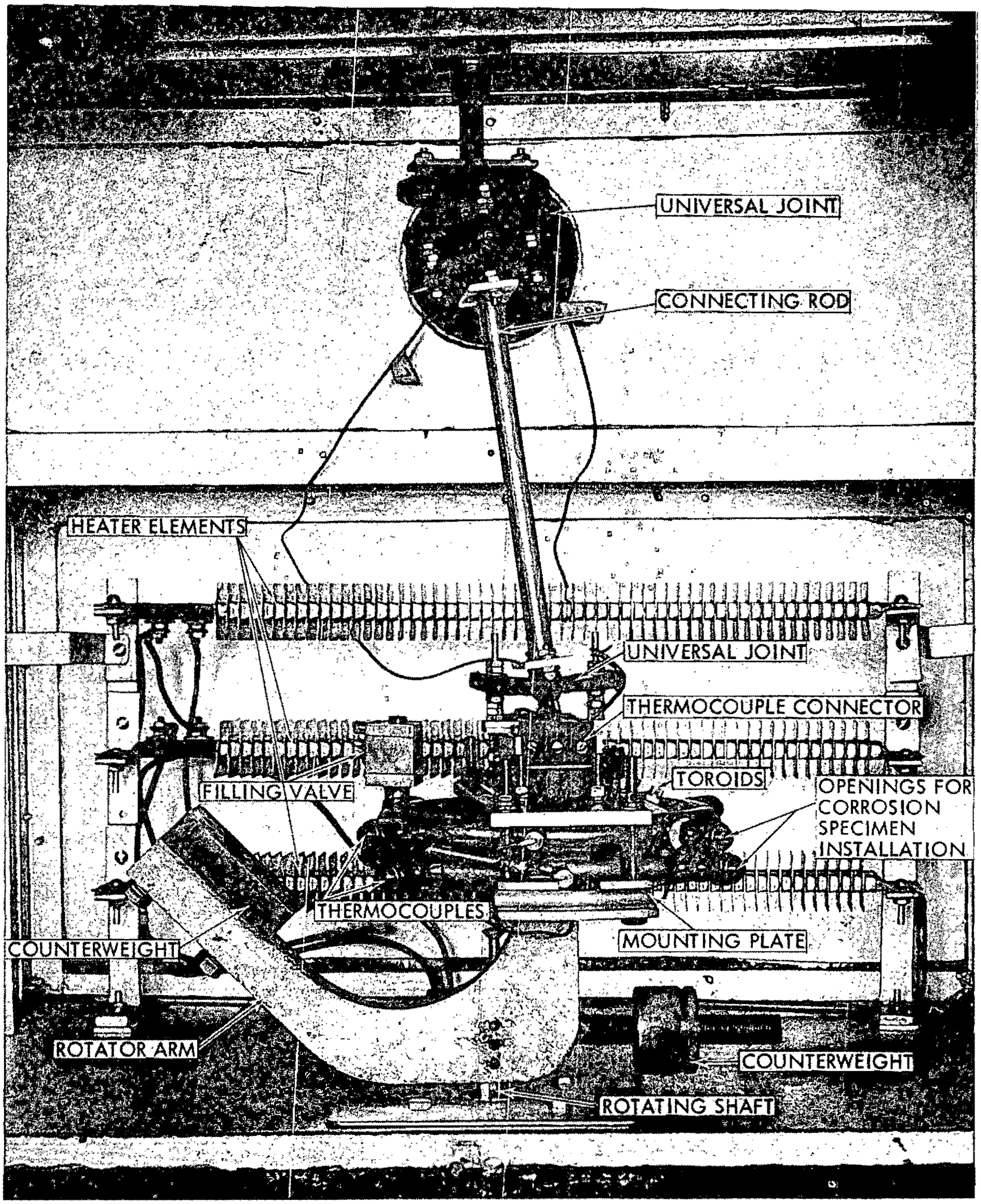

371-65-1384

FIGURE 3.1 TOROID

371-65-1385

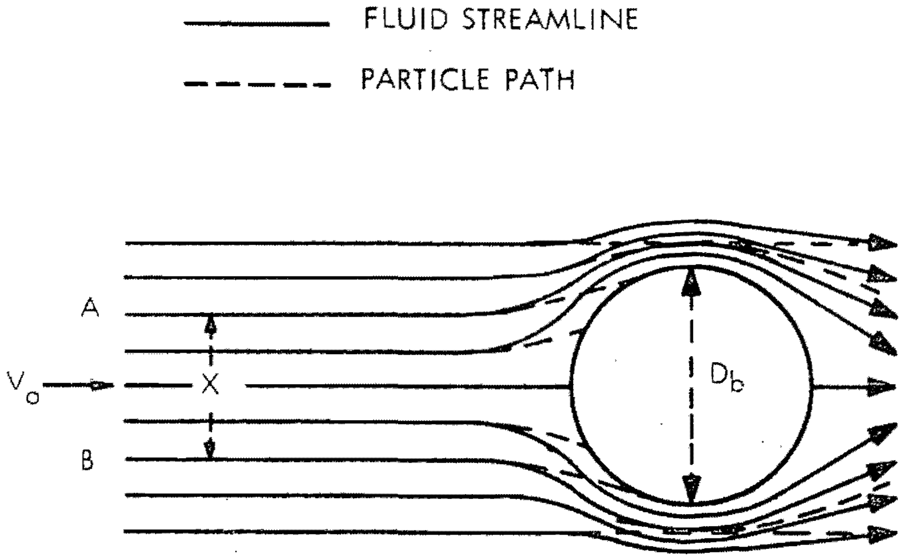

FIGURE 3.2 IMPINGEMENT SEPARATION OF SLURRY PARTICLES

ρ_s = particle density

ρ = fluid density

μ = fluid viscosity

For simple shapes the relationship between the two sides of the equation can be derived; e.g., there will be 50% more impingements on a ribbon placed in a flowstream than on a cylinder. For more complex shapes, such as pump impellers, etc., experimental determinations are required.

Using the erosion data generated in the toroids on the Homogeneous Reactor Program (HRP) at ORNL, the erosion rates to be expected in the hydrazine system were estimated. ORNL used slurries of ThO_2 in water at 300°C. In Table 3.1 are comparative values of the physical properties of interest for NH_3 at 160°F and H_2O at 300°C.

TABLE 3.1

SLURRY PROPERTIES

	ρ_s (g/cc)	ρ (g/cc)	μ (centipoise)	$(\rho_s-\rho)$ (g/cc)
ThO_2-H_2O (300°C)	10.1	0.73	0.09	9.37
UO_2-NH_3 (160°F)	10.96	0.52	0.11	10.44

For comparative purposes, identical values of V_o, D_p, and D_b will be assumed in the ThO_2-H_2O and the UO_2-NH_3 systems. The ratio of target efficiencies of the two systems then can be calculated.

$$\frac{\left(\frac{X}{D_b}\right) UO_2\text{-}NH_3(160^oF)}{\left(\frac{X}{D_b}\right) ThO_2\text{-}H_2O(300^oC)} = \frac{10.44}{9.37} \times \frac{0.09}{0.11} = 0.91$$

Or, in other words, at similar flow rates, and for equivalent size particles, UO_2 in NH_3 at 160°F will not impinge as frequently on a pin specimen as ThO_2 in H_2O at 300°C.

Table 3.2 lists the measured erosion rates of various materials by a ThO_2-H_2O slurry[24] and predicts the erosion rates expected in a reference UO_2-NH_3 slurry. Both the reduced solids concentration and the reduced target efficiency act to minimize the predicted erosion. Since UO_2 is a somewhat softer material than ThO_2, a still greater reduction in erosion rates may be expected although the extent of this latter advantage cannot be quantitatively predicted.

TABLE 3.2

SLURRY EROSION RATES

Material	Measured HRP Pin Attack Rate(1) (mil/yr)	Predicted Hydrazine Pin Attack Rate 2 (mil/yr)
Platinum	2	0.09
Gold	2	0.09
Zircaloy 2	3	0.14
Titanium and Alloys	4	0.18
Type 347 and other SS	7	0.32
Nickel	12	0.54
Inconels	24	1.1
Stellites	14 - 20	0.63 to 0.90
Al_2O_3	280	12.5
Graphitar	Consumed	?

---

(1) 1000 g ThO_2/kg of H_2O; 20 fps; 300°C

(2) 50 g UO_2/l of NH_3; 20 fps; 160°F

3.1.3 Measured Ammonia Slurry Erosion Rates

The initial rates of erosion by UO_2- and ThO_2-liquid ammonia slurries in toroid experiments were too small to be measured. (Table 3.3). After circulating the slurry for 100 hr, the weight loss of stainless steel specimens exposed to a 50 g/liter UO_2-liquid ammonia slurry at 20 fps and 160°F was not detectable on the analytical balance.

Both the predictions and the initial erosion tests indicated that erosion rates of UO_2-NH_3 slurries used in the Hydrazine Program were

TABLE 3.3

MEASURED EROSION RATES OF NH_3 FUEL SLURRIES

Slurry	Particle Size (microns)	Erosion Rate (mil/yr)						
		50g/l; 20 fps; 160°F	500 g/l; 30 fps; 160°F					
		347 SS	347 SS	440C SS	17-4SS	304 SS	Teflon	Al_2O_3
H_2O	-	N.D.*						
H_2O-ThO_2-sol	0.03-0.05	0-2						
NH_3	-	N.D.*						
NH_3-dried ThO_2	0.03-0.05	0-1	7.2	2.9	10.2	N.T.	13.5	N.T.
NH_3-unfired UO_2	1.65		2.2	3.4	3.4	N.T.	W.G.+	N.T.
NH_3-1300°C fired UO_2	1.65		2.4	N.D.	0-1	6.6	W.G.+	N.T.
NH_3-1400°C fired UO_2	1.65	0-1	2.4	3.6	3.6	N.T.	W.G.+	N.T.
NH_3-1600°C fired ThO_2	2.3		3.0	4.1	3.1	N.T.	W.G.+	N.T.

* N.D. - no detectable weight change

\+ W.G. - weight gain

N.T. - No Test

very small. To better evaluate the erosion resistance of various construction materials, more severe conditions than those existing in the in-pile loop were chosen. Slurry loadings were increased tenfold to 500 g/l, flow rates were increased to 30 fps, and test times were doubled to 200 hr. By calculation, these changes in slurry conditions should have increased the erosion rates about twentyfold.

A second series of erosion tests was run under the new conditions; the results appear in Table 3.3. The erosion rates of UO_2 in ammonia, even at the excessive conditions of 500 g/l and 30 fps, are acceptably low for the in-pile test loop; the measured rates are slightly less than predicted. The weight gains shown for Teflon are due to UO_2 embedding in the soft material.

The tests performed using ThO_2 indicated erosion rates somewhat higher than for UO_2. Since UO_2 is softer than ThO_2, and since ORNL has successfully run an in-pile ThO_2-H_2O slurry loop for over 3000 hr at 300°C, it was concluded that erosion rates in the hydrazine in-pile slurry loop would not be a serious problem.

3.2 Hydrazine Decomposition

A literature search to investigate the compatibility of NH_3-N_2H_4 mixtures with other materials was conducted early in the program.[25,26,27,28] No data on NH_3-N_2H_4 mixes were located, but considerable information was available on the compatibility of either ammonia or hydrazine (separately) with other materials. The literature reported that hydrazine was easily decomposed by many materials (Inconel, copper, molybdenum, graphitar, neoprene rubber) at temperatures below 200°F.

The possible effect of the structural materials of the loop on the decomposition of N_2H_4 in a N_2H_4-NH_3 mixture was not known. It was necessary to determine, first, if hydrazine would decompose when in contact with the loop structural materials and, second, the rate of such decomposition.

3.2.1 Experimental Technique

The toroid assembly was adapted and used to determine the decomposition rate of N_2H_4-NH_3 mixtures in contact with many materials. Hydrazine produces gaseous products when it decomposes. By measuring and recording the pressure buildup within the toroid as a function of time, the extent and the rate of hydrazine decomposition can be determined.

Hydrazine when it decomposes will do so by one of the following three reactions:

1)	$N_2H_4 \longrightarrow N_2 + 2H_2$	catalytic at any temperature (n = 3),
2)	$2N_2H_4 \longrightarrow N_2 + 2NH_3 + H_2$	catalytic probably above 100°F (n = 1),
3)	$3N_2H_4 \longrightarrow N_2 + 4NH_3$	thermal and catalytic probably above 150°F (n = 1/3).

An indication of which reaction has occurred is given by the N_2/H_2 ratio. The weight of N_2H_4 decomposed can be calculated from the formula

$$W_d = \frac{\Delta P_t \cdot V_g}{37.7 \cdot n \cdot T_t} + \frac{1.43 \cdot W_L \cdot S_t}{10^3 \cdot n} \qquad (3.2)$$

where:

W_d = weight of N_2H_4 decomposed (grams),

W_L = weight of ammonia in the system (grams),

S_t = solubility of H_2 and N_2 in ammonia at temperature t and pressure T_t (cm^3/gram at STP),

n = moles of permanent gas produced,

V_g = volume of gas phase (cm^3),

T_t = final temperature (°K),

ΔP_t = change in pressure at temperature t (psi).

3.2.2 Results

The first material evaluation test was performed on 304 SS toroid rings. The temperature was 190°F, the flow rate was 10 ft/sec, and the test lasted for 415.9 hr. No pressure rise was detected throughout this run. It was concluded that 304 SS toroids would not affect any of the structural material decomposition tests.

The following materials were tested in NH_3-N_2H_4 mixtures containing from 3 to 7 wt% hydrazine at test temperatures between 130 and 217°F in mixtures or slurries circulated at a velocity of 10 fps:

Structural Materials (as pins)

Inconel
Copper
Molybdenum
Graphitar

Powders

UO_2 (loaded in air)
UO_2 (baked in H_2 and loaded in vacuum)
Copper
Fe_2O_3

The structural materials were selected because they were reported to be capable of decomposing pure hydrazine. Total exposed area of the pins was approximately 0.6 in.^{2}. None of the structural materials produced a rise in pressure, nor was there a significant quantity of gas generated. It was concluded that ammonia inhibits reaction, reducing the rate of hydrazine decomposition in N_2H_4-NH_3 mixes in contact with the test materials to a level that would not affect the program.

A slurry of 10 grams of UO_2, fired at 1300°C but exposed to air after cooling, was made with 14.2 grams of 5.5% N_2H_4-NH_3 mixture, and was rotated in the toroid at 10 fps and 190°F for 50 hr. The overpressure of the system rose 118 psi and leveled off after 40 hr, indicating decomposition of the hydrazine into gaseous products. Analysis of the slurry and the gaseous products after the runs revealed that most of the hydrazine had been decomposed, and that the gaseous products were N_2 and H_2 in the ratio of 2.7 to 1. The test was repeated with UO_2, which was not exposed to air after being fired in a hydrogen atmosphere so that absorbed oxygen was excluded from the toroid. Unfortunately, the chemical analysis of the N_2 to H_2 ratio was not successfully performed in this latter test.

Surface dependency was demonstrated in this test since the decomposition rate during the first two hours was 17.4 wt%/hr for the

UO_2 exposed to air and 13 wt%/hr for the unexposed UO_2. The average decomposition rates for the entire runs were, respectively, 2.2 wt%/hr and 1.1 wt%/hr. The higher decomposition rate is attributed to the presence of more oxygen on the surface of the UO_2. This is corroborated by the fact that in both cases the hydrazine ceased to decompose after 45 hr. Only 55% of the hydrazine decomposed with the vacuum-loaded UO_2 and 90% decomposed with the air-loaded UO_2. Both the Fe_2O_3 and copper powders decomposed hydrazine; the Fe_2O_3 faster than the copper which was faster than the UO_2. The results are shown in Table 3.4. In conclusion, it has been shown that powders induce hydrazine decomposition rates which are much higher than are the hydrazine decomposition rates on solid, low surface area materials.

The significance of the decomposition caused by the UO_2 powder has been calculated by applying these results to a hydrazine production plant design reported in the final technical engineering report for Phase I of this program (July, 1961).[1] For a 175 Mw(t) reactor with a hydrazine production rate of 3650 lb/hr (G = 1), only 0.65% will be lost by decomposition; this is not enough to alter production cost significantly.

3.3 Fuel Preparation

After consideration of all the process parameters for producing hydrazine in a reactor, a decision was made to use 1 to 3 micron uranium dioxide particles as the source of fission fragments. This choice was made for the following reasons:

1) UO_2 is stable in anhydrous ammonia;
2) It is stable in air, requiring no special handling other than that required for health considerations;
3) It is easily procured in a wide range of particle sizes; and
4) A considerable amount of literature on its technology is available.

3.3.1 Uranium Dioxide Powder Preparation

The depleted uranium dioxide powder used in the hydrazine development program is a low-fired product of the ammonia diuranate precipitation process, and is produced by the Davison Chemical Corporation. The particles are irregular in shape and relatively soft, but their

TABLE 3.4

N_2H_4 DECOMPOSITION RATES

Slurry	Temp.(°F)	Weight % N_2H_4 (1)		N_2H_4 Decomposition Rate Wt% /hr of Original Amount		Possible Reactions (2)
		Initial	Final	During First 2 hr	Ave. of Entire Run	
UO_2-NH_3-N_2H_4	192	4.1	0.51	17.4	2.2	2
UO_2-NH_3-N_2H_4 (vacuum loaded UO_2)	193	4.5	1.92	13.0	1.1	3
UO_2-NH_3-N_2H_4	160	6.5	5.50	6.0	0.3	2
Cu Powder - NH_3-N_2H_4	160	6.4	3.30	9.0	1.4	2
Fe_2O_3-NH_3-N_2H_4	160	3.1	0.33	13.0	2.5	2,3

---

(1) Calculated from recorded pressures.

(2) Refers to mechanisms listed in Section 3.2.1.

resistance to degradation can be increased by refiring at a higher temperature, provided the temperature is below that at which the particles begin to sinter together and form clinkers. This maximum temperature was determined by measuring the clinker content of UO_2 powder samples fired in dry hydrogen at temperatures ranging from 1000° to 1600°C in a Hevi-Duty, molybdenum-wound, single-end tube furnace. The clinker content was measured with a settling apparatus consisting of a pyrex tube, 14 mm ID and 7 ft long fitted with a stopcock and clinker receiving receptacle at one end, and a funnel at the other. The procedure used was as follows:

One-half gram samples of unfired and fired powder were agitated by an Eberbach clinical shaker for 16 hr in a 0.005 molar solution of trisodium phosphate (Na_3PO_4).

A sample of unfired UO_2 was washed into a funnel at the top of the settling apparatus which was also filled with Na_3PO_4. The time required for the first particles to fall to the stopcock was measured and found to be 9 min.

In measurements of the fired UO_2 samples, the stopcock was closed after 9 min had elapsed. During the 9 min, the clinkers, being heavier, fell though the stopcock into the bottom receptacle. The smaller, slower settling particles were retained in the settling apparatus.

The clinkers were removed from the bottom receptacle, dried and weighed.

Results of these tests,shown in Figure 3.3, indicated that the fired UO_2 powder was not well dispersed in a 0.005 M solution of Na_3PO_4, as shown in Curve A of Figure 3.3. Curve B shows the results of tests repeated with a 0.002 M solution of Na_3PO_4 as the dispersant. For Curve C, the UO_2 was fired at 1200°C for 2 hr, and then refired for an additional 2 hr at a higher temperature. From the curves, it is seen that sintering begins somewhere above 1300°C.

One kilogram of 93% enriched UO_2 was procured from United Nuclear Corp. This material had been produced by the fluoride reduction process and ranged in size from 0.7 to 1.0 μ. The material assayed as 93.074 wt% U-235 and 87.67% uranium. AGN processed the fuel by firing

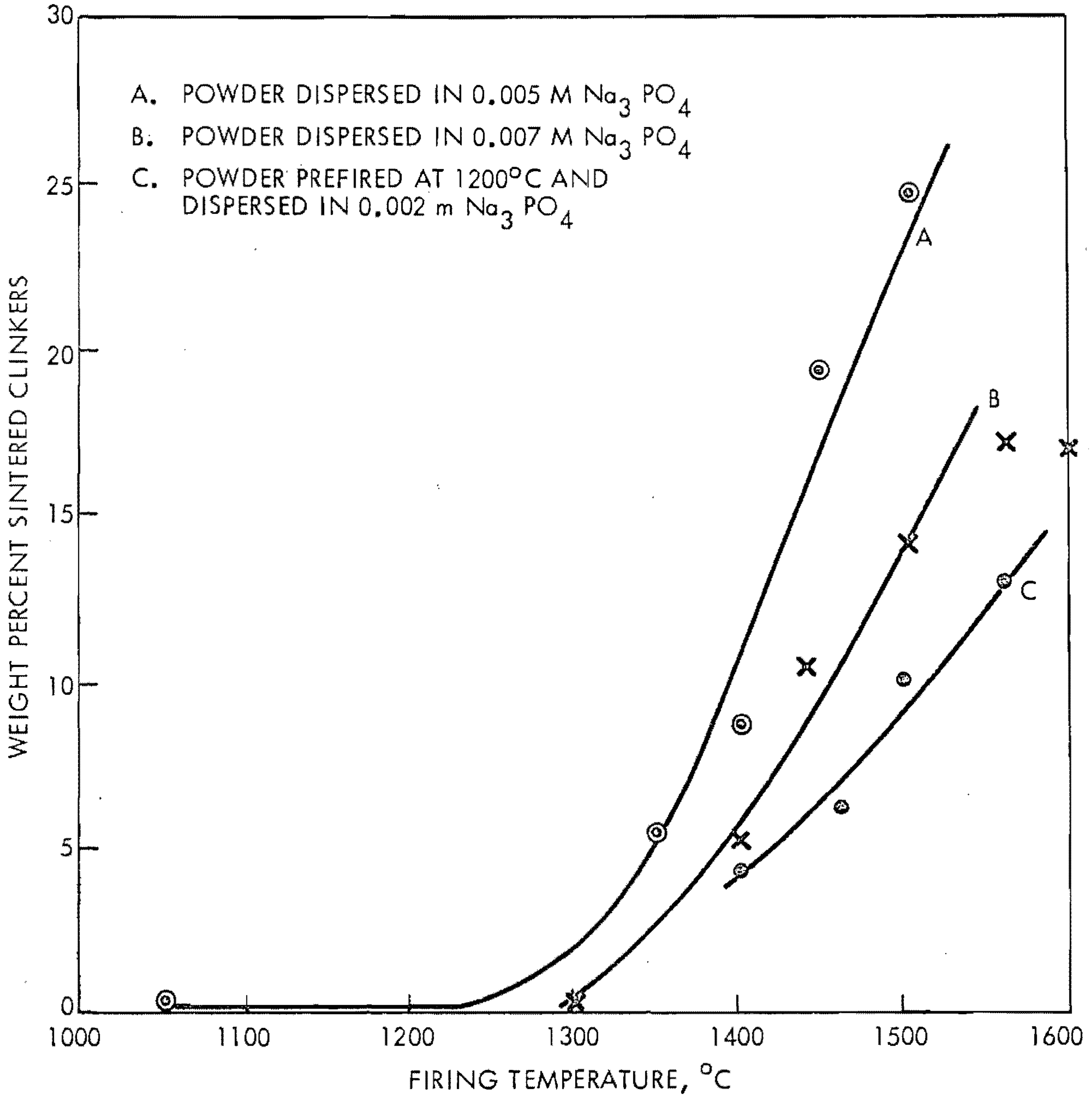

FIGURE 3.3 PERCENT SINTERING OF UO$_2$ POWDER AS A FUNCTION OF FIRING TEMPERATURE

371-65-1386

it to 1300°C for four hours, cooling, crushing, and screening it through 100-mesh screens.

3.3.2 Uranium Dioxide Ammonia Sol Preparation

Some of the difficulties in handling a slurry of UO_2 powder suspended in liquid ammonia (particle settling, slurry caking, erosion, etc.) might be overcome if it were possible to prepare a stable sol of UO_2 in liquid ammonia. The Research Division of W. R. Grace & Co. at the Washington Research Laboratories, Clarksville, Maryland, had been successful in suspending UO_2 in water as a sol. Under subcontract to AGN, W. R. Grace & Co. made a preliminary study to determine whether a stable urania dispersion in liquid ammonia was feasible, and to establish procedures for preparing such a dispersion.

The aqueous urania sols previously developed by Grace were used as starting materials for this work. The basic problem was to prevent extensive aggregation during the drying process. Generally, during the drying of sols, surface tension forces act to irreversibly bond the material into a soft and dense mass. Grace successfully separated the urania from the sol by centrifuging the sol at 1500 rpm for 15 min. and decanting the supernate. The slurries were then dried at room temperature under an ammonia atmosphere using silica gel as dessicant. This urania was then suspended in liquid ammonia. The resulting ammonia dispersions were altered and aggregated from their original sol form; a slow-settling suspensoid resulted. The extensive alteration of the initial urania colloidal structure is a complicating factor that indicates the need for complete dehydration and stabilization of the colloidal urania prior to resuspension in the liquid ammonia. Conditions during preparation, material handling, and dispersing must be further investigated to avoid any concurrent reaction of water and ammonia or possible oxidation effects on the colloidal urania, particularly while in the reactive hydrated form. Grace feels confident that the difficulties can be overcome and a stable urania-liquid ammonia sol is feasible.

These efforts were of an exploratory nature and were designed to learn first, if there was any possibility of forming an ammonia based urania sol and second, to learn the extent of the problems which must be overcome. The efforts were less in direct support of the in-pile loop experiment than in support of any possible future phases of operation.

3.4 Effect of Irradiation on UO_2 Fuel Suspended in Liquid Ammonia

M. E. A. Hermans and his associates,[29] have reported the results of their irradiation experiments with aqueous fuel suspensions of PuO_2, $ThO_2 \cdot 20\%\ UO_2$ (20% U-235) and $ThO_2 \cdot 20\%\ UO_2$ (4% U-235). They found that irradiation of these suspensions can result in the formation of colloidal suspensions of the solids. For a total integrated flux of approximately $3 \times 10^{15}\ n/cm^2$, the colloid formation reaches a maximum of about 25 wt% for $ThO_2 \cdot 20\%\ UO_2$ (4% U-235) with a surface area of 3 m^2/gram, and that such formation decreases to about 8 wt% as the doses increase to approximately $2 \times 10^{16}\ n/cm^2$ (Figure 3.4). Hermans, et al, explain this drop-off by proposing a "saturation" theory to the effect that part of the colloidal debris recrystallizes to form particles of microscopic size which associate with the bulk solid.

Hermans also reports that noticeable irradiation damage occurs to the particles when they are irradiated in dispersing media (H_2O, 10^{-2} HNO_3, 10^{-3} KOH, etc.), and that the damage is markedly reduced when irradiation is conducted under flocculating conditions. Figures 3.5, 3.6 and 3.7 illustrate, respectively, fuel before irradiation, after irradiation under dispersing conditions, and after irradiation in flocculating media. The loss of the original particle shape, and the formation of pores 500 to 1000 Å in size, are apparent in the fuel irradiated in dispersing media (Figure 3.6), whereas the fuel irradiated in flocculating media (Figure 3.7) retains its form and exhibits minimal porosity.

A careful review of Hermans' reports led to the conclusion that UO_2 particles suspended in liquid ammonia might not be stable under irradiation. It was considered possible that the particles would partly degrade and form a sol when irradiated by thermal neutrons, and that this could occur at fairly low burnups. Probable effects as determined from the literature include: change in particle size and size distribution, formation of a colloid, change in specific surface area, and changes in the rheological properties resulting from changes in the surface characteristics of the particles. Because the nature and extent of these changes would greatly affect the design, construction, and estimate of the reliability of the in-pile loop, an irradiation program was carried out early in the hydrazine program in the

371-65-1387

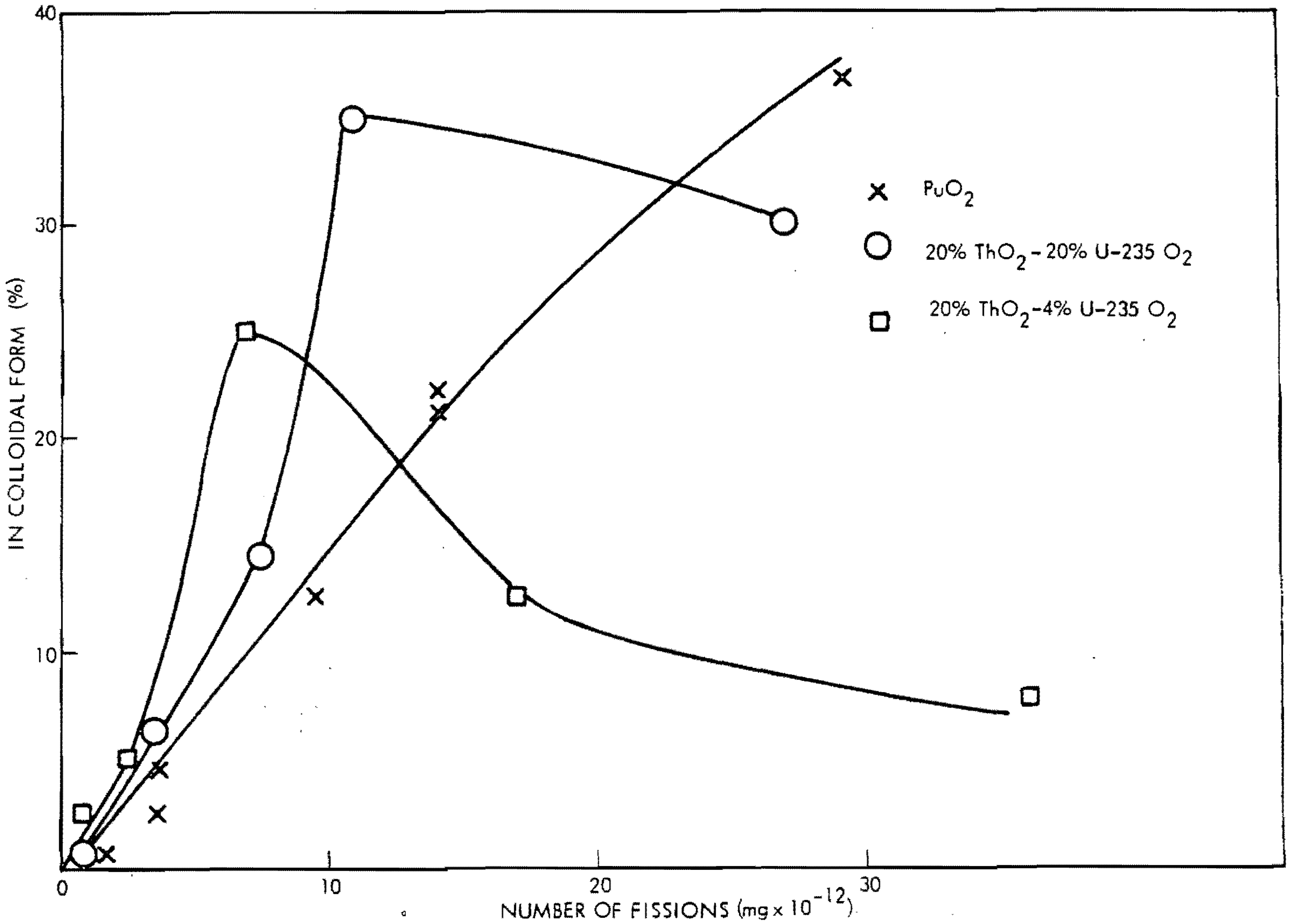

FIGURE 3.4 PERCENTAGE VARIATION OF METAL ATOMS IN COLLOIDAL FORM WITH TOTAL DOSE (ALL SOLIDS 3 m^2/grams)

371-65-1388

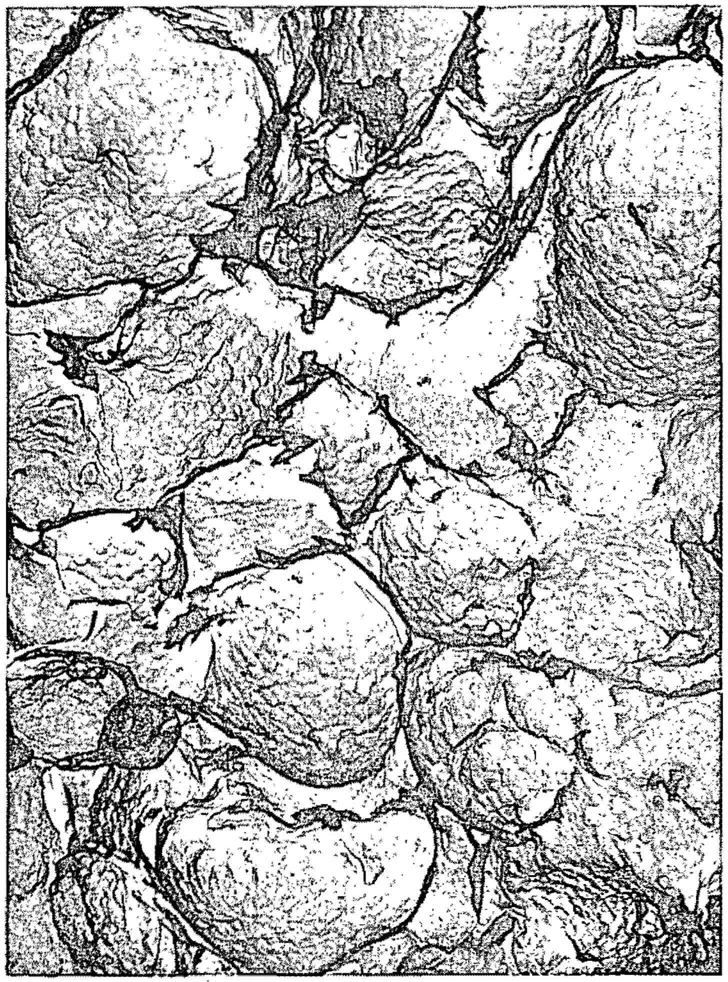
10,400X

FIGURE 3.5 ELECTRON MICROSCOPE TRIAFOL REPLICA OF NON-IRRADIATED 20% U-235 O_2 - 80% ThO_2 (1150°C FIRED)


32,000X

FIGURE 3.6 ELECTRON MICROSCOPE TRIAFOL REPLICA OF 20% U-235 O_2 - 80% ThO_2 (1150°C FIRED) IRRADIATED IN A DISPERSING MEDIUM TO A TOTAL INTEGRATED FLUX OF 2×10^6 n/cm^2

10,400 X

37.1-65-1349

FIGURE 3.7 ELECTRON MICROSCOPE TRIAFOL REPLICA OF 20% U-235 O_2-80% ThO_2 (1150°C FIRED) IRRADIATED IN A FLOCCULATING MEDIUM TO A TOTAL INTEGRATED FLUX OF 4×10^{16} n/cm^2

Battelle Research Reactor (BRR) to determine the extent, if any, of the irradiation effect on the properties of UO_2 suspended in liquid ammonia.

3.4.1 Equipment

The capsule (Figure 3.8) used to irradiate UO_2 suspended in liquid ammonia in the BRR was a doubly-contained pressure vessel capable of withstanding the pressure buildup caused by ammonia decomposition and gaseous fission products. The slurry (1/2 gm 93% enriched uranium and ~200 cm^3 liquid anhydrous NH_3) was loaded through a valve and loading tube into a stainless steel liner. Standard Oil's Alkyl-Benzene 250, a liquid of proved radiation stability, was placed between the stainless steel liner and the capsule walls to facilitate heat transfer. Slurry temperatures were read, using two wells, each holding two thermocouples, and maintained at approximately 140°F. Pressures were read in each capsule with pressure transducers and continuously recorded. A nickel-laminated ultrasonic vibrator was affixed to the bottom of the capsule with an epoxy cement and surrounded by a waterproof casing in order to keep the UO_2 suspended throughout the irradiation. The capsules were approximately 60 in. high and 4 in. in diameter.

Post-irradiation tests required careful transfer of the irradiated slurry into several pieces of equipment. To be sure that no solids or supernate were lost, a special transfer apparatus was designed and constructed (Figure 3.9). The apparatus consisted of a vacuum-pressure chamber designed to receive the stainless steel liner from the irradiated capsule, a slurry bomb connected to the chamber, and special ball valves to which a settling rate sight glass could be connected. The chamber, the slurry bomb, and valves "A", "B", and "C" were designed to permit transfer of all the slurry in the downward direction. Two Dewar flasks were used to liquefy or freeze the slurry, as required.

3.4.2 Operating Details

Three irradiation capsules and one control capsule were suspended in the Battelle Research Reactor pool. The control capsule remained in its original position in the non-irradiated section of the pool; the irradiation capsules were successively positioned at the center of the reactor core face in an estimated average flux of 2×10^{13} neutrons/cm^2/second. At a reactor power level of 1.8 Mw, one capsule was irradiated for 13.2 hr,

371-65-1348

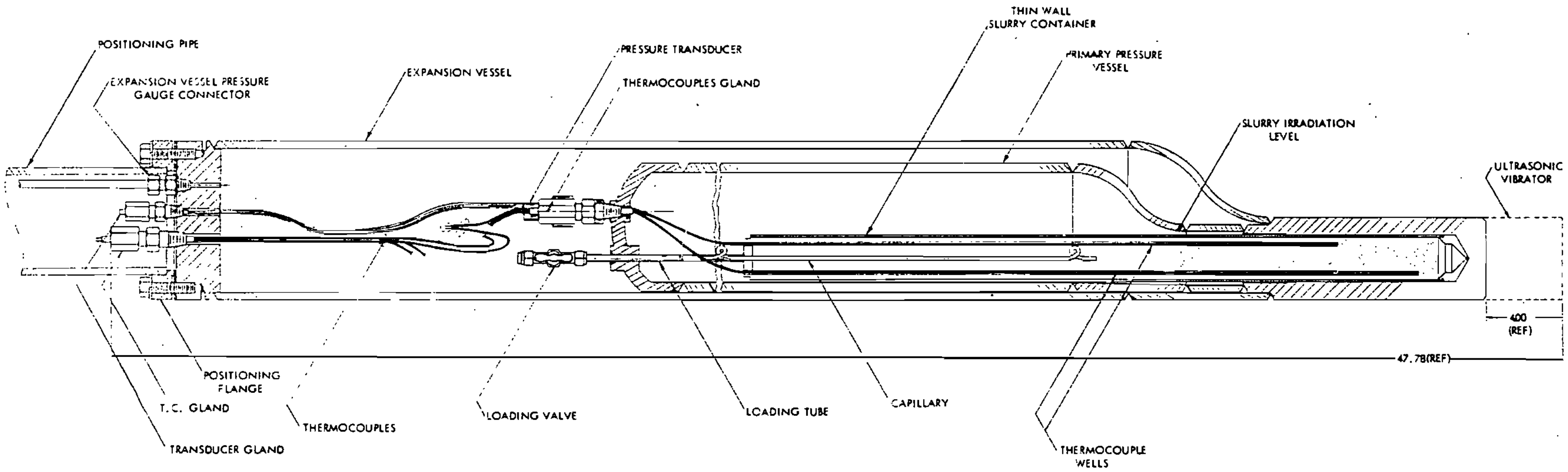

FIGURE 3.8 SLURRY IRRADIATION CAPSULE - FINAL DESIGN.

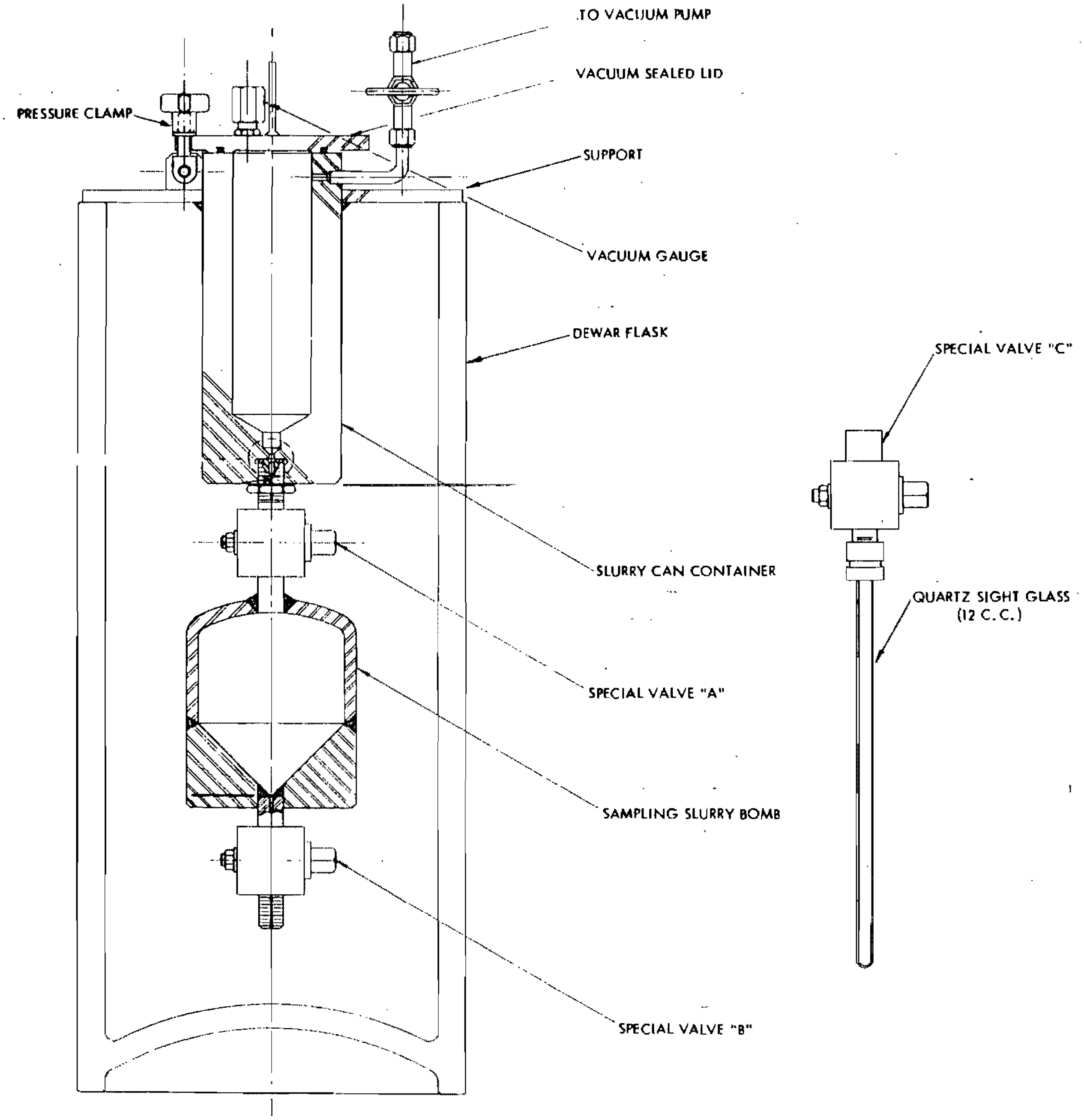

FIGURE 3.9 SLURRY TRANSFER APPARATUS

37.1-65-1347

another capsule for 24 hr, and the third for 70.15 hr. The measured temperature of the slurry throughout the irradiations was 127° to 130°F. As ammonia decomposed, pressure inside each irradiation capsule gradually increased, reaching 980 psi in the 13.2 hr irradiation and 1750 psi in the 70 hr irradiation.

After the three capsules had been irradiated, they were removed from the reactor core and allowed to cool in the pool water until they could be transported to the hot cells. In the hot cell, the ammonia slurry in each capsule was frozen, the capsules were cut open, and the liners removed. Each liner was allowed to thaw slowly until the ammonia melted. Then the transfer apparatus was used to put the slurry into a sample bomb. The same procedure was followed for the unirradiated control capsule. These bombs containing the irradiated samples were removed to the BMI radiochemical laboratory and subjected to the testing program outlined in Figure 3.10.

3.4.3 Results

The effective flux at the fuel, calculated from cobalt monitors, was approximately 4×10^{12} neutrons/cm^2/second. Calculated values of the percent burnups reached were 0.01, 0.022, and 0.056% for the low, medium, and high burnup capsules, respectively.

The settling rate in ammonia for all irradiated samples was 0.85 cm/second, essentially the same as for unirradiated UO_2. Unirradiated samples settled quickly and completely, leaving a clear supernate. In the highest burnup sample, a slight tail of extreme fines was observed to settle slowly for an hour after the bulk of the solids had settled. All samples produced a straw-colored supernate after complete settling. This supernate sample was rotated at 10,000 rpm in a Servall centrifuge for 4 to 5 min at atmospheric pressure with the ammonia at a temperature below its boiling point to separate particles larger than 500 Å from the supernate. Uranium analyses of the separated fractions are listed in Table 3.5. Less uranium was recovered in the fractions after centrifugation than was contained in the starting supernate, presumably because of handling losses. Using either value, the uranium content is low, indicating the absence of significant quantities of suspended sol. These data suggest that the UO_2 content of ammonia is between 30 and 90 milligrams per liter after gravity

371-65-1346

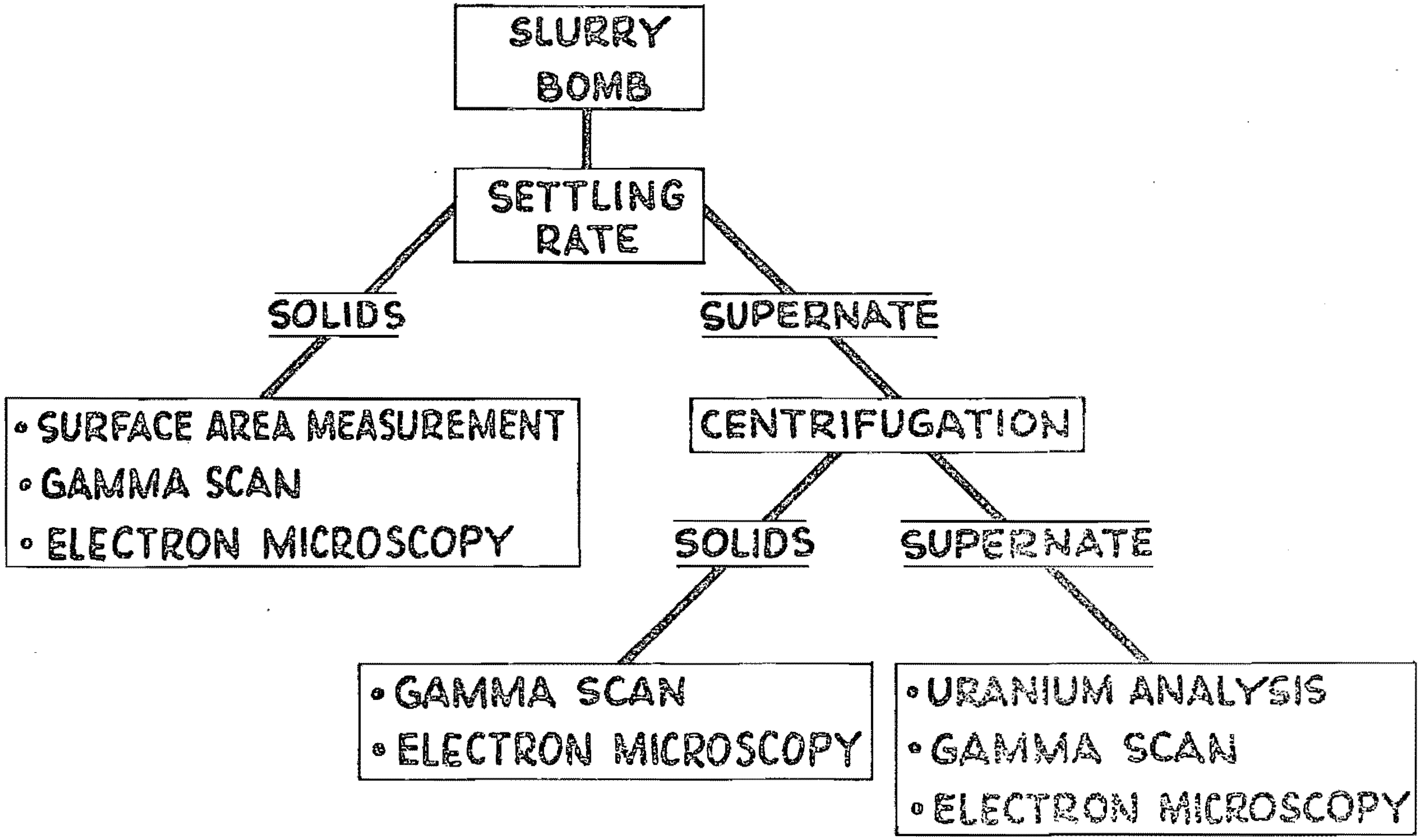

FIGURE 3.10 IRRADIATED SLURRY TEST PROGRAM

settling and between 10 and 20 milligrams per liter after centrifugation; that the thermal neutron irradiation of UO_2 slurried in liquid ammonia to burnups of as high as 0.055% results in some particle breakdown, followed by agglomeration of these particulate fines into discrete agglomerates; and that essentially no uranium-bearing sol is formed.

TABLE 3.5

UO_2 CONCENTRATION IN SUPERNATE AFTER IRRADIATION (GRAMS/LITER)

Burnup	Supernate After Gravity Settling	After Centrifugation Supernate	After Centrifugation Solids
0.01	--	0.019	0.002
0.022	0.090	0.007	0.025
0.056	0.080	0.018	0.020

The measured specific surface area of the unirradiated UO_2 was 0.60 m^2/grams, and that of the UO_2 after irradiation to 0.055% burnup was 2.0 m^2/grams. This increase is attributable either to a modest degree of particle breakdown caused by a combination of irradiation and mechanical attrition, or to increased porosity of the particles, perhaps resulting from hole formation similar to that shown in Figure 3.6. Hole formation is probably not the explanation, since current information suggests that holes are formed only in a dispersed system, and that UO_2 suspended in liquid ammonia is a flocculating system. The observations made during the settling rate tests and reported in the previous section support the particle breakdown explanation.

To determine particle size distribution and particle appearance, many electron micrographs were taken of the UO_2 samples before and after irradiation. Figure 3.11 shows a typical dispersion of the unirradiated enriched UO_2 used as starting material in all of the capsules. Most particles range between 0.1 and 1.8 micron diameter, the average being 1 micron; relatively few fines are present. Figure 3.12 is a transfer replica of irradiated UO_2 from the high burnup capsule. In contrast with Figure 3.11, this picture reveals a wide range of particle sizes, down to as small as 100 Å, supporting the settling test results and the increase of surface area noted earlier.

37.1-65-1344

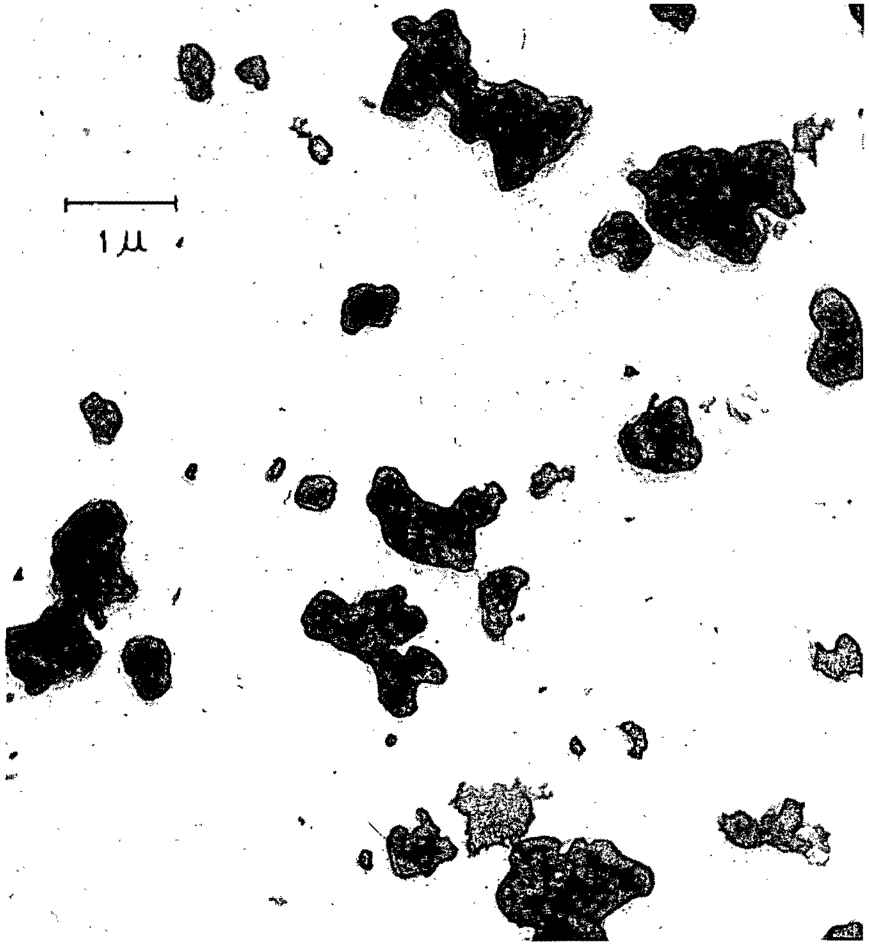

FIGURE 3.11 DISPERSION OF ENRICHED UO_2 PARTICLES PREPARED BY TRANSFER REPLICA METHOD

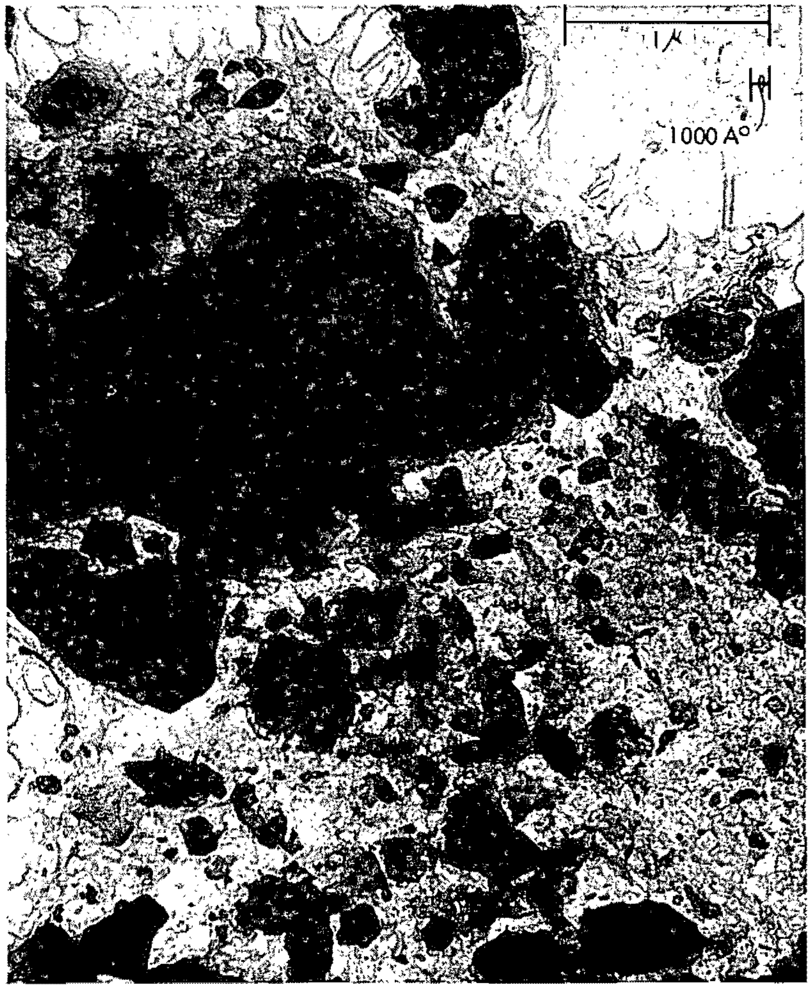

FIGURE 3.12 TRANSFER REPLICA OF THE IRRADIATED UO_2 FROM THE HIGH BURNUP CAPSULE (0.055%) AFTER REMOVAL OF THE VOLATILES BY HEATING TO 400°F FOR 30 MINUTES

Irradiation did not significantly change the shape of most of the solids. A few of the particles mixed in with the bulk of the UO_2 showed definite crystal formation; a few quite perfect single crystals were also found. The extent of this crystal growth did not seem to depend upon UO_2 burnup. Figure 3.13 shows a large UO_2 crystal taken from the bulk solids after gravity settling of the slurry from the low burnup capsule; it had developed several triangular faces. Figure 3.14 shows solids separated by centrifugation from the gravity-settled supernate; clearly, the crystals grew from the surface of the original irregular UO_2 particles. Figures 3.15 and 3.16 are photographs of UO_2 crystals, the first accumulated by gravity settling and the other by centrifugation from the highest burnup capsule. The most plausible explanation for the occurrence of these faceted crystals is that they have grown from solution. Growth from a low supersaturation solution dependent upon a step defect in a low index face has been demonstrated for many types of crystals. The most plausible lattice defect capable of providing such a step defect is dislocation whose Burger's vector has some screw component which terminates in the growing crystal face. The development of habit faces on UO_2 particles irradiated in anhydrous ammonia indicates the existence of such a defect structure. Although UO_2 is not normally considered soluble in liquid ammonia, uranium in the low parts per million range might exist in a liquid ammonia solution. The dislocation-generated, step-defect, crystal-growth mechanism usually presupposes a supersaturation of approximately 1% at the growth face. This supersaturation is most apt to be achieved during fissioning since the fission fragments leaving the surface probably "boil off" several atoms of uranium into the liquid ammonia. Hermans, et al, likewise observed crystal growth during the irradiation of UO_2 slurried in water.[29]

One of the objectives of the experiment was to ascertain the distribution of fission products. Samples of ammonia and uranium were withdrawn after each irradiation, and gamma-scanned, using a 128-channel pulse height analyzer. Several scans were repeated so that the decay rates of certain isotopes could be calculated. On the basis of the gamma scans, other samples were selected for radiochemical separation analyses.

Iodine and ruthenium radioisotopes were found in the liquid phase and all other radioisotopes, except for the gases, appeared in

371-65-1389

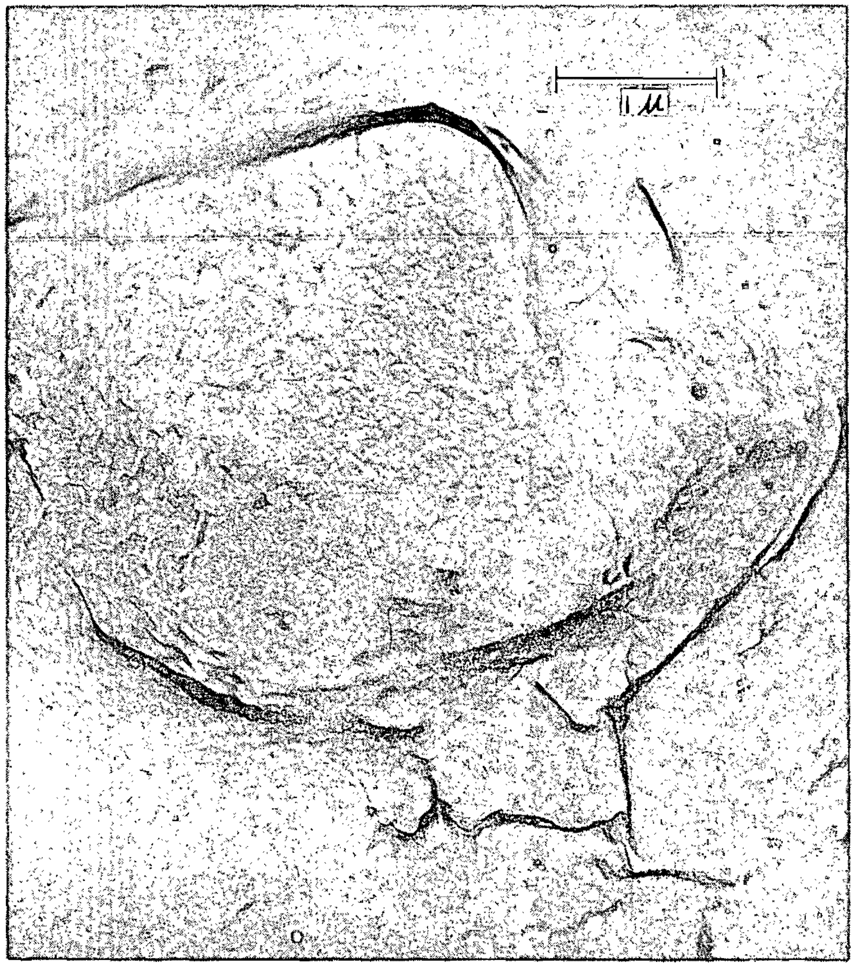

FIGURE 3.13 TRIANGULAR-FACED UO_2 CRYSTAL FOUND IN THE BULK SOLIDS AFTER GRAVITY SETTLING (0.01% BURNUP)

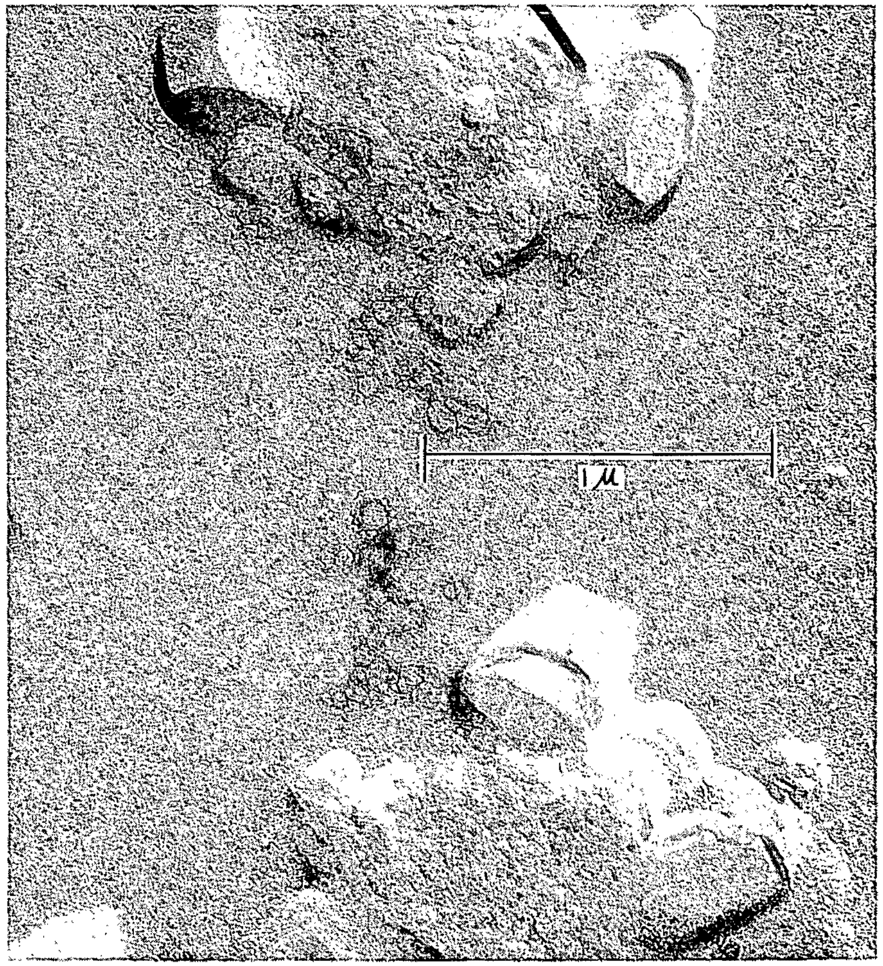

FIGURE 3.14 CRYSTALLINE UO_2 GROWING ON SOLIDS COLLECTED BY CENTRIFUGATION OF SUPERNATES (0.01% BURNUP)

371-65-1390

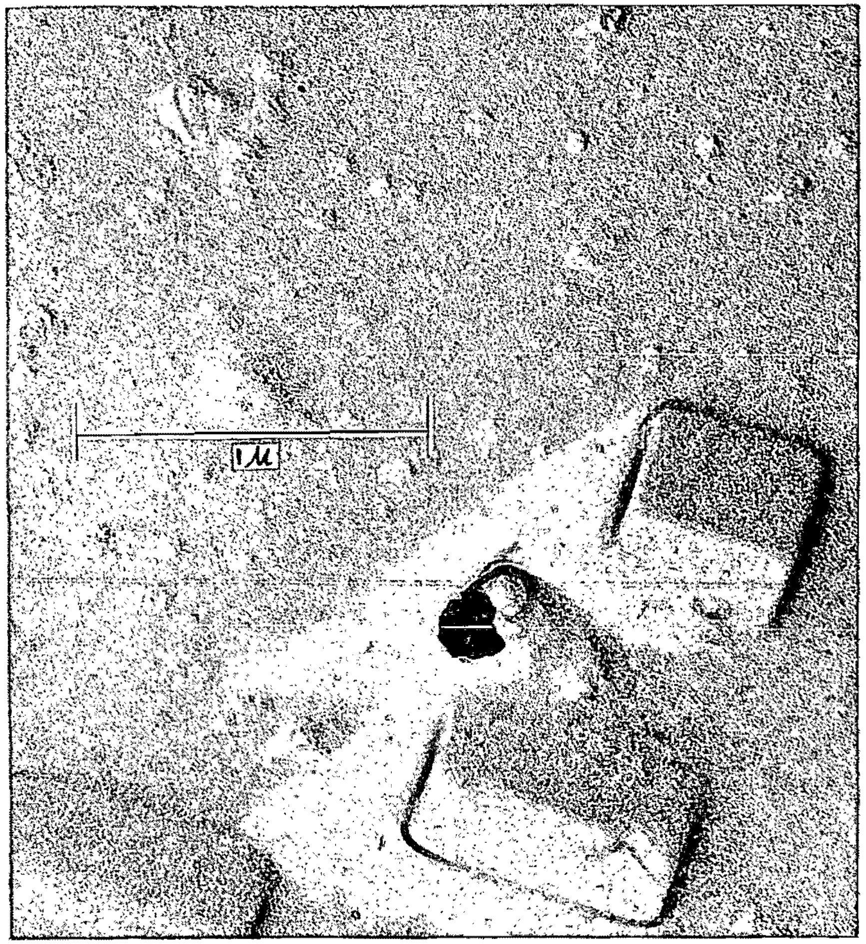

FIGURE 3.15 CRYSTALLINE UO_2 FROM GRAVITY-SETTLED SOLIDS OF HIGH BURNUP CAPSULE

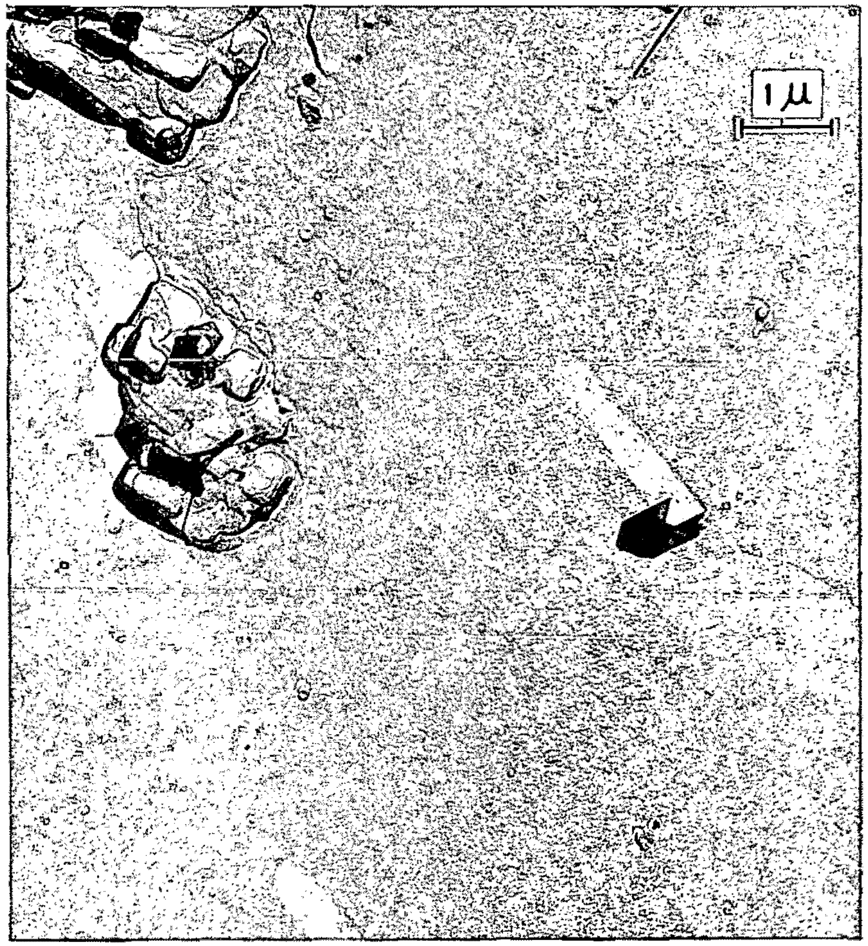

FIGURE 3.16 SOLID PARTICLES SEPARATED FROM GRAVITY-SETTLED SUPERNATE BY CENTRIFUGATION

the solids, as summarized in Table 3.6. Almost all of the iodine was present in the liquid ammonia. Tests have demonstrated that iodine is not volatile in liquid NH_3-UO_2 within the investigated temperature range -80° to $+100^\circ C$. It is therefore deduced that the iodine is in ionic form rather than in the form of free molecules. Ruthenium was found in randomly varying proportions between the liquid phase and the solid phase (Section 2.4). Since it is not completely tied to the solids as are the other metallic elements, it is presumed to form a complex bond with the ammonia, as do several noble metals.

TABLE 3.6

FISSION PRODUCT DISTRIBUTION

Radioisotope	Distribution (%) Liquid Ammonia	UO_2 Solids
Iodine-131	80	20
Ruthenium-103	50	50
Zirconium-Niobium-95	NIL	100
Cerium-141	NIL	100
Cerium-144	NIL	100
Lanthanum-140	NIL	100
Barium-140	NIL	100
Strontium-90	NIL	100
Cesium-137	NIL	100

The results obtained on samples of different fuel burn-up and mean particle size showed no significant change in fission product distribution.

The distribution of fission products among the liquid, solid, and vapor phases is crucial to the processing of a crude product in a fissiochemical production plant. The lack of volatility of all fission products other than the rare gases suggests that hydrazine can be decontaminated by a simple distillation procedure.

3.4.4 Conclusions

While the settling rate tests evidenced only the possible presence of a fraction of fines in the irradiated UO_2, surface area measurements and electron microscopy corroborate the occurrence of particle degradation during irradiation of UO_2 in an ammonia suspension. When UO_2 suspended in liquid ammonia is irradiated up to 0.055% burnup, it will not form sols as it will in a dispersing aqueous medium. Enriched UO_2, during irradiation in liquid ammonia, will form crystal habits, and will occasionally develop into almost perfect crystals. Finally, it has been shown that iodine and ruthenium are essentially the only radioisotopes which remain with the supernate, and that quite probably distillation will suffice to decontaminate the hydrazine.

The results of the capsule irradiation program indicated no reason to doubt that particulate UO_2 would be a satisfactory fuel for the in-reactor loop test. The extent of particle breakup and fines formation in the BRR tests was not sufficient to cause significant differences between in-reactor and ex-reactor loop behavior. The effect of crystal growth, if it should occur in a pumped loop, is unpredictable although such a phenomenon might result in fuel growth on the walls or the cementing of individual particles into large agglomerates.

3.5 Effect of NH_3 on 304 Stainless Steel

Type 304 SS is prone to sensitization since it is non-stabilized. Welding temperatures (800 to 1600°F) during fabrication of the 304 SS loop could cause carbide precipitation at the grain boundaries, thus making the loop susceptible to intergranular corrosion. Reported data from tests on the compatibility of 304 SS with mixtures of anhydrous ammonia showed severe embrittlement after 1600 hr at 1500°F which was attributed to ammonia exposure and sensitization. The embrittlement also is caused by nitriding which occurs during exposure to anhydrous ammonia atmospheres in temperatures above 800°F. Little information was available on the corrosion resistance and mechanical properties of 304 SS after exposure to ammonia in the 100 to 200°F range.

Samples were prepared from two lots of solution-annealed 304 SS sheet of 0.020 and 0.185 in. thicknesses containing low (0.03%) and high

(0.07%) carbon content. Half of the samples were sensitized by heating for 4 hr at 1300°F. Tensile and bend specimens were sealed in two stainless steel, pressure tight capsules and heated by immersing them in a bath containing silicone oil kept at a constant 200°F. One capsule contained liquid anhydrous ammonia at 1000 psi and the other a mixture of approximately 50% ammonia vapor, 25% nitrogen, and 25% hydrogen pressurized at 1000 psi. The samples were taken from the capsules after 500, 1500, and 2000 hr of exposure.

Metallographic examination revealed no nitriding or intergranular corrosion. The sensitized samples did exhibit some carbide precipitation at the grain boundaries. Tensile test results showed that the sensitized samples exhibited a small loss in ultimate strength and about three times as much yield loss as the solution annealed samples. (Figures 3.17 and 3.18 show results of the tests.) The yield strength loss appeared to be greater with increased exposure time to gaseous and cracked ammonia. It was also determined that the loss was not affected by the carbon content. The samples showed no detectable loss in ductility. The slight change noted in the 304 SS properties after heat treatment and exposure to the worst possible conditions indicate no cause for concern in either loop construction or operation.

3.6 Component Test Loop

3.6.1 Introduction

Because of the complexity of the in-reactor loop and the reliability assurance deemed necessary, a component test loop was constructed and operated.

This test loop was used as an out-of-reactor test stand to determine the performance and reliability of all components used in the main slurry irradiation loop, together with the operating characteristics of the entire loop system. A schematic drawing of the test loop, with all components and associated hardware in place, appears in Figure 3.19. The following components were tested: main circulating pump, backflush filter, test section, gas disengager, and instrumentation for the main irradiation loop. A detailed description of each component can be found in Section 4. Additionally, the procedure for loading fuel into the loop via a fuel induction system was checked to determine its effectiveness. (See Section 3.7.) The loop was also used to perform the series of heat transfer experiments described in Section 7.1.

371-65-1391

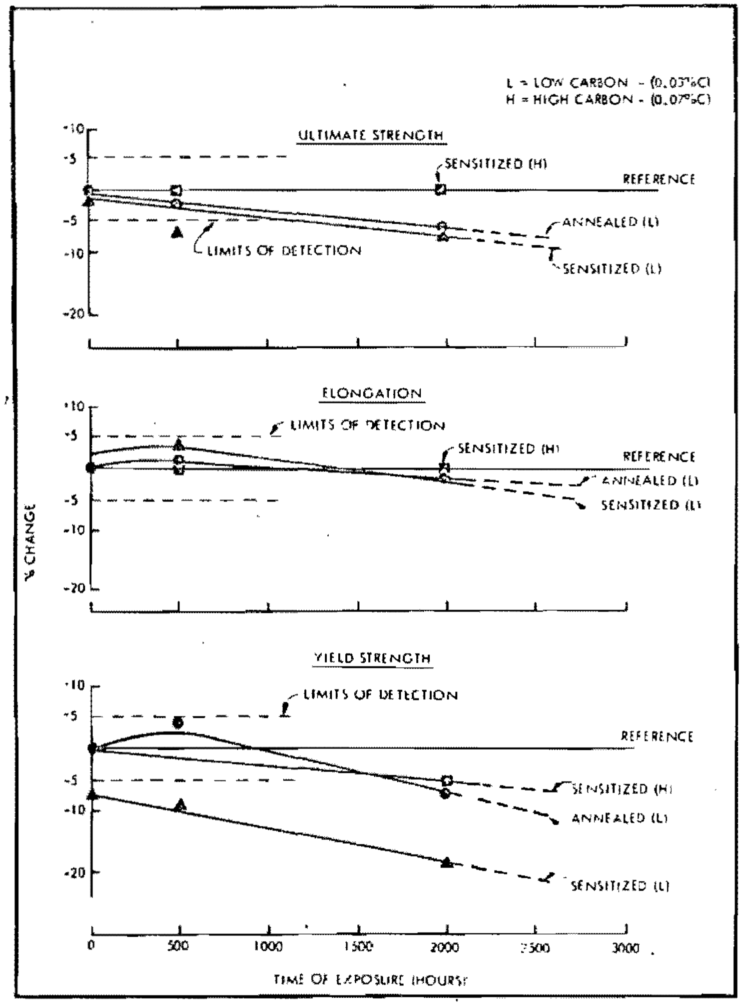

FIGURE 3.17 EFFECTS OF EXPOSURE TO LIQUID ANHYDROUS NH_3 AT 200°F ON MECHANICAL PROPERTIES OF 304 STAINLESS STEEL

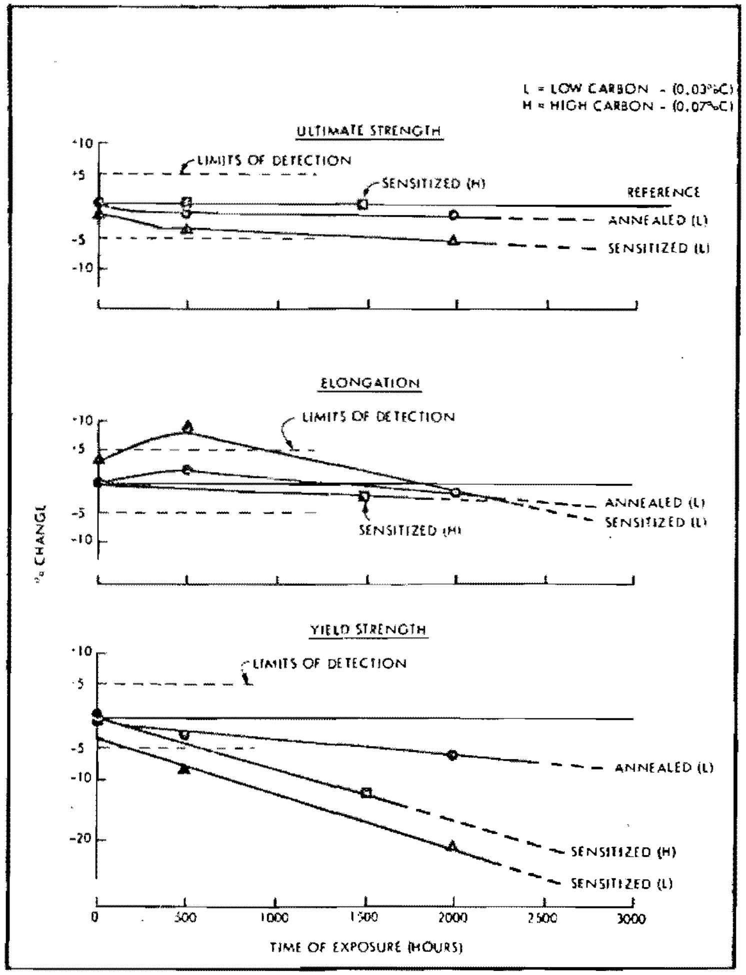

FIGURE 3.18 EFFECTS OF EXPOSURE TO NH_3 VAPOR PLUS CRACKED NH_3 AT 200°F ON MECHANICAL PROPERTIES OF 304 STAINLESS STEEL

37.1-65-1345

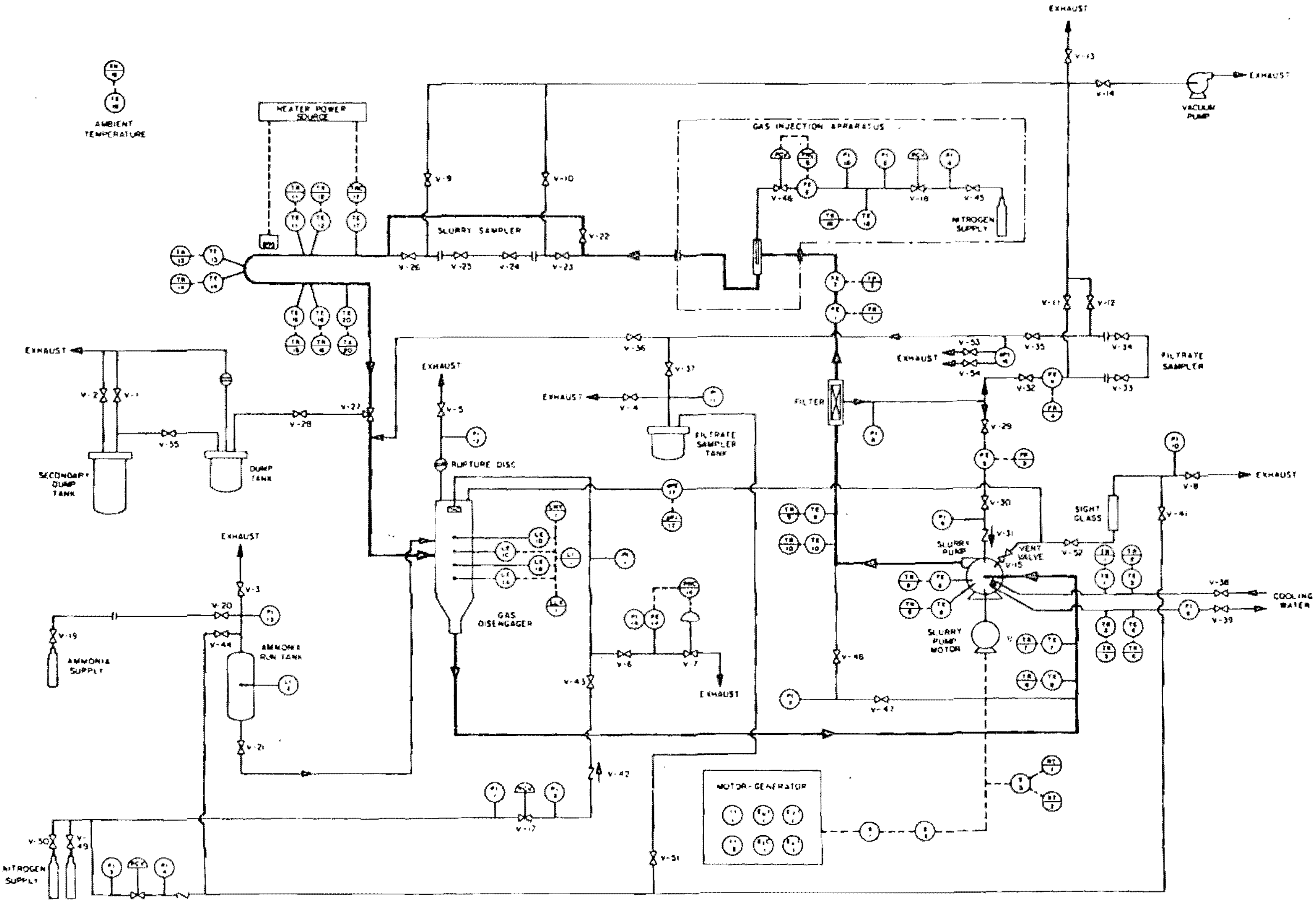

FIGURE 3.19 PIPING AND INSTRUMENTATION DIAGRAM OF COMPONENT TEST LOOP

Figures 3.20, 3.21 and 3.22 are photographs of the assembled loop: Figure 3.20 illustrates the relative positions of the gas disengager and pump and shows the operating console. Figures 3.21 and 3.22 are side views showing the positioning of the main components of the loop. The component loop was arranged to resemble the geometry and displacement of the in-reactor loop so that out-of-reactor test conditions would simulate actual operations.

3.6.2 Component Testing Program

The parameter affecting component performance evaluation is slurry density during test. Accordingly, the component test experimental conditions were arranged to span the entire range of slurry density expected during in-reactor operations.

The experimental conditions of each test run with respect to UO_2 concentration and temperature are given in Table 3.7.

TABLE 3.7

NOMINAL AND EXPERIMENTAL SLURRY TEMPERATURES AND FUEL CONCENTRATIONS

	Nominal			Experimental Data		
Run	Temp. °F	Fuel Conc. gm/liter	Calculated Density gm/cc	Temp. °F	Fuel Conc. gm/liter	Calculated Density gm/cc
1	75	0	0.606	79 ± 10	0	0.601
2	135	0	0.550	136 ± 2	0	0.550
3	200	0	0.477	195 ± 5	0	0.482
4	75	4.3	0.610	-	-	-
5	75	21.5	0.628	73 ± 5	24.6 ± 6	0.634
6	135	21.5	0.571	135 ± 1	21.5 ± 10	0.572
7	75	43.0	0.649	78 ± 5	35.8 ± 4	0.630
8	135	43.0	0.593	135 ± 2	35.8 ± 3	0.578
9	75	64.5	0.671	79 ± 4	60.6 ± 4	0.663
10	135	64.5	0.614	136 ± 4	60.6 ± 4	0.610
11	200	64.5	0.542	179 ± 5	66.9 ± 10	0.570
12	165	64.5	0.586	164 ± 2	66.9 ± 10	0.586

All temperatures were measured with unsheathed chromel-alumel (20 gage) thermocouples, uncalibrated. Slurry temperature was taken to be the average

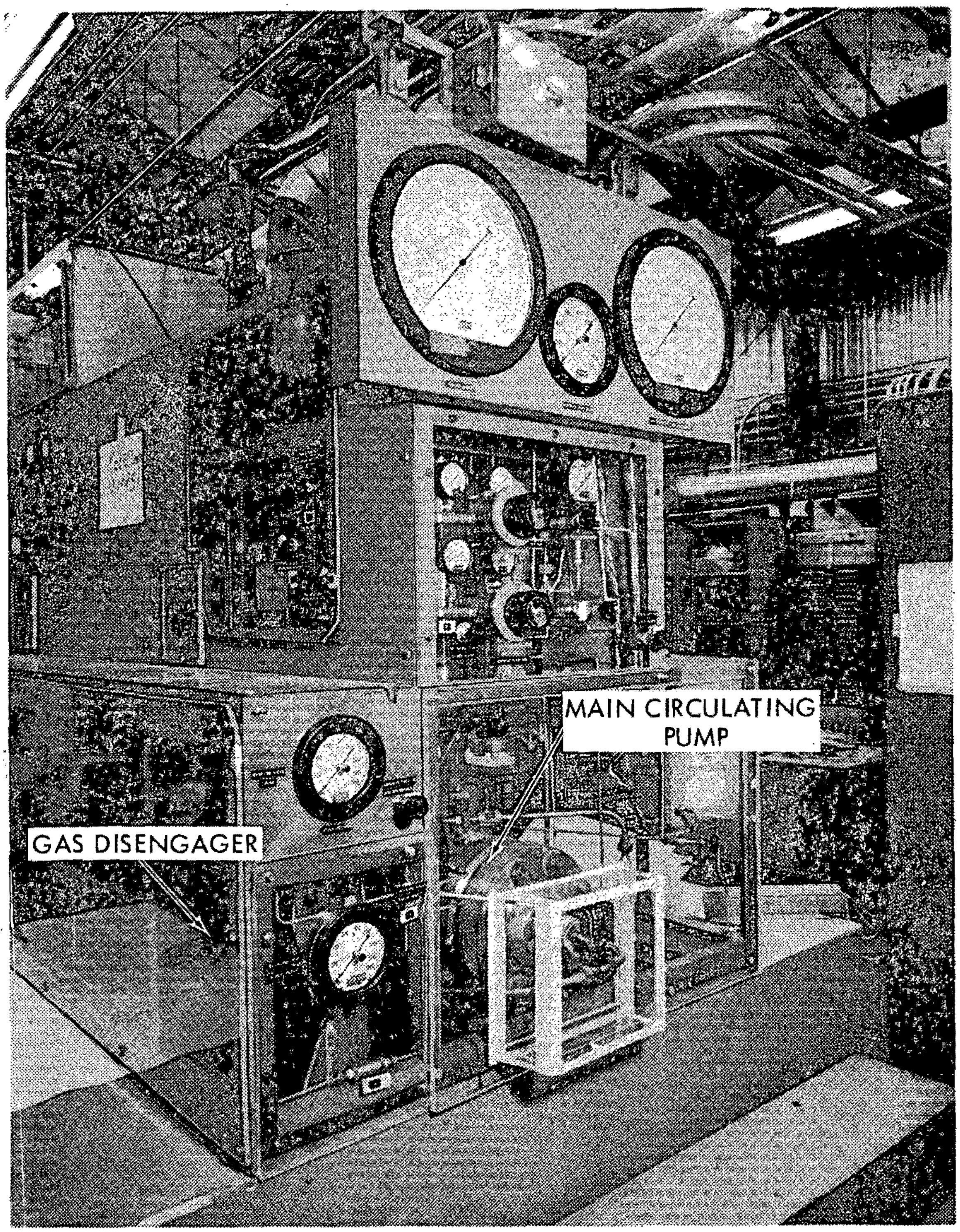

371-65-702

FIGURE 3.20. COMPONENT TEST LOOP - END VIEW AND OPERATING CONSOLE

37.1-65-704

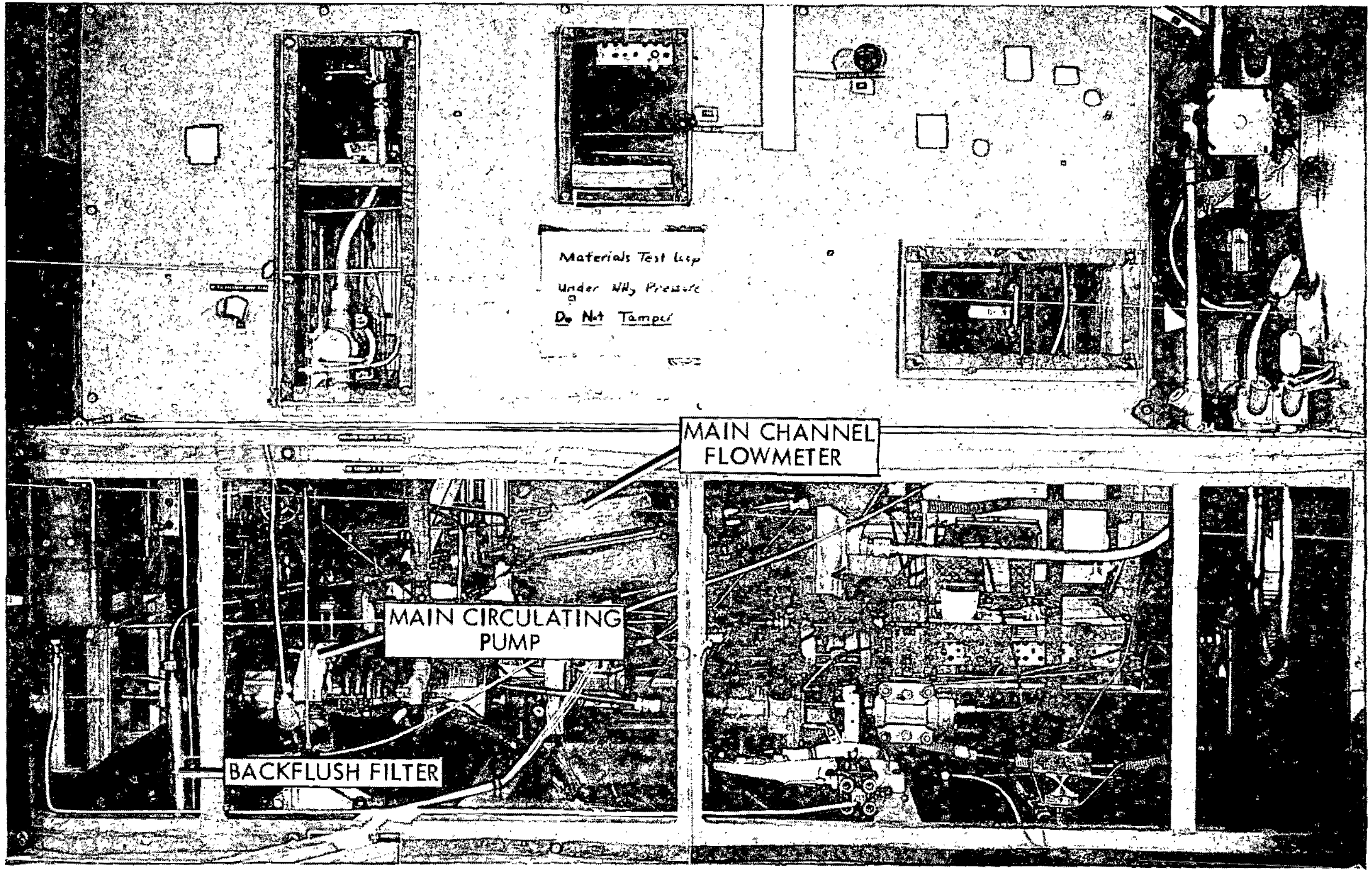

FIGURE 3.21 COMPONENT TEST LOOP - RIGHT SIDE

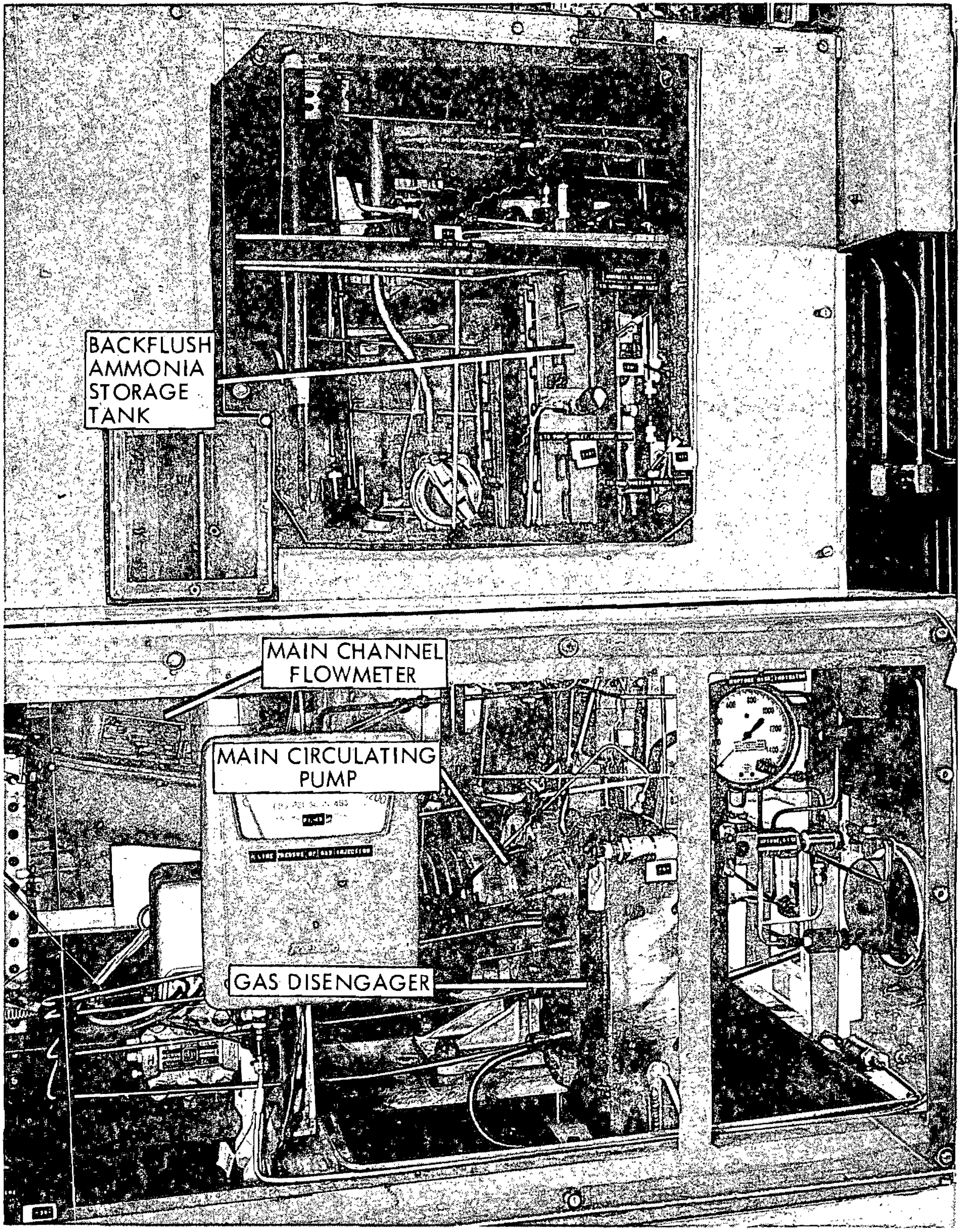

37.1-65-703

FIGURE 3.22 COMPONENT TEST LOOP - LEFT SIDE of thermocouples TR-12, TR-14, and TR-16 (Figure 3.19). These thermocouples were taped and insulated to the outer main flow channel wall. The main flow channel was 9/16 in. OD x .060 in. wall AISI 347 stainless steel seamless tubing. No compensation was made for temperature drop through the tube wall. The main loop flow rate was measured by a Fisher & Porter electromagnetic flowmeter Model No. 10 D 1416 B (FR-2). Bearing purge flow rate was measured by a Foxboro differential pressure recorder flowmeter Model No. 613-DM (FE-3 - FR-3). The same type of instrument was used to measure filtrate flow rate (FE-3-FR-4). The pressure head developed by the pump was measured with a Heise pressure gage and a valving arrangement (PI-7, V-48, V-47). The pressure drop through the filter element wall was measured as the difference in pressure between two Heise dial pressure gages (PI-7 and PI-8).

Table 3.8 briefly outlines the purpose of the twelve experimental runs.

3.6.3 Component Test Results

3.6.3.1 Pump

Figures 3.23 to 3.33 show power input, input power frequency, and pressure head developed by the pump as functions of flow rate (measured by FR-1 and FR-2) for the conditions of each run described in Table 3.8 (except for Run No. 4 during which no component test measurements were made).

Figure 3.34 shows the pressure head developed by the pump as a function of flow. The data spread is about ± 1.5 psi at any flow rate in the range 3 to 7 gpm.

Figure 3.35 shows pump power input frequency as a function of flow rate for each test. The band spread here is about ± 1.5 cycles per second throughout the flow rate range. Note that the four heavy points above the general band from 5.5 up to 7 gpm are from Run No. 11, the only run in which measurements were made while gas was being injected into the loop. At flows lower than 5.5 gpm, points for this run fell within the general band with all other such data. It is probable that during operation below 5.5 gpm the loop was not in equilibrium with respect to gas injection since gas injection was started approximately 10 minutes prior to

TABLE 3.8

COMPONENT TEST EXPERIMENTS

Run	Purpose
1	Head-flow curves for clear ammonia from 3 to 7 gpm flow rate (75°F)
2	Head-flow curves from 3 to 7 gpm for clear ammonia. Determine maximum flow rate through filter such that bearing purge flow does not decrease below 40 cc/min with main loop flow at 5 gpm (135°F).
3	Head-flow curves from 3 to 7 gpm for clear ammonia with gas injection to loop to simulate in-reactor operation. Check performance and operating characteristics of gas disengager. Repeat maximum filtrate flow test under gas injection condition (200°F).
4	Initial fuel (UO_2) addition to the loop. Experiments with slurry sampling. No other measurements (4.3 g/liter; 75°F).
5	Head-flow curves from 3 to 7 gpm. Further slurry sampling experiments (21.5 g/liter UO_2; 75°F).
6	Head-flow curves from 3 to 7 gpm. Determine maximum filtrate withdrawal capacity consistent with 40 cc/min minimum bearing purge flow rate (21.5 g/liter UO_2; 135°F).
7	Head-flow curves from 3 to 7 gpm (43 g/liter UO_2; 75°F).
8	Head-flow curves from 3 to 7 gpm. Determine maximum filtrate withdrawal capacity as above (43 g/liter UO_2 concentration; 135°F).
9	Head-flow curves for slurry from 3 to 7 gpm (64.5 g/liter UO_2; 75°F).
10	Head-flow curves for slurry from 3 to 7 gpm (64.5 g/liter UO_2; 135°F).
11	Head-flow curves for slurry from 3 to 7 gpm with gas (N_2) injection at rate of 0.6 scfm to simulate in-reactor operation. Add hydrazine to loop and by filtrate sampling determine decomposition rate (64.5 g/liter UO_2 concentration; 200°F; 5 wt% N_2H_4). Determine maximum filtrate withdrawal rate consistent with minimum permissible bearing purge flow rate under conditions of gas injection.
12	Head-flow curves for slurry from 3 to 7 gpm. Further hydrazine decomposition rate measurements (64.5 g/liter UO_2 concentration; 165°F; 5 wt% N_2H_4).

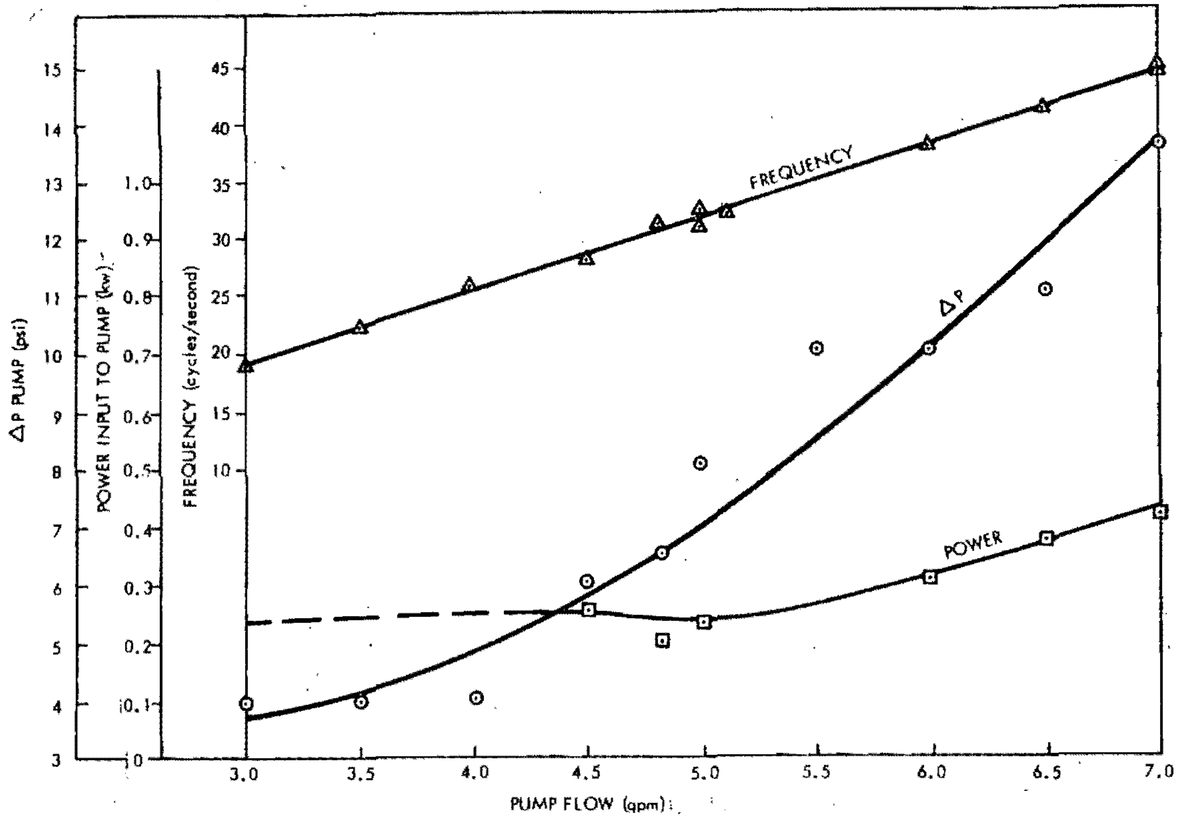

FIGURE 3.23 MAIN PUMP FLOW VERSUS PUMP ΔP, POWER INPUT AND FREQUENCY (RUN NO. 1)

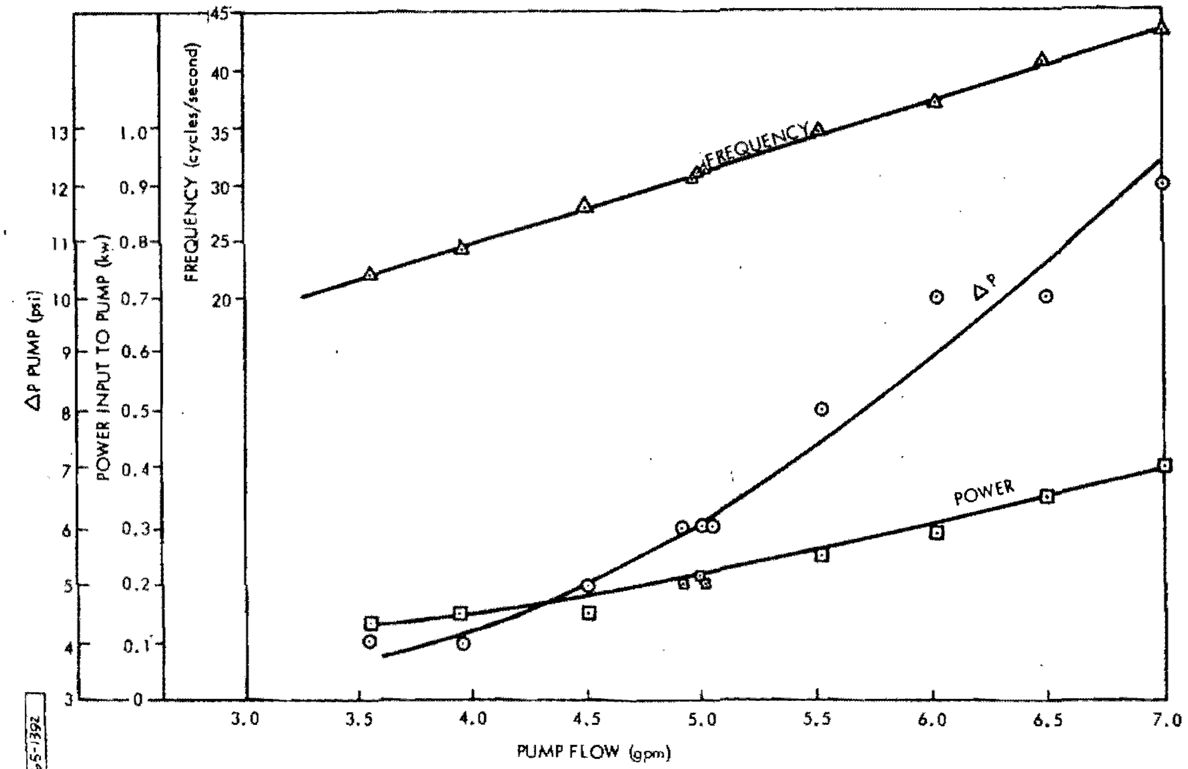

FIGURE 3.24 MAIN PUMP FLOW VERSUS PUMP ΔP, POWER INPUT AND FREQUENCY (RUN NO. 2)

371-65-1392

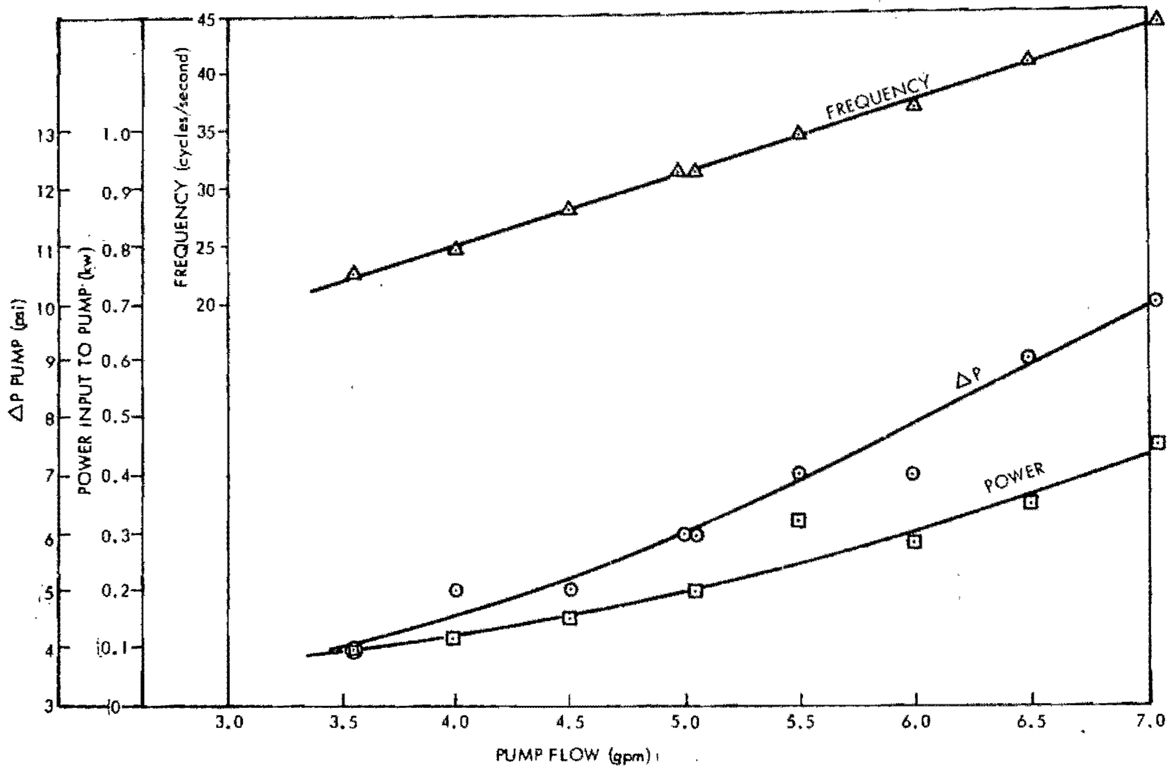

FIGURE 3.25 MAIN PUMP FLOW VERSUS PUMP ΔP, POWER INPUT, AND FREQUENCY (RUN NO. 3)

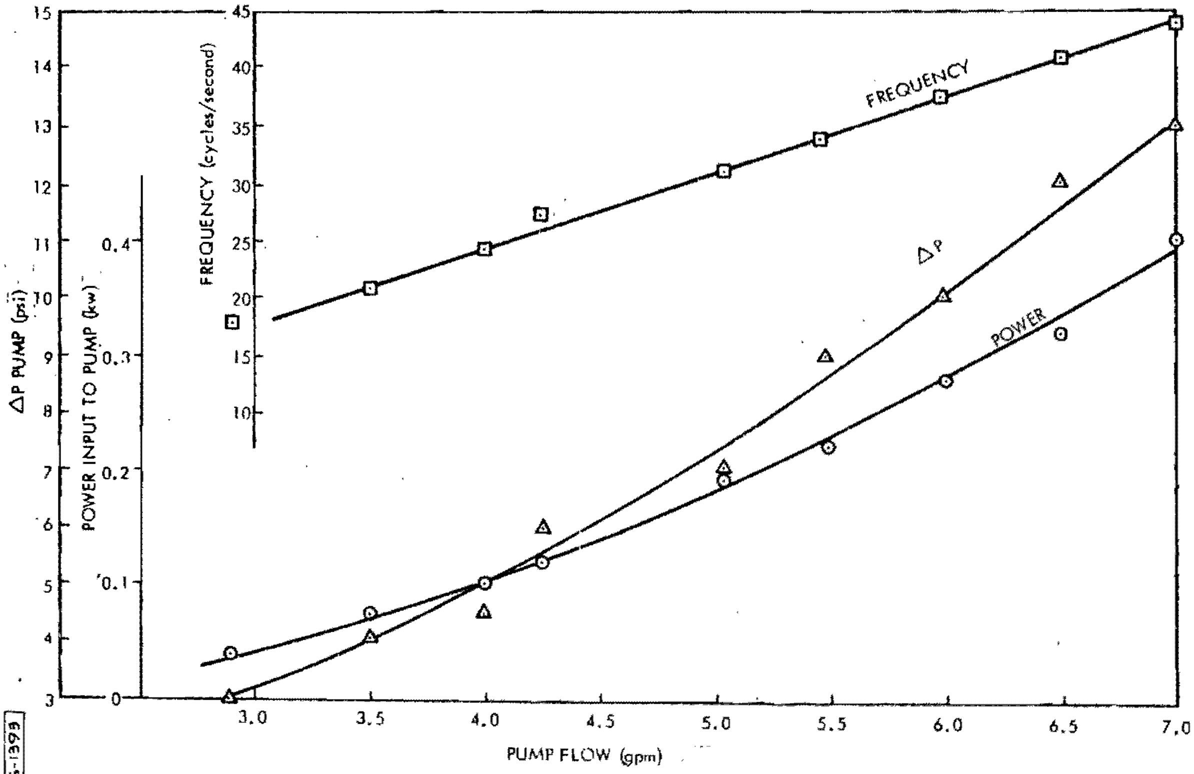

37I-65-1399

FIGURE 3.26 MAIN PUMP FLOW VERSUS PUMP ΔP, POWER INPUT, AND FREQUENCY (RUN NO. 5)

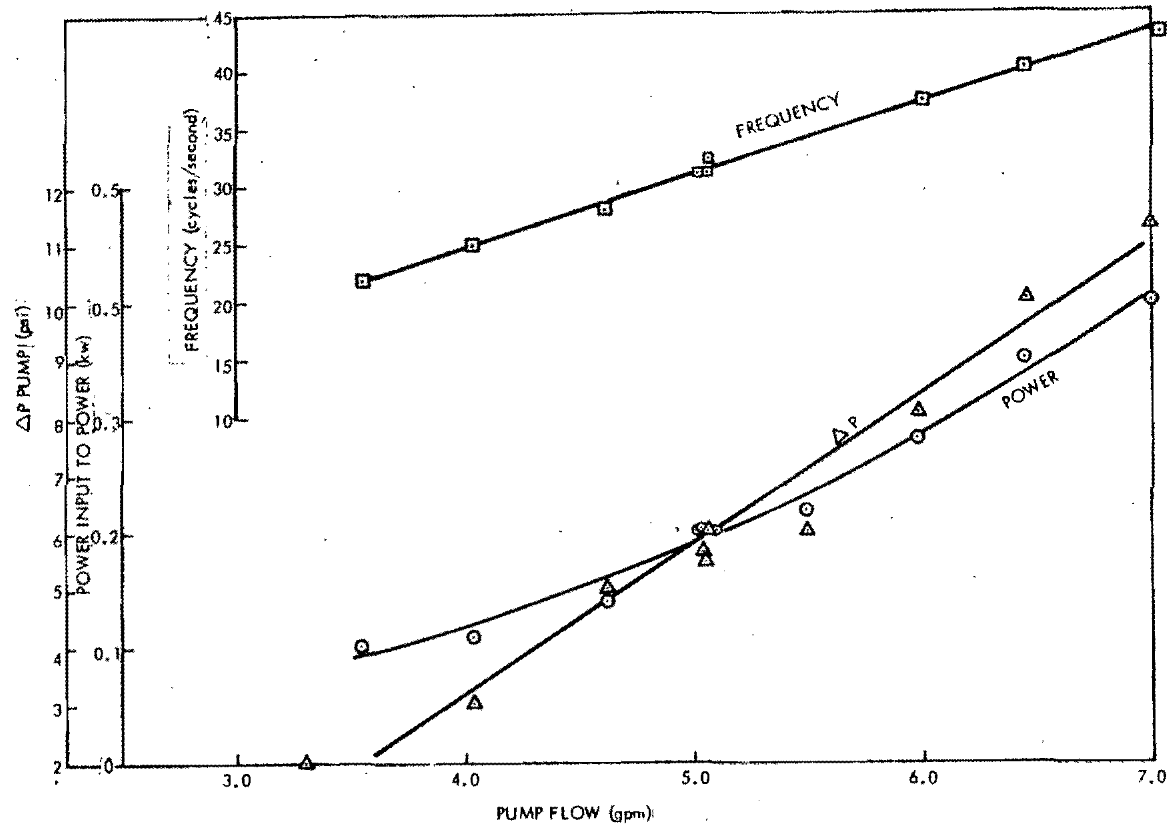

FIGURE 3.27 MAIN PUMP FLOW VERSUS PUMP ΔP, POWER INPUT, AND FREQUENCY (RUN NO. 6)

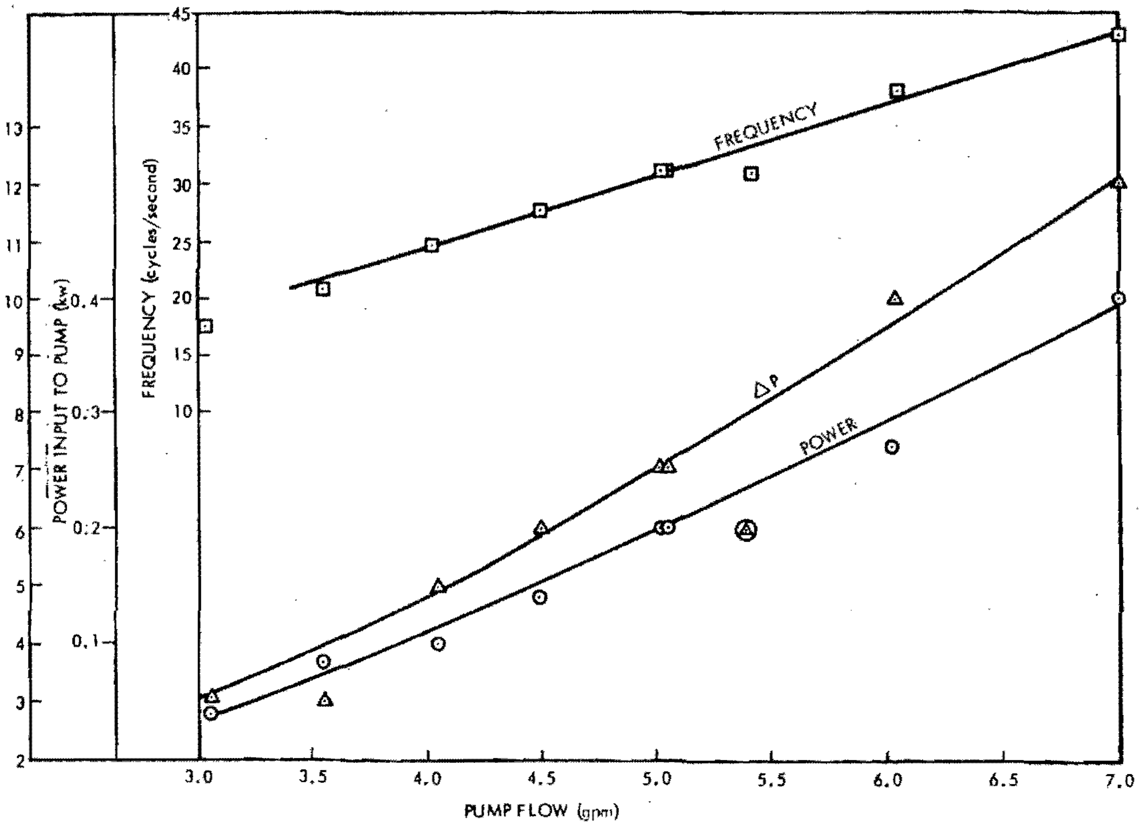

37-1-65-1394

FIGURE 3.28 MAIN PUMP FLOW VERSUS PUMP ΔP, POWER INPUT AND FREQUENCY (RUN NO. 7)

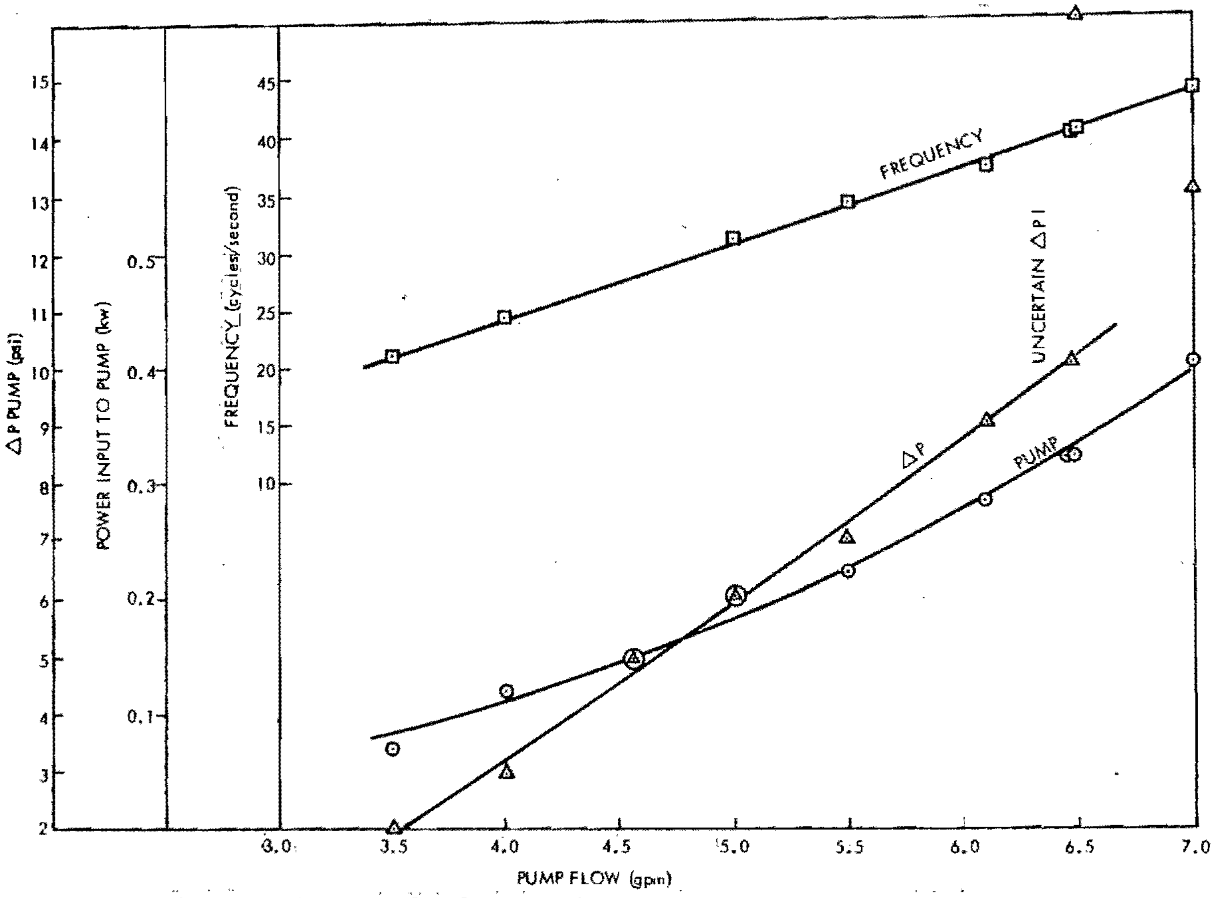

FIGURE 3.29 MAIN PUMP FLOW VERSUS PUMP ΔP, POWER INPUT AND FREQUENCY (RUN NO. 8)

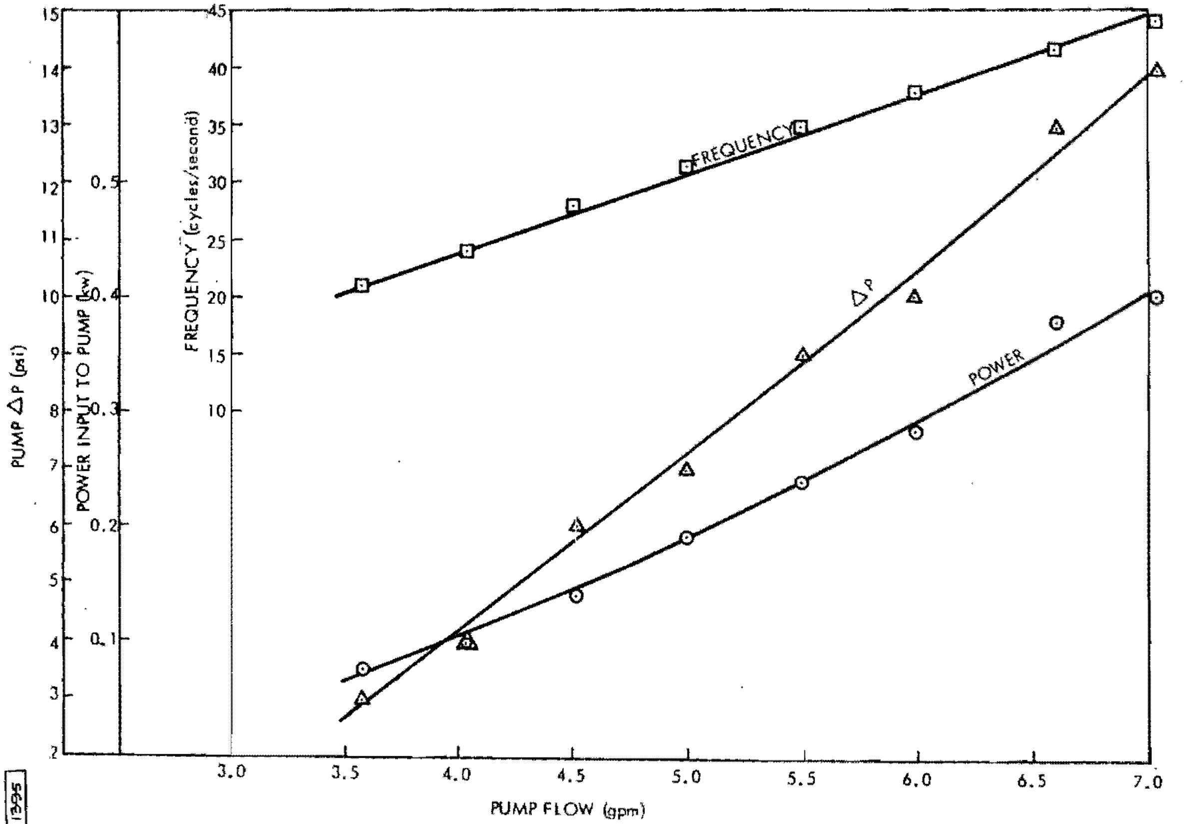

FIGURE 3.30 MAIN PUMP FLOW VERSUS PUMPΔP, POWER INPUT AND FREQUENCY (RUN NO. 9)

371-66-1395

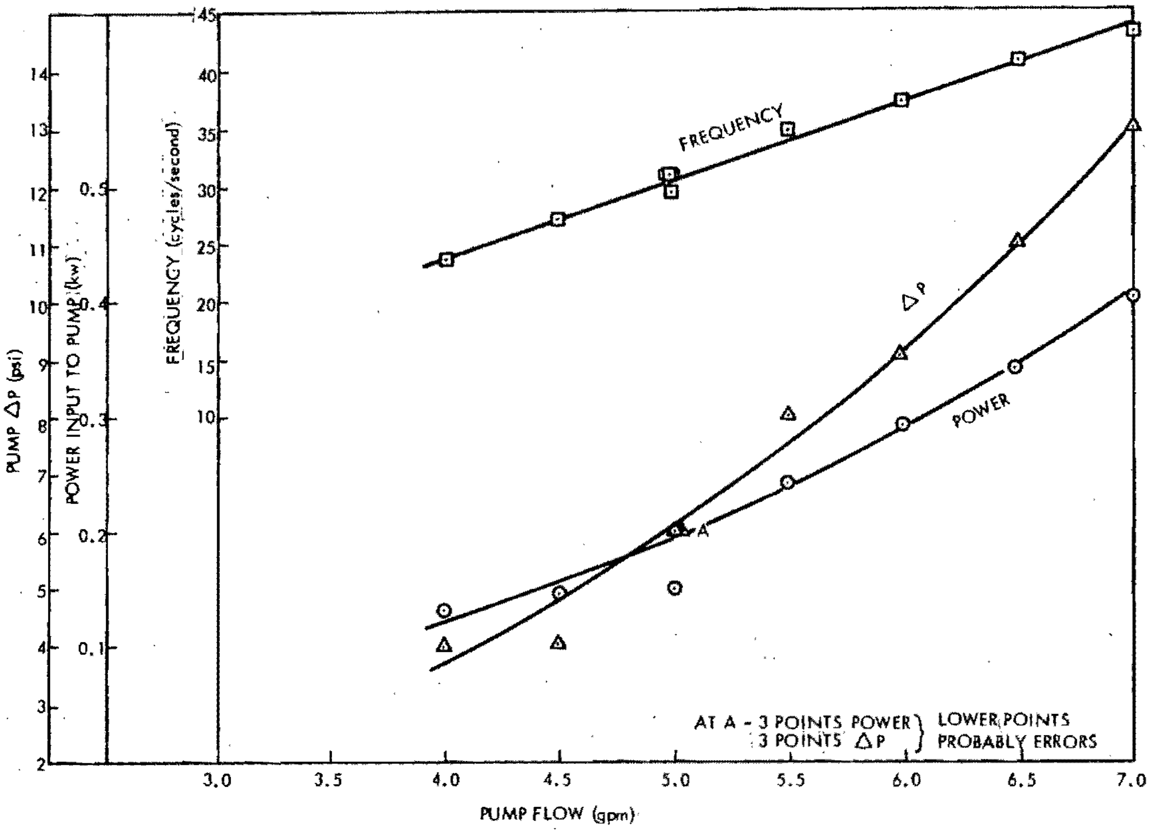

FIGURE 3.31 MAIN PUMP FLOW VERSUS PUMP ΔP, POWER INPUT AND FREQUENCY (RUN NO. 10)

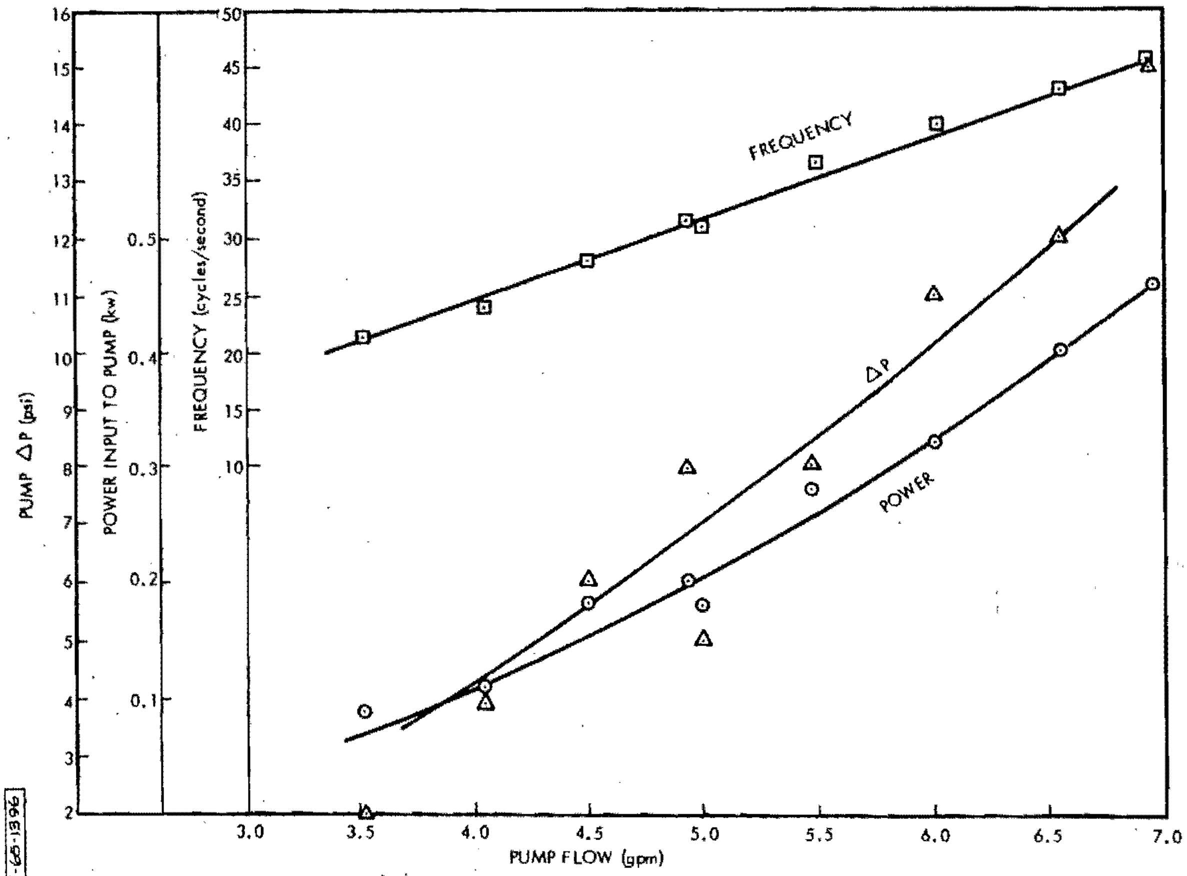

FIGURE 3.32 MAIN PUMP FLOW VERSUS PUMP ΔP, POWER INPUT AND FREQUENCY (RUN NO. 11)

37.-66-1396

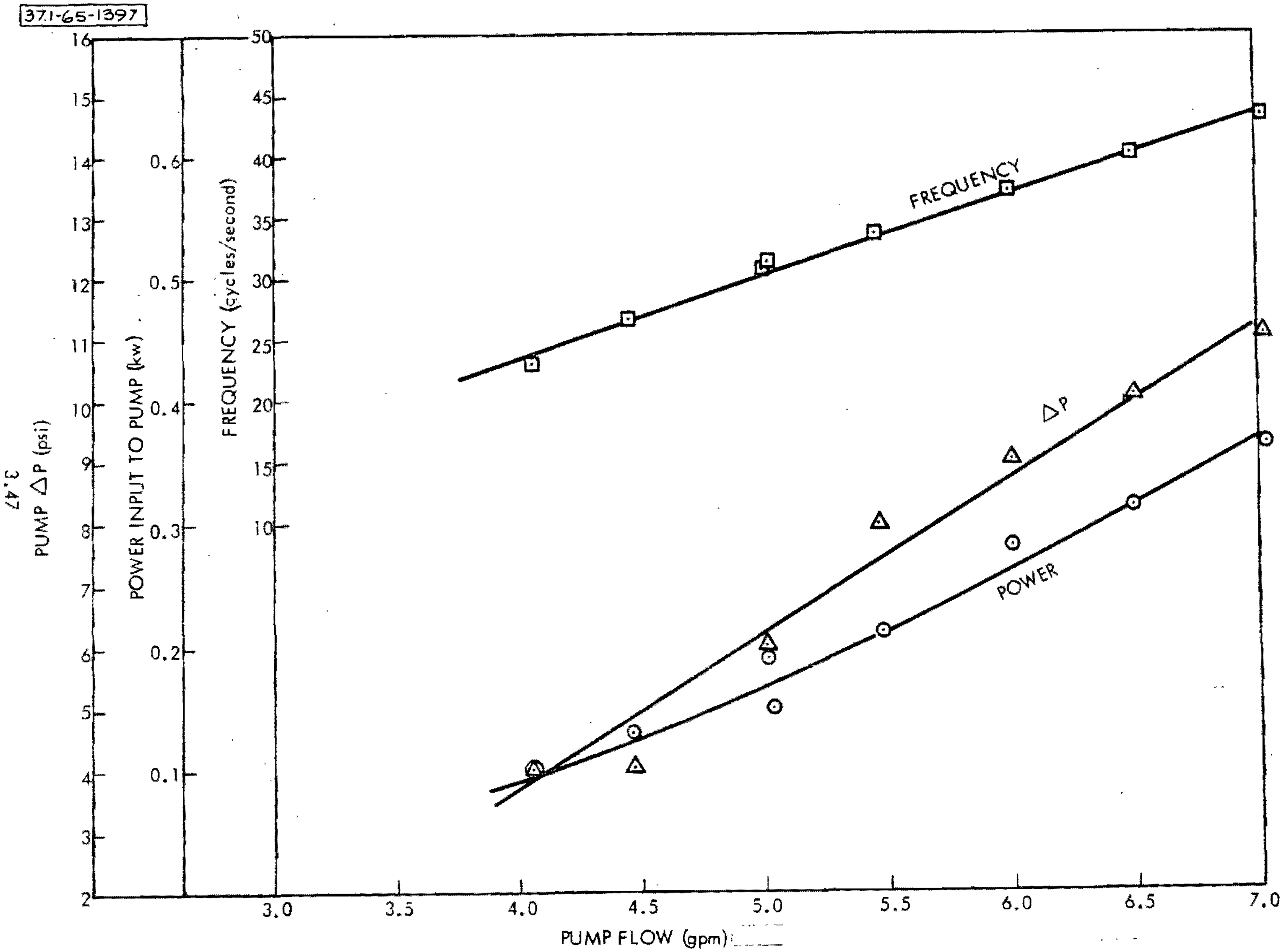

FIGURE 3.33 MAIN PUMP FLOW VERSUS PUMP △P, POWER INPUT, AND FREQUENCY (RUN NO. 12)

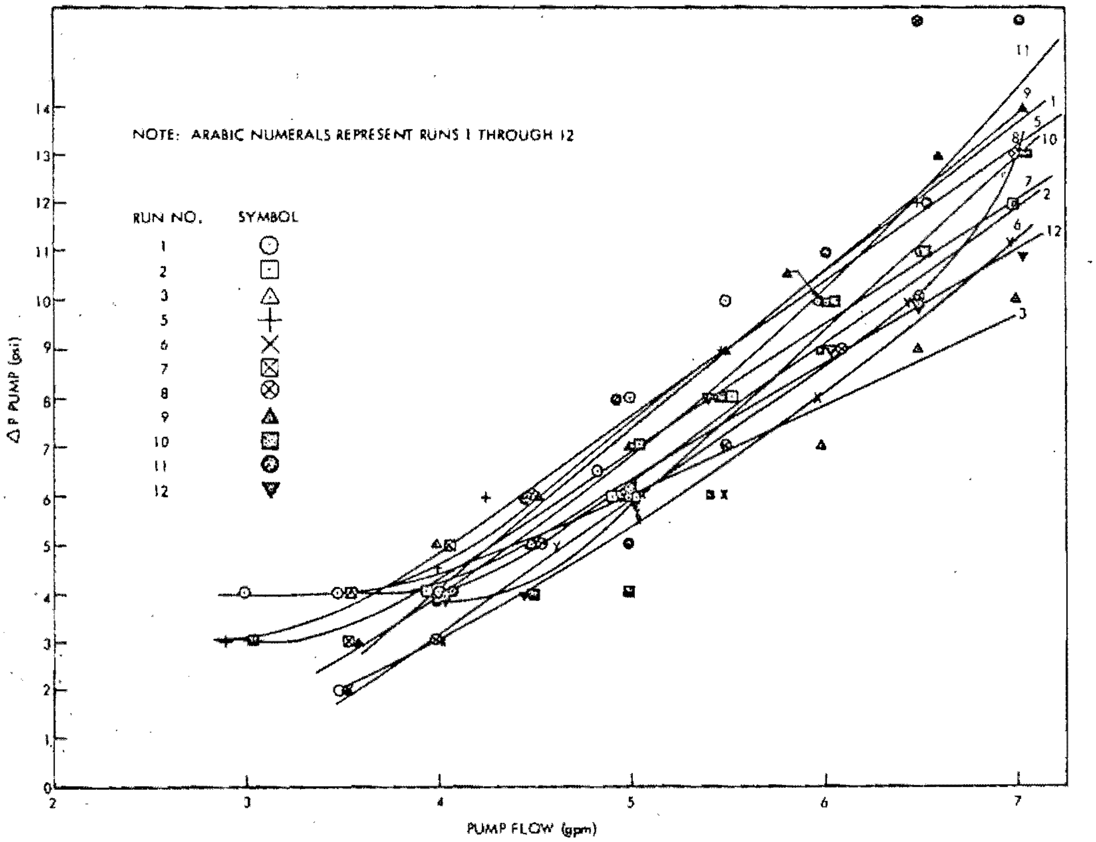

FIGURE 3.34 PUMP PRESSURE HEAD VERSUS FLOW

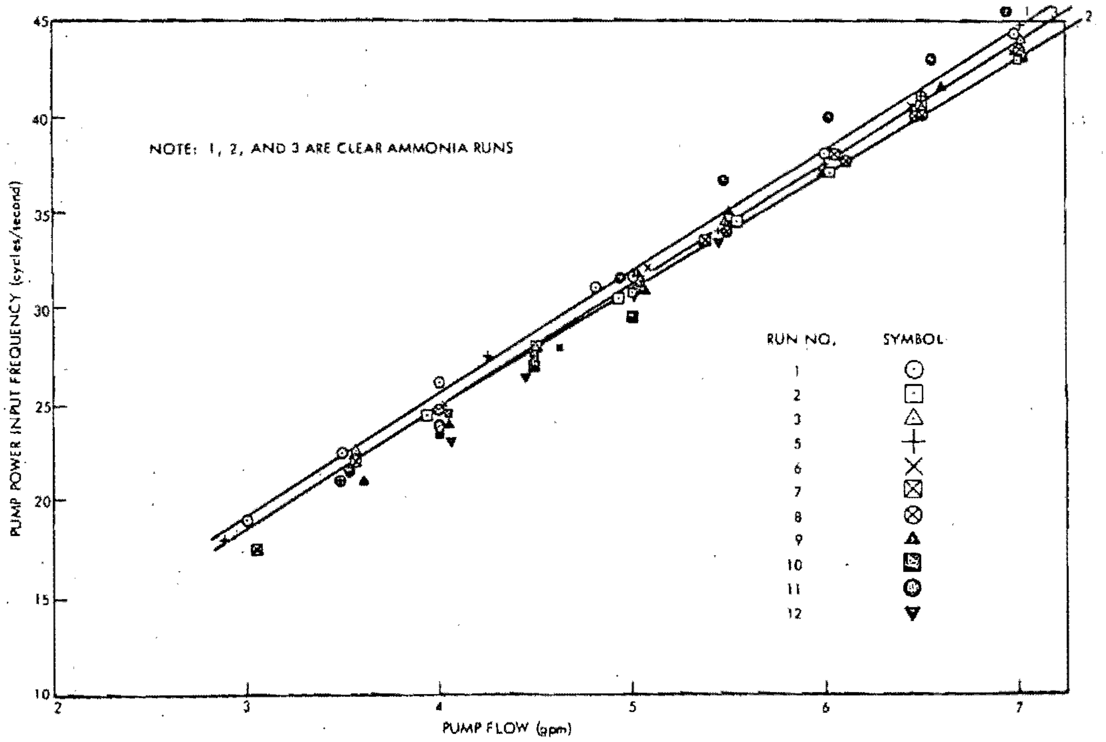

FIGURE 3.35 POWER INPUT FREQUENCY AS A FUNCTION OF FLOW RATE FOR RUNS 1 THROUGH 12

37.1-65-1340

the beginning of the test. Since the points above 5.5 gpm define a nearly straight line, the loop was probably in equilibrium after that time. Thus, during in-reactor operation, an input frequency requirement 2 to 3 cps higher than the band indicated would not be unexpected. It was recommended that this parameter, power input frequency, be used to control the in-reactor loop flow rate.

Figure 3.36 shows pump power consumption as a function of a loop flow in the range 3 to 7 gpm for each experimental run. All runs except Nos. 1 and 11 lie in the band shown on the figure. The band spread is about ± 0.05 kw in the flow rate range. There is no clearly discernible trend with respect to density within the band. As before, the points in the upper half of the flow range for Run 11 lie above the band indicating that the effect of gas injection is to increase the pump power consumption about 0.025 kw over that required for equivalent operation without gas injection.

Figure 3.37 shows the loop slurry concentration throughout the test period. Each point on the chart represents a single sample, of which there were 111. The spaces on the chart designated by run number are regions of operating time in which the nominal slurry concentrations listed in Table 3.8 were to be attained. The shorter bars within each run space are the time intervals during which the 1/2 gpm increment parameter measurements were performed. Slurry concentrations for each set of parameter measurements were calculated from only those samples in the immediate time vicinity of the measurements because of the wide sampling data spread.

All parts of the Westinghouse in-reactor pump were weighed or measured, or both, before and after operations. After 24 hours operation on clear ammonia and 560 hours operation on slurry, the following changes were noted:

Casing ID at rotor labyrinth seal:	+0.0048 in.
Thermal barrier ID at rotor labyrinth seal:	no measurable change
Labyrinth seal OD on rotor (both seals) and impeller:	+0.001 in. on each
Axial end play of rotor:	+0.002 in.

371-65-1339

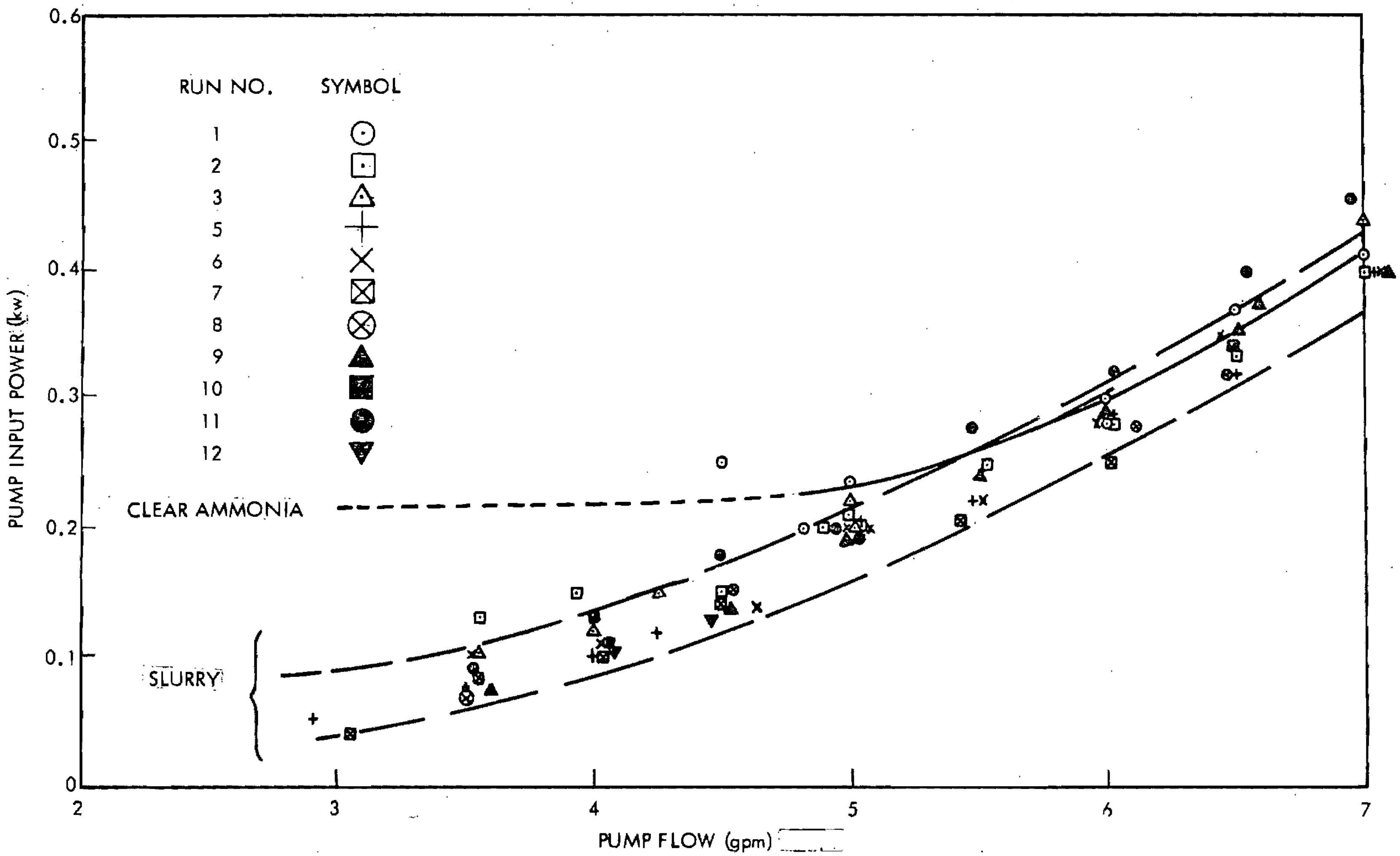

FIGURE 3.36 PUMP POWER CONSUMPTION VERSUS FLOW

371-65-1538

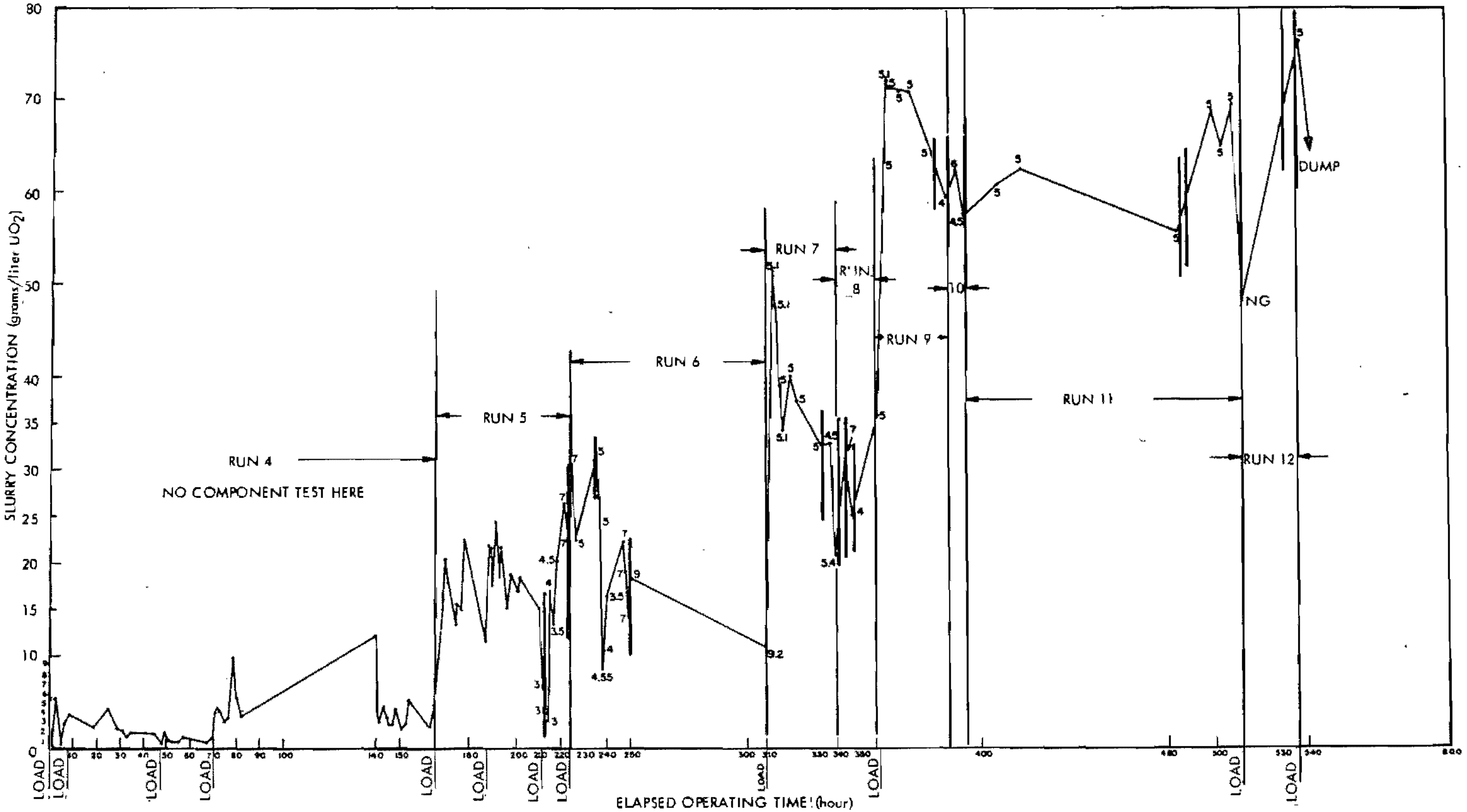

FIGURE 3.37 CHART OF FUEL CONCENTRATION VERSUS TIME FOR COMPONENT TESTS

Vertical play at impeller end of rotor:	+0.002 in.
Horizontal play at impeller end of rotor:	+0.0015 in.
Change in bearing diameters, all:	-0.001 in.
Change in impeller weight:	-0.2 g

The appearance of the mating surfaces on bearings and journals changed from a smooth ground ceramic surface before operation to a glass-like mirror polish after operation. No other significant changes were observed.

3.6.3.2 Filter Performance

The filter operated satisfactorily throughout the test period; pressure drop through the filter wall, which determines filter flow rate, is shown in Figure 3.38. The data are not smooth because this pressure drop parameter was a difference between two pressure gages operating in the range 990 to 1010 psia. Thus, it is really an upper bound plot of the filter element wall pressure drop. It is clear that pressure drop showed no continuous increase with time during slurry operation up to 560 hr.

The filter pressure drop increased when gas injection was made but again decreased to the initial value when gas injection was stopped; no permanent change was noted.

During operation of the filtrate sampling circuit two types of tests were made:

1) The filtrate sampler was operated as a by-pass line returning the filtrate to the suction side of the loop through valve V-36; V-37 closed (Figure 3.19).

2) The filtrate was dumped from the loop through valve V-37 with V-36 closed. This simulates withdrawing a liquid sample from the in-reactor loop.

The pressure drop level through the filter wall for a type 1 test above, with and without gas injection is shown on Figure 3.38. The pressure drop for tests of type (2) with gas injection is about 6 psi as shown on Figure 3.38. In all filter pressure drop tests, the filter

371-65-1337

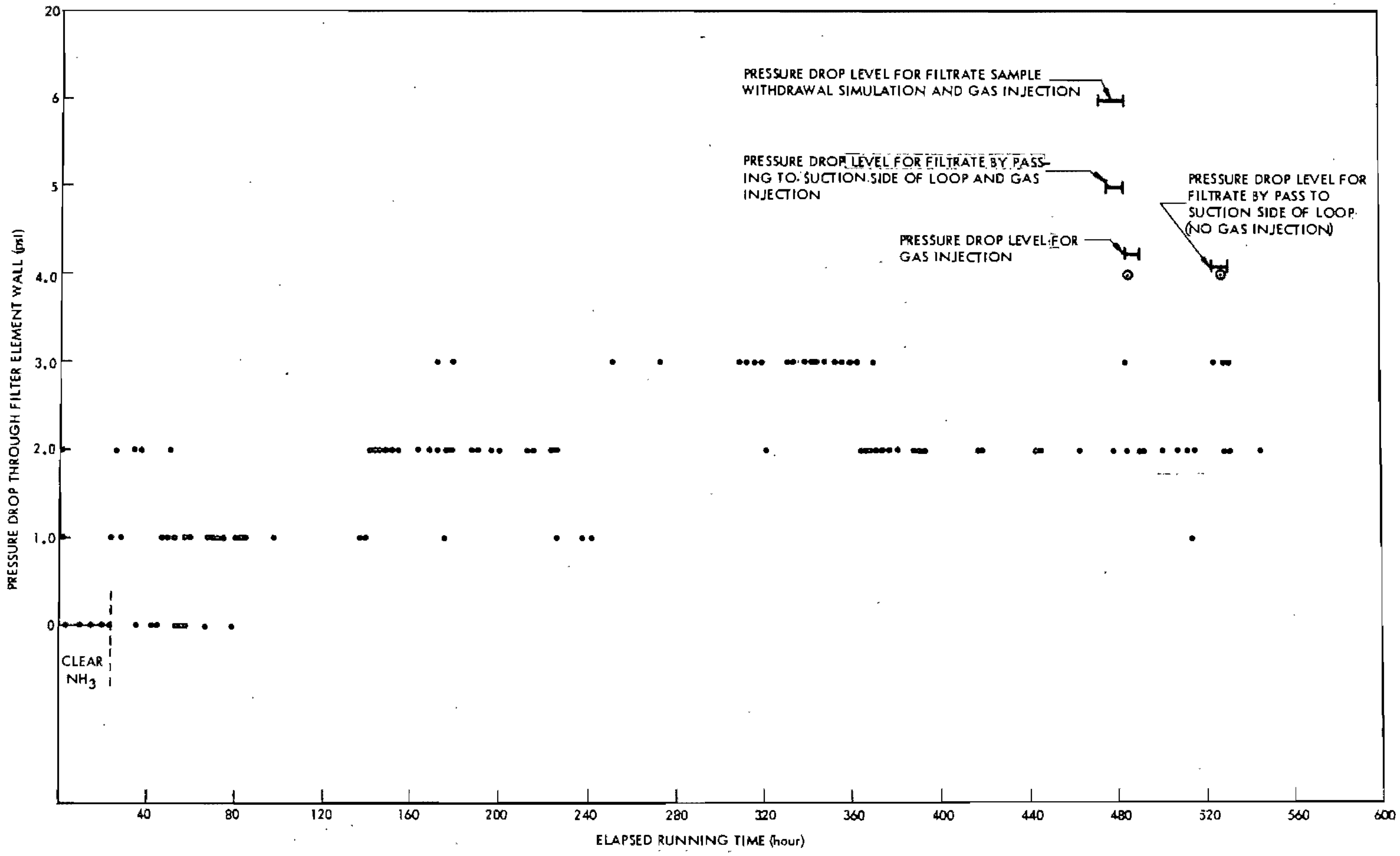

FIGURE 3.38 PRESSURE DROP THROUGH FILTER WALL

pressure drop was measured at the maximum attainable flow and 1/2 maximum filtrate flow. This is represented on Figure 3.39 when two points corresponding to the same time are shown. The maximum levels of ΔP for various experimental conditions as shown on Figure 3.38 are for maximum filtrate flow.

Figure 3.39 shows the decrease of bearing purge flow rate with increase in filtrate sampling rate for the various runs, all at 5 gpm main flow rate.

Figure 3.40 shows the same measurements but with gas injection as noted. For both Figures 3.39 and 3.40, the sum of the two flows, bearing purge plus filtrate, is the total flow rate through the filter under the given experimental conditions. Under in-reactor loop operating conditions, liquid sample flow rates up to 300 cc per minute under the given experimental conditions should not cause the bearing purge flow rate to decrease below 40 cc per minute.

Figure 3.41 shows bearing purge flow as a function of main loop flow for several different runs. It is clear that, when operating on slurry, the main loop flow must not be decreased below 3.5 gpm or the minimum permissible bearing purge flow of 40 cc/min will not be maintained.

3.6.3.3 Gas Disengager and NH_3 Loss Rate

The gas disengager was tested by injecting 0.6 standard cubic feet of N_2 gas at room temperature into the loop during Run No. 3 and Run No. 11 while operating the loop at flow rates from 3 to 7 gpm. The loop did not suffer any large changes in performance. Power consumption, input power frequency, and probably pump pressure head showed slight increases to maintain the desired flow rate; pump cavitation was never observed.

It was observed that NH_3 was lost from the loop with the N_2 expelled from the gas disengager. During Run No. 3, it was found that loop flow rate decreases markedly if the gas disengager liquid level is allowed to fall to the point at which only the bottom (No. 1) liquid level probe is covered. During Run No. 11, the NH_3 loss rate while injecting 0.6 scfm N_2 was found to be 56 cc/min. The loss rate was also determined by measuring the NH_3 addition rate to the loop necessary to maintain the gas disengager liquid level between the second and third probes while injecting N_2. The loss rate determined in this manner was 42 cc/min.

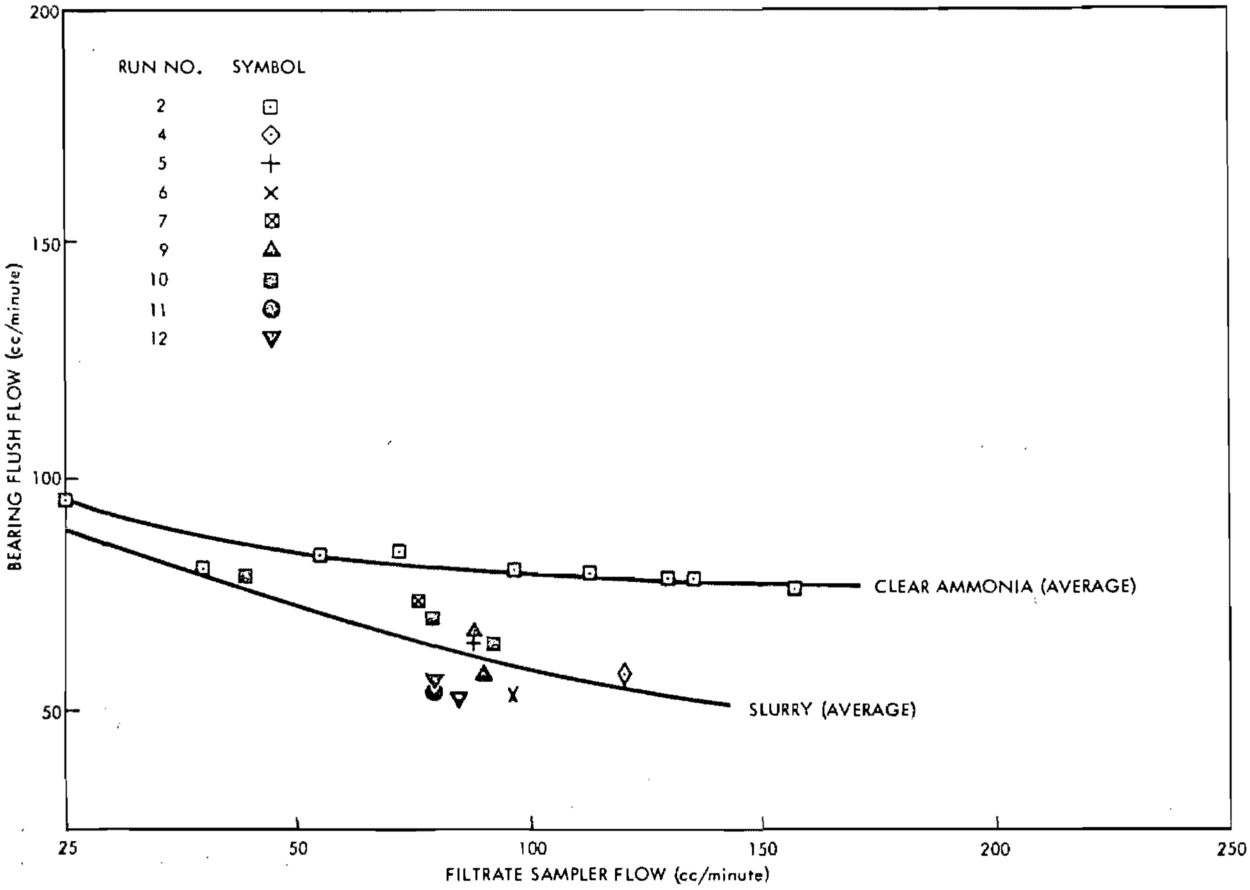

FIGURE 3.39 BEARING FLUSH FLOW VERSUS FILTRATE SAMPLER FLOW AT 5 gpm PUMP FLOW

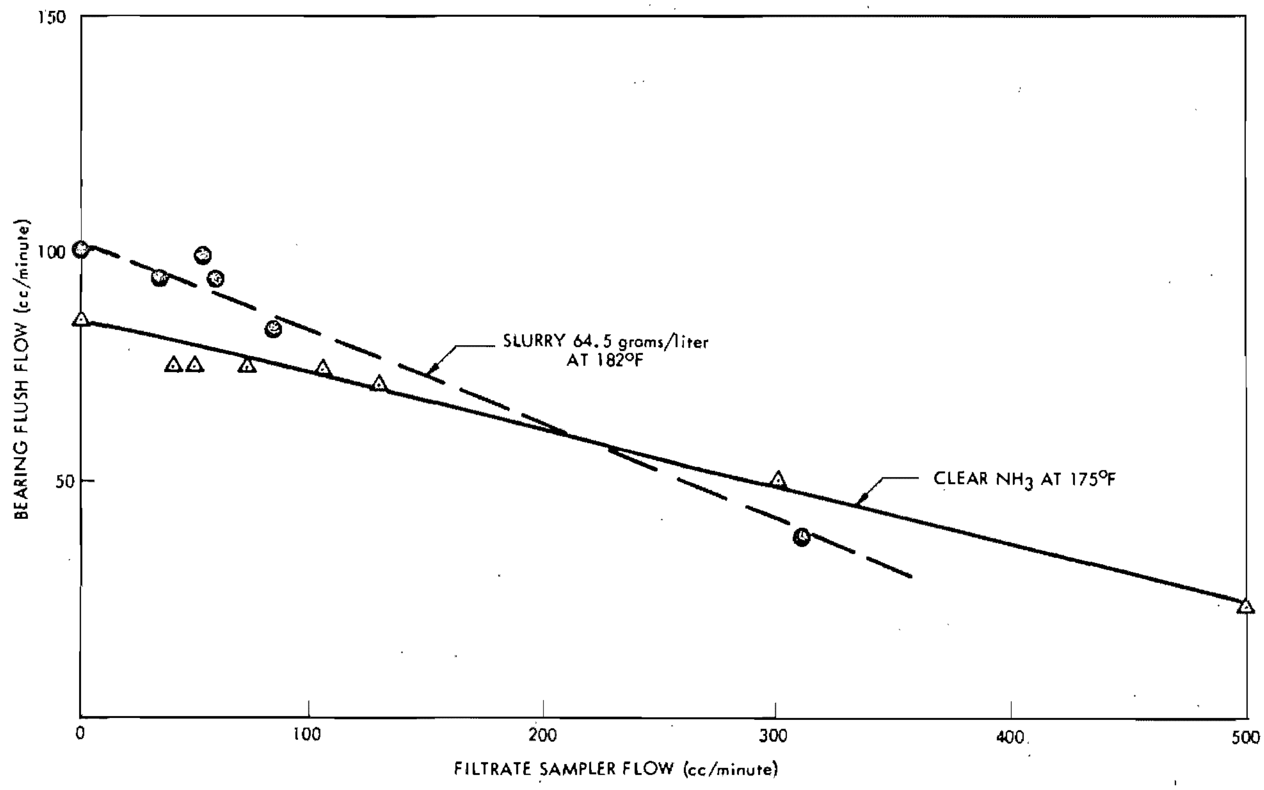

FIGURE 3.40 BEARING FLUSH FLOW VERSUS FILTRATE SAMPLER FLOW AT 5 gpm PUMP FLOW WHILE INJECTING N_2 GAS AT THE RATE OF 0.6 scfm

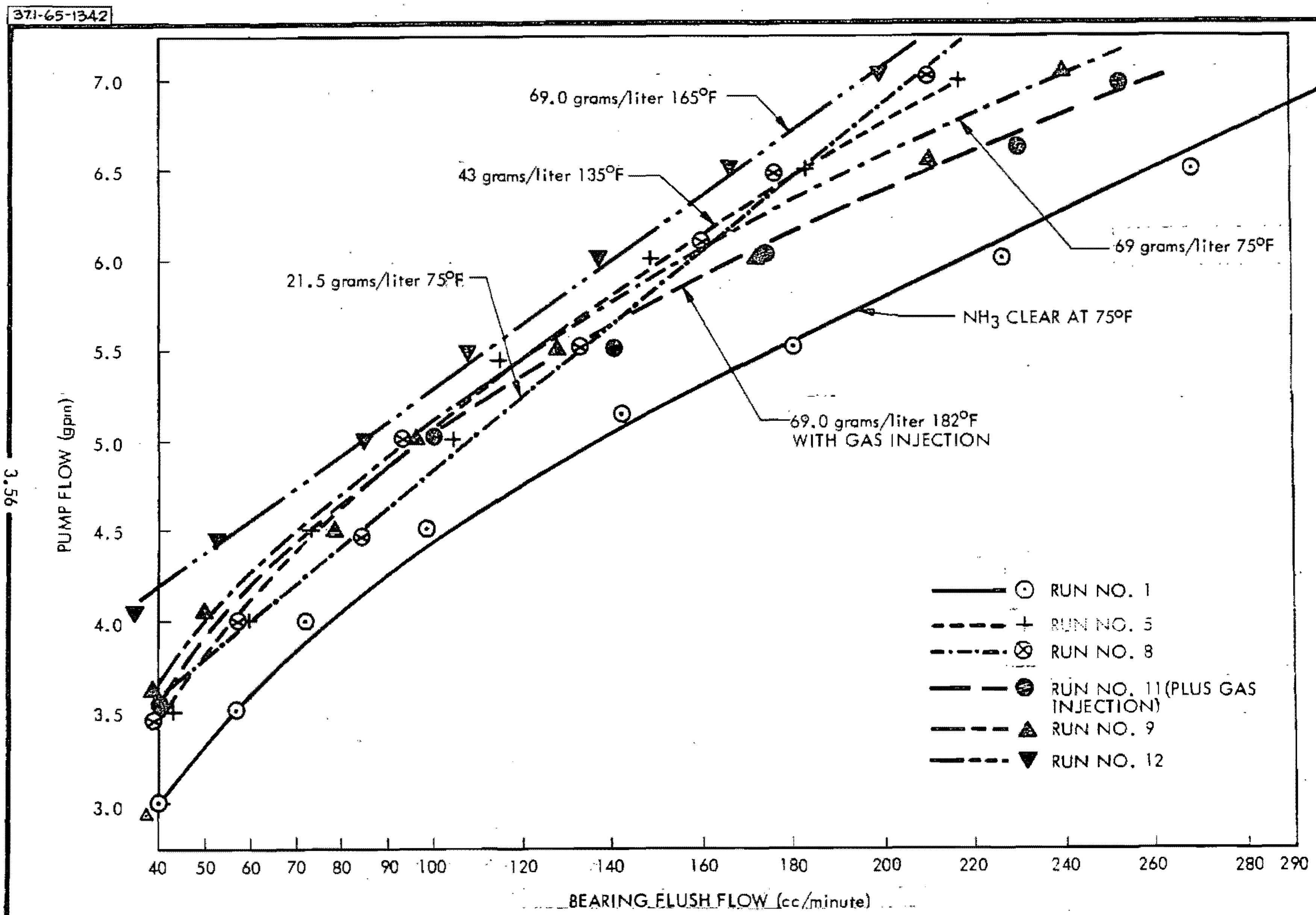

FIGURE 3.41 PUMP FLOW VERSUS BEARING FLUSH FLOW

3.6.4 Fuel Inventory

Upon completion of component testing, the loop was disassembled and a quantitative account made of the UO_2 found in the loop.

Table 3.9 shows the amount of UO_2 loaded into the loop and the amounts removed during operation for samples. The net UO_2 remaining at 560 hr is 390.54 g.

TABLE 3.9

SUMMARY OF UO_2 INVENTORY

	UO_2 g
UO_2 Loadings	
Total loaded into loop in 11 successive loadings	574.42
UO_2 Removals and Waste	
removal through sampling	119.50
removal in cleaning ends of samplers	40.98
removal during venting of samplers, replacement of gaskets, etc.	23.40
Total UO_2 removed	183.88
UO_2 present in system at the end of the tests	390.54

The 119.5 and 40.98 g losses from sampling and sampler cleaning are measured values. The 23.4 g loss from venting, etc., is an estimate based on an assumed 10% loss of the UO_2 contained in the sampler end fittings during venting, evacuating, disassembling, etc.

Table 3.10 lists the UO_2 recovered during loop disassembly.

The balance of fuel unaccounted for is 20.70 g; the accuracy of the balance would more nearly be represented by 21 $\pm$ 5 g. In Table 3.10 it can be seen that total fuel trapping in the pump is 8.86 g, in the filter 5.23 g, in the gas disengager 2.64 g, and in the Venturi and pressure transducers 0.35 g. The total reference component trapping excluding small plate-out in pipe lines is 17.08 g UO_2. The other equipment shown in Table 3.10 is nonreference and not part of the in-reactor loop.

TABLE 3.10

FUEL RECOVERED FROM LOOP COMPONENTS

	Weight UO_2, g
Total fuel in dump tank	301.40
Filter	5.23
Front pump casing and impeller	1.00
Pump front bearing, front of rotor and thermal barrier	4.28
Pump rear cover, rear bearing and rear area of rotor	1.38
Pump front casing behind thermal barrier and rotor casing	0.85
Pump back casing and rotor	1.35
Barton gage casing (ΔP gage)	11.48
Total of 20 Marman fittings	0.14
Total of 11 ball valves	1.76
Total of 1/4 in. tubings (0.01 g/ft length)	1.40
Dump tank 3-way valve (V-27)	1.20
Total of 9/16 in. tubing (main slurry loop) (0.055 g/ft length)	1.55
Two Foxboro flowmeters	6.10
Bearing vent sight glass	17.70
Gas disengager	2.64
E.M. flowmeter and flanges	5.15
Filtrate removals and sampling	1.68
Venturi and pressure transducers	0.35
Pump cooling coil	0.45
Slurry sampler valves (12); check valve; 8 needle valves, 8 T fittings	2.75
Total UO_2 recovered	369.84
UO_2 present in the loop at the end of the test (Table 3.9)	390.54
Total UO_2 recovered	369.84
Unaccounted Fuel	20.70

The missing 21 g, or 3.6% of the total fuel loaded (574.42 g), has not been fully explained. Examination of the gas-disengager off-gas line has shown that fuel passed through the filter in the top of the gas-disengager. The inside surface of this line was coated with a slight amount of UO_2. The outlet port of Valve V-7 also was slightly contaminated. The inside of the valve was not visibly contaminated with UO_2. These observations indicate that the amount of UO_2 passing through the top of the gas disengager was minimal and cannot account for all of the 21 g missing.

We conclude that the 21 g inventory loss results either from under-estimation of the fuel loss during sampler venting and evacuation or fuel transport from the small dump tank to the large dump tank during loop draining operations, or both. The large dump tank was not opened because it contained an unknown amount of UO_2 from previous runs and therefore the amount of UO_2 resulting from the present run could not be determined from it.

3.6.5 Filtrate Uranium Analysis

Filtrate samples taken during Run Nos. 11 and 12, primarily for N_2H_4 decomposition analysis, were also analyzed for uranium dioxide content (as U) by the polarographic method. Table 3.11 shows the results of the analysis. The last column gives uranium concentration as grams U (not UO_2) per liter of sample.

TABLE 3.11

URANIUM ANALYSES - RUN NOS. 11 AND 12

Sample	Sample Volume, cc	Total Weight of Uranium Found in the Sample, mg	Uranium Concentration, g/l
11-1	1.365	0.135	.10
11-4	1.151	.123	.11
11-7	1.365	.111	.08
11-11	1.365	.133	.10
11-14	1.365	.115	.08
11-17	1.151	.122	.11
11-18	1.365	.129	.10
12-2	1.365	.107	.09
12-6	1.365	.116	.08
12-10	1.365	.136	.10
12-16	1.365	.116	.08

This data confirms the indicated passage of UO_2 fines through the filter as described in Section 3.6.4 above.

3.6.6 Hydrazine Decomposition

The rate of N_2H_4 decomposition in a pumped ammonia-UO_2 slurry was measured during Run Nos. 11 and 12. A known weight of N_2H_4 was added to the loop during each run. The addition was made through the pump bearing venting port on the motor end of the pump, top side (Valve V-15). Forty-five minutes to one hour was allowed for N_2H_4 mixing in the slurry before samples were taken.

Samples were analyzed for NH_3 and N_2H_4 by titration and the coulometric method, respectively.

Results of the decomposition experiments are shown in Tables 3.12 and 3.13. At 200°F about 33% of the N_2H_4 in the loop was decomposed in 24 hr and about 50% in 48 hr with an initial hydrazine concentration of 3.76 wt%. At 165°F (Run 12), the initial N_2H_4 concentration was 4.75 wt% of which 17.7% was decomposed in 23 hr.

TABLE 3.12

DECOMPOSITION - RUN NO. 11

All data based upon temperature of 200°F. The initial loading of N_2H_4 reresulted in a concentration of 0.0376 g N_2H_4 g sample.

Sample	Elapsed Time Since N_2H_4 Addition,hr	NH_3,g	N_2H_4,g	Observed Ratio (g N_2H_4/g sample)	Apparent N_2H_4 Decomposition, %
11-1	0.25	0.630	0.0178	0.0275	26.86
11-2	0.83	.534	.0199	.0359	4.52
11-3	1.17	.648	.0244	.0363	3.46
11-4	1.50	.480	.0179	.0360	4.26
11-5	2.00	.649	.0244	.0362	3.72
11-6	2.50	-	-	-	-
11-7	3.00	.645	.0241	.0360	4.26
11-8	3.50	-	-	-	-
11-9	3.75	.662	.0247	.0360	4.26
11-10	4.00	-	-	-	-
11-11	4.25	.667	.0235	.0340	9.57
11-12	5.00	-	-	-	-
11-13	5.50	.676	.0225	.0322	14.36
11-14	6.00	.638	.0208	.0316	15.96
11-15	6.50	-	-	-	-
11-16	7.00	.649	.0224	.0334	11.17
11-17	7.25	-	-	-	-
11-18	23.50	.606	.0157	.0253	32.71
11-19	43.00	.615	.0117	.0187	50.27

TABLE 3.13

DECOMPOSITION - RUN NO. 12

All data based upon temperature of 165°F. The initial loading of N_2H_4 resulted in a concentration of 0.0475 g N_2H_4/g sample.

Sample	Elapsed Time Since N_2H_4 Addition, hr	NH_3, g	N_2H_4, g	Observed Ratio (g N_2H_4/g sample)	Apparent N_2H_4 Decomposition, %
12-1	1.00	-	-	-	-
12-2	1.50	0.689	0.0332	0.0460	3.16
12-3	2.00	.595	.0286	.0459	3.37
12-4	2.30	.685	.0330	.0460	3.16
12-5	3.00	.574	.0282	.0468	1.47
12-6	3.30	.695	.0310	.0427	10.11
12-7	4.00	-	-	-	-
12-8	4.30	.690	.0321	.9445	6.32
12-9	5.00	.576	.0269	.0446	6.11
12-10	5.30	.691	.0318	.0440	7.37
12-11	6.00	.532	.0251	.0451	5.05
12-12	6.30	.694	.0314	.0433	8.84
12-13	9.83	-	-	-	-
12-14	13.83	.686	.0314	.0438	7.79
12-15	22.83	-	-	-	-
12-16	23.00	.699	.0285	.0391	17.68
12-17	23.75	-	-	-	-

3.6.7 General Observations

All in-reactor components operated throughout the testing program without malfunction. It was found that the loop flow rate was affected by gas disengager liquid level. If this liquid level decreases to the point at which it is below the second probe from the bottom of the disengager, the flow rate can be expected to decrease from the initial value of 5 gpm to 3.5 gpm in about 20 min. The flow decreased to about 2.6 gpm in 35 min. under similar conditions.

The sampling data were so erratic as to preclude correlation of operating parameter measurement with slurry density. This result was not entirely unexpected; it is the same result obtained by personnel of the HRE project at ORNL before the extensive development of isokinetic sampling by the out-of-reactor test group. The HRE in-reactor loop operations group, which did not adopt the isokinetic sampling technique after it was developed, experienced similar erratic sampling during in-pile operations.

A question remains concerning the actual behavior of fuel during circulation in the loop. A large part of the scatter in the sampling data is undoubtedly due to sampling technique. The scatter in pump ΔP and power input versus loop flow data evident from Figures 3.23 to 3.33 is evidence that either the fuel concentration in the slurry is fluctuating or some other experimental variable is not being adequately controlled and is causing the resulting scatter. Further analysis of experimental data has shown that pump ΔP and power consumption are influenced by liquid level in the gas disengager regardless of the absolute level in the disengager and bearing purge flow rate. The degree of sensitivity of the parameters of present interest such as pump ΔP, power consumption and frequency to these variables is not determinable from existing experimental data.

3.7 In-Pile Fuel Induction System

The reference method for fueling the in-reactor loop was to transfer a premixed quantity of relatively concentrated slurry from a loading bomb into the gas disengager using nitrogen gas pressure as the driving force. The fuel induction system consisted essentially of a detachable slurry loading bomb assembly and a connecting length of 1/4 in. tubing.

3.7.1 Test of Simulated System

A geometrically identical mockup of the fuel induction system was assembled and a series of loadings were undertaken to determine the efficiency of the proposed fuel transfer technique. A flow diagram of the mockup is shown in Figure 3.42; the heavy line indicates the critical slurry injection path. Valves V-20 (ammonia and nitrogen injection valve) and V-14 (slurry induction valve) are quick shut-off ball valves which permit fast operation of the system to insure that the UO_2 will not settle before the slurry is injected into the disengager. Transfer test results are given in Table 3.14. The tests are described below:

Run No. 1

The fuel loaded in this run was the amount which would be necessary to raise the loop in-reactor slurry concentration to 4.3 g/liter plus an additional amount (19.0 g) equal to that expected to be stopped in the components (see Section 3.6.4). The fuel was not screened and the NH_3 and nitrogen overpressure were admitted at the top of the fuel loading bomb.

37.1-65-1341

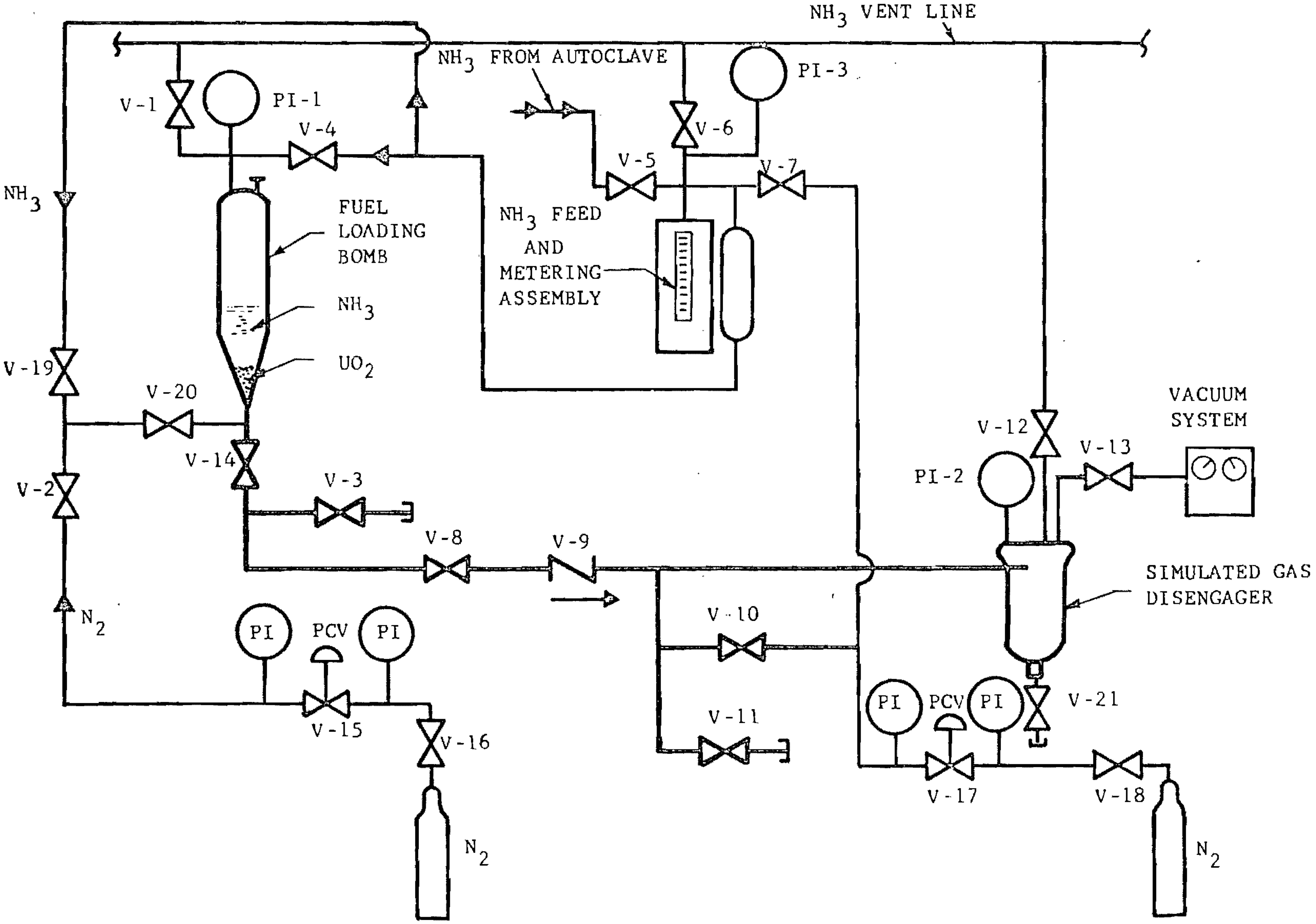

FIGURE 3.42 PIPING AND INSTRUMENTATION DIAGRAM OF TEST FUEL INDUCTION SYSTEM

TABLE 3.14

TEST DATA FOR FUEL INDUCTION SYSTEM TESTING

Run No.	UO_2 Loaded (grams)	Total UO_2 in system (grams)	UO_2 Recovered (grams)			Total UO_2 hang up (grams)	Pressures (psia)				Equilibrium Pressure (psia)	Time to reach the equilibrium pressure (sec)
							Initial		After 5 sec			
			Gas Disengager	Load Bomb Flush	Total Recovered		Load Bomb	Disengager	Load Bomb	Disengager		
0	-	-	-	-	-	-	300	1700	950	880	910	20
1	36.3	36.3	no transfer occurred	35.0	35.0	1.3 (in load bomb)	300	1700	315	1675	(350)(1605)	10 min.
1A*	35.3	36.6	0.3	27.3	27.6	9.0	300	1700	1170	850	1010	22
2*+	27.1	36.1	0.3	21.9	22.2	13.9	300	1685	1090	850	940	27
3*	69.0	82.9	0.4	65.9	66.3	16.6	302	1700	850	800	870	26
5*	87.2	103.8	0.3	87.0	87.3	16.5	305	1650	1020	700	965	30

---

* Run Nos. 1A, 2, 3, 5 performed with revised system and procedure

\+ Run No. 2 performed with clear NH_3 after flush

When fuel induction was attempted by opening Valve V-14, the only change resulting was an increase in pressure of 15 psi in the gas disengager; no fuel transfer occurred.

A system checkout revealed that line plugging occurred in the fuel loading bomb above Valve V-14.

Run No. 1A

After the first fuel injection test (Run No. 1) some changes in procedure became necessary; these were:

1) The fuel should be passed through a 150-mesh screen before loading and should be handled in dry atmosphere. This will break up hard lumps, one of the causes of line plugging.

2) The fuel should be thoroughly wetted by the ammonia prior to injection. This will prevent dry packing of the UO_2 in the 1/4 in. tubing at the bottom of the fuel loading bomb and promote fuel dispersion.

3) A thorough fuel suspension should be achieved before fuel injection to prevent packing of the UO_2 in the narrow section. This is achieved by bubbling the overpressure nitrogen through the UO_2-NH_3 mixture rather than admitting it at the top of the fuel loading bomb.

The fuel from the previous run was recovered and the run was repeated by injecting the ammonia and the nitrogen through the UO_2 using Valves V-19, V-20 (NH_3), and V-2, V-20 (N_2). The fuel was successfully transferred except for 9.0 g which had evidently settled in the lines and valves.

Run No. 2

This run was a repeat of Run No. 1A except that it was followed by a line flush with 750 cc of clear NH_3 to test the possibility of better fuel transfer by following with a clear NH_3 line flush. An additional 4.9 g of fuel were hung up in the lines during this run. This indicated that a clear NH_3 flush did not improve fuel transfer.

Run Nos. 3 and 5

These runs followed the same procedures as Run No. 1A. No ammonia flush followed, and the UO_2 loadings were sufficient amounts to simulate successive increases in the loop slurry concentration from 4.3 to 21.5 g/l (Run No. 3), 21.5 to 43.0 and 43.0 to 64.0 g/l (Run No. 5).

In Run No. 3 an additional 2.7 g of UO_2 were lost in the lines, and in Run No. 5 the fuel recovered was 0.1 g in excess of the loaded amount (87.2 g) indicating that no further fuel hang-up had occurred even though the amount of fuel loaded was more than three times as much as in Run No. 2.

3.7.2 Fuel Balance

During the fuel induction test runs, a total of 16.5 g of UO_2 had hung up in the lines and valves between the loading bomb and the simulated gas disengager.

A 2000 cc flush of the lines and Valves V-11 and V-10 (ammonia makeup line and filtrate return line) was performed, and 11.3 g of fuel were recovered. Valves V-8 and V-9 were sectioned and cleaned and 1.90 g UO_2 recovered. The fuel loading bomb and Valves V-14 and V-20 were cleaned and 2.3 g UO_2 recovered.

The following Table 3.15 gives a complete account of the fuel balance.

TABLE 3.15

FUEL BALANCE

	UO_2 Loaded, g	UO_2 Recovered, g
Run No. 1 (no transfer occurred)	36.3	35.0
Run No. 1A	35.3	27.6
Run No. 2	27.1	22.2
Run No. 3	69.0	66.3
Run No. 5	87.2	87.3
Ammonia makeup and filtrate return lines and valves (V-10, V-11)		11.3
Simulated valves (V-8, V-9)		1.9
Fuel load bomb and Valves V-14, V-20		2.3
	254.9	253.9
Fuel unaccounted for	1.0 (0.4% of total loaded fuel)	

The 1.0 g missing fuel represents the fuel plate-out in the lines between the loading bomb and the gas disengager and some small losses in fuel handling during fuel recovery.

Since a continuous flow of ammonia to the disengager will be maintained through Valves V-10 and V-11, the 11.3 g fuel hang-up in these valves and lines is considered to be only temporary. The permanent fuel hang-up is thus 16.5 - 11.3 = 5.2 g.

3.7.3 Recommendations

In view of the test results the following recommendations were made:

1) Screen all fuel (in dry atmosphere) through at least a 150-mesh screen prior to loading into the fuel bomb.

2) To insure thorough wetting of the UO_2, load the ammonia slowly through the bottom of the fuel loading bomb (V-20).

3) Inject the nitrogen overpressure through the same valve at the bottom of the fuel loading bomb to insure fuel suspension during transfer and avoid plugging of the lines.

4) Open the fuel loading Valve V-14 immediately after closing the quick shut-off nitrogen inlet ball valve (V-20). (This will inject the slurry into the disengager before it starts settling out.)

LIST OF REFERENCES

1. J. H. Cusack, et al, "Nuclear Hydrazine Program," AD 261324 (1961).

2. B. Carlin, "Ultrasonics," McGraw-Hill, N.Y., N.Y. (1949).

3. R. W. Boyle, et al, Cavitation in the Track of an Ultrasonic Beam, Trans Roy. Soc. Canada, 23, 187 (1929).

4. O. I. Babikov, "Ultrasonics and its Industrial Application," Consultants Bureau, N.Y. (1960).

5. E. L. Youngblood, P. A. Haas, An Evaluation of Hydroclones for Size Classification of Thorium Oxide, ORNL-2689 (1959).

6. P. A. Haas, Solids Separation by a Hydraulic Cyclone with a Batch Underflow Receiver, ORNL-2876 (1960).

7. N. Yoshioka and Y. Hotta, "Liquid Cyclones as a Hydraulic Classifier", Chem. Eng. Japan 19, 632-40 (1955).

8. D. Bradley, "A Contribution to the Theory of the Hydraulic Cyclone and Data on the Performance of Small Diameter Cyclones", AERE CE/R 2016, October 1956.

9. P. A. Haas, Hydraulic Cyclones for Application to Homogeneous Reactor Chemical Processing, ORNL-2301 (1957).

10. North American Aviation, Inc., Report AL-312, 29 October 1947.

11. Audrieth and Ogg, The Chemistry of Hydrazine, Wiley, New York, 1951, pp 45, 47.

12. Ibid, p 200.

13. Brown and Houeban, JACS 33, 1734-42 (1911).

14. Drago and Sisler, J. Physical Chemistry 60, 245-9, 1956.

15. Lewis and Kay, Oil and Gas J. 32, No. 45, 40, 29 March 1934.

16. Edmister, Petroleum Refiner, Vol. 39, No. 6, 7, 8, 10, 11, 12, 1960.

17. Maxwell, "Data Book on Hydrocarbons," D. Van Nostrand Col., 1950.

18. Fenske, Ind. Engr. Chem. 24, 485 (1932).

19. Oak Ridge National Laboratory Status and Progress Reports for October 1962, ORNL-3377, 29 November 1962.

20. Heath, R. L., A Scintillation Spectrometry Gamma Ray Spectrum Catalogue, DIO-16408, 1 July 1957.

21. National Academy of Sciences, National Research Council, Nuclear Data Sheets.

22. R. C. Bolles and N. E. Ballou, Calculated Activities and Abundances of U-235 Fission Products, USNRDL-456, 30 August 1956.

23. J. Belloni, et al., J. Phys. Chem. 63, 881-7, January 1959.

24. Aqueous Fuel Systems, Reactor Handbook, 2nd Edition, Vol. I, pp 416 Interscience Publishers, Inc. 1960.

25. V. R. Evans, The Corrosion and Oxidation of Metals, N. Y., St. Martins Press, 1960, pp 354-355.

26. H. H. Uhlig, Corrosion Handbook, John Wiley & Sons, N. Y., 5th Printing, 1955, p 799.

27. Compatibility of Rocket Propellants with Materials of Construction, DMIC Memorandum 65, September 15, 1964.

28. "Hydrazine Handling Manual", AD-266145, September 1961.

29. M. E. A. Hermans, R. G. Sowden, and S. G. Slooten, "Irradiation Experiments with Fuel Suspensions," paper presented at Symposium on Radiation Damage in Solids and Reactor Materials, Venice, Italy, May 1962.

DISTRIBUTION LIST

for

AFML-TR-6598

Contract AF 33(600)-42996

Project 7-840a

U. S. Atomic Energy Commission (1)
Office of Isotope Development
Washington, D. C.
Attn: Dr. Paul C. Aebersold, Director

U. S. Atomic Energy Commission (1)
Chemical Separations & Development Branch
Washington 25, D. C.
Attn: Dr. E. L. Anderson, Jr.

U. S. Atomic Energy Commission (3)
San Francisco Operations Office
2111 Bancroft Way
Berkeley, California 94704
Attn: Walter H. Brummett, Jr.

U. S. Atomic Energy Commission (1)
Research Division
Washington 25, D. C.
Attn: Dr. Paul W. McDaniel, Director

U. S. Atomic Energy Commission (1)
Division of Reactor Development and Technology
Washington, D. C.
Attn: Dr. Milton F. Shaw

U. S. Atomic Energy Commission (1)
Research Division
Washington 25, D. C.
Attn: Dr. Alex Van Dyken

U. S. Atomic Energy Commission (1)
Washington 25, D. C.
Attn: Dr. E. E. Sinclair, D.R.D.& T.

Oak Ridge National Laboratory (1)
Oak Ridge, Tennessee
Attn: R. P. Briggs

AFR & TD(1)
Wright-Patterson AFB, Ohio
Attn: MAX (Dr. A. Lovelace)

AFR & TD(1)
Air Force Systems Command
Wright-Patterson AFB, Ohio
Attn: SEKRB

Office of Aerospace Research (1)
Headquarters, USAF
Directorate of Material Sciences
Washington 25, D. C.

Commander (1)
Aeronautical Research Directorate
Aeronautical Research Laboratory
Wright-Patterson AFB, Ohio
Attn: Col. Robert E. Fontana

Space Systems Division (1)
Air Force Unit Post Office
Los Angeles 45, California
Attn: SSR

San Francisco AFCMD (1)
Western Contract Management Region
Air Force Systems Command
U. S. Air Force
880 Doolittle Drive
San Leandro, California 94577
Attn: E. Kreick, ACO

Air Force Systems Command (1)
Andrews Air Force Base
Washington 25, D. C.
Attn: C. W. Kniffin, RDRAW-F

Commander (1)
Ballistic Systems Division
Air Force Unit Post Office
Los Angeles 45, California
Attn: BSR

Air Force Flight Test Center (1)
Edwards AFB, California
Attn: FTRPL-2

Commander (1)
Aeronautical Systems Division
Wright-Patterson AFB, Ohio
Attn: Mr. C. Perry, ASWKR

Commander (3)
Aeronautical Systems Division
Manufacturing Technology Laboratory
Wright-Patterson AFB, Ohio
Attn: MATC - C. Tanis

SEPIE (1)
Wright-Patterson AFB, Ohio

SEPIR (1)
Wright-Patterson AFB, Ohio

Commander (1)
AFR & TD
Nuclear Division FDFN
Wright-Patterson AFB, Ohio
Attn: Mr. S. G. Fidler

U. S. Army (1)
Quartermaster Research & Engineering Command
Quartermaster Research & Engineering Center
Natick, Massachusetts

Office of Naval Research (1)
Washington 25, D. C.
Attn: Dr. Ralph Roberts

AFDRT (1)
The Pentagon
Washington 25, D. C.

Dr. J. P. Kincaid (1)
Advanced Research Project Agency
Department of Defense
The Pentagon
Washington, D. C.

Advanced Research Projects Agency (1)
Institute for Defense Analysis
The Pentagon
Washington 25, D. C.

Dr. Harold Brown (1)
D.D.R.E., O.S.D.
The Pentagon
Washington 25, D. C.

Defense Documentation Center (10)
Arlington Hall Station
Arlington 12, Virginia

Office of the Special Assistant
for Science & Technology (1)
The White House
Washington 25, D. C.
Attn: E. Mahoney

National Aeronautics & Space Administration (1)
Lewis Research Center
2100 Brookpark Road
Cleveland 35, Ohio
Attn: Dr. E.J. Maganiello

National Aeronautics & Space Administration (1)
George C. Marshall Space Flight Center
Huntsville, Alabama
Attn: Dr. W. R. Lucas (M-S & M-M)

ASMA (1)
George C. Marshall Flight Test Center
Huntsville, Alabama
Attn: Dr. Wernher Von Braun
Director of Development Operations

National Aeronautics & Space Administration (1)
1512 H Street
Washington 25, D. C.
Attn: Harold B. Finger
Chief, Nuclear Propulsion

A&M College of Texas (1)
College Station, Texas
Attn: Chemical Engineering Dept.

Battelle Memorial Institute (1)
505 King Avenue
Columbus, Ohio
Attn: Dr. C. H. Lorig

Radiation Effects Information Center (1)
Battelle Memorial Institute
505 King Avenue
Columbus 1, Ohio
Attn: R. E. Bowman

Brookhaven National Laboratory (1)
Associated Universities, Inc.
Upton, Long Island, New York
Attn: Research Librarian

Brookhaven National Laboratory (2)
Associated Universities, Inc.
Upton, Long Island, New York
Attn: B. Manowitz

Case Institute of Technology (1)
Chemical Engineering Department
10900 Euclid Avenue
Cleveland 6, Ohio

IIT Research Institute (1)
10 West 35th Street
Chicago, Illinois 60616
Attn: Alice L. Jones
Document Librarian

Liquid Propellant Information Agency (1)
John Hopkins University
8621 Georgia Drive
Silver Springs, Maryland

Massachusetts Institute of Technology (1)
Chemical Engineering Department
Cambridge 39, Massachusetts

Pennsylvania State University (1)
Chemical Engineering Department
University Park, Pennsylvania

Princeton University (1)
Princeton, New Jersey
Attn: R. C. Axtmann, Associate Professor of
Chemical Engineering for Nuclear Studies

Purdue University (1)
Chemical Engineering Department
Lafayette, Indiana

Rensselear Polytechnic Institute (1)
Troy, New York
Attn: Professor Paul Hartech

Southwest Research Institute (1)
San Antonio 6, Texas
Attn: Dr. P. M. Ku

Stanford Research Institute (1)
Economics Research Division
Menlo Park, California
Attn: Dr. Leland H. Towle

University of California (1)
Lawrence Radiation Laboratory
Post Office Box 808
Livermore, California

University of Cincinnati (1)
Chemical Engineering Department
Cincinnati, Ohio

University of Dayton (1)
Chemical Engineering Department
Dayton, Ohio

Aerojet-General Corporation (1)
Post Office Box 296
Azusa, California
Attn: Dr. D. L. Armstrong
Department 3201

A. D. Little, Inc. (1)
30 Memorial Drive
Cambridge 42, Massachusetts

Lovell Lawrence, Jr., Director (1)
Advanced Projects Organization
Chrysler Corporation
Post Office Box 1827
Detroit 3, Michigan

Air Reduction Company, Inc. (1)
Central Research Laboratories
Murray Hill, New Jersey

Allis-Chalmers Manufacturing Company (1)
Atomic Energy Division
Glendale, Wisconsin
Attn: Mr. C. R. Bracon
Manager of Marketing

American Potash & Chemical Corporation (1)
3000 W. Sixth Street
Los Angeles 54, California
Attn: J. C. Schumacher, Vice President
Research

Astra, Inc. (1)
Post Office Box 226
Raleigh, North Carolina

Bettis Atomic Power Division (1)
Post Office Box 1568
Pittsburgh 30, Pennsylvania
Attn: Mrs. Virginia Sternberg
Librarian

Bristol-Aerojet, Ltd. (1)
Banwell
Weston-Super-Mare
England
Attn: Mr. A. G. Shove

California Research Corporation (1)
200 Bush Street
San Francisco 20, California
Attn: Mr. J. R. MacGregor

Callery Chemical Company (1)
Callery, Pennsylvania
Attn: C. N. Clayton, Literature Chemist

Convair Astronautics (1)
Division of General Dynamics Corporation
Mail Zone 592-10
San Diego, California
Attn: Dr. E. B. Miros

E. I. du Pont de Nemours, Inc. (1)
Atomic Energy Division
Wilmington 98, Delaware
Attn: Document Custodian

E. I. du Pont de Nemours, Inc. (1)
Development Department
Wilmington 98, Delaware
Attn: Dr. Daniel St. John

Food Machinery & Chemical Company (1)
Princeton Laboratories
Princeton, New Jersey
Attn: Dr. Louis Diamond

General Electric Company (1)
Chemical Engineering Department
Post Office Box 100
Richland, Washington
Attn: M. F. McHale

The General Tire & Rubber Company (1)
1708 Englewood Avenue
Akron 9, Ohio
Attn: Dr. E. E. Gruber, Director
Research Division

The General Tire & Rubber Company (2)
1708 Englewood Avenue
Akron 9, Ohio
Attn: Dr. R. J. Belner, Technical Director
Chemical/Plastics Division

Hercules Powder Company (1)
Propulsion Division
Wilmington 99, Delaware
Attn: C. T. Butler

International Minerals & Chemical Corporation (1)
Florida Experiment Station
Post Office Box 437
Mulberry, Florida

Kaiser Engineers Division (1)
Henry J. Kaiser Company
Kaiser Building
Oakland 12, California

Knolls Atomic Power Laboratory (1)
Schenectady, New York

Director, USN Research Laboratories (1)
Code 6180
Washington 25, D. C.

National Distiller & Chemical Corporation (1)
U. S. Industrial Chemicals Division
1275 Section Road
Cincinnati 37, Ohio
Attn: Dr. H. Horvitz

Nuclear Development Association, Inc. (1)
White Plains, New York

Olin Mathieson Chemical Corporation (1)
Chemical Research Energy Division
275 Winchester Avenue
New Haven, Connecticut
Attn: Dr. John W. Churchill, Director

Phillips Petroleum Company
AEC Division
Idaho Falls, Idaho
Attn: Dr. R. L. Shank, Manager, (1)
CPP Analytical

Attn: F. L. McMillan, Manager (1)
Project Engineering Branch

Attn: J. H. Ronsick, Manager (1)
Metallurgy & Hot Cell Branch

Attn: L. L. Meyers (1)
Project Engineer

Rand Corporation (1)
Santa Monica, California

Rocketdyne (1)
Liquid Propellant Division
6633 Canoga Avenue
Canoga Park, California

Sylvania Electric Products, Inc. (1)
Atomic Energy Division
Bayside, New York

Temco Aircraft Corporation (1)
Manufacturing Department
Post Office Box 6191
Dallas 22, Texas
Attn: Doyle T. Brooks, Jr.
Department Manager

Monsanto Chemical Company (1)
Research & Engineering Division
Everette Station
Boston 49, Massachusetts
Attn: Emery N. Wescott

Thompson-Ramo Wooldridge, Inc. (1)
Industrial Engineering
23555 Euclid Avenue
Cleveland 17, Ohio
Attn: K. C. White, Staff Director

Union Carbide Corporation (1)
270 Park Avenue
New York, New York 10017
Attn: H. D. Kinsey, Vice President

Union Carbide Corporation (2)
Mining and Metals Division
P.O. Box 324
Tuxedo, New York
Attn: J. C. Brantley

U. S. Rubber (1)
137 North Main Street
Dayton 2, Ohio
Attn: Mr. Ray Lozar

Westinghouse Electric Corporation (1)
Materials Laboratory
East Pittsburgh, Pennsylvania
Attn: Gordon C. Gainer

W. R. Grace & Company (1)
Research Division
Washington Research Center
Clarksville, Maryland
Attn: Mr. W. K. O'Loughlin

Unclassified
Security Classification

DOCUMENT CONTROL DATA - R&D

(Security classification of title, body of abstract and indexing annotation must be entered when the overall report is classified)

1. ORIGINATING ACTIVITY (Corporate author) Aerojet-General Nucleonics San Ramon, California	2a. REPORT SECURITY CLASSIFICATION Unclassified 2b. GROUP

3. REPORT TITLE CONTINUOUSLY CIRCULATING FISSIOCHEMICAL PROCESS DEVELOPMENT APPLICABLE TO HYDRAZINE SYNTHESIS. Vol. I - Program Survey, Processing, and Materials; Vol. II - In-Reactor Engineering, and Support; Vol. III - Basic Studies, Nuclear Engineering, Plant Design, and Loop Operations.

4. DESCRIPTIVE NOTES (Type of report and inclusive dates)
Final Technical Engineering Report

5. AUTHOR(S) (Last name, first name, initial)
Cusack, J. H., Groff, C. C., Carpenter, L. G., et al

6. REPORT DATE June 1965	7a. TOTAL NO. OF PAGES 903	7b. NO. OF REFS 66

8a. CONTRACT OR GRANT NO. AF 33(600)-42996	9a. ORIGINATOR'S REPORT NUMBER(S) AN-1425
b. PROJECT NO. ASD 7-840a	
c.	9b. OTHER REPORT NO(S) (Any other numbers that may be assigned this report) AFML-TR-65-98
d.	

10. AVAILABILITY/LIMITATION NOTICES Qualified requesters may obtain copies of this report from DDC. DDC RELEASE TO OTS NOT AUTHORIZED. The distribution of this report is limited because the report contains technology identifiable with items on the strategic embargo.

11. SUPPLEMENTARY NOTES	12. SPONSORING MILITARY ACTIVITY Chemical Processing Branch (MATC), Manufacturing Technology Division, AF Materials Laboratory, Wright-Patterson Air Force Base, Ohio

13. ABSTRACT The primary goal of this program was to design, construct, and operate a continuous in-reactor loop to further the development of the fissiochemical process; the conversion of ammonia to hydrazine was chosen as the demonstration synthesis. Direct support included studies in decontamination, purification, fuel cycle materials, chemical and energy deposition analysis, basic radiation chemistry, new product development, and reactor physcis. Techniques and equipment to accomplish gas-liquid and liquid-solid separation and the removal of radioactive contamination from the concentrated product were developed. The compatibility of materials of construction, particulate UO_2, and process chemicals was demonstrated. Fission fragment range and energy deposition rates within solid fuel bodies were derived theoretically and confirmed experimentally. Colorimetry, coulometry, titrimetry, chromatography, UV and x-ray spectrometry, sedimentometry, and polarography were utilized in the development of analytical techniques. The effects of product concentration, gas overpressure, gamma to fission fragment ratios, and chemical additives upon hydrazine yield were studied in stirred capsule irradiations. The fissiochemical formation of several new high energy rocket fuel oxidizers was attempted; NF_3 was produced. The economics of hydrazine production in self-critical reactors and in production loops was evaluated. The AGN-6 loop experiment involved the circulation of a slurry of fully enriched particulate UO_2 fuel through the high thermal neutron flux region of a testing reactor; the design, construction and testing of all supporting systems are described. Loop experimental operation at fission power levels of 0 to 9 kw is discussed; operational and analytical data and the conclusions derived therefrom are presented. (U)

DD FORM 1 JAN 64 1473

Unclassified
Security Classification

14. KEY WORDS	LINK A		LINK B		LINK C	
	ROLE	WT	ROLE	WT	ROLE	WT
nuclear reactor						
fissiochemistry						
radiochemistry						
radiation chemistry						
hydrazine						
rocket fuel oxidizer						
chromatography						
slurry handling						
ammonia						
uranium dioxide						
distillation						
evaporation						
ion exchange						
fission fragment						
solid-liquid separation						
gas-liquid separation						

INSTRUCTIONS

1. ORIGINATING ACTIVITY: Enter the name and address of the contractor, subcontractor, grantee, Department of Defense activity or other organization *(corporate author)* issuing the report.

2a. REPORT SECURITY CLASSIFICATION: Enter the overall security classification of the report. Indicate whether "Restricted Data" is included. Marking is to be in accordance with appropriate security regulations.

2b. GROUP: Automatic downgrading is specified in DoD Directive 5200.10 and Armed Forces Industrial Manual. Enter the group number. Also, when applicable, show that optional markings have been used for Group 3 and Group 4 as authorized.

3. REPORT TITLE: Enter the complete report title in all capital letters. Titles in all cases should be unclassified. If a meaningful title cannot be selected without classification, show title classification in all capitals in parenthesis immediately following the title.

4. DESCRIPTIVE NOTES: If appropriate, enter the type of report, e.g., interim, progress, summary, annual, or final. Give the inclusive dates when a specific reporting period is covered.

5. AUTHOR(S): Enter the name(s) of author(s) as shown on or in the report. Enter last name, first name, middle initial. If military, show rank and branch of service. The name of the principal author is an absolute minimum requirement.

6. REPORT DATE: Enter the date of the report as day, month, year; or month, year. If more than one date appears on the report, use date of publication.

7a. TOTAL NUMBER OF PAGES: The total page count should follow normal pagination procedures, i.e., enter the number of pages containing information.

7b. NUMBER OF REFERENCES: Enter the total number of references cited in the report.

8a. CONTRACT OR GRANT NUMBER: If appropriate, enter the applicable number of the contract or grant under which the report was written.

8b, 8c, & 8d. PROJECT NUMBER: Enter the appropriate military department identification, such as project number, subproject number, system numbers, task number, etc.

9a. ORIGINATOR'S REPORT NUMBER(S): Enter the official report number by which the document will be identified and controlled by the originating activity. This number must be unique to this report.

9b. OTHER REPORT NUMBER(S): If the report has been assigned any other report numbers *(either by the originator or by the sponsor)*, also enter this number(s).

10. AVAILABILITY/LIMITATION NOTICES: Enter any limitations on further dissemination of the report, other than those imposed by security classification, using standard statements such as:

(1) "Qualified requesters may obtain copies of this report from DDC."

(2) "Foreign announcement and dissemination of this report by DDC is not authorized."

(3) "U. S. Government agencies may obtain copies of this report directly from DDC. Other qualified DDC users shall request through
_______________________."

(4) "U. S. military agencies may obtain copies of this report directly from DDC. Other qualified users shall request through
_______________________."

(5) "All distribution of this report is controlled. Qualified DDC users shall request through
_______________________."

If the report has been furnished to the Office of Technical Services, Department of Commerce, for sale to the public, indicate this fact and enter the price, if known.

11. SUPPLEMENTARY NOTES: Use for additional explanatory notes.

12. SPONSORING MILITARY ACTIVITY: Enter the name of the departmental project office or laboratory sponsoring *(paying for)* the research and development. Include address.

13. ABSTRACT: Enter an abstract giving a brief and factual summary of the document indicative of the report, even though it may also appear elsewhere in the body of the technical report. If additional space is required, a continuation sheet shall be attached.

It is highly desirable that the abstract of classified reports be unclassified. Each paragraph of the abstract shall end with an indication of the military security classification of the information in the paragraph, represented as *(TS)*, *(S)*, *(C)*, or *(U)*.

There is no limitation on the length of the abstract. However, the suggested length is from 150 to 225 words.

14. KEY WORDS: Key words are technically meaningful terms or short phrases that characterize a report and may be used as index entries for cataloging the report. Key words must be selected so that no security classification is required. Identifiers, such as equipment model designation, trade name, military project code name, geographic location, may be used as key words but will be followed by an indication of technical context. The assignment of links, rules, and weights is optional.